

CHALMERS



Methods for Verification of Post-Impact Control including Driver Interaction

Master's Thesis in the Master's programme Automotive Engineering

JAVIER BELTRAN

YUJIAO SONG

Department of Applied Mechanics
Division of Vehicle Engineering and Autonomous Systems
Vehicle Dynamics Group
CHALMERS UNIVERSITY OF TECHNOLOGY
Gothenburg, Sweden 2011
Master's Thesis 2011:11

Methods for Verification of Post-Impact Control including Driver Interaction

Master's Thesis in the Master's programme Automotive Engineering

JAVIER BELTRAN

YUJIAO SONG

Department of Applied Mechanics
Division of Vehicle Engineering and Autonomous Systems
Vehicle Dynamics Group
CHALMERS UNIVERSITY OF TECHNOLOGY
Gothenburg, Sweden 2011

Methods for Verification of Post-Impact Control including Driver Interaction

Master's Thesis in the Master's programme Automotive Engineering

JAVIER BELTRAN

YUJIAO SONG

© JAVIER BELTRAN, 2011

© YUJIAO SONG, 2011

Master's Thesis 2011:11

ISSN 1652-8557

Department of Applied Mechanics

Division of Vehicle Engineering and Autonomous Systems

Vehicle Dynamics Group

CHALMERS UNIVERSITY OF TECHNOLOGY

SE-412 96 Gothenburg

Sweden

Telephone: + 46 (0)31-772 1000

Cover:

Volvo S60 which is the car used as example in the thesis work. <Source: (Volvo Cars Corporation, 2009)>

Chalmers Reproservice / Department of Applied Mechanics

Gothenburg, Sweden 2011

Methods for Verification of Post-Impact Control including Driver Interaction

Master's Thesis in the Master's programme Automotive Engineering

JAVIER BELTRAN

YUJIAO SONG

Department of Applied Mechanics

Division of Vehicle Engineering and Autonomous Systems

Vehicle Dynamics Group

Chalmers University of Technology

Abstract

This thesis project focuses on the verification method of a safety function called PIC that stands for Post-Impact Control which controls the vehicle motion of passenger cars after being exposed to external disturbances produced by a 1st impact, aiming at avoiding or mitigating secondary events.

The main objective was to select a promising method, among several candidates, to develop further for testing the function and the interaction with the driver. To do this it was first necessary to map the real destabilized states of motion that are targeted by the function. These states are referred as Post-Impact problem space and are a combination of variables that describes the host vehicles motion at the instant the destabilizing force has ceased. Knowing which states are requested by the solution candidates, it is possible to grade the rig candidates based on the capability of covering the problem space. Then, simulating the proposed rig solutions with Matlab/Simulink models to investigate which candidate fulfils best the problem space.

The result of the simulations and other criteria is that a moving base simulator (Simulator SIM4) is most fitted to research verification. The second most advantageous solution is the rig alternative called Built-in Actuators.

Key words: Verification of function, Multiple Event Accidents, Active safety, Vehicle motion control, Post-Impact, Triggered instability, Collision simulation.

I

CHALMERS, *Applied Mechanics*, Master's Thesis 2011:11

Metoder för verifiering av Post-Impact Control med förarinteraktion

Examensarbete inom Fordonsteknik

JAVIER BELTRAN

YUJIAO SONG

Institutionen för Tillämpad Mekanik

Avdelningen för Fordonsteknik och autonoma system, Gruppen för fordonsdynamic

Chalmers Tekniska Högskola

Sammanfattning

Detta examensarbete fokuserar på verifieringsmetoder av en säkerhets-funktionsom kallad PIC som står för Post-Impact Control, vilken är menad att förbättra stabiliteten på personbilar efter att ha utsatts för yttre störningar som alstras av en första kollision i en seriekrock.

Huvudsyftet var att välja en lovande metod, bland flera alternativ, för att ytterligare utveckla provningen av funktionen och dess samspel med föraren. För att göra detta var det först nödvändigt att kartlägga de verkliga destabiliserade rörelsetillstånd som är det som funktionen siktar på. Dessa tillstånd är samlade under begreppet Post-Impact problemrummet som är en kombination av variabler som beskriver den bärande fordonets rörelser i det ögonblick som den destabiliserande kraften har upphört. Att veta vilka tillstånd som eftersträvas av kandidatlösningarna gör det möjligt att gradera dem utifrån dess förmåga att täcka problemrummet.

Sedan, kommer rigsimuleringar med Matlab / Simulink-modeller att undersöka vilken kandidat som bäst uppfyller problemrummet.

Resultat av simuleringar och andra kriterier är att Simulatoren SIM4 är den rig som är mest lämpad för en inledande forskning av interaktionen med föraren. Den näst bästa lösningen är den så kallade Inbyggda aktuatorer som besitter en genomsnittlig täckning över problemrummet och de praktiska kriterier.

Nyckelord: Funktions verifiering, Multipla händelser i fordonsolyckor, Aktiv säkerhet, Fordonsdynamisk kontroll, Triggad instabilitet, Kollisionssimulering.

III

CHALMERS, *Applied Mechanics*, Master's Thesis 2011:11

Contents

ABSTRACT	I
SAMMANFATTNING	III
CONTENTS	V
PREFACE	VIII
1 INTRODUCTION	1
1.1 Background	1
1.1.1 Volvo profile	1
1.1.2 Vehicle collisions	1
1.1.3 Safety systems	2
1.1.4 PIC	3
1.2 Objectives	3
1.3 Method	5
1.4 Delimitations	5
2 LITERATURE REVIEW	7
2.1 Accident statistics	7
2.2 PIC Collision scenarios	8
2.3 Post Impact Control	10
2.4 Earlier simulation models in accident scenarios	11
2.5 Improvement suggestions from earlier works	12
2.6 Collision Mechanics	16
2.7 Different solution alternatives on hand	16
2.7.1 Skidcar System	16
2.7.2 Water cannon	17
2.7.3 Kick plate	17
2.7.4 PIT manoeuvre	18
2.7.5 Simulator SIM3	18
3 PROBLEM SPACE	19
3.1 Pre-Impact Problem Space	21
3.1.1 Impulse x-Position	24
3.1.2 Impulse Magnitude	25
3.1.3 Impulse Angle	26
3.2 Post-Impact Problem Space	27
3.2.1 PIYR frequency distribution	28
3.2.2 Post-Impact Side Slip Angle	29
3.2.3 PI Side Slip Angle and PI Yaw Rate	30
4 EVALUATION CRITERIA	33
4.1 Interview	33
4.2 Characteristics	34
4.3 Implementation of criteria in evaluation matrix	36

5	COLLISION MODEL	37
5.1	Momentum method	37
5.1.1	Four-DOF vehicle model	37
5.1.2	Matrix method based on momentum-conservation	39
5.1.3	Critical parameters	40
5.2	Proposed collision model and validation	43
5.2.1	Proposed collision model	43
5.2.2	Collision model validation	44
5.3	GIDAS verification	45
5.3.1	Verification method	45
5.3.2	Representative verification examples	46
5.3.3	Summary of example cases	50
6	RIG CANDIDATES	53
6.1	Skidcar System	54
6.2	Water cannon	56
6.3	Kick plate	58
6.3.1	Parameters	58
6.3.2	Limitation analysis	59
6.3.3	Kick plate strategy	61
6.3.4	Simulation result	61
6.4	PIT manoeuvre	63
6.4.1	Limitation	64
6.4.2	Simulation result	64
6.5	Built-in actuators	68
6.5.1	Vehicle dynamic analysis and phase portrait	68
6.5.2	Actuator and friction sensitivity analysis	70
6.5.3	Actuator strategy analysis	73
6.5.4	Built-in actuator capability	75
6.6	Simulator SIM4	76
6.6.1	Limitation	77
6.6.2	Advantages	80
6.6.3	Disadvantages	80
7	RESULTS	81
7.1	Objective evaluation	81
7.1.1	Rig capabilities on Problem Space	81
7.1.2	Ten representative cases	89
7.2	Subjective evaluation	98
7.2.1	Ranked characteristics	98
7.2.2	Performance Matrix	99
7.2.3	Brief feedback from interview	101
8	CONCLUSIONS	103
9	FUTURE WORK	105
10	REFERENCES	107

APPENDIX A. NOTATIONS	109
APPENDIX B. ASSUMPTIONS INFLUENCE	115
APPENDIX C. FILTERS	119
APPENDIX D. PROBLEM SPACE, CONT.	123
APPENDIX E. INTERVIEW QUESTIONER	129
APPENDIX F. COLLISION MODEL	130
APPENDIX G. RESULTS, CONT.	132
APPENDIX H. OTHER 6 GIDAS VERIFICATION CASES	138
APPENDIX I: OTHER 7 REPRODUCED CASES	139

Preface

In this preface a brief account of how this thesis came about, the universities involved and the people that stands behind this project are presented.

The present work is part of the Post-Impact Control project that handles collision mitigation and avoidance in multiple collision accidents. The department of Vehicle Dynamics & Active Safety at Volvo Cars Corporation and Vehicle Safety division at Chalmers University of Technology have held this thesis during autumn 2010 and spring 2011.

Two students are working together from two Swedish universities; Chalmers University of Technology at Gothenburg and KTH Royal Institute of Technology at Stockholm. Yujiao Song from the Systems, Control and Mechatronics program and Javier Beltran from the Mechanical Engineering program, respectively.

Following the earlier work done by our supervisor MSc. Derong Yang, from Chalmers University of Technology - department of Applied Mechanics, have this present thesis been based on.

Herein, we would like to thank to our supervisor Derong Yang, our examiner Professor Bengt Jacobson, both at Chalmers University for the endless support and guidance during the thesis, and thank our mentors at Volvo Cars Corporation PhD. Mats Jonasson and our co-examiner at KTH Associate Professor Lars Drugge for their valuable feedback and support. Grateful thanks and appreciation to all these people for giving us the possibility to carry out this thesis.

We want to express our gratitude to Jianbo Lu, Wolfgang Ferlitz, Fredrik Bruzelius, Martin Fischer and Curt Cedergren who provided valuable information and ideas about the rig candidates.

Javier Beltran wants to thanks: my family and teachers that has supported me over the years, especially to my mother Arch. Visnhia Gutierrez for her unconditional love.

"The science is equally important as the art of knowing how to explain it"

Gothenburg April 2011

Javier Beltran

Yujiao Song

1 Introduction

In this chapter a brief introduction to the topics that will be handled in the thesis, the meaning of the project, objectives to reach and the delimitations of the project, are presented. Reading this chapter aims to determine the questions that are attempted to be answered and the problems that comes along the study.

1.1 Background

1.1.1 Volvo profile

In the safety progress among car manufacturers Volvo Car Corporation leads the stipulations of safety requirements worldwide, holding a safety profile alongside the social stakeholders, further have VCC formulated its own "Zero Vision" implying that no one will suffer a fatality or injury in a new Volvo car by 2020 and a long term vision is to create cars that can not crash at all. For that reason have several strategies been performed in order to fulfil these goals (Volvo Cars Corporation, 2009).

1.1.2 Vehicle collisions

One task in the "safe car" development is to study the harmful environment, at which the injuries are produced, i.e. the collisions in the real world from statistical databases. In order to scrutinize these accidents it is necessary to filter the relevant accident cases by the types of accidents that are intended to be handled in the studied safety function.

One classification regards the number of collisions suffered in the traffic accident. In a single event collision the car experience a first and only collision, and thereafter no more harmful events (such as collisions) neither with other cars nor obstacles. At the other hand Multiple Event Accidents, MEA, involves more than one harmful event in the accident sequence.

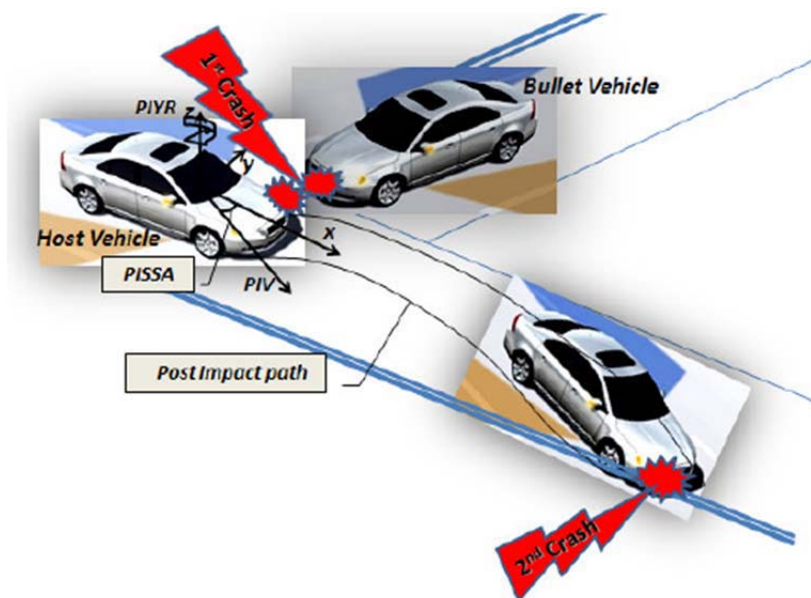


Figure 1.1. Multi impact event collision. <Source: (Yang, 2009)>

Only cars in a MEA where the first event is a collision will be handled, referred in the future as "host vehicle". The other vehicle in the collision, triggering the instability, will be referred as "bullet vehicle", see Figure 1.1. The focus will stay on the "host vehicle" if nothing else is said.

In a MEA the first collision might not be severe for the host vehicle but destabilizes it and drags it into a second event that might be of more serious character. The second event is denominated as a PI event. This accident type forms part of the accident statistics and represents a great number of accidents that have the potential to be mitigated and even avoided. As seen in Chapter 2.1 Accident statistics.

The collisions events develop through the time in sections where the dynamic conditions evolve from an original state until a final state. In Figure 1.2 the actions taken until the first collision are evolving in four steps. At the collision the PIC functions will be activated and prepared to operate in the fifth step where, provided right conditions, it prevents and mitigates the negative effects of subsequent collisions. The PIC function is intended to do so for all the collision events, but in this thesis is just the first collision the most interesting.

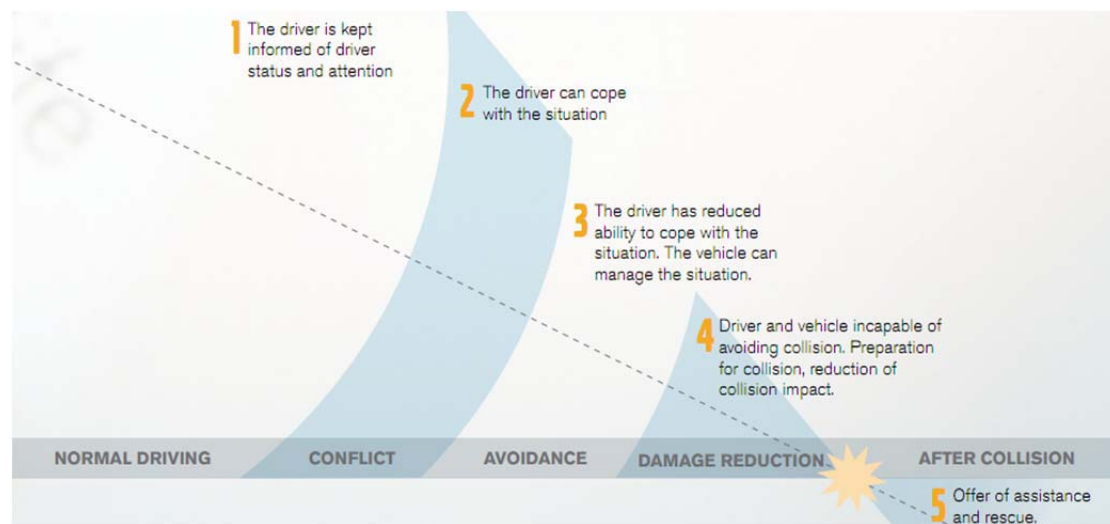


Figure 1.2. Collision time sections: Pre-Impact, Impact or collision, Post-Impact. <Source: (Volvo Cars Corporation, 2009)>

In this time line the most critical time phases are shown. Additionally between the fourth and fifth phase here there is a very short time segment, the collision time. More about this time line will be explained later in Chapter 2.2 PIC Collision scenarios.

1.1.3 Safety systems

The different safety systems are intended to act in different forms and at specific time segments, making two main categories: by physiology or by time segments.

- By physiology there are Active Safety systems and Passive Safety systems, these subcategories are intended to enclose the safety functions by the operation process. The passive safety systems are called so because they do not participate in taking actions or giving feedback to the driver. On the other hand the active safety systems can, and are targeted to, interact with the driver

and even take actions by themselves in order to improve the stability and restraining risky driving.

- By time segment there are Primary Safety systems and Secondary Safety systems. The primary systems act before the collision taking measures to reduce the effects of an anticipated collision during the pre-impact time segment. The secondary systems aim to reduce the effects of an ongoing accident, protecting the driver at the cabin during the collision and during post-impact time segment. Notorious are the simple seat belts, air bags and deformation zones improving the "survivability".

The primary safety systems have been taking more place in the modern vehicle industry the last twenty years due to technology development and method development, noteworthy functions are Anti-lock Brake System (ABS) and Electronic Stability Control (ESC) both being European legal requirements since 2005 and 2011 respectively for new cars. Surplus there are numerous functions that produce warnings intended to alert the driver of a risky driving, as Lane Departure Warning System, LDWS, and Seat Belts Warning Systems by dash light or buzz.

1.1.4 PIC

Post Impact Control or abbreviated PIC targets the instability generated by a bullet vehicle, attempting to either brake to stop or stabilize the host vehicle before a second collision occurs. The ultimate goal of the PIC system is to reduce or avoid further injury to the driver by consequent collisions in the post-impact time section. PIC system is an Active Safety system and Secondary Safety system, according to the previous categories. More information about this in Chapter 1.1.4 Post Impact Control.

1.2 Objectives

The main objective is to propose a verification method capable to reproduce the instable motion at the PI time point; this means that mainly the driver interaction and the vehicle motion actuation can be verified, but not the detection and characterization of the first impact. The verification method has to destabilize the host vehicle according to a safe and controlled method, allowing a scientific approach to the human response.

In Table 1.1 below there are two sets of data, the upper is data from a PIC-relevant accident, and the lower is data of what the destabilization rig is intended to replicate showing no constrains in the pre impact problem space. In other words, the way of producing this motion is not vital, but to obtain the PI states at command.

Table 1.1. Data from an accident example highlighting the key Post-Impact states¹.

(Time pt.) State	Time [s]	Impulse [Ns]	X [m]	Y [m]	V [km/h]	β [deg]	ψ [deg]	$\frac{\omega_z}{s}$ [$\frac{deg}{s}$]
(1) Original	0	-	0	0	40	0	0	0
(2) Pre-Impact	0.1	0	1.1	0	40	0	0	0
(3) Post-Impact	0.3	6000	3.1	0.6	34	5.7	12	91
(4) Second C.	1.1	-	11	5.3	8.2	17	67	44

Replicate

(Time pt.) State	Time [s]	Impulse [Ns]	X [m]	Y [m]	V [km/h]	β [deg]	ψ [deg]	$\frac{\omega_z}{s}$ [$\frac{deg}{s}$]
(1) Original	?	?	?	?	?	?	?	?
(2) Pre-Impact	?	?	?	?	?	?	?	?
(3) Post-Impact	0.3	?	3.1	0.6	34	5.7	12	91
(4) Second C.	1.1	-	11	5.3	8.2	17	67	44

Simultaneously it is essential to map the requested states from a real accident database, searching after which motions are most likely to happen. Then the requirements of the destabilizing method can be set, this can also be seen as quantifying the problem space to focus the efforts in the most frequent motion types. Here the wording “Problem Space” refers to the real world data set of pre-impact and post-impact variables; the Pre-Impact Problem Space describes the properties of destabilization action, and Post-Impact Problem Space describes the resulting destabilized state. Meeting the problem space with simulated models will serve as an objective criterion. Beside this objective criterion, there are some practical criteria that have to be analysed in order to suggest the most proper method. This subjective criteria as: driver safety, repeatability, investments, etc for each rig or method will be explained in Chapter 4 Evaluation Criteria.

Objectives in list form:

- Present information of motion states from a real accident database study
- Synthesise information about ideas, reflections and advices
- Establish subjective evaluation criteria in a ranked list of importance
- Present physical and physiological information about the possible candidates
- Evaluation of each candidate:
 - in practical advantages and drawbacks (Subjective)
 - in a simulation environment (Objective)
- Brief description of verification method(s) for foremost candidate(s).

¹ Time and Impulse are specified as the integral over earlier time intervals, and not the instant state.

1.3 Method

Following methodology is planned to commit the objectives.

- Literature review of earlier thesis related to the topic.
- Survey of candidates and their characteristics by searching information in published papers, homepages at internet and by contacting the manufacturers.
- Brief survey of internal interests through an interview in the safety related departments at VCC.
- An extent model simulation study carried out in Matlab/Simulink.
- Quantify the characteristics of each candidate by analysis of results.
- Select the foremost candidate(s) based on objective and subjective criteria.

1.4 Delimitations

This chapter handles about the limitations of the thesis scope, this assumptions and simplification are made for two main reasons, one, in order to fulfil the time plan, and two, in order to fill gaps in the available information sources.

Verification scope

As mentioned before the verification method aimed for this work does not intended to cover the detection and characterisation of the first impact; however during the thesis, the feedback gathered claims that this possibility is highly advantageous as criteria and will enter into account at the final evaluation among the most promising candidates, see Chapter 4 Evaluation Criteria and 7.2.2 Performance Matrix.

Accident scope

Principally the accident scope is delimited by the type of collision objects, including only passenger cars, a host vehicle and a bullet vehicle. As stated before is just the first impact of a multiple event accident of interest in the collision analysis. Further is the driver assumed to not being able to react by steering, remaining all four wheels oriented along the longitudinal direction of the vehicle. In the same way the driver is not able to react by braking or by accelerating during the accident analysis.

Impulse properties

The influence of the impulse properties as: the shape, the collision time and the constant impact angle are neglected, more about this will be in 2 Literature review. In some cases there are researches that are made outside these limitations in order to quantify how much the results change with these assumptions, and at Feasibility. See Appendix B. Assumptions influence.

Collision time

The collision time (t_c) used in the present thesis is held in constant 0.2 seconds, due to the earlier utilisation of it by the authors in (Zhou, J. et al., 2008) whose study of collision models will be introduced at Chapter 5 Collision Model.

Simulation model

When using the simulation model some assumptions are made. The environment is completely flat with a constant friction coefficient and no medium around the model. The model has two rigid bodies, the suspended body attached to the unsuspended body along the fixed roll axle. The model simulates the load transfer in lateral direction and longitudinal direction but having only roll dynamics for the suspended mass. Because of PIC function acts using the independent braking at the four wheels the model is not designed to cover the cases when one or more tyres lift from the ground. The horizontal forces at the wheels do not have wheel driving components. See Chapter 5 Collision Model. The 3-DOF bicycle model is used in some cases.

Severity level

The first delimitation that expressively were requested in the first meeting was about discarding the idea of making real collisions, implying high forces and therefore accelerations that may result in injuries to the test driver and or the test equipment. This requested norm is evaluated and form part of Chapter 4 Evaluation Criteria. The maximum impulse threshold is set to a maximum magnitude explained in Appendix C. Filters.

Safety systems

In the present thesis there are no studies of how the safety systems and procedures for the test method should be implemented, assuming all candidates have at least roll cage, six point belt, HANS device, air bags, etc. It is important to clarify that these safety upgrades will have some implications in the suggested solutions capabilities regarding the increment in the vehicle mass and inertia.

Data gaps and error in GIDAS database

The GIDAS accident is more extendedly introduced at 2 Literature review and 3 Problem Space but here it is important to make clear that this data have some gaps from a vehicle dynamics point of view. The lack of essential variables; as the vehicle side slip angle, collision time and others that are absolutely vital but near to impossible to gather from real accidents due to practical and legal reasons, which affects the precision of the study. The variables: Impulse, yaw angle, attitude angle and collision time are calculated with help of six assumptions. The mentioned database is also imperfect due to the presence of zero data instead of the established code for unknown data. More about the filtering of errors and unknowns is explained in Appendix C. Filters.

Limited presentation of results

The information from GIDAS database and simulation are a huge amount of variables with trends of high complexity, the presentation and evaluation of them will be focused on just some key variables that are relevant to the rig design.

For simplicity reasons the materials about parameter calculations, simulation models used, statistical data management programs, 3D figures, etc. will be available at (Beltran J. & Song Y.) for the more interested reader.

2 Literature review

A short recommendation before continuing reading the present work is to read the Appendix A. Notations, this in order to be familiarized to the topic basic terms and notations. Beside that a basic knowledge of the vehicle engineering and vehicle industry terms are needed for a complete understanding of the thesis. Consulting the following chapters will be of advantage;

2.1. *Basic Vehicle Dynamics*, in *The Efficiency of Electronic Stability Control*, (Thor, 2007).

1. *Introduction*, in *Vehicle Stability Control for Side Collision by Brake and Steering Wheel Torque Superposition*, (Petersson & Tidholm, 2007).

2.1 Accident statistics

The number of accidents per vehicle and per kilometre travelled has decreased the last three decades with the constant improvement of traffic rules, better road planning, public awareness, and technology development; despite this fact the total number of fatal crashes are still in a constant number due to the increased vehicle usage. As seen in Figure 2.1 from NHTSA-2004 study (NHTSA, 2004).

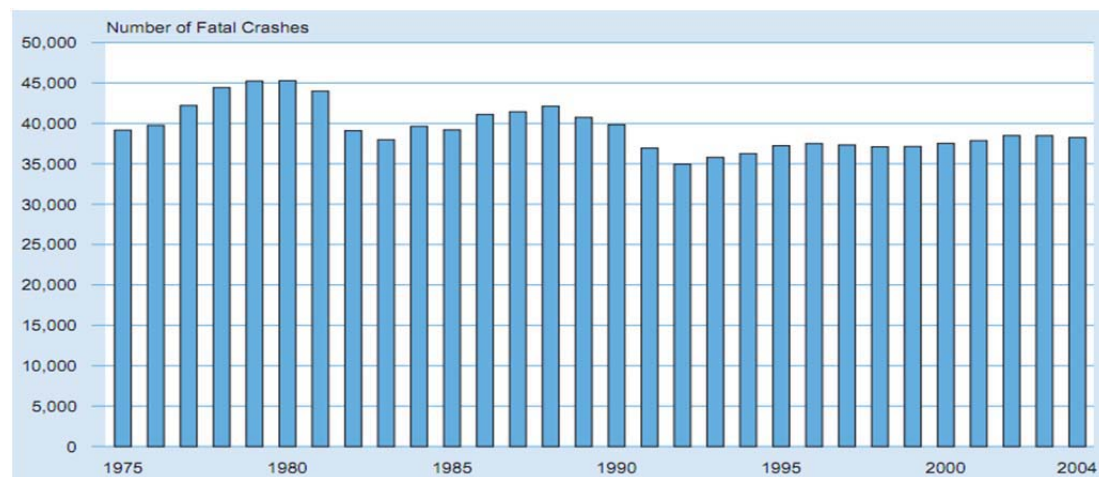
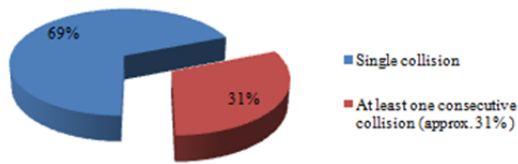


Figure 2.1. Fatal crashes per year during period 1975-2004. <Source: (NHTSA, 2004)>

Where passenger cars represent almost 57 % of the 11 million vehicles involved in motor vehicle crashes, together with Light trucks forms nearly 95 % share.

The statistical study NASS-CDS during period 1988-2004 at United States claims that about 2.9 million light passenger vehicles are involved in tow-away crashes annually. Of these vehicles approximately 31 % have at least one consecutive collision event (Zhou, J. et al., 2008). The following accident studies showed similar results: CCIS 1992-2000 at United Kingdom, GIDAS 1996-2000 at Germany and MHH 1996-2000 at Germany (Yang, 2009). About 33 % of all accident cases involving severe injuries consist of multi-impact events (Langwieder, K. et al., 1999). See Figure 2.2.

Light passenger vehicle involved in tow-away crashes/ year (1988-2004)



Accident cases involving severe injuries/year (1996-2000)

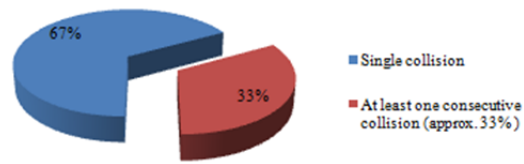


Figure 2.2. Share of multi event accidents from accident databases.

The study of the PISC relevant cases in "Method for Benefit Prediction of Passenger Car Post Impact Stability Control" (Yang, 2009) handle the GIDAS database where applying a number of filters to the entire accident database. For the present work two filters will be released enabling PIB relevant cases as well, more about the filters used in Appendix C. Filters.

2.2 PIC Collision scenarios

The time space develops through time frames and sections where the dynamic conditions evolve from an original stable state until a final unstable state. Below in Figure 2.3 it is shown in another representation how the collision develops through four time points, the time frames at each side of the collision frame between time point (2) and (3) forms the time sections: Pre-Impact time section before the collision and Post-Impact time section after the collision.

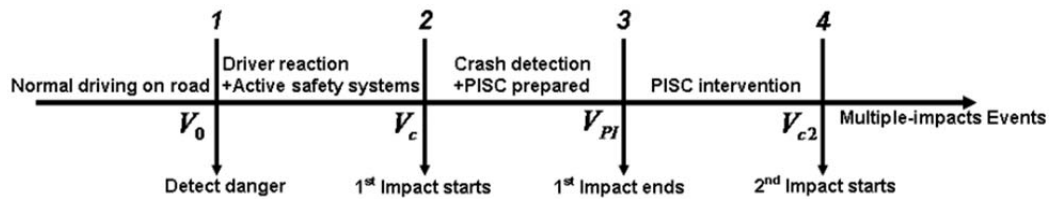


Figure 2.3. Time line of the first collision in a multi impact event collision. <Source: (Yang, 2009)>

Firstly is the driver of the host car driving in a normal and desired way, undisturbed at an original velocity, V_0 , unaware that a collision is near to happen. If the host car have detection systems and/or the driver detects the danger of an possible crash, in (1), the active safety systems and/or the driver takes measures provided enough time for that, until the Collision time section begins in (2) (Coelingh, 2005).

After the probable detection and possible reaction will the first collision begin at the second time point (2) at a collision speed V_c where the induced forces destabilize the host car until the forces ends at time point (3). Time point (3) is the most important time point for this thesis because the intention of the verification method is to replicate this motion state of the host vehicle. This means that the truly essential for the test rig is to generate the same Post Impact states as the statistical data suggest, making it possible then to study the benefit of PIC system in a test environment. From the PI states and the posterior time sections are the safety functions intended to act synchronized in benefit of the driver.

An example will be helpful to visualize the type of motion that is targeted. For instance imagine that a normal passenger car crosses an urban intersection at a modest speed of 40 [km/h], suddenly of unknown reason, another vehicle hits you from the right side at a low speed but far ahead of the centre of gravity producing a certain lateral acceleration and yaw acceleration, see Figure 2.4.

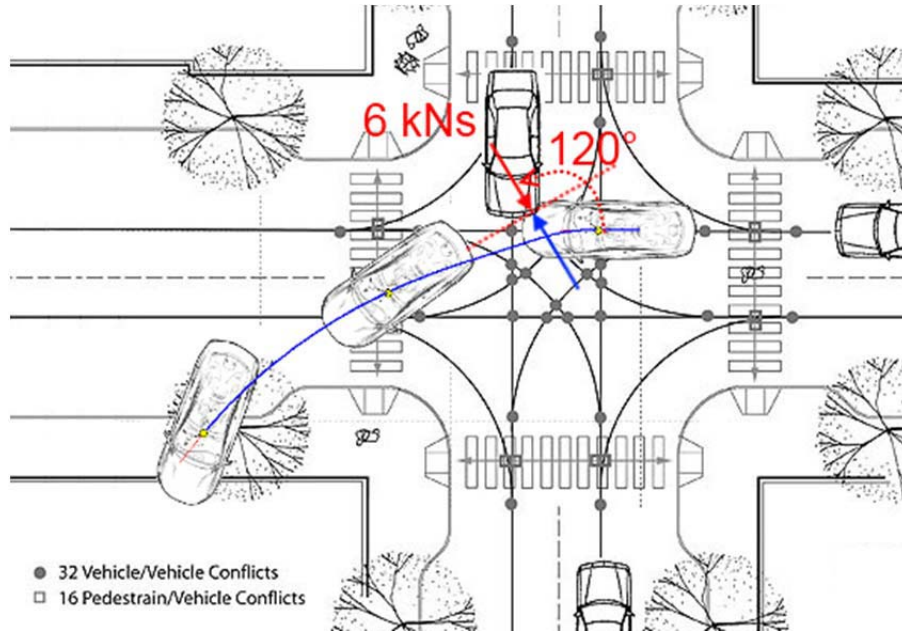


Figure 2.4. Intersection example. <Source background: (ITE, 2010)>

The host vehicle and driver do not suffer significant damage at this point, most surprise and disorientation due to air bag deployment and loud noise. Besides that is the change of direction during the impact 12 [deg] in just 0.2 [s], unlucky the car follows a path directed to the other side of the street, as seen in Figure 2.4. The object of the second collision could be a concrete wall, a tree or other object that will stop the car in a very short collision time. In the example the wall is located 6 meters at the left of the original path and 10 meters from the collision place. See data in Table 2.1.

Table 2.1. Motion data from the intersection example in Figure 2.4.

(Time pt.) State	Time [s]	Impulse [Ns]	X [m]	Y [m]	V [km/h]	β [deg]	ψ [deg]	ω_z [$\frac{deg}{s}$]
(1) Original	0	-	0	0	40	0	0	0
(2) Pre-Impact	0.1	0	1.1	0	40	0	0	0
(3) Post-Impact	0.3	6000	3.1	0.6	34	5.7	12	91
(4) Second C.	1.1	-	11	5.3	8.2	17	67	44

The first collision is not a very dangerous event for the driver and passengers (provided seat belts) but without any steering and/or braking intervention the host vehicle will collide with an side object, that will brake the car in a very short time if stiff enough. The pattern of the example is unfortunately very common among the PIC-relevant cases, as shown in the Table 2.2 forming 10 percent of the chromosome cases from the previous study, (Yang, 2009).

Table 2.2. Chromosomes of PIC relevant cases. <Source: (Yang, 2009)>

Chromosome Group No.	Key Characteristics					Car amount {frequency, N=944}
	PIYR [deg/s]	PIV [km/h]	Impact Area	Road Type	Road Layout	
1	≥ 150	21-60	Side	Urban road	Intersection	38 (4%)
2	0-150	21-60	Side	Urban road	Intersection	98 (10.4%)
3	0-150	21-60	Side	Country road	Continuous road	34 (3.6%)
4	0-150	21-60	Side	Country road	Intersection	37 (3.9%)
5	0-150	21-60	Front	Urban road	Intersection	37 (3.9%)
6	0-150	21-60	Front	Country road	Continuous road	42 (4.5%)
7	0-150	61-120	Front	Country road	Continuous road	42 (4.5%)
8	0-150	61-120	Front	motorway	Continuous road	42 (4.5%)
9	0-150	61-120	Side	Country road	Continuous road	33 (3.5%)
10	0-150	21-60	Rear	Any	Any	31 (3.3%)
11	0-150	61-120	Rear	Any	Any	36 (3.8%)
12	≥ 150	21-60	Front	Any	any	32 (3.4%)
13	≥ 150	61-120	Any	Any	Continuous road (mostly straight)	29 (3.1%)
14	0-150	21-60	Front	Country road	Intersection	29 (3.1%)

2.3 Post Impact Control

During the PI time section the Post Impact Control function (PIC) reacts and tries to mitigate the following collision either by braking to stop (PIB) or by stabilizing the car with the potential of totally avoiding it (PISC).

This function will probably reside in the Brake or Vehicle Dynamics control system where it can operate directly at the four wheels. Information from air bag system might be required to trigger the function, and other vehicle dynamics behaviour should be in synchronicity with ABS, ESC, etc.

As described earlier the driver reaction defines the input to the crash scenario in form of braking or steering but because the time section between crashes is very short the reliability of human response is deficient, additionally can other factors degrade the reaction as surprise, panic, airbag deployment, or simply because of not many people have the experience of regaining vehicle stability after a car collision.

Further some aspects as the integrity of the steering system, detection of traffic situation and road layout are needed to be taken into account in order to avoid non desirable interventions by the function.

More information of how the function operates and about the stability criteria for it is explained in the MSc thesis (Yang, 2009).

2.4 Earlier simulation models in accident scenarios

In the area of accident analysis there is a great number of texts, among them there are some studies done analysing ESC, (Thor, 2007). In this thesis study have light accidents been simulated using a veDYNA environment, which have a vast possibilities to combine different models and solvers. The goal was to identify the added benefit with ESC activated and the added benefit with a skilled driver behind the steer wheel. The study revealed that the added benefit increase with higher initial host speed. In both the presence and absence of driver model, and as well ESC on/off, the study shows that the higher the host vehicle is travelling the higher destabilisation is induced.

The variable study, in order to visualize the instability threshold, consisted of a range of impulse magnitudes and a range of impulse x-positions, from 500 [Ns] to 5000 [Ns] and between 2 [m] ahead and 3 [m] behind of CoG, respectively.

The impact angle remained perpendicular to the length of the vehicle during all the cases resulting in three sets of data, one for each original velocity of the ESC-host vehicle. In Figure 2.5 it is shown "where" in the problem space the host car passed the stability criteria, represented with squares and dots. The squares were achieved with the ESC both On and Off, the dots just for the cases where the host car has the ESC On marking the added benefit. In the cases marked with crosses the stability criteria of the study were not reached for ESC On or ESC Off.

Because the vehicles usually has less turning stability at higher speeds, behaving understeer or oversteer, it is common sense that the cars are even less stable with a induced turn force at higher speeds.

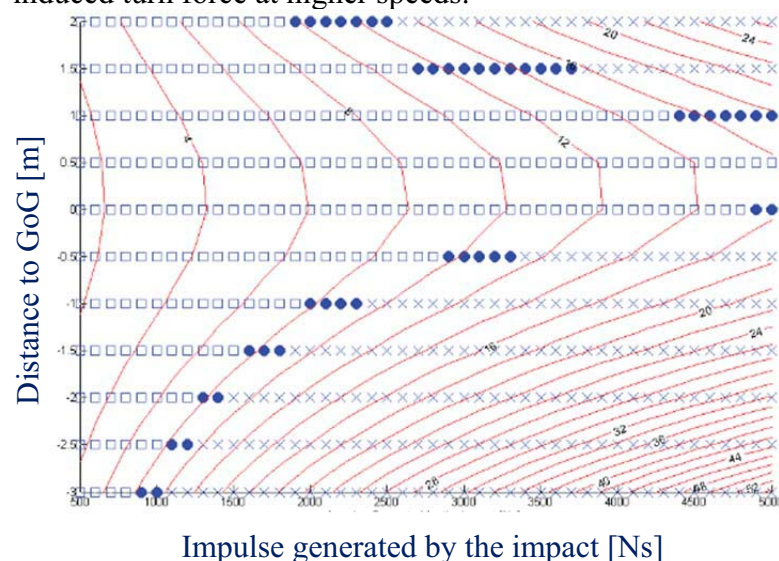


Figure 2.5. ESC added benefit batch plot for the original speed of 100 [km/h] and an active driver, the topographic curves represent the bullet vehicles speed. <Source: (Thor, 2007)>

In the study of A. Andersson about ESC, *Implementation, validation and evaluation of an ESC system during a side impact using an advanced driving simulator*, (Anderson, 2009) is the human behaviour and response to the activity or inactivity of the ESC function in focus. The Simulator SIM3 in the Swedish National Road and

Transport Research Institute brings a versatile tool for performing test of added functions as ESC, ABS, etc.

Several test persons proved to drive and regain the control of the vehicle in a predefined accident scenario. The result of having the ESC On and Off is showed in following graph, Figure 2.6.

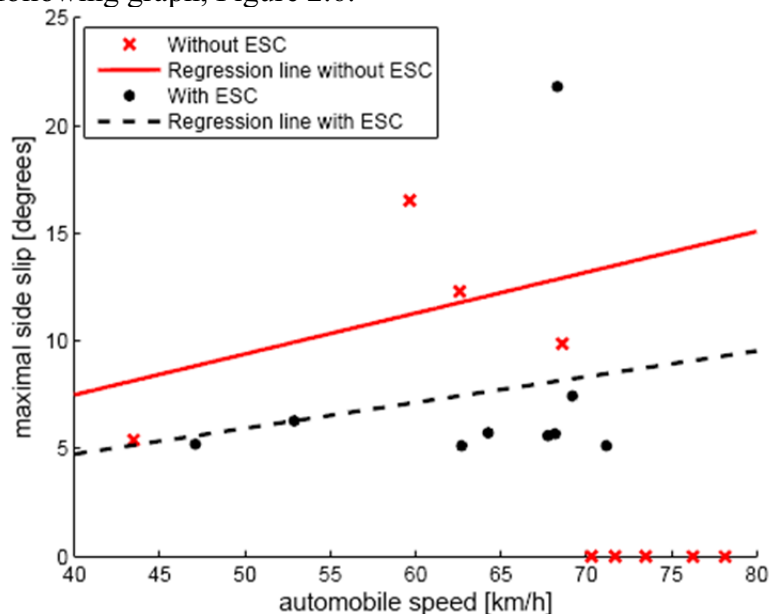


Figure 2.6. Test cases where the ESC On and Off can be distinguished. Drivers that lost control are marked with a maximal side slip at zero. <Source: (Anderson, 2009)>

2.5 Improvement suggestions from earlier works

The recommendations of earlier work can be resumed as follows:

- Better tyre model (Magic formula tyre model block)
- Better vehicle model (more DOF, roll and pitch dynamics)
- Better collision model (impulse shape, impulse fixed coordinates, friction and coefficient of restitution)

The authors concluded that the influences of such improvements are not major for the Post-Impact study setting an acceptance for light collision scenarios. The short time for error growth support this in a moderate yaw rate span.

Nevertheless for the present thesis it is interesting to point where the impulse becomes medium or severe. And if the influences grow far from the reality, at which threshold our models will diverge. Some studies have been done to map this and will be available in Appendix B. Assumptions influence.

The tyre model, as the most influential contact points to the environment plays a major role in the yaw stability and translational path in all the vehicle dynamics simulations. But how much are these differences?

When there are small angles and stable driving situation it is indicated that the simple models and linearization do not affect too much but in the accident space that forces

can appear and disappear suddenly, where neutral steer and stable motion are highly uncommon there is a need of researching more in deep the influence of better models.

For that reason there are numerous of texts that explains the most important characteristics of the tyres that are worth to simulate in the vehicle models, one very complete and therefore challenging text to understand is *Tyre and Vehicle Dynamics* (Pacejka, 2006). In the Chapter of 4.3. *The Magic Formula Tyre Model* it is possible to find the basic information of how the shape of saturation is represented in a mathematical way based on semi-empirical tyre models, Figure 2.7.

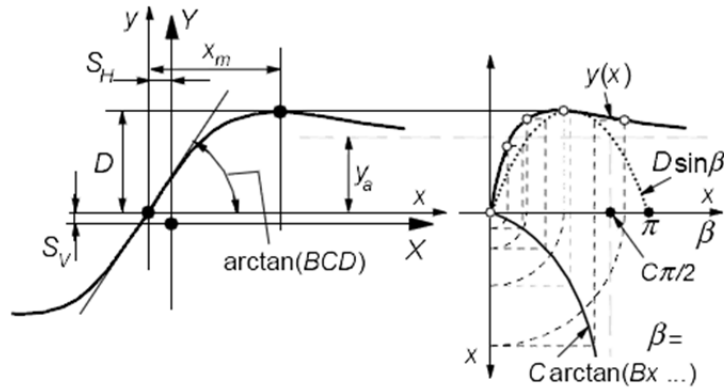


Figure 2.7. Magic Formula using curve parameters that are related to tyre parameters. <Source: (Pacejka, 2006)>

Other important model descriptions of the vehicle as the number of tracks and tyres have as well influence in the vehicle motion. The flat single track model, Figure 2.8, shows to be a common used model form when looking at vehicle dynamics at normal driving, i.e. a safe and controlled motion.

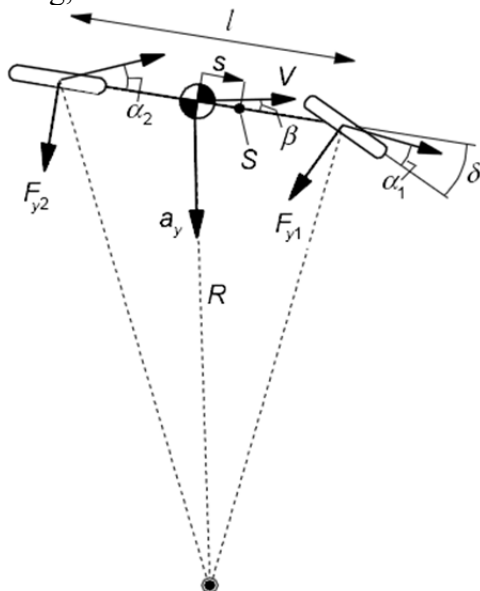


Figure 2.8. Vehicle model showing three degrees of freedom: surge, sway and yaw. <Source: (Pacejka, 2006)>

As mentioned earlier the accident scenario have to deal with a more aggressive driving dynamics than that, therefore it is of interest of this study to look in to the differences of using a more complex model, Figure 2.9.

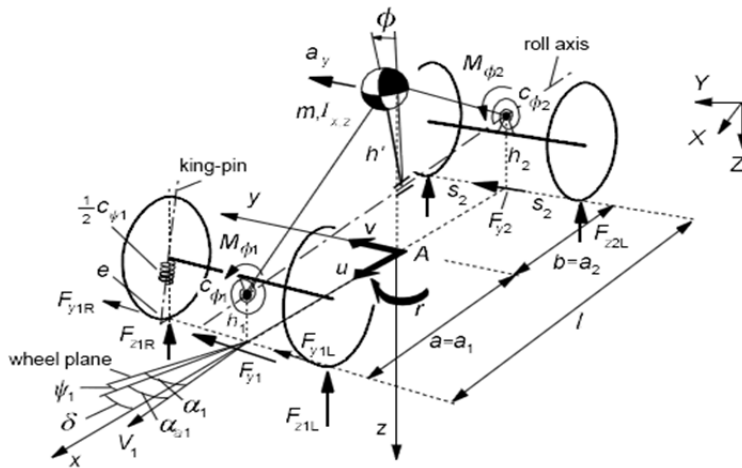


Figure 2.9. Vehicle model showing four degrees of freedom: surge, sway, yaw and roll around the roll axle. <Source: (Pacejka, 2006)>

This expansion in the car's y-coordinate and z-coordinate is beneficial when major load transfer and impulses that are far away from the roll axle. At the same time a fourth degree of freedom represents an improvement when analysing the reaction of a combination of mass bodies as a group instead as a rigid block, which have definitely influences in the behaviour.

The impulse model is at the most a car coordinate fixed force anchored in a certain location generating a translational and a rotational impulse. The impact force that triggers the instability has a number of parameters that governs the interaction with the vehicle body.

In the study of M. Thor (Thor, 2007), the shape on the impact is represented in two forms, a squared and a triangular. The impact, that starts at time point 2 and lasts until time point 3 from the 1 Introduction Chapter, and its shape have the same impulse if the integral area under it encloses the same amount. This means that the duration time and or the maximum force can vary during the collision but having the same impulse, this may affect the post impact states of the vehicles motion, however the influence may be limited and the principal researching goal is to replicate the post impact states of the vehicle at this point. In (Thor, 2007) two impulse shape have been studied resulting in a similar yaw rate, see Figure 2.10 and Figure 2.11.

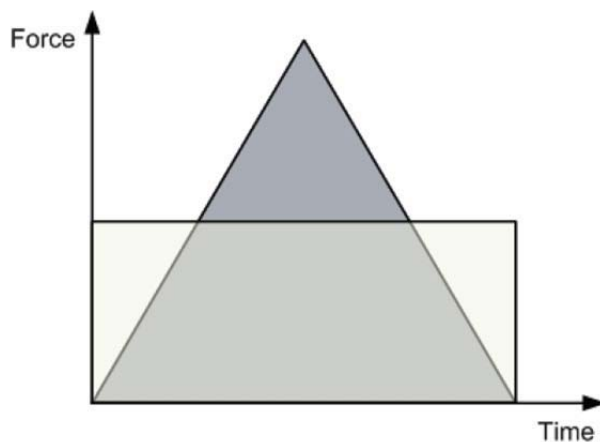


Figure 2.10. Two impact shapes, squared and triangular. <Source: (Thor, 2007)>

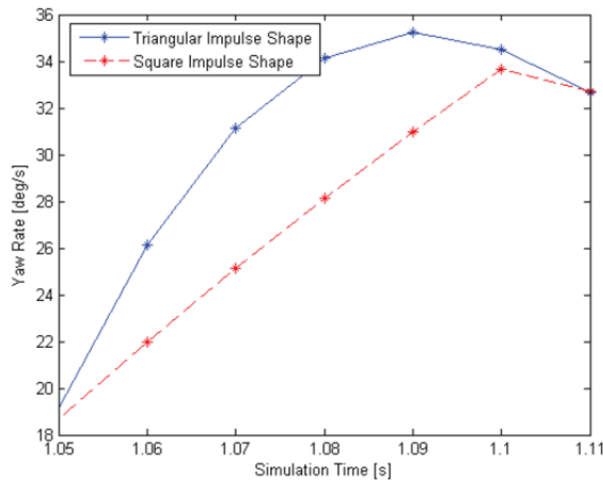


Figure 2.11. Yaw rate response produced by the two impact shapes with the same amount of impulse. <Source: (Thor, 2007)>

In A. Anderson's study there is a suggestion; using a sinusoidal shape shifted to the first half of the impulse, this is said to be the most realistic shape, see Figure 2.12. A brief study about the impulse shape is done and the results are presented in Appendix B. Assumptions influence.

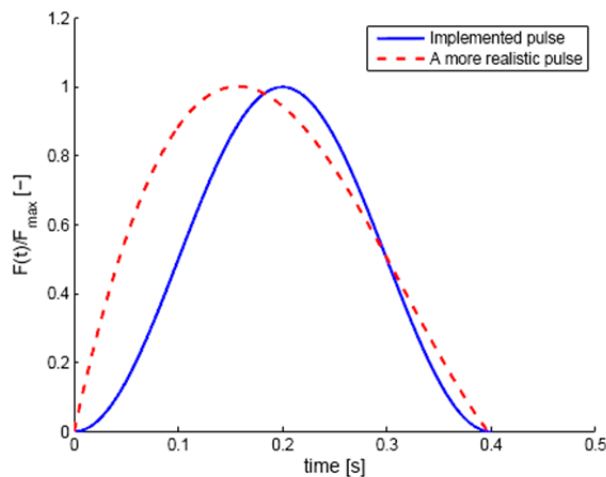


Figure 2.12. Two impact shapes, a realistic one and a sinusoidal one. <Source: (Anderson, 2009)>

In both reports, (Thor, 2007) and (Anderson, 2009), the authors recommends the use of realistic shapes in accident simulations, however, the present thesis main goal is to reproduce the post impact states at the moment the impulse ends in a safe and controlled way. Therefore the shape used is mostly squared, additionally the duration of the impulse can be modelled in order to fulfil the safety criteria and at the same time reach higher impulse magnitude without hurting the test driver or damaging the test equipment. A statistical study, among several cars fitted with acceleration pulse recorders, finds an average collision duration against passenger cars to 94.8 [ms] in frontal crashes and to 70.3 [ms] in rear-end crashes, (Trafikverket, 2010). Still the collision time or impact duration is maintained constant through all the work at 200 [ms] or 0.2 [s].

2.6 Collision Mechanics

Collision mechanics is useful in accident reconstruction, vehicle crashworthiness and prediction of PI vehicle dynamics. Light impact, which refer to those collisions that structural deformation is not substantial, could use constant impulse angle and magnitude, specific crash point to describe the collision process (Zhou, J. et al., 2008).

For a real accident, the generated impulse not only contributes to change kinematic states but also to the deformation consumption. An empirical Coefficient of Restitution, CoR, could be used to describe the energy loss through deformation. CoR is a fractional value representing the ratio of speeds after and before collision, which always belong the interval of 0 to 1. For CoR= 0, the two objects are stuck together and consume more energy. An accident with CoR= 1 is called elastic collision, which has less deformation and less energy loss.

Most well-known impact models are built based on the conservation of momentum method, which hides the impact force variation during the collision, since it assumes an infinitely short impact duration time. If assuming the tyre friction can be neglected during the collision and the pitch motion is not critical for the vehicle dynamics, PC-Crash or 3-DOF model is good enough to reconstruct the collision (Cliff & Montgomery, 1996). However, some papers also provided a 4-DOF model with tyre friction included, which is more accurate (Segel, 1956).

2.7 Different solution alternatives on hand

A number of solution alternatives that can be obtained, without new development from scratch, are presented here in a list. The source of the information is gathered by contacting the companies and studying the information available at their homepages. Here is just a brief description of these solutions with their homepage links. The solutions adapted to this work with pictures, description, simulation and results of simulations will be found at the Chapter 6 Rig Candidates.

2.7.1 Skidcar System

The Skidcar System is a driver training solution aimed for training over low friction surfaces or less grip conditions. The customer target are most the law enforcements, security agencies other institutions that have to act correctly under unexpected instability situations. Very easy to adapt and maintain (Skidcar.com, 2011). Figure 2.13 shows the rig dolly wheels sustaining the training vehicle.



Figure 2.13. Mounted Skidcar System under vehicle. <Source:(Skidcar.com, 2011)>

2.7.2 Water cannon

The Water cannon is equipment developed in the department of Active Safety Research and Advanced Engineering Group at Ford Motor Company at US during 2009. It is designed to replicate the impact of another vehicle slamming the test vehicle from the side without actually crashing another vehicle into it. This diminishes the risk of driver injury (Jalopnik.com, 2009). Figure 2.14 show the implementation of the cannon at the cargo compartment of the test vehicle.



Figure 2.14. Water cannon mounted the test vehicle <Source: (Jalopnik.com, 2009)>

2.7.3 Kick plate

Some test tracks e.g. The Rockingham Motor Speedway, UK, facilities provide a Dynamic Wet Grip Area that is intended for the vehicle manufacturer testing and driver training. The test track consists of three components: a kick plate, water walls and a polished surface.

The Kick plate is a hydraulic powered sliding plate at the ground with the intention of kicking the rear tyres as the vehicle passes over it. When being destabilized the vehicle enters a low friction surface where water walls simulates obstacles and lubricates the skid track. The method is very safe and provides a complete test environment. (rockingham.co.uk, 2011). Figure 2.15 shows the plan view of the training complex at Rockingham.

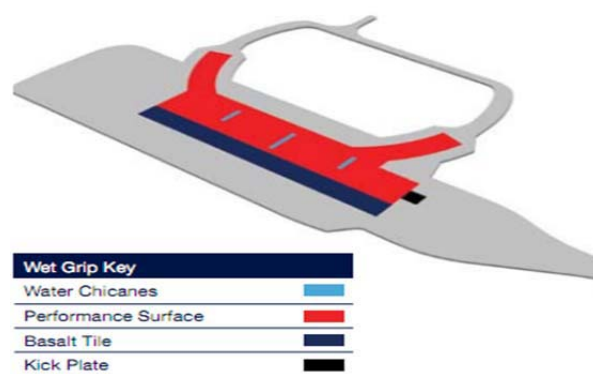


Figure 2.15. The test track components. <Source: (rockingham.co.uk, 2011)>

2.7.4 PIT manoeuvre

The Precision Immobilization Technique or PIT manoeuvre is a destabilization method and not a rig in the same sense of the other alternatives, this method is used by law enforcement in some situations, where the pursued vehicle needs to be stopped efficiently (Zhou, J. et al., 2008). Figure 2.16 shows the principle of a PIT manoeuvre in three steps, Bullet vehicle in blue and host vehicle in red.

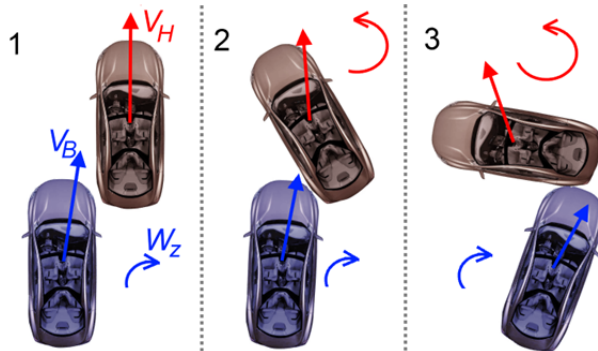


Figure 2.16. PIT manoeuvre principle.

2.7.5 Simulator SIM3

The simulators are used to emulate the driver's interaction with the vehicles by generating acceleration forces that the test person will feel when "driving" in a virtual environment. This type of simulator has a broad range of applications in studies of human-machine interface, road design, vehicle manufactures and safety agencies, Figure 2.17

One example is Simulator SIM3 at the Swedish National Road and Transport Research Institute (VTI) head office in Linköping-Sweden where three independent motion parts, a linear sliding base, a tilting platform and a vibration table provides the accelerations mentioned above. All of these parts supports the interchangeable cabin where the driver sits, looking in synchronized projection screen at the front and three additional screens as rear view mirrors. The outstanding safety and high reproducibility is vastly appreciated by the vehicle industry (VTI, 2011). Figure 2.17 shows the driver at the cabin mounted on the Simulator SIM3.



Figure 2.17. Simulator SIM3's human interface. <Source: (VTI, 2011)>

3 Problem Space

The overall problem, that vehicles are opposed to secondary events, can be described using several dimensions such as PI speed, PI yaw rate, road friction, distance to road edge, etc. The space spanned by those delimited dimensions is here called Problem Space.

The purpose of the spanned dimensions is to see the "size" and "shape" of the scattered data across it. A data cloud from targeted motion will describe the operational range that the rig alternatives strive to fill with their own data clouds in this problem space. Some patterns and trends are then possible to identify by analyzing the different variable combinations. This trends and patters might be common for real accidents and evaluated rigs.

The statistical motion database is however incomplete and can be completed in some extent by using some assumptions as mentioned earlier in 1.4 Delimitations. The total or partial lacks of variables are then completed with the following approximations:

- [i]. Some accident database cases do not have the crash weight, but have the dry weight of the vehicle available. The dry weight is by definition the weight the vehicle has without passengers, spare tyre, fuel and all necessary consumables (e.g. Motor oil, brake fluids, coolant, etc.) Therefore a simple calculation can approximate this variable in order to "rescue" some data that would be filtered out otherwise later, according to equation (3.1).

$$m_{Crash} = m_{Dry} + m_{Additional} [kg] \quad (3.1)$$

So how much weight should be added to the dry weight?

The manufacturing specifications are commonly based in adding a 75 [kg] driver and all added load being the result a 125+ [kg] of added weight (pistonheads.com, 2010), from dry- to curb- weight. From dry- to crash-weight is then the number of average occupants in accident necessary, this research is not done but assuming the weight of one and a half occupants plus added equipment will result in a reasonable 150 [kg], See equation (3.2).. By doing this, of course neglecting an eventual overload of the vehicle or in the other case overestimating the load of it, it is possible to rescue 30 cases from being filtered later.

$$\begin{aligned} m_{Additional} &= 1.5 \cdot m_{Occupant} + m_{Equipment} [kg] \\ &= 1.5 \cdot 75 + 40 \approx 150 [kg] \end{aligned} \quad (3.2)$$

- [ii]. None of the accident cases have the impulse magnitude for which it is necessary to estimate it using the assumption that the change of linear momentum is enough. In most of studies between crash severity and injury outcome is the impact severity described as the change of linear velocity ΔV , studies made of the magnitude of such errors often indicate standard deviations between 10 % and 15 %. But also a systematic underestimation of between 11 % and 33 % (Trafikverket, 2010).

The impulse magnitude is calculated by the change of the linear momentum, according to equation (3.3), a product of the vehicles scalar mass and the vectorial change of velocity represented in Figure 3.1 with a red vector.

Linear impulse:

$$p = m \cdot \Delta V = m \cdot (v_{PI} - v_c) \quad [Ns] \quad (3.3)$$

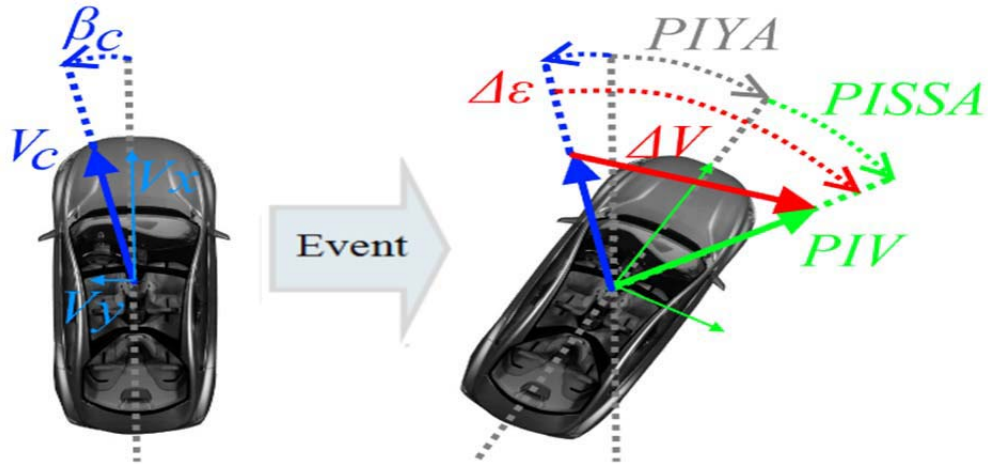


Figure 3.1. PISSA calculation according to (3.3). <Background Source: (uptodatedesign.com, 2008)>

- [iii]. Fixed 0.2 [s] or 200 [ms] for all collisions and calculations if nothing else is said.
- [iv]. The fourth assumption is present in the calculation of the Post-Impact Yaw Angle, PIYA. Because the original GIDAS database has not this variable an approximation is calculated by assuming that the Post-Impact Yaw Rate grows constantly during the collision. Therefore the PIYA is the result of a constant PI acceleration acting over the collision time, t_c . Notice the area below the yaw rate growth during the impulse time in Figure 3.2.

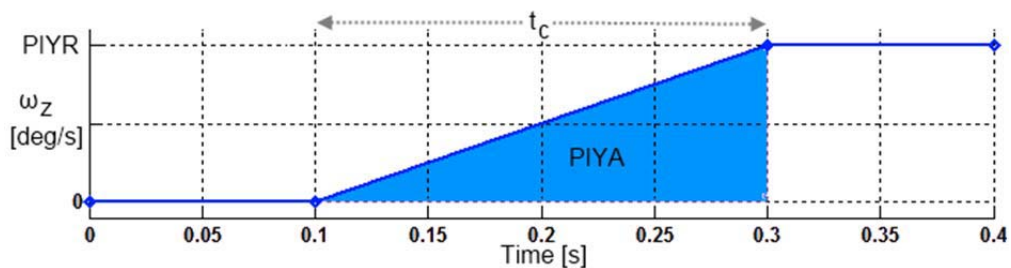


Figure 3.2. Constant yaw rate growth and yaw angle development.

- [v]. Once the PIYA is calculated it is possible to calculate the Post-Impact Side Slip Angle according to equation (3.5). See Figure 3.2.

$$\Delta \epsilon = PIYA + PISSA - \beta_c \quad [deg] \quad (3.4)$$

$$PISSA = \Delta \epsilon - PIYA + \beta_c \quad [deg] \quad (3.5)$$

- [vi]. Further a normalisation of the available data to Volvo S60's parameters is made making it useful for later comparison. Because the GIDAS database is a

study grounded on real traffic accidents in Germany during 1999-2007 and not intended originally to the vehicle dynamics the statistical study use units that are more comprehensive and not the vehicle dynamics academic units.

However it is seen during the study that expressing the velocity and angles in kilometres per hour [km/h] and degrees [deg], respectively, are much more intuitive when looking at plots and tables, for instance expressing 1.57 [rad/s] is the same as 180 [deg/s], and 5.56 [m/s] is the same as 20 [km/h]. Using these units will save time and effort when looking and comprehending the information, at the same time making it more accessible to the reader.

All variables are at the CoG if nothing else is said, and all the calculation are made in SI units, however for the readers effective and effortless understanding they are presented in common daily used units. Velocity units in tables and plots may differ and the writers ask for comprehension; however the colours relate them to each other.

In the following chapters the variables correspond to these time point the chapters are specifying.

3.1 Pre-Impact Problem Space

Despite of the definition regarding time dependent states, pre- impact and impact, the variables in Table 3.1 will be referred as Pre-Impact problem space because the both time segments are before the Post-Impact time point, but it is important to clarify that the impact variables belongs to the collision time interval, see Chapter 2.2 PIC Collision scenarios.

This problem space encloses the relevant information of the accident case by the following variables:

Table 3.1. Variables in Pre-Impact Problem Space, Calculation from data given in GIDAS.

Name		Description	Calculation	Unit
Collided Part	-	Vehicle part that takes the first impact	Given	-
Imp. magnitude	$Imag$	Linear change of momentum	$\frac{\Delta V \cdot m_{GIDAS}}{1000}$, [i]&[ii]	[kNs]
Imp. angle	$Iang$	The angle of the impulse	Given	[deg]
Imp. x-position	$xPos$	x position of the impulse on the vehicle body	$\frac{xPos_{GIDAS} \cdot BX_{S60}}{BX_{GIDAS}}$, [vi]	[m]
Imp. y-position	$yPos$	y position of the impulse on the vehicle body	$\frac{yPos_{GIDAS} \cdot BY_{S60}}{BY_{GIDAS}}$, [vi]	[m]
Original velocity	$V0$	Vehicle velocity before any collision detection	Given	[km/h]

After filtering unknowns and irrational data, see Appendix C. Filters showing the impact location and impact angle of the collision cases is the first step in this statistical study.

The Cartesian area on the vehicle is divided in four parts, N , according to the GIDAS code book. The lateral parts has been additionally been divided into four areas each, making a total of ten small areas. Later, the side parts groups are added in the physical distribution study, making six area groups: Front, Back and four Sides' 1-4 from the front. The groups are shown with six different colours in Figure 3.3 and are quantified in Table 3.2.

Table 3.2. Impact physical distribution, see Figure 3.3.

Physical impact distribution						Cases: 931
Front	Sides				Rear	
412	430				89	
44.3%	46.2%				9.6%	
F	S1	S2	S3	S4	B	
412	158	96	110	66	89	
44.3%	17.0%	10.3%	11.8%	7.1%	9.6%	

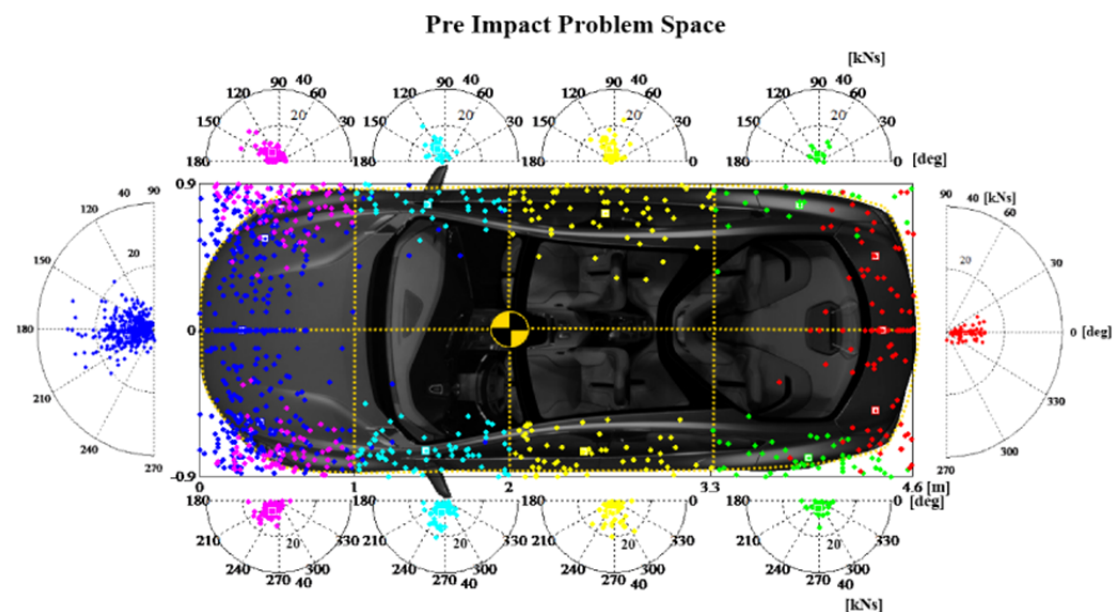


Figure 3.3. Impact physical distribution, top view. <Source background: (uptodatedesign.com, 2008)>

The most notorious trend is that the Front part and the foremost parts of the Sides are more crowded than the rear part. Other noticeable trends are; that the more further in front the higher impulse magnitude, and the further in front the higher impulse angles are generated.

By looking at the Table 1.1 the question "Why these trends are so notorious and what can be concluded from them?" raises.

Well there are two aspects that can partly explain this. For the first the vehicles travels to the front making the front more exposed to the first collision, this because of the objects the collision is made against can have any speed below its own (in that forward direction). At the other end, the objects that will collide from the rear must to have higher speed (than the own forward direction). For a similar reason the vehicles that collides from the sides will have less time to do it if the target vehicle will move faster, as a duck shooter will have less time to aim a moving target.

Table 3.3. Pre-Impact problem space average variables distribution, see Figure 3.3.

Variable		Front ²	Side1	Side2	Side3	Side4	Back	Vehicle
<i>Imag</i> [kNs]	Max	30.0	24	23.3	24	15	13.0	30
	Average	9.0	6.7	8	7.2	4.5	7.0	7.7
	Min	1.2	1.1	1.7	1.9	0.9	1.3	0.9
<i>Iang</i> [deg]	Max	101	180	180	180	180	87.0	180
	Average	180	120	110	100	96	3.7	120
	Min	-90	0	30	0	0	-40.0	0
<i>V0</i> [km/h]	Max	200	150	200	160	150	140	200
	Average	84	69	62	62	76	65	74
	Min	15	15	15	15	15	15	15

Be aware that the average calculation for the Sides in Table 3.3 is based on the mirrored data. The mirrored data means that all dots at the left side are inverted as they have been produced at the right part. Doing this have the advantage that average values become positive and concentrating information, and drawback of wipe away the asymmetry induced by the traffic situation.

However, in overall there in no big improvement in the following tables because the data is spread over the intended plots anyway. So if nothing else is said the data represented in the Tables are based on the "both" sides data. The both sets will be found in (Beltran J. & Song Y.). Knowing at which position intervals, at which angles intervals, and at which magnitude intervals are the most frequent accidents will bring more information on how to prepare for this cases, expecting some outcome at different speeds intervals and therefore at different road layouts. For that reason, the original velocity *V0* will be useful to map-in all variables in pre impact problem space.

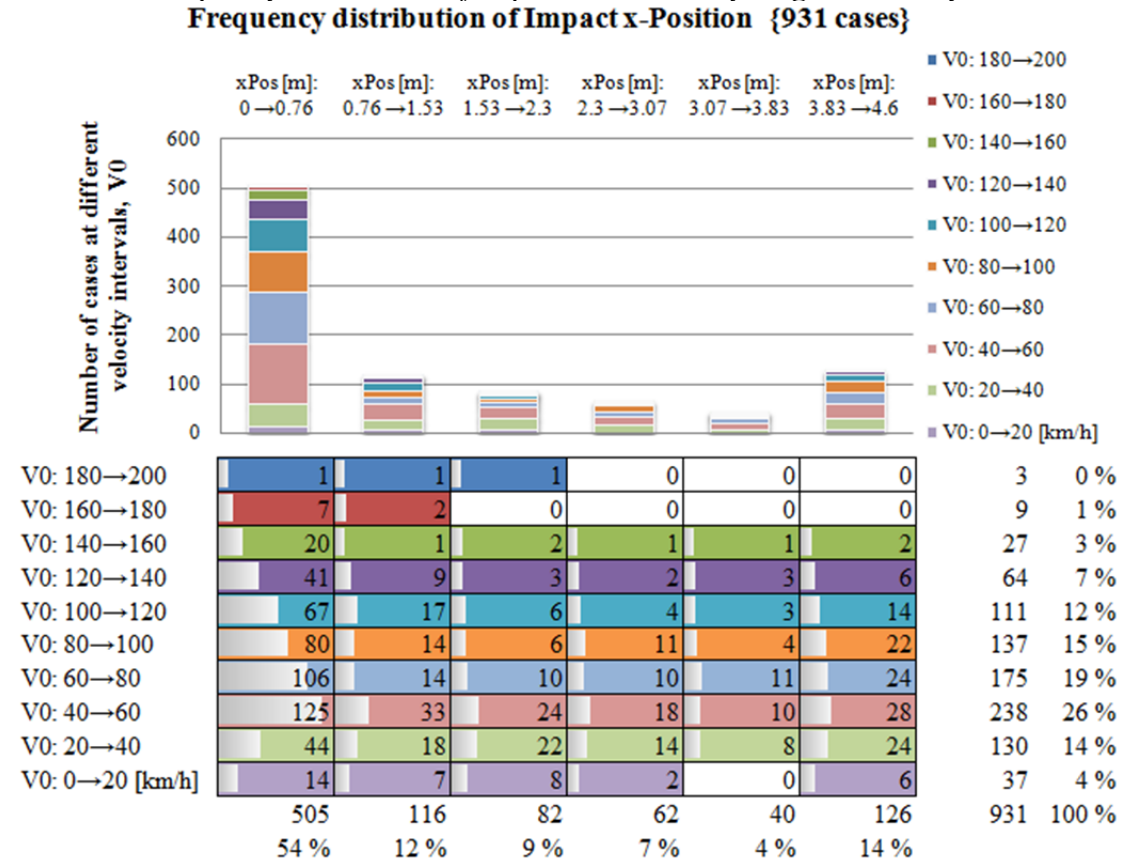
The tables are constructed in a way that the interval counts the cases in between the boundaries including the higher boundary of the interval. In the lowest interval the cases include both the higher boundary and the lower boundary, i.e. The PISSA interval between [-30 0] degrees includes all the cases that have zero degrees and not the cases that have minus thirty degrees, See Table 3.9. This partly explains why the asymmetry of yaw rate shifted to the positive or counterclockwise, other explanation resides in the traffic situation that encourages counterclockwise PI yaw rate.

² The average angle in Front part are calculated based on [0 360] degrees angles and transformed back to [-180 180] degrees.

3.1.1 Impulse x-Position

The first trend suspect that the frequency of collision cases decreases as the impact x-position goes further back. Dividing the x-length of the normalized vehicle in six equal sections and counting the number of cases that are inside the interval boundaries will result in Table 3.4.

Table 3.4. Frequency distribution of impact x-Position by original velocity.



The column bars are the representation of stacked cases that have been counted at different velocity intervals, and corresponds to an own x-Position interval, for instance it is easy to identify the most crowded velocity row, the pink one with 26 % of all cases. All these 238 cases have different x-Position were the most numerous corresponds to the interval between 0 [m] to 0.76 [m] of the first column. This column groups 54 % of all cases at the foremost sixth of the car.

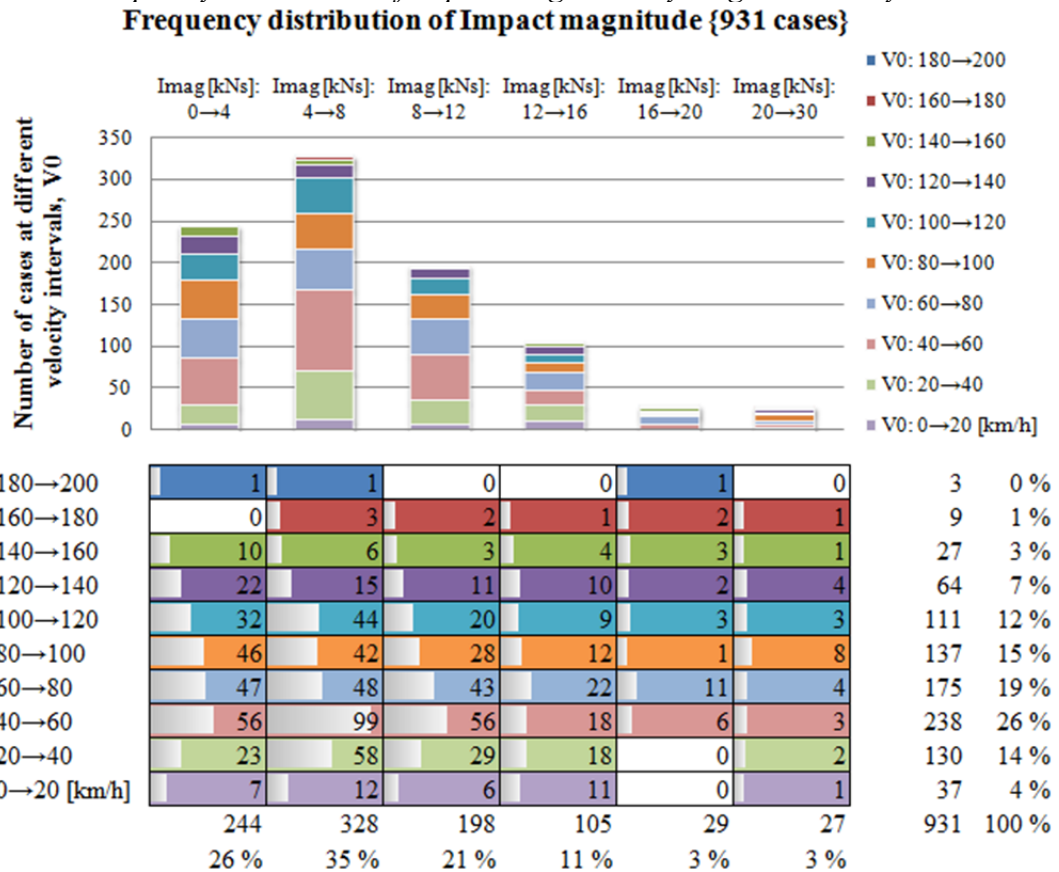
Because the total number of cases in each velocity interval (at the right of Table 3.4) are not the same it is not possible to compare directly the frequency of the interval cases but is instead useful to see the frequency normalized to the total number of cases at each velocity interval, with reservation for the speed intervals with spare cases. These normalized charts will be found in (Beltran J. & Song Y.)

In the Table 3.5 it is possible to see that the problematic velocities intervals lay in between 20 and 120 [km/h] of $V0$, it encloses the most of the road speed limits that the accidents are produced at. However because there are more roads and less visibility in the "slow roads" category there is substantial more accidents at the lower speed range that in the "fast road" category.

3.1.2 Impulse Magnitude

Without looking at the traffic conditions the most probable velocity interval where the accidents are done lays in between 40 and 60 [km/h], and the rest of the intervals decreases from that speed interval. And the representative group of impulse magnitude lay in between 4 and 8 [kNs]. The cases inside these two intervals represent the 10 % of all cases. The second trend talked about earlier said that the impulses generated at the front tend to be higher in impulse magnitude will be shown plotting the impulse magnitudes over the physical distribution location of them, see Appendix D. Problem Space, cont.

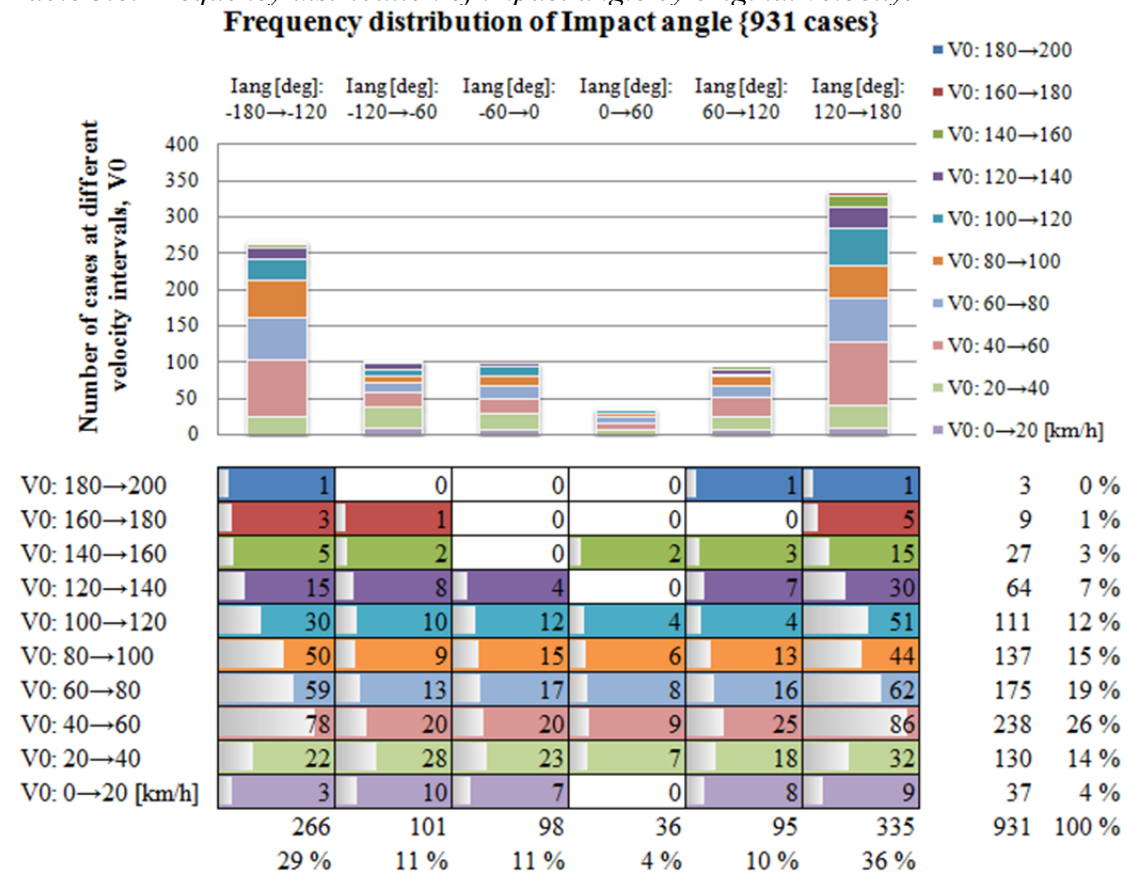
Table 3.5. Frequency distribution of impact magnitude by original velocity.



3.1.3 Impulse Angle

The third trend talked about earlier said that the impulses generated at the front end have a higher impulse angle in GIDAS coordinates, i.g. near ± 180 [deg] impulse angle, see Appendix A. Notations. In Table 3.6 the two columns with high angle intervals enclose almost 66 % of the 931 cases. The lower impulse angle columns, between $[-60, 60]$ degrees, represents hardly the 15 %. In Appendix D. Problem Space, cont. it is shown the complete physical distribution of them.

Table 3.6. Frequency distribution of impact angle by original velocity.



3.2 Post-Impact Problem Space

This time segment variables describes the behaviour of the vehicle at instant the destabilisation force has just ceased, this time point is referred as Post-Impact. The most relevant variables are given and calculated. Combining some variables in a certain form will generate new variables that interpret the behaviour in a more theoretical way that can not sees as a real motion but a way of representing this motion. Table 3.7 shows the variables that will be combined in different ways. Because in the Pre-Impact Problem Space the variable used to map-in was the original velocity the variable chosen to do the same here is the Post-Impact Velocity.

Table 3.7. Variables in Post-Impact Problem Space³.

Post Impact..		Description	Calculation (made with SI units)	Unit
Velocity	PIV	Vehicle velocity	Given	[m/s]
Side Slip Angle	$PISSA$	Vehicle side slip angle	$\Delta\varepsilon - PIYA + \beta_c$, ^[v]	[deg]
Yaw angle	$PIYA$	Vehicle yaw angle rotated during t_c	$\frac{t_c \cdot PIYR}{2}$, ^{[iii]&[iv]}	[deg]
Yaw Rate	$PIYR$	Vehicle yaw rate	Given	$\left[\frac{\text{deg}}{s}\right]$
Velocity x-component	PIV_x	Vehicle longitudinal velocity	$PIV \cdot \cos(PISSA)$	[m/s]
Equivalent PISSA	$ePISSA$	The absolute value of PISSA, extended to ± 180	$\text{atan}_2\left(\frac{ V_{y\ PI} }{V_{x\ PI}}\right)$	[deg]
Equivalent PIYR	$ePIYR$	Rotational contribution to lateral speed over translational longitudinal	$\text{atan}_2\left(\text{sign}(V_{y\ PI} \cdot \omega_{z\ PI}) \cdot \frac{L}{2} \cdot \frac{\omega_{z\ PI}}{V_{x\ PI}}\right)$	$\left[\frac{\text{deg}}{s}\right]$
Beta Front	$BetaF$	Front axle side slip angle	$\left \text{atan}\left(\frac{V_{y\ PI} + \omega_{z\ PI} \cdot l_f}{V_{x\ PI}}\right) \right $	[deg]
Beta Rear	$BetaR$	Rear axle side slip angle	$\left \text{atan}\left(\frac{V_{y\ PI} - \omega_{z\ PI} \cdot l_r}{V_{x\ PI}}\right) \right $	[deg]

³ The index 2 in atan indicates the function atan2 that extends the function arctangent to ± 180

3.2.1 PIYR frequency distribution

Higher yaw rate generates higher side slip angles at one axle and reduce it at the other, increasing the grip difference between both axes, this result in oversteer or understeer behaviour. Figure 3.4 shows that most of the cases have a moderate post impact yaw rate in between ± 90 [deg/s] with approx. 64 %, according to Table 3.8. This could be a result of that the most of the impacts proceed from the front with high angles and very high impulse magnitude, this could produce rotation around the y-axis instead of around the z-axis, in other words pitch rate instead of yaw rate. There are four cases less in Figure 3.4 than in Table 3.8 is because four cases with unknown PISSA have been filtered out for plotting in Matlab.

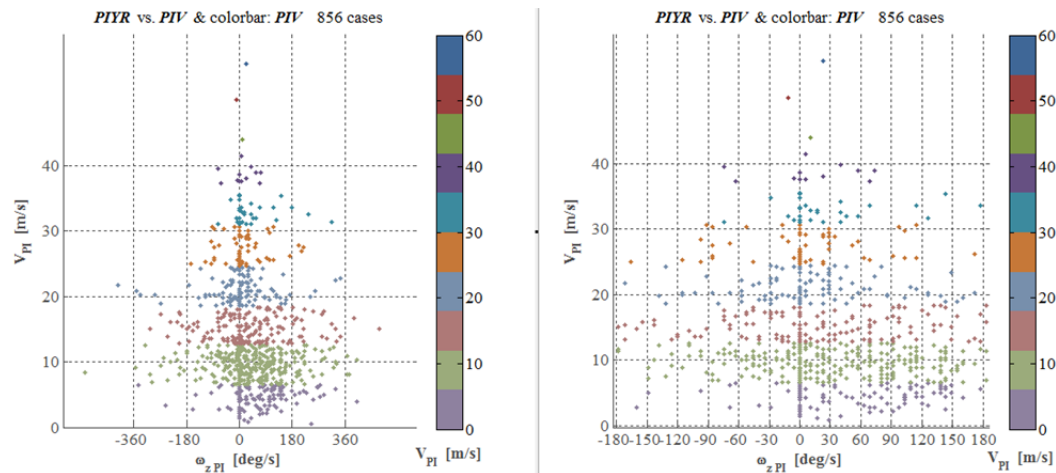
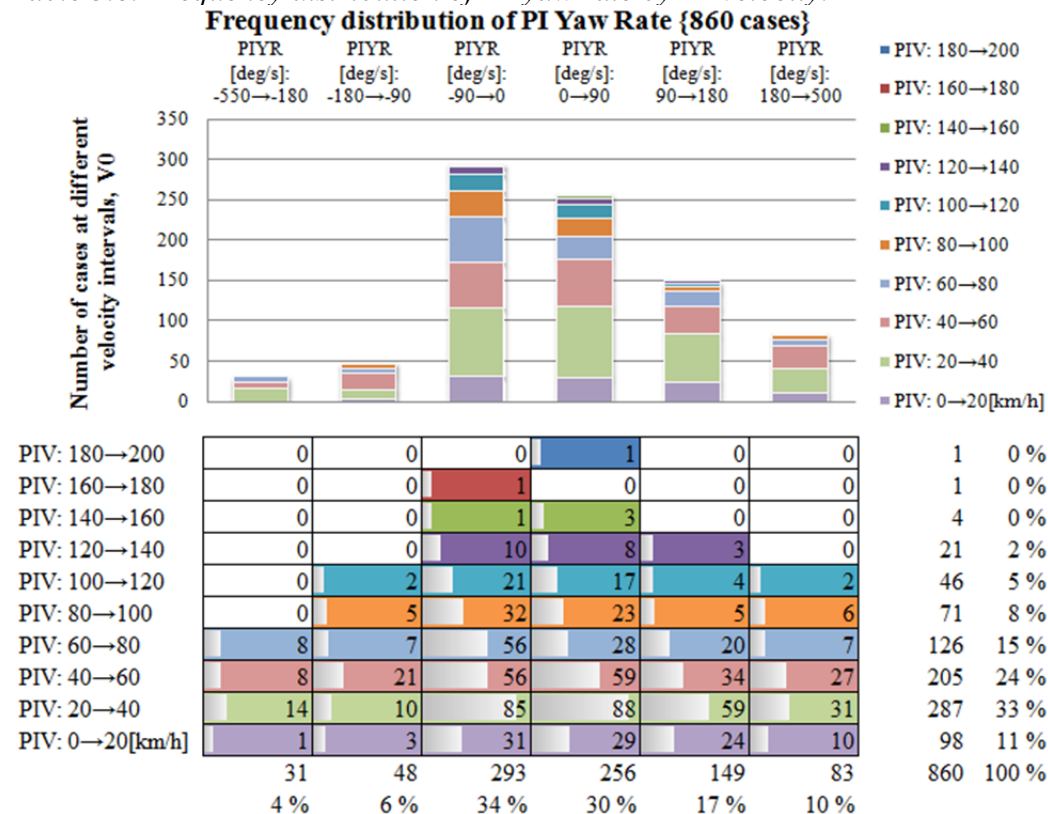


Figure 3.4. Frequency distribution of PI-yaw rate by PI-velocity, zoom at the right.

Table 3.8. Frequency distribution of PI-yaw rate by PI-velocity.



3.2.2 Post-Impact Side Slip Angle

For the side slip induced by the impulse, the concentration towards the zero pattern is repeated here. The cases in between ± 30 degrees represent around 66 % of the cases, according to Table 3.9. Note how the most numerous V_0 interval has shifted down in the most numerous V_{PI} interval.

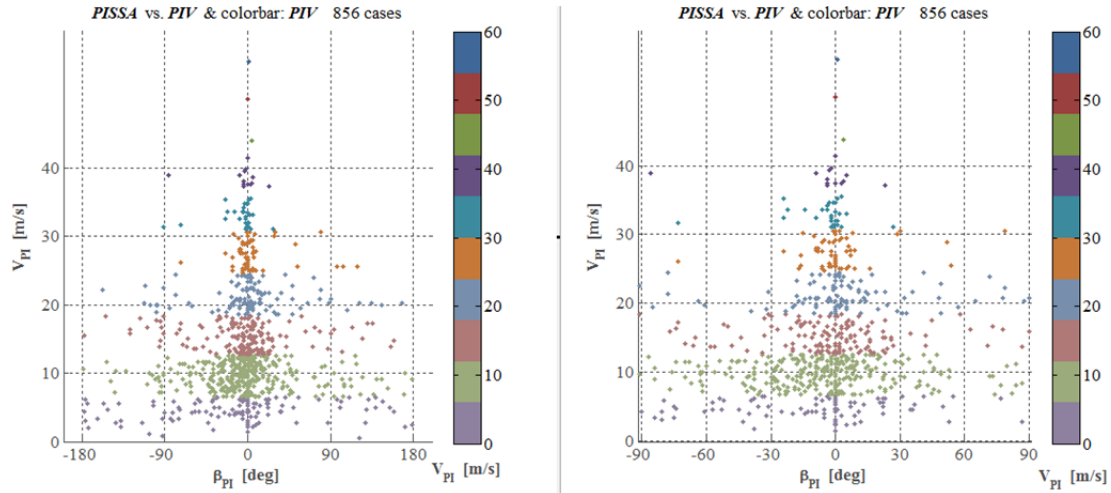
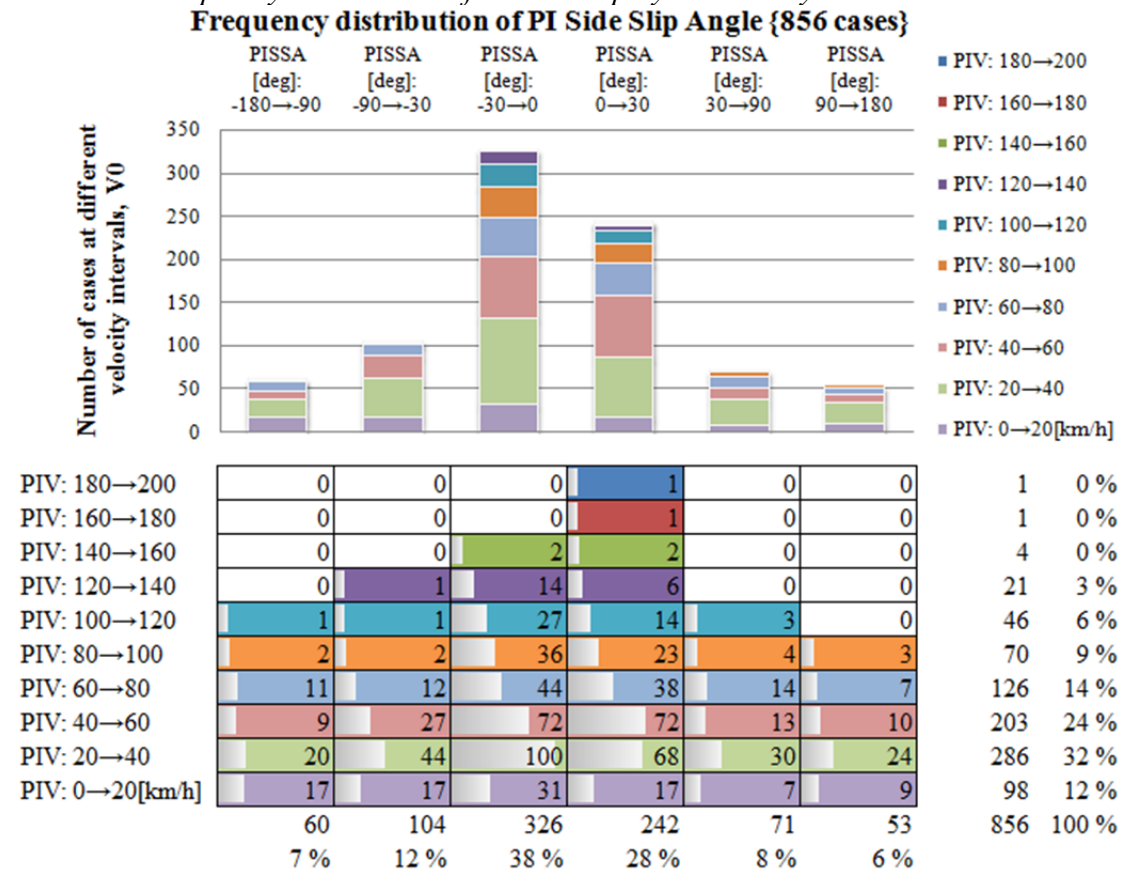


Figure 3.5. Frequency distribution of PI-side slip by PI-velocity, zoom at the right.

Table 3.9. Frequency distribution of PI-side slip by PI-velocity.



3.2.3 PI Side Slip Angle and PI Yaw Rate

The last two sets of data are combined resulting in Figure 3.6.

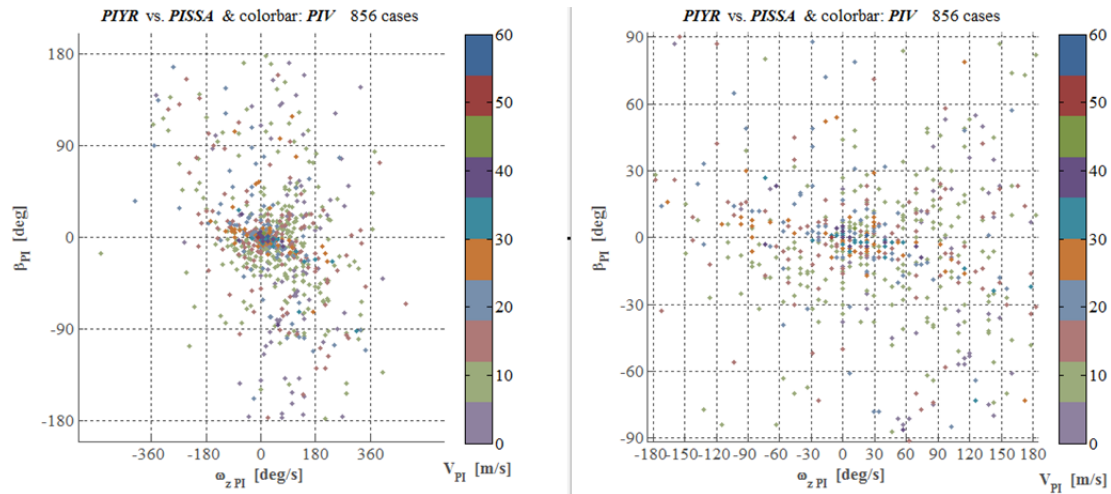
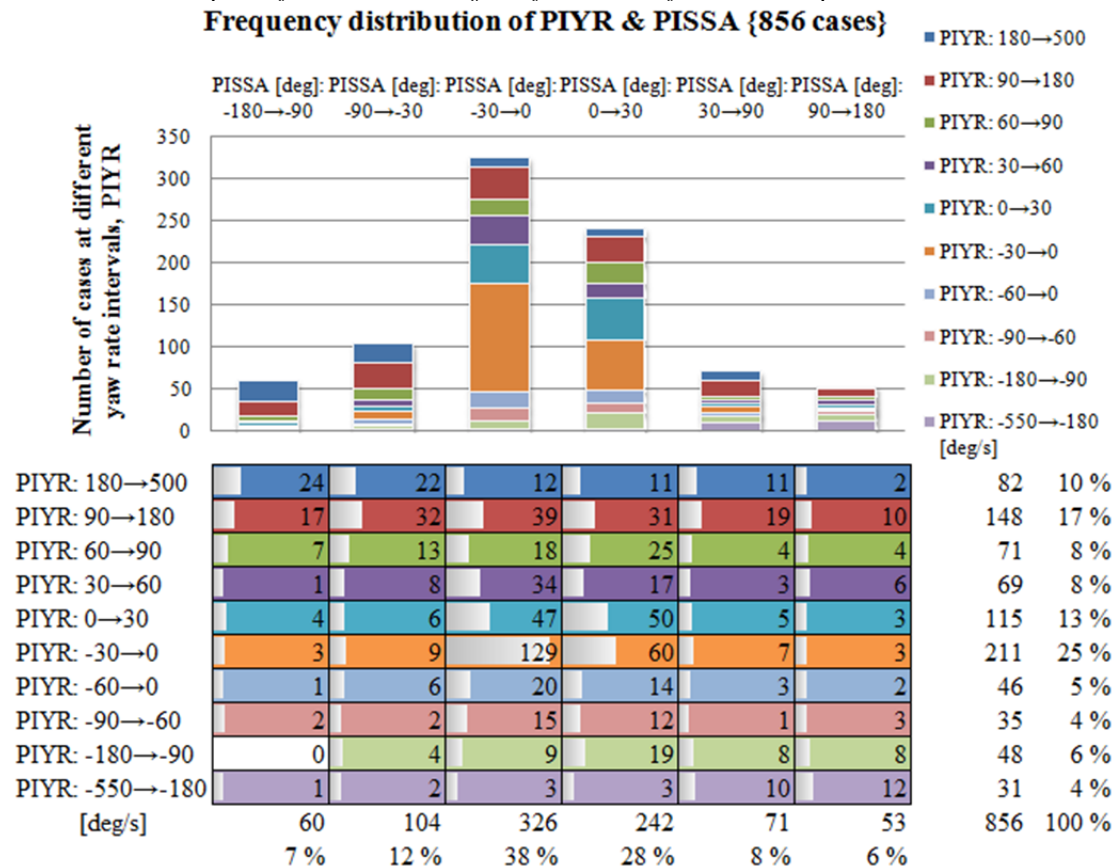


Figure 3.6. Frequency distribution of PI-yaw rate by PI-side slip, zoom at the right.

These two variables together with the velocity are the most interesting motion states that will be handled and combined in search of patterns. In this particular combination the colour of the table intervals are not related to the velocity, but the plots are.

Table 3.10. Frequency distribution of PI-yaw rate by PI-side slip.



Changing the interval boundaries in Table 3.10 reveals that there are 73 cases that have both zero yaw rate and zero side slip. These cases are plotted along the z-axis from origo in the three-dimensional plot of these variables, Figure 3.7.

PIYR vs. PISSA vs. PIV & colorbar: *PIV* 856 cases

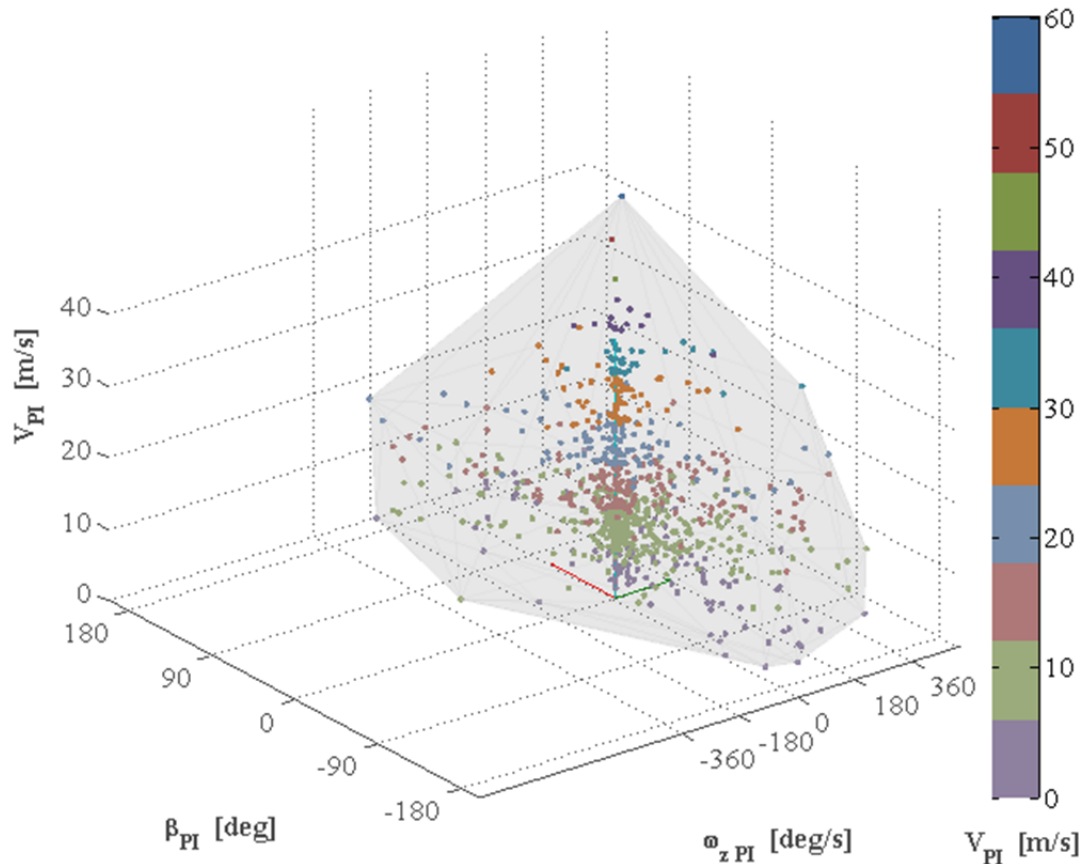


Figure 3.7. Frequency distribution of PI-yaw rate by PI-side slip and by PI-velocity, 3D view.

This cloud of points in these three variable coordinates will be referred as Post Impact cloud, and will be useful when evaluating the capabilities of the rigs to cover this variable cloud. This three-dimensional space can be represented by a volume constructed by the points at the foremost out of the centroid, see Figure 3.7.

This volume brings a recognizable shape to the point clouds but it covers more volume than just the point clouds, good to have in mind later, when using the rig simulation generated volumes.

4 Evaluation Criteria

In this thesis the main objective is to suggest the most proper ways of generating the instable motions, without off course hurting the test driver or the measurement object, the host car with all the test equipment. Evaluating the different rig solutions requires then a multidisciplinary study that maps the criteria by importance and type. Because of the vast rig alternatives to study a list of main characteristics was formulated in a very early stage of the study in order to have a gross compass to know where to look at when selecting the most promising candidates for further analysis. The characteristics will be rated in a subjective way by the interviewed personal.

4.1 Interview

The interview have in intention to rank the different criteria according to the importance of them, for that have a list of the characteristics and two questions been asked to fill to the interviewed people in a questionnaire sheet, Appendix E. Interview questioner. After the interview have the thoughts and feedback been summarized into a chapter that express the most commonly quotes. The five departments at which at least one person have been asked to participate in the survey are:

- Safety Centre
- Active Safety
- Passive Safety
- Vehicle Dynamics Requirements and Verification
- Vehicle Dynamics Functions

The questionnaire sheets consist of a list of $N=16$ characteristics with an empty slot where the participants were asked to grade the importance of each characteristic with a number from zero to ten, with possibility of decimals and blank votes. This weighting factor is averaged according to equation (4.1).

$$Average_n = \frac{\text{weighing factor}}{\text{Filled slots}} , \quad n = 1,2,3, \dots N \quad (4.1)$$

The questioner of Characteristic importance has been done by people that have already an insight in validation projects similar to the PIB and PISC functions. Despite of this fact, may some participants not be familiar with the meaning of this thesis project, and for that reason the interview precedes with a brief presentation in order to have an accurate interpretation of the characteristics before filling the questioner.

Besides the ranking slots there are two questions that followed:

"Why is the Post Impact rig important for Volvo Car Corporation?"

"Which other test do you think it could be useful for?"

The synthesized quotes and feedback from the interview are handled in the Results chapter.

The Questionnaire sheets in the interview have two versions; the internal to Vehicle Dynamics team and other to the Safety related departments. The only difference is that the internal one has four characteristics retained in the Vehicle Dynamics Group because they seemed to be too intricate for the external interview.

4.2 Characteristics

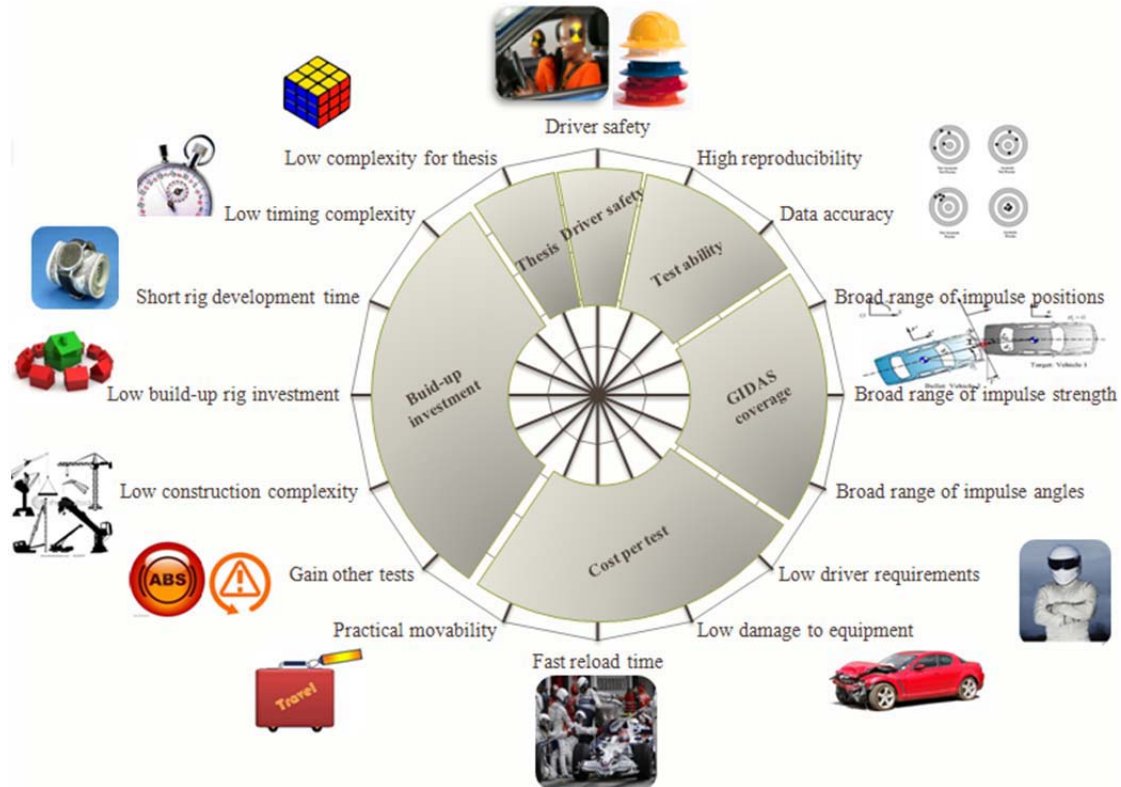


Figure 4.1. Graphical description of rig characteristics. <Icon source: (Google)>

All these characteristics are intended to describe the advantages and disadvantages of all possible rig designs without taking into account hardware or software solutions, however some characteristics may not be applicable to all rigs. In Figure 4.1 there is a graphical description of the characteristics used in the interview presentation. They are presented here in main groups together with the ranking number of importance that they become after the interview input⁴. Being the #1 the most important characteristic.

Indispensable characteristic

#1. Driver safety: The major guideline is the drivers and the test staff safety regardless the convenience in other characteristics. This characteristic discards tests that might involve some risks for the test crew.

⁴ Characteristics retained internally are marked with an asterisk (*).

Test ability characteristics

#2. High reproducibility: The reproducibility is a factor that describes the robustness against the sensibility to factors that might influence the performance; external factors can be extreme temperature sensibility, driver or operator skills, terrain, etc.

#3. Data accuracy: Data accuracy tells how well the rig meets the requested state of motion, being the impact properties decisive for maximum performance.

GIDAS coverage characteristics

#4. Broad range of impact positions: The impulse force acts on the car body in one average location point making the force projection from this point to the CoG very influential.

#5. Broad range of impact strength: the impact strength is referred to the impulse strength that can be reached with long impact time or high impact forces. Being the last one, undesirable because the first safety characteristic at the same time is the force strength useful in order to trigger the sensors located at different places.

#8. Broad range of impact angles: The impulse angle is important in order to vary the proportion of side slip and yaw rate triggered, this might be useful for using the same strength for the tests but varying only the angle in combination with a variation of impact position.

Cost per test characteristics

#7. Low driver requirements: The test system sensibility to different driver skills, meaning if the test requires a skilled test driver with stunt experience or the test can even be done with a regular amateur driver.

#9. Low damage to equipment: Implying the advantage of lower maintenance and replacement costs.

#13. Fast reload time: This characteristic describes the cost that represents the lag between tests. This is related to necessities to change parts or configure the system to other test.

#14. Practical movability: If ability to moving the equipment from one location to another. This might save costs in tack rearrangement, but here it just qualifies the practical movement between locations.

Build-up investment

#6. Gain other tests/Extra quality: The rig may be useful to other tests as ESP or passive safety systems, besides that could other qualities may be have passed unaware in the other points, as the cost reduction by test track rearrangement or climate control.

#10. Low construction complexity *: The advantage of limited number of parts, all costs in general grow with the number of parts and code requirements.

#11. Low build-up rig investment: This cost have to put in accordance to the result that the rig is capable to replicate, however it is relevant to know the importance of this characteristic criteria in order to discard some expensive solutions before the evaluation part.

#12. Short rig development time *: The development time refers to the time it will take to the first test. Design, construction, coding, incorporation could be important for the company.

#15. Low timing complexity *: Because the accidents are about being in the wrong spot at the wrong time it is presumable that the timing is key characteristic. Even if the applied disturbance is operate by request there is a timing complexity in the system that controls it.

Thesis

#16. Low complexity for thesis *: This point attempts to rank the importance of the available skills in the thesis team, influencing the autonomous work, having to consult more often the supervisors and require more time to develop more complex methods or combinations.

4.3 Implementation of criteria in evaluation matrix

Because the selection of a rig solution have the risk of being favoured by subjective grades and individual preferences an objective approach can limit that by using a grading system that set qualification points depending in how well the rig perform at these characteristics.

All the candidates have a particular performance in each characteristic, then quantifying this performance with a grading number from zero to five will make possible to quantify the advantages across the N numbers of characteristics. Further the performance grade will be multiplied with its correspondent average importance points and will be summed into the rig score as in (4.2).

$$Rig\ score = \sum_{n=1}^N Performance_n \cdot Average_n \quad (4.2)$$

A control item in form of a perfect rig has the highest performance grade in all the characteristics, gathering the maximum rig score. All other individual rig scores are then normalized to the control item score as percentage as in (4.3).

$$Percentage_{Candidate} = \frac{Rig\ Score_{Candidate}}{Rig\ Score_{Control\ item}} \cdot 100 \quad (4.3)$$

The answers, importance ratings, matrix and score percentage are presented in Chapter 7 Results.

5 Collision Model

Collision model is a combination of one vehicle simulation model and matrix method based on momentum conservation theory. Different with simulation model, energy losses through plastic deformation and through friction dissipation could be accounted for through this collision model. Hence, it can be used to reconstruct GIDAS accident and verify the PISSA calculation method done in Chapter 3 Problem Space. Besides, simulation model with rear end impact can be validated by momentum method. For later evaluation of rig – PIT manoeuvre, collision model helps to get two cars pre-impact states to fulfil desired host vehicle post-impact states.

5.1 Momentum method

The force commonly used to calculate accelerations and velocity are not constant during the collision. To simplify the problem, the momentum method does not attempt to solve the trajectories over time, but use integrated forces, i.e. the impulse, to solve for velocity changes from before to after the collision. The time traces during collision is not calculated and accordingly, the method assumes that the collision happens during infinitely short time, but with limit integral value of impact forces. This solution method is the so called momentum method.

Some assumptions are necessary to use this simplified method to describe the collision process. First of all, structural deformation is too complex to be exactly calculated, which is determined by surface material properties, surface geometry (Cannon, 2001) and initial normal velocity (Antonietti, 1998). Assuming that the crash happened at a specific point and would not vary during the collision implies that the impact force magnitude and angle remains constant during the collision, which would not affect the result dramatically (Thor, 2007). Energy dissipation by material plasticity is substituted with the coefficient of restitution, CoR.

5.1.1 Four-DOF vehicle model

As a preparation of later matrix method, a 4-DOF dynamic model is demonstrated in this section. Heave and pitch motions of the vehicle are ignored, which acts as weak influences for post-impact states. The ground force considered dynamic model is 4-DOF, which is compatible with the simulation model in Chapter 5.2 Proposed collision model and validation.

To describe roll motion, the vehicle mass is separated into rolling mass m_R and unrolling mass m_{NR} . The connection between these two masses is described by an equivalent torsional spring and damper with coefficient of K_s and D_s . Figure 5.1 shows the three orthogonal views of vehicle model, which is crashed at the rear end (x_A, y_A, z_A) with impact force (F_x, F_y) . Newton's equations of motion relating longitudinal, lateral velocities, as well as rotational motion about the x-axis and z-axis can be written as equation (5.1) to (5.4)..

$$m(\dot{v}_x - v_y w_z) = F_x \quad (5.1)$$

$$m(\dot{v}_y + v_x w_z) - m_R h \dot{w}_x = F_y + F_{yf} + F_{yr} \quad (5.2)$$

$$I_{zz}\dot{w}_z + I_{xz}\dot{w}_x = x_A F_y - y_A F_x + a F_{yf} - b F_{yr} \quad (5.3)$$

$$\begin{aligned} I_{xxs}\dot{w}_x + I_{xz}\dot{w}_z - m_R h(\dot{v}_y + v_x w_z) = \\ F_y(z_A - h) + (m_R g h - K_s)\phi - D_s w_x \end{aligned} \quad (5.4)$$

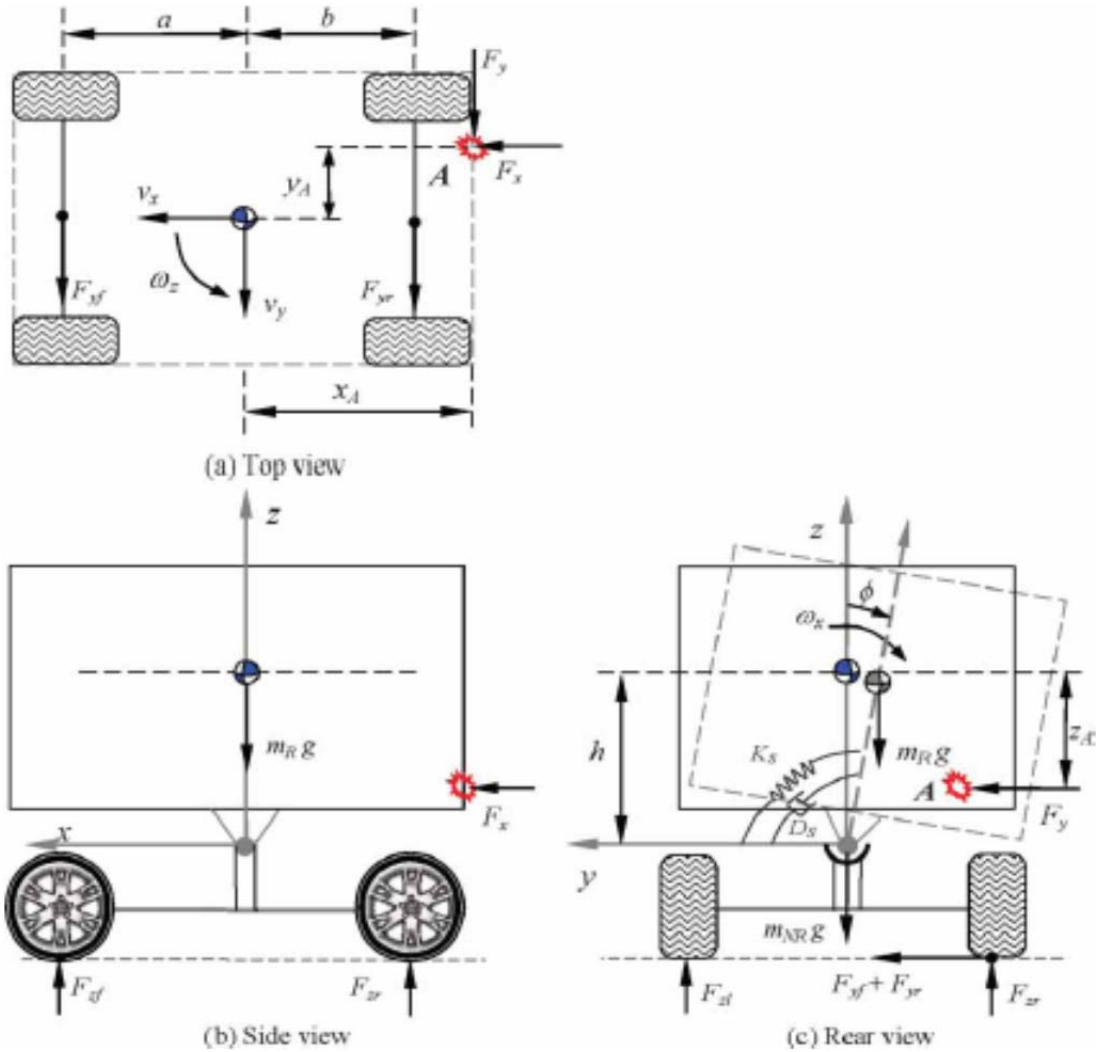


Figure 5.1. Schematic diagrams of the vehicle model with impact forces applied <Source: (Zhou, J. et al., 2008)>

The tyre lateral friction F_{yf} and F_{yr} are proportional to tyre side slip angle at the beginning and saturated after side slip angle increase to 10 [deg]. During the linear section, the relationship between tyre lateral friction and side slip angle could be written as equation (5.5).

$$\begin{cases} F_{yf} = C_f \left(\delta_f - \frac{v_y + a w_z}{v_x} \right), & |F_{yf}| < m g \mu_R \frac{b}{L} \\ F_{yr} = C_r \left(\frac{-v_y + b w_z}{v_x} \right), & |F_{yr}| < m g \mu_R \frac{a}{L} \end{cases} \quad (5.5)$$

Momentum method is an integral based solution, which asks the variable have approximately linear changing according to time. However, as impulse magnitude increase, lateral tyre friction would be saturated before the end of collision ($t = 0.15$ [s])

for instance). In this case, it is not appropriated to assume the friction is a time linear function, integrated over the pre- and post-impact friction. In addition, tyre friction is a complex function that relies on the dynamic states. This determines that without simplifying the tyre model; it is hard to find friction integral within collision period – 0.15 [s]. In this case, a parameter η is introduced to decrease the slope of tyre friction, and get the same mean value of lateral friction over 0.15 [s] as Figure 5.2 shows. The parameter η is chosen by comparisons to a certain rear-end impact collision, which would be shown in Chapter 5.1.3.1 Friction characteristic parameter η . The expression of tyre friction is written as equation (5.6) without tyre slip angle boundary.

$$\begin{cases} F_{yf} = \eta C_f \left(\delta_f - \frac{v_y + aw_z}{v_x} \right), \\ F_{yr} = \eta C_r \left(\frac{-v_y + bw_z}{v_x} \right), \end{cases} \quad (5.6)$$

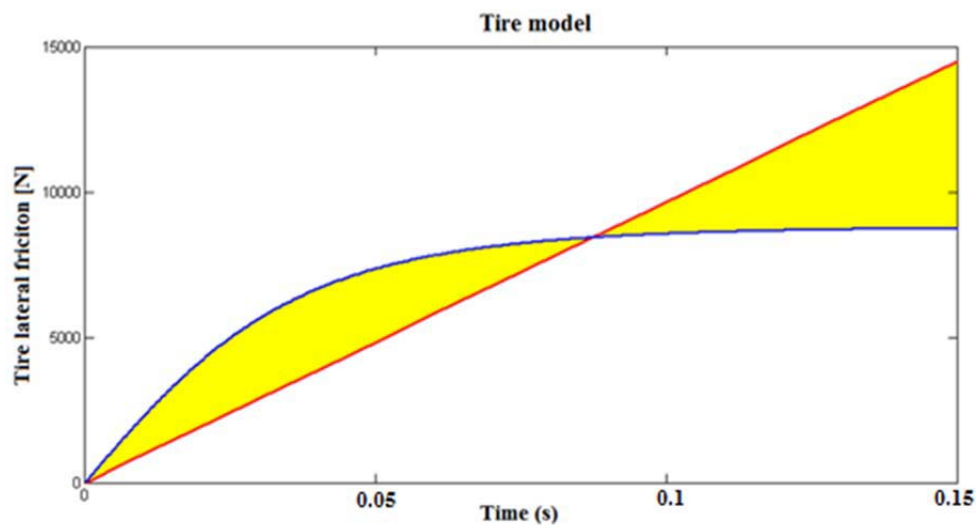


Figure 5.2. Comparison of linear tyre model.

5.1.2 Matrix method based on momentum-conservation

In this section, a mathematical matrix based on Jing’s paper (Zhou, J. et al., 2008) is built to estimate the PI states and impulse information by given PI states. Matrix method only focuses on the final changes in vehicle kinematic states due to the impact; without analysing component deformation and kinematic process.

Figure 5.3 shows a common collision, where vehicle1’s local coordinate is overlapped with the earth fixed coordinate. The typical collision duration is around 0.2 [s] (Brach, 2003). Within this short period, assuming that the acceleration integral is approximately equal to velocity changes and the integral of cross-terms is a trapezoidal area. Since the collision-induced impulse should be the same between two vehicles, two more equations can be generated to describe the projection between bullet vehicle coordinate impulse and host vehicle one.

According to the definition of CoR, negative ratio of the final to initial relative normal velocity components, one equation is derived to describe the energy losses through CoR. The frictional dissipation is expressed by the coefficient of tangential interaction (μ) equation. These two parameters CoR and μ are assumed to be known a priori. Consequently, 12 equations are collected to generate the matrix method.

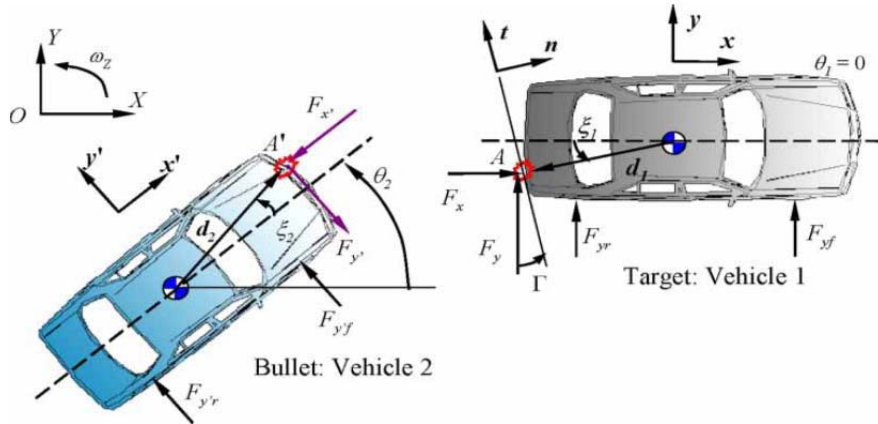


Figure 5.3. Planar view of two car collision <Source: (Zhou, J. et al., 2008)>

There are twelve unknown variables in the matrix: post-impact states of two cars (V_{1x} , V_{1y} , Ω_{1z} , Ω_{1x} , V_{2x} , V_{2y} , Ω_{2z} , Ω_{2x}) and the collision-induced impulse (P_{1x} , P_{1y} , P_{2x} , P_{2y}). Besides, the eight pre-impact states of two vehicles (v_{1x} , v_{1y} , w_{1z} , w_{1x} , v_{2x} , v_{2y} , w_{2z} , w_{2x}) and collision position (x_A , y_A , z_A), angle θ , deformation angle Γ , CoR and collision surface μ should be available previously. The crash point is described through local spherical coordinates by angle ξ and distance d , as Figure 5.3 demonstrated. Then the block-matrix formulation could be written as equation (5.7), where $\mathbf{x} = (V_{1x}, V_{1y}, \Omega_{1z}, \Omega_{1x}, V_{2x}, V_{2y}, \Omega_{2z}, \Omega_{2x}, P_{1x}, P_{1y}, P_{2x}, P_{2y})$. The specific term of matrix A and B is shown in Appendix A. Equation (5.7) is not a linear matrix, which could be solved by least-square optimisation method by Matlab.

$$\begin{pmatrix} A_{11} & 0 & A_{13} \\ 0 & A_{22} & A_{23} \\ A_{31} & A_{32} & A_{33} \end{pmatrix} \cdot \mathbf{x} = B \quad (5.7)$$

There are some drawbacks of this momentum conservation based matrix method. First of all, to simplify matrix, the initial v_y , w_z , w_x have been assumed to be zero. Further, even if η is introduced to describe the linear tyre lateral friction, the value of η should change according to different collision time period and impulse information. Therefore, this model is not reliable. Additionally, the matrix method is have some differences with the simulation model; the weight transfer, tyre relaxation and other dynamic information can not be included in the matrix elements. Based on above disadvantages, the matrix method only is used as a reference data or initial value for certain iteration in later sections.

5.1.3 Critical parameters

There are two critical parameters; friction characteristic parameter η and coefficient of restitution CoR, which are used to describe linear tyre friction and energy losses respectively. Both of them would change according to different collision proprieties such as collision time, impact position, impulse magnitude and so on. Fortunately, these two parameters are limited in certain interval.

5.1.3.1 Friction characteristic parameter η

The tyre friction parameter η is used to decrease tyre stiffness and should be located within [0 1]. For $\eta=0$, the ground force is completely neglected during the collision; for $\eta=1$, the model is only accurate in case that tyre lateral friction does not saturate

at the end of collision. The value of η should decrease as impulse magnitude or impulse duration grows.

To study friction characteristic parameter η , a simple collision scenario of two ‘baseline big SUV’ front-rear collision is chosen, which is quite similar to the Figure 5.3 situation. Table 5.1 shows the parameter of vehicle model and pre-impact states are shown in Table 5.2. The matrix formulation result with $\eta=0.45$ is given in Table 5.3. The comparison between CarSim (commercial vehicle dynamics software), 4-DOF (Zhou, J. et al., 2008), Planar (3-DOF and without ground force) and matrix formulation result are also listed in Table 5.3.

Table 5.1. Vehicle parameter for matrix method.

Parameter	Value	Unit	Parameter	Value	Unit
m	2450	[kg]	I_{zz}	4946	[kgm ²]
m_R	2210	[kg]	I_{xz}	40	[kgm ²]
m_{NR}	240	[kg]	I_{xxs}	1597	[kgm ²]
a	1.105	[m]	K_s	94000	[Nm/rad]
b	1.745	[m]	D_s	8000	[Nms/rad]
h	0.4	[m]	C_f	145750	[N/rad]
h_{CG}	0.66	[m]	C_r	104830	[N/rad]

Table 5.2. Collision information and pre-impact states.

Parameter	Value	Unit	Parameter	Value	Unit
d_1	2.75	[m]	d_2	1.85	[m]
ζ_1	2	[deg]	ζ_2	0	[deg]
z_A	0.66	[m]	$z_{A'}$	0.66	[m]
θ_1	0	[deg]	θ_2	25	[deg]
v_{1x}	29	[m/s]	$v_{2x'}$	33.5	[m/s]
v_{1y}	0	[m/s]	$v_{2y'}$	0	[m/s]
w_{1x}	0	[deg/s]	$w_{2x'}$	0	[deg/s]
w_{1z}	0	[deg/s]	$w_{2z'}$	0	[deg/s]
μ	0	[1]	μ_R	0.9	[1]
Γ	25	[deg]	CoR	0.2	[1]
Δt	0.15	[s]	η	0.45	[1]

Table 5.3. Comparison of matrix result with $\eta=0.45$.

Kinematic states		Target vehicle			
		CarSim	4-DOF	Planar	Matrix
Pre-impact	v_{Ix} [m/s]	29			
	v_{Iy} [m/s]	0			
	w_{Iz} [deg/s]	0			
Post-impact	V_{Ix} [m/s]	31.3	31.1	31.9	31.4
	V_{Iy} [m/s]	4.3	4.5	1.4	4.4
	Ω_{Iz} [deg/s]	-89.9	-95.3	-109	-89
	Ω_{Ix} [deg/s]	-13.2	-15.8	–	-15.7

We can see that the matrix method with $\eta=0.45$ is quite accurate compared to the other three methods' results. As mentioned above, η need to be changed by different collision situation. To see how this would influence the result, Table 5.4 shows the post-impact states' sensitivity for different η .

Table 5.4. Friction characteristic parameter η sensitivity analysis.

Kinematic states		Target vehicle (CoR = 0.2)				
		$\eta = 0$	$\eta = 0.3$	$\eta = 0.45$	$\eta = 0.6$	$\eta = 1$
Pre-impact	v_{Ix} [m/s]	29				
	v_{Iy} [m/s]	0				
	w_{Iz} [deg/s]	0				
Post-impact	V_{Ix} [m/s]	31.2	31.4	31.4	31.5	31.7
	V_{Iy} [m/s]	5.2	4.7	4.4	4.2	3.8
	Ω_{Iz} [deg/s]	-95.2	-91	-89	-87.2	-82.6
	Ω_{Ix} [deg/s]	-1.83	-11.6	-15.7	-19.5	-27.8
Impulse magnitude	P_x [Ns]	6922	7162	7271	7372	7615
	P_y [Ns]	3228	3340	3390	3438	3551

As η is varying, PIV would not change noticeably, this is because CoR guarantee the PIV changes and impulse magnitude will increase to generate similar PIV to compensate η and tyre friction growing influence. Besides, the impulse angle is determined by collision information, which would not change and the ratio of P_x and P_y keep constant in Table 5.4. For PIYR and PISSA, the maximum difference is around 10 %. Roll-rate would changes dramatically but not important for our post-impact states estimation. Consequently, use $\eta=0.45$ to estimate all rear-end collisions are reasonable, maybe even for all collision situations.

5.1.3.2 Coefficient of Restitution

Coefficient of Restitution, CoR, is defined as a fractional value representing the negative ratio of speeds after and before collision. The energy losses of deformation could be accounted for with CoR, which is also depends on body material, geometry, impact velocity, and vehicle mass difference, etc. Figure 5.4 shows the rear end collision experimental results of CoR, it implies that if the two collision car has the same mass, CoR approximates to 0.2.

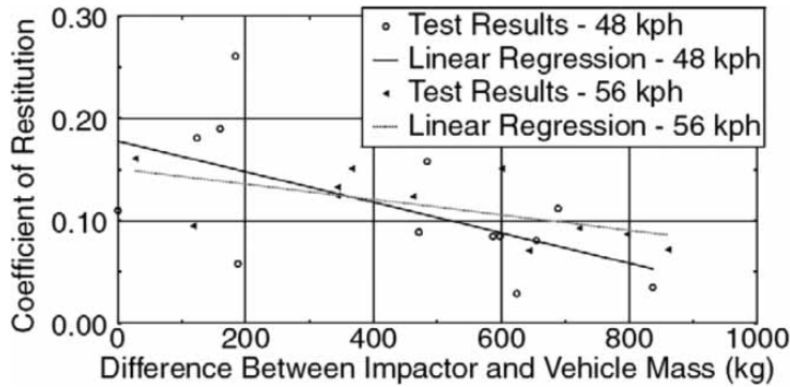


Figure 5.4. CoR versus mass difference. <Source: (Monson, 1999)>

To test the relationship between CoR and impulse magnitude different CoR are used as test parameter, obtaining the result shown in Table 5.5. where it is shown that the impulse magnitude is proportional to CoR. As CoR increase and energy losses increase as well, more impulse or say collision force is needed to compensate these losses.

Table 5.5. Coefficient of restitution sensitivity analysis.

CoR	Post-impact states				Impulse magnitude	
	V_x [m/s]	V_y [m/s]	W_z [deg/s]	W_x [deg/s]	P_x [Ns]	P_y [Ns]
0.1	31.3	4	-81.3	-14.4	6639	3096
0.2	31.4	4.4	-89	-15.7	7271	3391
0.3	31.6	4.9	-96.9	-17.1	7901	3688

5.2 Proposed collision model and validation

5.2.1 Proposed collision model

Momentum method presented in previous section could describe two collided vehicles' information, but the dynamic states during the collision and tyre friction introduced errors that make it not accurate enough. For more precise one vehicle simulation model, energy losses and friction dissipation is impossible to be considered. Hence, a new collision model which combines those two models together is proposed.

The simulation model used here is a 4-DOF two track vehicle dynamics model. This model is developed by the author of (Yang, 2009) in MATLAB/Simulink software

and has been validated by veDYNA. It has the impulse as input signal, with four degrees of freedom or dynamic states; longitudinal velocity V_x , lateral velocity V_y , yaw rate w_z and roll rate w_x . Besides, the magic formula tyre model also includes tyre relaxation, which introduces time delay after sudden increase of tyre side slip angle. This simulation model is designed for one car collision.

The collision test is as following:

- a) Given information such as: pre-impact states of two colliding vehicles, collision parameters, Γ , CoR and μ are settled as critical parameters in both simulation model and momentum-matrix method.
- b) Calculate impulse magnitude by matrix method, which is used as the initial value of later iteration.
- c) The vehicle model is used twice with correspondent impulse and car properties, target car and bullet car. Calculate CoR by the two collided vehicles' dynamic states at t_{PI} by the equation given in matrix method.
- d) Compare the new CoR with the reference value of 0.2, if the calculated CoR is within interval [0.19 0.21] stop iteration and show the post impact states got by step c). Otherwise go to step e).
- e) Since impulse magnitude is proportional to CoR (proved in Chapter 5.1.3.2 Coefficient of Restitution), tuning impulse magnitude with principle as: if CoR is larger than 0.2, decrease impulse magnitude to 99 % and vice versa.
- f) Back to step c) with new impulse magnitude and iterate until CoR belongs to [0.19 0.21].

5.2.2 Collision model validation

To further validate the simulation model with rear end impact and test if the collision model runs good, it is compared to the results in (Zhou, J. et al., 2008). The comparison shows that the proposed collision model performs well for rear-end collisions.

As the friction parameter is $\eta = 0.45$ here, which has been compared with a single case shown in Chapter 5.1.3.1 Friction characteristic parameter η . The tested method is in following way:

- a) Use the information given in Table 5.1 and Table 5.2, except the two variables, bullet vehicle orientation angle θ_2 and collision offset along y-axis Δy , to settle critical parameter in simulation model. These two varied parameters are changing within [0 30] degrees and [-0.5 0.5] meters respectively.
- b) Use collision model get two vehicle's post-impact states.
- c) The simulated contour plot is shown in Figure 5.6 and the result in (Zhou, J. et al., 2008) in Figure 5.5.

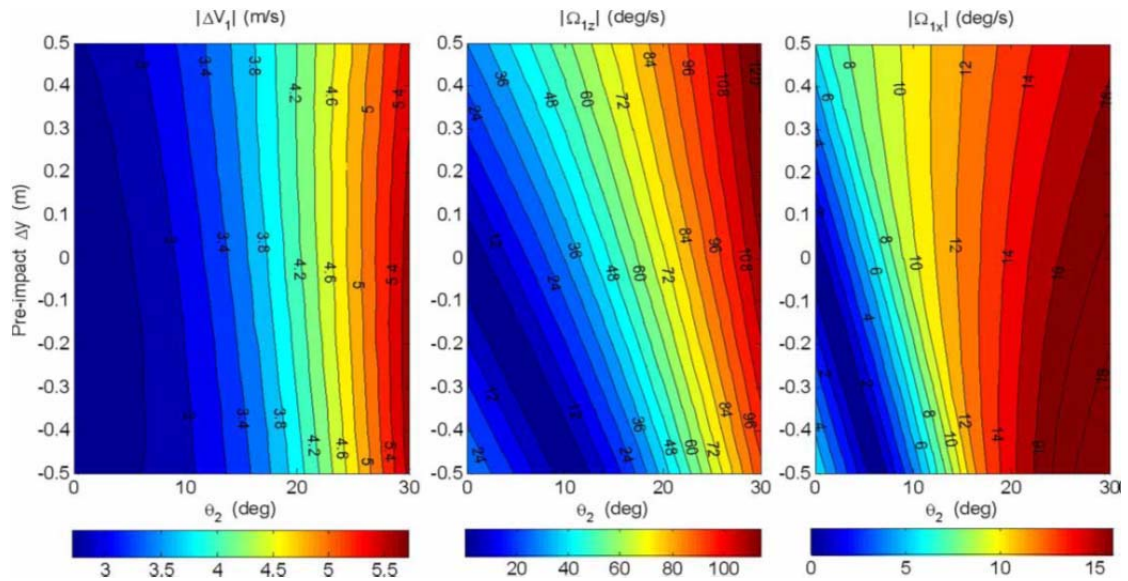


Figure 5.5. Benchmark contour plots <Source: (Zhou, J. et al., 2008)>

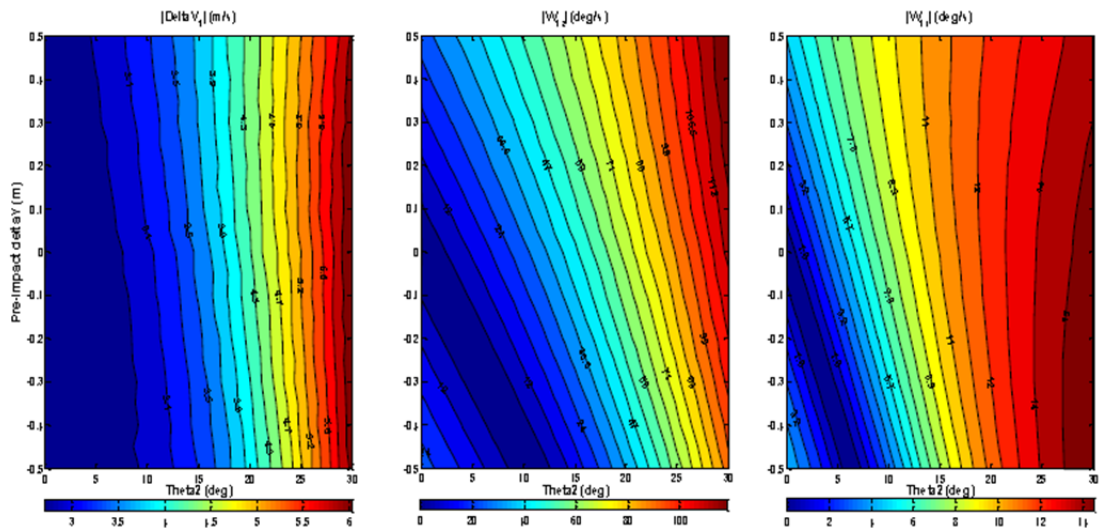


Figure 5.6. Simulation model contour plots.

The difference between these two contours is hard to see. Hence, the collision model is feasible and simulation model with rear-end impact behaves correctly. For later verification, the results provided by the collision model can be used as criterion.

5.3 GIDAS verification

5.3.1 Verification method

The representative cases here are nine accidents picked from GIDAS database. GIDAS database accident involves two sets of collision information, pre-impact information and post-impact states. Since impulse magnitude is calculated by velocity changes during collision, one car simulation model is enough to estimate the post-impact states.

There are two steps done to validate the accident. First of all, trust the pre-impact information and use simulation model to generate post-impact states. If these states are similar with GIDAS database, the collision case is correct. In this case, the pre- and post-impact information is compatible with each other. Otherwise, use the second step to tune the pre-impact information. The principle is trust post-impact states if GIDAS is not compatible. Pre-impact states could be tuned by the assumption that GIDAS reconstruction neglected or miscalculated the friction on collision surface, which would be large for side collision cases. If none of these steps is confirmed, make a conclusion that GIDAS is wrong.

The extra-standards of above judgment are μ and CoR. As mentioned above, CoR should be positive and always located within [0 1]. The sign of μ need to fulfil the friction definition – opposite to the relative motion. For rear end or front collision, surface friction could be neglected because of the lower relative speed.

For first step, since GIDAS only gives the impact point distance to the foremost point of the vehicle and relevant wheelbase (checked according to vehicle type), it is hard to find accurate location of CoG thus the distance between CoG and impact point. Use SL_f as a variable to tune CoG location, which should be a positive and smaller than the subtraction between vehicle length and wheelbase. The other variable is the inertia around z-axis, I_{zz} , which is estimated by its crash weight and wheelbase. I_{zz} could only help to tune the absolute value of PIYR, but not the sign of it. Since the impulse magnitude is calculated by velocity changes, estimated PIV would be correct all the time. PIYR is chosen as a priority to determine relevant SL_f and I_{zz} .

Vehicle data, especially the height of CoG, impact height position and distance between CoG to roll centre, could also be changed in some extent if necessary (rollover case). To decrease the impact force, prolong the impact duration and keep same impulse magnitude can help the model based car to not rollover. In most real collision cases, the first impact would not result in rollover, so that the simulation should be matched as well. The crash duration is 0.2 [s] if not adjusted.

5.3.2 Representative verification examples

In this section, three representatives are shown how the verification method does work. These instances involve two correct cases with or without adjusting and a wrong case.

5.3.2.1 Correct without tuning Case A.

This case is one PIC relevant cars' crash, located at front and right respectively. Detailed collision position (according to GIDAS coordinate), impulse angle, post- and pre- impact states are shown in *Table 5.6*. Besides, the initial side slip angle of host vehicle is not zero but -112 degrees. This accident is happened at urban road and both cars are driven in low speed. The impulse magnitude of both cars is around 5500 [Ns].

Table 5.6. GIDAS collision information of case A.

Vehicle	Impact position [m]			Impact part	Impact angle [deg]	Pre-impact states [m/s],[m/s],[deg/s]			Post-impact states [m/s],[deg],[deg/s]		
	X	Y	Z			v_x	v_y	w_z	PIV	PISSA	$\Omega_{z,PI}$
Host	0.2	-0.7	0	Front (1)	-164	3.9	0	0	1.11	-107	17.2
Bullet	0.4	0.7	0	Right (2)	62	-3.6	-9	0	6.11	-130	166.2

To get the same result with GIDAS, suitable SLf and I_{zz} are chosen and the relevant post impact states are given in Table 5.7. We can see that PIYR, PISSA and PIV are quite similar to GIDAS data. The maximum difference is 8 % for PISSA, which is acceptable as well. Besides, for Γ is equal to -180 [deg], then CoR is equal to 0.74 and μ is 0.3. Both of them are satisfied with judgment standards, therefore this is a correct case and there is no need to tune the impulse information.

Table 5.7. Comparison between GIDAS and simulation model based result.

Vehicle	SLf [m]	PIV [m/s]		PISSA [deg]		PIYR [deg/s]	
		Sim.	GIDAS	Sim.	GIDAS	Sim.	GIDAS
Host	0.86	0.95	1.11	-98	-107	17	17.2
Bullet	0.43	6.11	6.11	-125	-130	166.6	166.2

5.3.2.2 Correct after tuning case B:

The case is one PIC relevant car's crash case, both collision located at left front side and crashed face to face. Detailed collision position (according to GIDAS coordinate), impulse angle, post- and pre- impact states are shown in Table 5.8. The vehicle trajectory is shown in Figure 5.7 and the first impact is illustrated by the red arrow. The accident is happened at a countryside road. After first collision, the host vehicle ran into bushes alongside the road. The impulse magnitude is around 3500 [Ns].

Table 5.8. GIDAS collision information of case B.

Vehicle	Impact position [m]			Impact part	Impact angle [deg]	Pre-impact states [m/s],[m/s],[deg/s]			Post-impact states [m/s],[deg],[deg/s]		
	X	Y	Z			v_x	v_y	w_z	PIV	PISSA	$\Omega_{z,PI}$
Host	0.6	-0.8	0	Left (4)	-133	20	0	0	18.6	-10	45.9
Bullet	0.6	0.7	0	Left (4)	-131	18.9	0	0	17.5	–	28.7

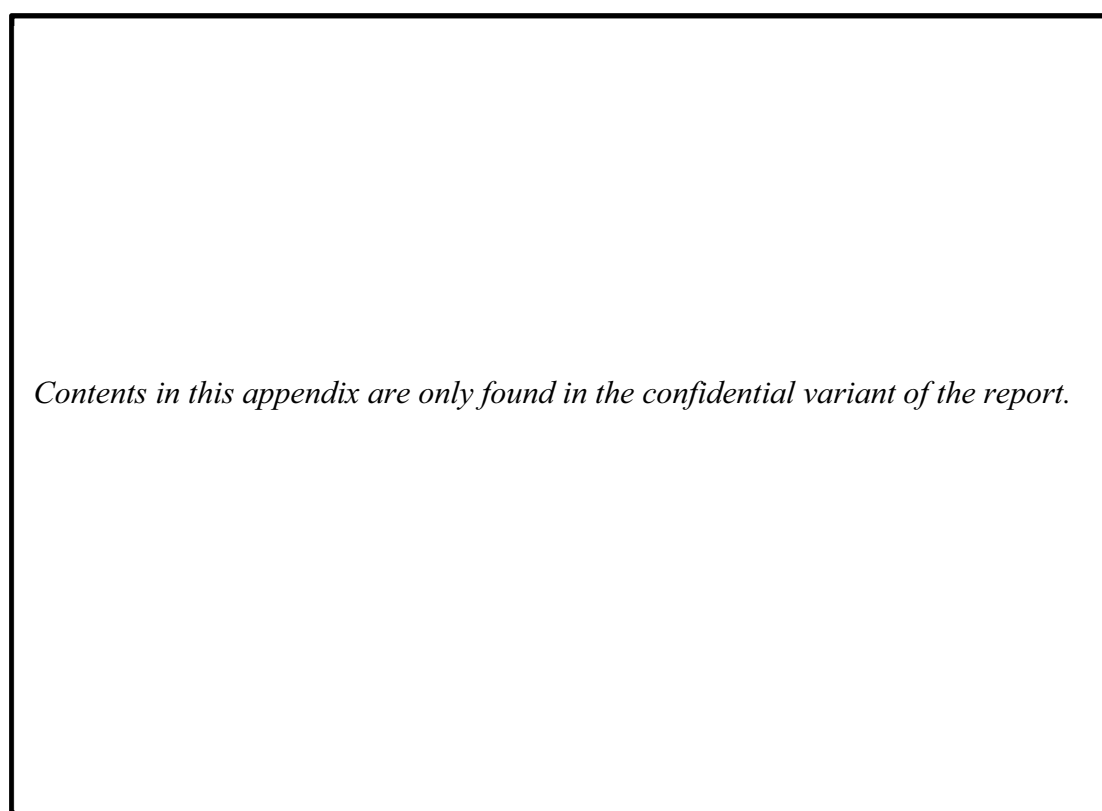


Figure 5.7. Collision trajectory of case B.

Table 5.9. Comparison between GIDAS and simulation model based result.

Vehicle	SLf [m]	PIV [m/s]		PISSA [deg]		PIYR [deg/s]	
		Sim.	GIDAS	Sim.	GIDAS	Sim.	GIDAS
Host	0	18.5	18.6	-3.4	-10	10.3	45.9
Bullet	0	17.3	17.5	-3.5	–	4.6	28.7

To get the same result with GIDAS, suitable SLf and I_{zz} are chosen and the relevant post impact states are given in Table 5.9. We can see that PISSA from vague estimation is ok. PIYR cannot reach GIDAS given value no matter how large I_{zz} and SLf is, which implies that GIDAS impulse information is miscalculated. For face to face side collision, the friction is too large to be ignored. The host vehicle surface friction is opposite direction to the velocity, which would generate positive yaw rate. After concerning surface friction, the absolute value of impulse angle and magnitude would increase simultaneously. With impulse of 4100 [Ns] and -163 [deg] better simulation results are shown in Table 5.10. For deformation angle $\Gamma = -92$ [deg], CoR = 0.47 and $\mu = -2.9$.

Table 5.10. Comparison between GIDAS and simulation model based result after adjustment.

Vehicle	Impact position [m]			Impact mag [Ns]	Impact angle [deg]	Simulation model [m/s],[deg],[deg/s]			GIDAS [m/s],[deg],[deg/s]		
	X	Y	Z			PIV	PISSA	$\Omega_{z,PI}$	PIV	PISSA	$\Omega_{z,PI}$
Host	0.6	-0.8	0	4100	-163	17.6	-5	41.5	18.6	-10	45.9
Bullet	0.6	0.7	0	4300	-161	16.2	-5.2	25.6	17.5	-	28.7

5.3.2.3 Incorrect case C.

This accident happened at the interaction of urban road, and host car is the PIC relevant vehicle, which was travelling straight until the border of the intersection. Then bullet vehicle crashed the host vehicle on the right middle side with its front nose, which generate positive yaw rate and side slip for host vehicle. Then the host vehicle turned left, ran into the curb stone and collided with one mailbox on the wall of the building finally. The yellow arrow and red curve shows the trajectory of host vehicle in Figure 5.8. Detailed collision position (according to GIDAS coordinate), impulse angle, post- and pre- impact states are shown in Table 5.11.

Table 5.11. GIDAS collision information of Case C.

Vehicle	Impact position [m]			Impact part	Impact angle [deg]	Pre-impact states [m/s],[m/s],[deg/s]			Post-impact states [m/s],[deg],[deg/s]		
	X	Y	Z			v_x	v_y	w_z	PIV	PISSA	$\Omega_{z,PI}$
Host	1.5	0.6	0	Right (2)	126	8.3	0	0	7.78	38	252
Bullet	0.4	0	0	Front (1)	-161	12.2	0	0	5.5	-	269

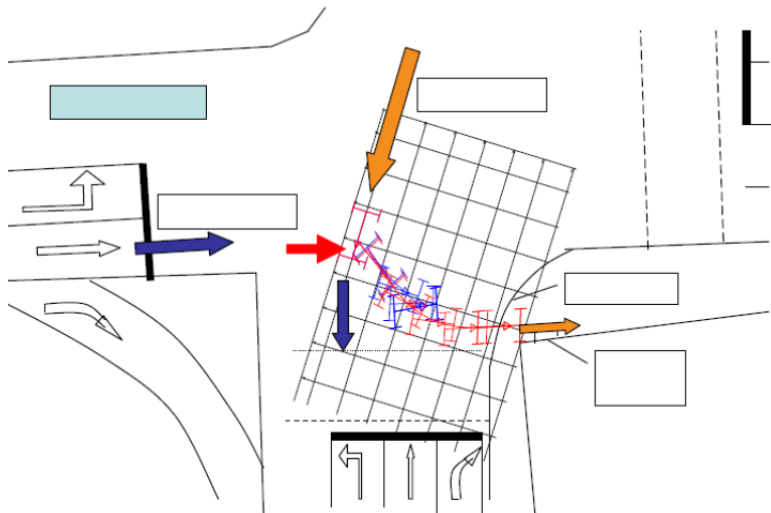


Figure 5.8. Collision trajectory of Case C. <Source: (Yang, 2009)>

If GIDAS given pre-impact information is used to reconstruct the accident, it is impossible to reach such large PIYR even with SLf at minimum zero value. For host vehicle, the surface friction is in opposite direction to the relative speed of these two vehicles, which only generate negative yaw rate and enlarge the PIYR differences. Therefore, the post-impact states differ from the ones supplied by GIDAS starting from the same pre-impact information; this implies that the GIDAS reconstruction model used differ significantly in some GIDAS cases. However, from the Figure 5.8, the positive PIYR and PISSA is reasonable to generate such trajectory.

5.3.3 Summary of example cases

There are nine representative cases (between 17 vehicles) that have been tested. These cover: three large yaw rate cases (all with $PIYR > 200$ [deg/s]), one pure side slip case, two cases of large PISSA with small PIYR or large one, and three middle level collision cases. The simulation model supplied results are shown in Table 5.12, where the two bold cases are incorrect.

There are two incorrect cases in total. One of them has large impulse magnitude for the host vehicle but relatively small one for the bullet car. The post-impact states generated by the simulation model even have different sign with GIDAS data. The other incompatible case's GIDAS post-impact states have similar trajectory, but the simulation result is much smaller in magnitude. However, for safety or capability reason, these severe cases would not be repeated by any rigs for later study.

Without the two incompatible cases (7 cases left), 13.3 % cases need to be tuned before they are similar to the GIDAS given post-impact states. As mentioned above, these nine cases almost covers and proves the accuracy of light impact cases, such as $PIYR$ within 220 [deg/s], PIV within 30 [m/s] and all PISSA situations. Hence, the rig evaluation could use GIDAS coverage database as standard. The detailed nine cases' simulation result and GIDAS information is shown in Appendix F. Collision Model.

Table 5.12. GIDAS verification result.

No.	SLf [m]	Vehicle	$Imag$ [Ns]		PIV [m/s]	PISSA [deg]	PIYR [deg/s]
1	0	Host	7740	Simulation	30.26	8.8	-81
				GIDAS	30.2	8	-86
	1	Bullet	7750	Simulation	25.21	7.2	-97.7
				GIDAS	25	9	-97.4
2	0.72	Host	4100	Simulation	17.6	-5	41.5
				GIDAS	18.61	-10	45.84
	0.72	Bullet	4300	Simulation	16.2	-5.2	25.6
				GIDAS	17.5	-7	28.65
3	0.5	Host	7873	Simulation	6.8	64.6	-75.4
				GIDAS	7.78	38	252.1
	0.6	Bullet	8945	Simulation	5	-8.3	-59.2
				GIDAS	5.5	-54	269.3
4	0	Host	8146	Simulation	12.9	-9.5	-96.9
				GIDAS	13.1	-12	-126
	0.72	Bullet	8250	Simulation	9.5	13.13	114
				GIDAS	10.56	19	114.6
5	0.8	Host	5000	Simulation	14.6	36.6	-132
				GIDAS	13.89	-48	343.8
	0.7	Bullet	26250	Simulation	6.56	-11.6	-163
				GIDAS	15.83	-92	315.1
6	1.15	Host	6300	Simulation	15.6	-38	219.7
				GIDAS	15	-44	217.7
7	0.49	Host	5500	Simulation	11.55	-13.9	-0.04
				GIDAS	11.94	-20	0
	0.64	Bullet	5480	Simulation	9.854	4.4	37.67
				GIDAS	10.23	11	37.38
8	0.86	Host	5625	Simulation	0.95	-98	17
				GIDAS	1.11	-107	17.2
	0.43	Bullet	5417	Simulation	6.11	-125	166.6
				GIDAS	6.11	-130	166.2
9	0.5	Host	11306	Simulation	6.8	65.6	175.6
				GIDAS	9.44	73	172
	0.6	Bullet	11519	Simulation	15.52	-21	71
				GIDAS	16.11	-27	68.8

6 Rig Candidates

From the brief list in Chapter 2.7 Different solution alternatives on hand a study of the capabilities of each rig solution is done based on data acquired through literature study, survey trough internet and contacting the manufacturers. Three candidates were studied without a complete collision simulation because they showed already at early stages not being suitable for the intended tests; Skidcar system, Water cannon and Kick bar.

The different test methods might destabilize the host vehicle by internal forces or by external forces, though the origin of them are not vital for the project but what is generated at the PI time point, as seen in Table 1.1. In this way of thinking the rig candidates will be able to adopt very different constructions appearances and different capability patterns. Then using a similar data post processing as in GIDAS cloud, the simulation results arranges in an own PI data cloud.

At the left part of Figure 6.1 there is a PI states in the so called phase plot, where the accident cases are distributed throughout. At the right there is a polygon formed by the most exterior points from the centroid, this area encloses all the cases despite at which velocity they happened. The area is calculated with the Surveyor area formula.

The plot at the left and right are based in the same data but the right one represent a volume that encloses the clouds with help of the most external points, making the polygons not 100 % accurate because they enclose volumes that have not been simulated. Nevertheless, this representation is useful for simplicity reasons, especially because then it is possible to reduce the amount of simulated velocities.

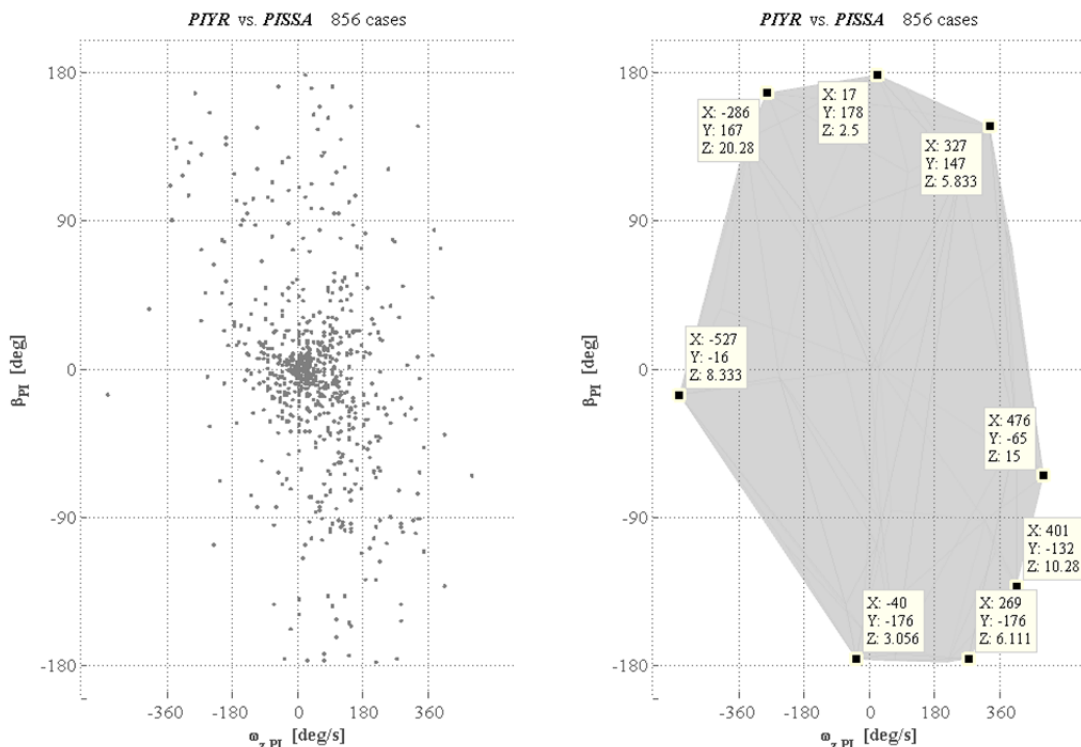


Figure 6.1. GIDAS cloud of real accident cases.

To differentiate them are the GIDAS cloud only coloured with grey scale colours, and the rig clouds will be distinguished with an own colour:

- Red for Kick plate
- Green for PIT manoeuvre
- Blue for Built-in actuators
- Yellow for Simulator SIM4

Then, all the rig solutions will be graded with a number from 0 to 5 on how well the solution meets the criteria in a vector that represents its strengths and weaknesses.

6.1 Skidcar System

As mentioned before, this solution is intended to generate a safe training environment where vehicle instability situations are desired. The skidcar effectively reproduces a loss of traction making the vehicle to behave in a very similar form that in situations where this occurs, as on icy roads or on wet leaves ground.

The metal frame under the vehicle provides two main positions, a lowered position and a raised position, where the control unit permits all the positions in between, including independent action at front or at rear. The frame is provided with four smaller dolly wheels that rotate freely in its local y- and z-axis, as a shopping cart wheel, see Figure 6.2. When raised all the weight of the car is suspended by the frame and this condition is the one that replicates a friction loss with the ground.

This ingenious method decreases the reaction forces from the tyres when inducing a destabilizing force, and this implies the possibility lowering the destabilization forces to reach the same requested destabilized state as in regular driving. It can be used alone or in combination with other solutions.



Figure 6.2. Skid Car System and a training vehicle. <Source: (Skidcar.com, 2011)>

This frame has four arms with a linear pneumatic actuator on each, attached to these actuators are the smaller dolly wheels. When injecting compressed oil into the pneumatic actuators the steel frame is raised, lifting the entire vehicle from the ground. Doing this the horizontal forces decrease because of the direct relationship with the current μ coefficient and the normal load.

The car is held to the dolly by four bushes that are attached to the wishbones, this restricts less the vehicle dynamics, according to the constructors. Once the requested

states are achieved the frame can drop the vehicle to regain the full grip where the intended verification method can begin.

Advantages are that the test vehicle requires no modifications at all to work, a relatively quick delivery time within a few months with a full customisation manufacture. Full customized equipment was estimated to 300 kSEK without taxes. This includes rig with oil compressor and controls, training course, different vehicle mounts and mounting tools. The high safety and flexibility has made this method already proven by different car manufacturers to test active safety functions as ESC.

Among the disadvantages is mainly the limited range of instability when working alone, the low repeatability and the low data accuracy, therefore a very high driver requirement to compensate. The heavy added weight and yaw inertia must be taken into account as disturbances to the host vehicle.

Nevertheless, the dolly frame has potential combined with other rig or rigs, making the host vehicle more susceptible to instability and taking less damage. And fortunately is the rig's CoG very close to the vehicle's CoG making the added rotational inertia less influential.

Parameters⁵:

Added mass \approx	310	[kg], 19 % of S60 mass
Added rotational inertia \approx	800	[kgm ²], 25 % of the S60 yaw inertia
Dimensions =	3.6	[m] x 2.7 [m]
Lift capacity, up to \approx	2000	[kg]
Raising time \approx	3-5	[s]
Sinking time \approx	1-2	[s]
Maximum speed \approx	80	[km/h] and more provided a proper test track.
Price \approx	33100	[€] (@February2011)

This solution will not be studied more in detail and will pass to Chapter 9 Future work as combination with other solution.

⁵ Calculation based in parameters from telephone interview with the manufacture, and information on the web page (Skidcar.com, 2011).

Rig candidates	Ranked characteristics															
	Driver safety	High reproducibility	Data accuracy	Broad range of impulse positions	Broad range of impulse strength	Gain other tests	Low driver requirements	Broad range of impulse angles	Low damage to equipment	Low construction complexity	Low build-up rig investment	Short rig development time	Fast reload time	Practical movability	Low timing complexity	Low complexity for tesis
Skidcar system	5	0	0	1	0	3	0	1	5	5	5	5	5	5	0	5

Performance 1. Ranked characteristics and performance grade of Skidcar System.

6.2 Water cannon

This device has been developed by Ford Cars aimed to produce instability similar to light collisions. The Water cannon is an equipment that shoots water. At the moment that the water is expelled at very high velocities the reaction forces destabilize the vehicle making it deviate from its intended direction. In Figure 6.3 it is seen how the combination of water and compressed air ejects from the rear side.



Figure 6.3. Water cannon expelling a blast of compressed air and water. <Source: (Jalopnik.com, 2009)>

The cannon consists of four main parts: A compartment of compressed air, a compartment of water, a valve between the compressed air and water, a thin plastic membrane between the water compartment and the exterior free air. Prior to the test some security features are removed as a steel plate between the water and the thin plastic membrane. Driving the vehicle at some original velocity and the destabilization is requested the valve that retains the compressed air opens suddenly pushing the water violently against the water volume, this breaks the fragile membrane that hold it on place.

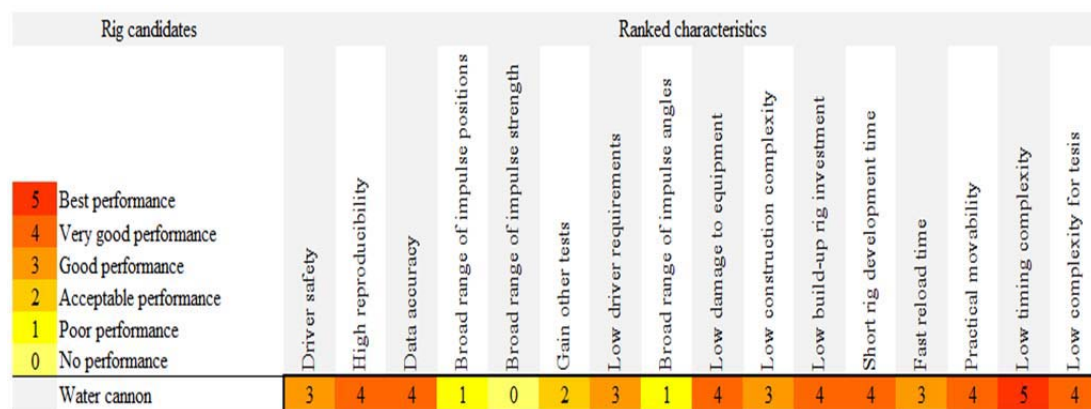
Some upgrades were planned in terms of higher power, reduced size and weight, more flexibility of location, and increased flexibility of the nozzle direction and position.

Advantages are mainly the simplicity of the rig and the practical aspects that comes along with it as a relative low price, reduced amount of parts and is relatively low tech. The added mass is relatively low at the Post-Impact time segment with just the discharged cannon. The fast reload time is a benefit as well.

The current solution has the drawbacks of: too weak impulse strength, added mass far from the CoG increasing the added yaw inertia and at the studied cannon layout only perpendicular impulses to the cars x-axis. A drawback for other studies is the pre-impulse weight change and CoG change.

Parameters⁶:

Added mass (unloaded) ≈	50 [kg], 3 % of S60 mass
Added rotational inertia (unloaded) ≈	130 [kgm ²], 4 % of the S60 yaw inertia
Dimensions ≈	0.3 [m] x 2.0 [m]
Approximated impulse capacity ≈	2.5g·m·tc ≈ 7800 [Ns]
	20 % of the maximum impulse threshold
	80 % of the impulses mean value
Reload time:	< 30 [min]
Speed range:	none provided a proper test track.



Performance 2. Ranked characteristics and performance grade of Water cannon.

⁶ Calculation based in parameters from telephone interview with the test personnel at Ford, and information on the web page (Jalopnik.com, 2009).

6.3 Kick plate

Kick plate is a part of a training track where the kick plate's function is to destabilize the vehicle passing over it, and forwarding it to a low friction surface as Figure 6.4 shows. The Wet Grip Area was designed for vehicle testing and driver training, the low friction surface recreates the slippery caused by icy roads, rain, or wet leaves. This method is a well proven destabilization method used by manufacturers, dealers and customers to test the benefits of new technology in a safe environment. It has a high repeatability and with the complete test track the possibilities are great. Drawbacks of this rig are the high price and high construction complexity.



Figure 6.4. Kick plate shifts a passing car into a low friction area. <Source: (rockingham.co.uk, 2011)>

For the test method regular asphalt in front of the kick area is needed. i.e. the same road condition as the traffic accident have. Hence, just the Kick plate will be considered in this section.

The plate is powered by a hydraulic piston buried near the plate that is suddenly filled with compressed oil when the vehicle triggers detection sensors slightly in front of the plate. As the vehicle's rear axle passes through the plate kick violently at the side.

6.3.1 Parameters

There are five components in Kick plate: galvanized sliding plate; galvanized frame with steel sheeting on the sides and open bottom; entire hydraulics beneath the sliding plate; control box with operating elements and external speed indicator (GmbH, 2010). The detailed parameters of each part are shown as follows.

Load Rating and Dimensions:

Max. Gross Axle Weight Rating	3000	[kg]
Max. Vehicle Gross Load Weight	6000	[kg]
Sliding Plate Depth	2.96	[m] or 4.96 [m] (two alternatives)
Clearance Width	3.75	[m]

Dynamic:

Speed Range (Vehicle)	30-90	[km/h] (lower and upper limit adjustable)
Max. Acceleration (Sliding plate)	2 g	[m/s ²]

Max. Speed (Sliding plate) \approx	3.0	[m/s]
Max. Offset (Sliding plate) \approx	0.45	[m]
Max. Stroke (Sliding plate) \approx	0.9	[m]
Reload time \approx	12	[s]

Hydraulic:

Main Tank Volume \approx	0.1	[m ³]
Operation Pressure \approx	170	[bar] or 17.0 [MPa]
Accumulate Tank Volume \approx	0.02	[m ³]

Price:

Kick plate \approx	114000	[€] (@December2010)
----------------------	--------	---------------------

(Without taxes, shipping and installation costs)

6.3.2 Limitation analysis

Kick plate uses the tyre generated friction force to build-up the impulse. There are five possible factors in total, which could be categorized into two factor groups:

Tyre friction factor:

- plate lateral acceleration
- hydraulically stored energy

Force build-up time:

- plate lateral speed
- plate lateral stroke
- plate size

6.3.2.1 Tyre friction limitation

With the highest plate acceleration, around $2g$ [m/s²], the physical analysis supply the vehicles highest lateral acceleration, around $1g$ [m/s²]. Through normal tyre parameters and conditions the largest friction coefficient $\mu=1$ is provided by the plates special surface.

The other limitation is the hydraulically stored energy. Assuming a linear decrease of the largest pressure until zero as the fluid fills the pneumatic chamber; the maximum stored energy could be calculated as equation (6.1), where W is the total stored energy, V is the tank volume, Y and P_{max} represents sliding plate's maximum offset and pressure respectively. From equation (6.2), knowing that the plates maximum acceleration, for a 1650 [kg] vehicle, exceeds $1g$ [m/s²] and thus would not significantly limit the kick plate. Consequently, the largest kick force that can be generated is the tyre normal load or equivalent axle load for $\mu=1$.

$$W = P_{max} \cdot \frac{V}{2} = 17 \cdot 10^6 \cdot \frac{0.02}{2} = 170 \text{ [kNm]} \quad (6.1)$$

$$a = \frac{F}{m} = \frac{W}{(2Ym)} = \frac{170 \cdot 10^3}{(2 \cdot 0.45 \cdot 1650)} = 114 \left[\frac{m}{s^2} \right] \approx 11.4 \cdot g \text{ [m/s}^2] \quad (6.2)$$

6.3.2.2 Kick duration constraint

Kick duration depends on two periods: how long time the vehicle would leave the plate and how long time the plate can provide kick force. The first effect is relying on the sliding plate size and the initial longitudinal speed of passing vehicle. The second one depends on sliding plate features: maximum speed and stroke.

The track width of common passenger car is about 1.8 [m], which is much less than the plate width. For short depth plate, it is easier if it is assumed that the plate depth have the same length as the wheelbase, so that there is no situation for both track axes locate on the sliding plate and use 2.7 [m] as the short depth instead of 2.96 [m] for later simulation.

The simulation result with the bicycle model shows that the longitudinal velocity is only varied within 5 % by the kick disturbance. Thus, the maximum time that the car would leave the plate can be expressed as equation (6.3), where D is the plate depth and V_0 represents the initial velocity of testing vehicle. Figure 6.5 demonstrates the single axle leaving time comparison between longitude velocity changes considered duration and equation (6.3) calculated result. Assuming the difference between them is negligible the equation (6.3) is used to obtain T_{leave} .

$$T_{leave} = \frac{D}{V_0} \quad (6.3)$$

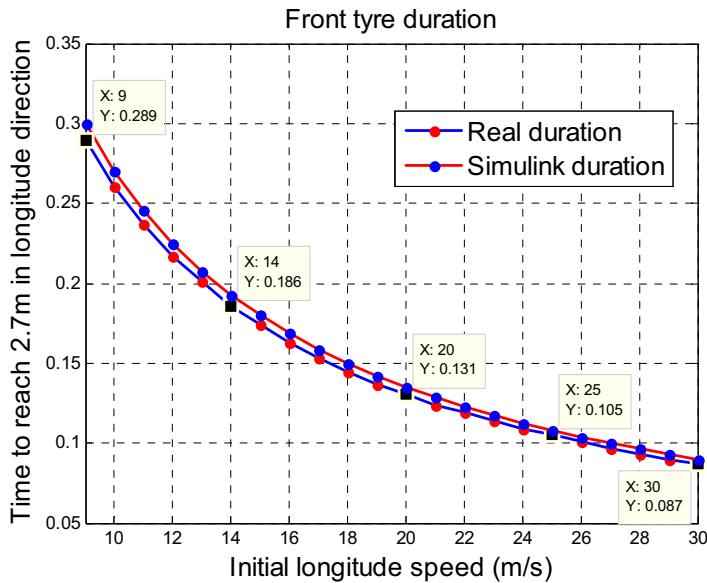


Figure 6.5. Comparison of time T_{leave} .

In the Kick plate datasheet it is stated that it takes 25 [ms] for a loaded plate to increase its acceleration to $1.1 \cdot 1g$ [m/s^2]. Assuming a linear acceleration, the velocity would increase to 0.14 [m/s] at 25 [ms]. In this case, the plate acceleration can step up to $1g$ [m/s^2] when vehicle axle reaches plate edge without any stroke consumption.

The second period is the time that sliding plate boundary is reached. The sliding plate acceleration is $1g$ [m/s^2] and the time that reach maximum speed and stroke are shown in equation (6.4) and (6.5) respectively. It is possible to see that the maximum speed is the real constraint. At 0.3 [s], only half of the maximum stroke is reached.

$$g \cdot T_{speed} \leq V_{max} = 3 \text{ [m/s]} \Rightarrow T_{speed} \leq 0.3 \text{ [s]} \quad (6.4)$$

$$\frac{1}{2} \cdot g \cdot T_{stroke}^2 \leq 2 \cdot 0.45 = 0.9 \Rightarrow T_{stroke} \leq 0.43 \text{ [s]} \quad (6.5)$$

By combined the above time limitations together, the kick time could be calculated by equation (6.6). It implies that for short depth plate, as initial speed lower than 9 [m/s], kick period reach its peak with 0.3 [s]. As vehicle speed increase, the kick time decrease simultaneously.

$$T_{kick} = \min(0.3s, T_{leave}) \quad (6.6)$$

6.3.3 Kick plate strategy

With two different depth plate alternatives it is possible to generate five destabilizing strategies: wheelbase depth's sliding plate (2.7 [m]) with only front or rear kick, long depth sliding plate (4.96 [m]) with only front or rear kick and two short depth sliding plates generating simultaneous kicks. Whatever the strategy is, the kick force is equal to the normal load on the plate and directed towards the plates movement.

The short depth plate movements are shown in Figure 6.6, where X is the axle position in plate coordinates and Y is the sliding plate movement from -0.45 [m] to 0.45 [m], or vice versa. Front kick strategy starts at front axle reach $X=0$ and rear one starts at rear axle reach. Plate stops when the front or rear axle leave the plate. Kick time is calculated by equation (6.6). For two simultaneously kicks' case, the two sliding plates are combination of Figure 6.6 but with opposite moving direction for rear kick.

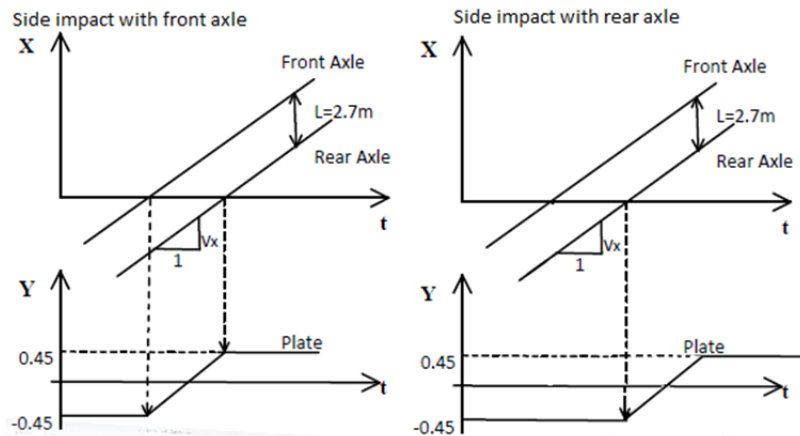


Figure 6.6. Short depth plate with only front or rear kick strategy.

Long depth plate kick strategy has the same start time as short ones does and the ending time is also based on equation (6.6), where T_{leave} is calculated with $D=4.96$ [m] this time. Long depth plate allows two axles stand on the sliding plate at the same time and generate larger side slip angle. Besides, Long depth plate has longer T_{leave} which is suitable to test larger speed cases.

6.3.4 Simulation result

Except above sliding plate limitations, kick plate capability is also determined by the passing vehicle's initial longitudinal velocity. The maximum kick time is defined as the post-impact point and post-impact states is the vehicle dynamics at that point. The relevant post-impact states of different speed are shown in Figure 6.7. It is easier to image that as kick period decrease, PIYR and PISSA would reduce simultaneously.

Kick plate is suitable to simulate lower speed case with PIYR smaller than 81 [deg/s] and PISSA smaller than 13 [deg]. Besides, except two only front kick cases, all other strategies generate different sign's PIYR and PISSA. Compare to front axle, rear axle kick is easier to destabilize passing vehicle and get larger post-impact states.

Figure 6.8 shows the trends of PIYR vs. PISSA as kick time varies. It is clear to see that not all dots in right rectangle could be reached by kick plate but somehow limited around its maximum kick time curve, except long depth plate with only rear kick. The largest PIYR and PISSA are happened when initial velocity is lower than 9 [m/s].

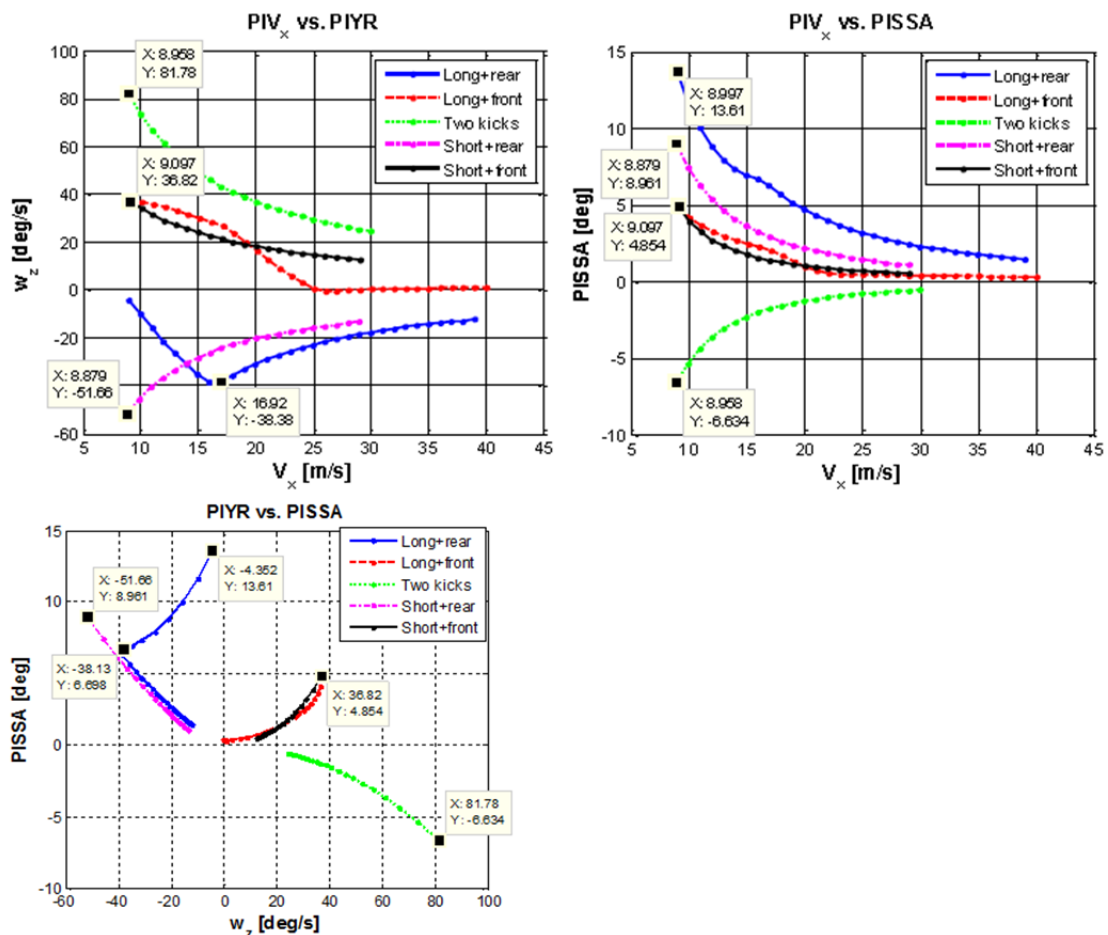


Figure 6.7. Peak value of PIYR and PISSA.

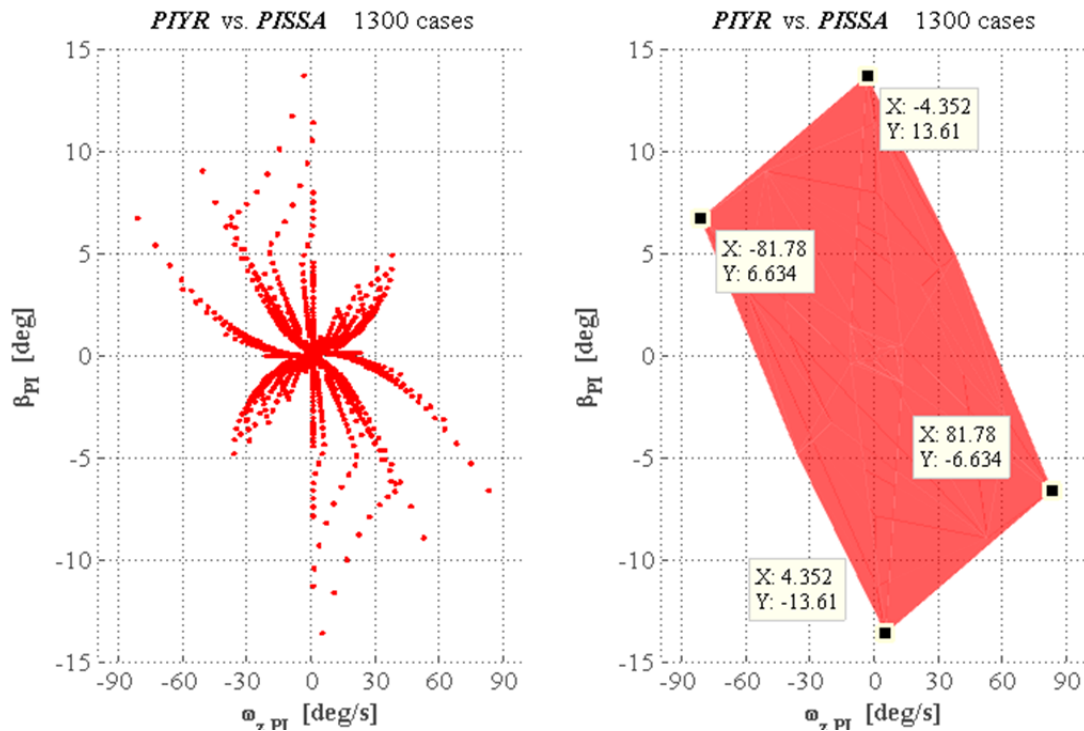


Figure 6.8. Rig cloud of simulated Kick plate.

Rig candidates		Ranked characteristics															
		Driver safety	High reproducibility	Data accuracy	Broad range of impulse positions	Broad range of impulse strength	Gain other tests	Low driver requirements	Broad range of impulse angles	Low damage to equipment	Low construction complexity	Low build-up rig investment	Short rig development time	Fast reload time	Practical movability	Low timing complexity	Low complexity for tests
		5	4	3	2	1	0	0	0	0	0	0	0	0	0	0	0
		4	4	4	1	3	5	5	2	4	0	0	3	4	0	4	3
	Kick plate	4	4	4	1	3	5	5	2	4	0	0	3	4	0	4	3

Performance 3. Ranked characteristics and performance grade of Kick plate.

6.4 PIT manoeuvre

Precision Immobilization Technique or PIT manoeuvre is a method by which one car pursuing another can force the pursued vehicle to abruptly turn sideways to the direction of travel, render the driver lose control. This is a judicious method for policemen to terminate a hazardous vehicle pursuit situation. By vehicle collision, certain impact is purposely generated to reach PI states of host vehicle, which is used for safety function verification. In difference with real accidents, the test colliding vehicles can be previously protected by steel covers to minimize the damage. Besides that, a significant factor is the willingness of being stopped and the environment layout that should be safer.

One procedure is (Zhou, J. et al., 2008): the PIT begins when the pursuing vehicle pulls alongside the fleeing vehicle so that the portion of the pursuer's vehicle forward of the front wheels is aligned with the portion of the target vehicle behind the back

wheels; the pursuer gently makes contact with the target's side, then steers sharply into the target; as soon as the fleeing vehicle's rear tyres lose traction and start to skid, the pursuer brakes quickly while continuing to turn in the same direction until clear of the target. The impact of this procedure is happening on the rear side as Figure 6.9 shows.

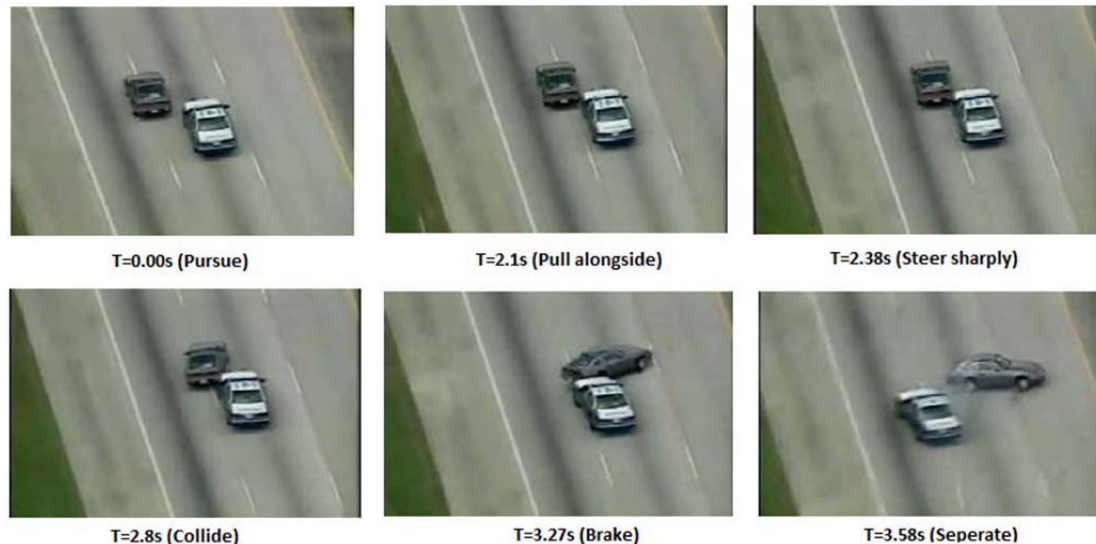


Figure 6.9. A real PIT manoeuvre record (Zhou, J. et al., 2008)

6.4.1 Limitation

After considering driver safety, PIT manoeuvre is applicable under certain situations. In some studies, PIT is considered as non-deadly force when properly executed at the maximum speed of 80 [km/h] (Pinellas County, 2007). The other two limitations are maximum transient acceleration and velocity changes after collision on CoG.

Ground force is a form of resistance for an object in motion, which would decrease the impact force effect. Hence the maximum transient acceleration is at the collision start point. In Figure 6.9, the collision duration is around 1 [s] but 0.2 [s] for most real accident (Brach, 2003). To guard for the purpose of safety, 0.2 [s] is used to calculate relevant impulse and impact force. Although not fully validated, the neck injury criterion below $1.53 \cdot g$ [m/s^2] is suggested to avoid risk for long-term impairment (Boström, O. et al., 1996) and (Eichberger, A. et al., 1998). For rear-end collision, driver seat could supply good protection and decrease the acceleration to almost half (Jacobson, L., 2000). Consequently, choose maximum acceleration at CoG to be $2 \cdot g$ [m/s^2] for rear-end crash and $0.8 \cdot g$ [m/s^2] for side impact. PIT manoeuvre capability is limited within 6500 [Ns] for rear and 2500 [Ns] for side impact. The velocity change is 14.2 [km/h] and 5.5 [km/h], which would not trigger the airbag protection system.

6.4.2 Simulation result

PIT manoeuvre is a purposely two vehicles' collision. During simulation, the input signal for each vehicle is an impulse or say 0.2 [s] step impact force. Hence, the simulation result analysis only includes one car with certain impulse as input, but not two collided vehicle as real accident. For safety purpose, host vehicle is crashed at rear-end or side rather than face to face collision at front.

6.4.2.1 Influences of road adhesion

To study the influence of road adhesion, choose one rear side impact case with perpendicular impulse. The magnitude of impulse is 6700 [Ns] or 2250 [Ns] with road friction coefficient equal to 0.5 or 0.9. The initial velocity is 15 [km/h] and relevant PIYR and PISSA is shown in Figure 6.10. Friction coefficient influence is so small that could be neglected for both large and small magnitude impact cases. It is mainly because tyre relaxation limits the increase rate of tyre lateral force within collision duration (0.2 [s]) and impact force (33500 [N] or 11250 [N]) is large enough to be the main determination of post-impact states.

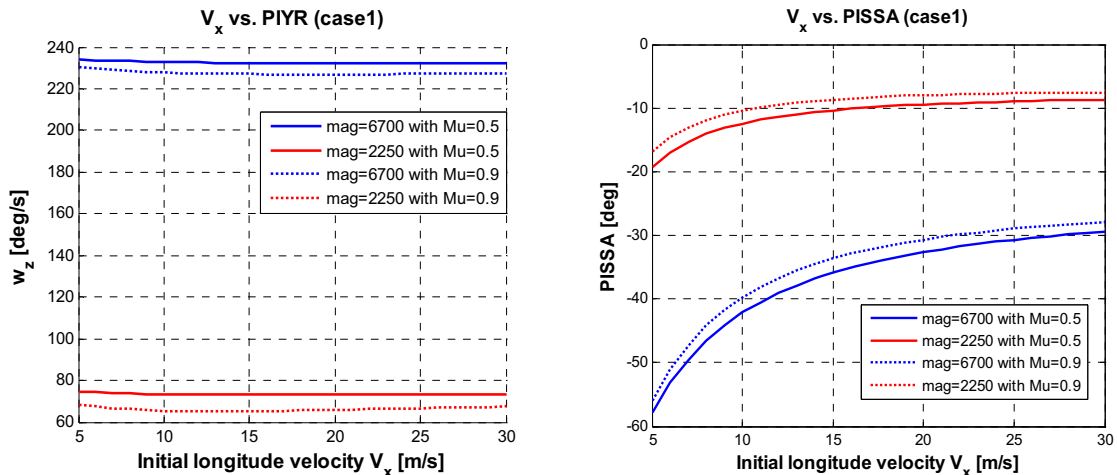


Figure 6.10 Influences of road adhesion.

This section demonstrates the trend of PIT manoeuvre provided PI states through two groups of impulse information: rear-end kick and side impact. The initial velocity of host vehicle is 15 [m/s] (54 [km/h]). Figure 6.11 shows the post-impact states with all possible impulse angle [-90 90] degrees and y-axis position [0 0.8] meters of rear-end impact case. Besides, two different impulse magnitudes are studied.

Each group of dots represents the same impulse angle but different position, which implies the position would not influence the post-impact states dramatically for rear-end cases. Hence, there is no exact demand for bullet driver to crash the bullet car with specific rear-end point but correct angle. The 'PIYR vs. PISSA' figure shows that rear-end PIT manoeuvre only can reach the case where PIYR's absolute magnitude is around ten times of PISSA's, even with smaller impulse magnitude. Besides, PIYR and PISSA should have opposite sign with each other unless PISSA is around zero.

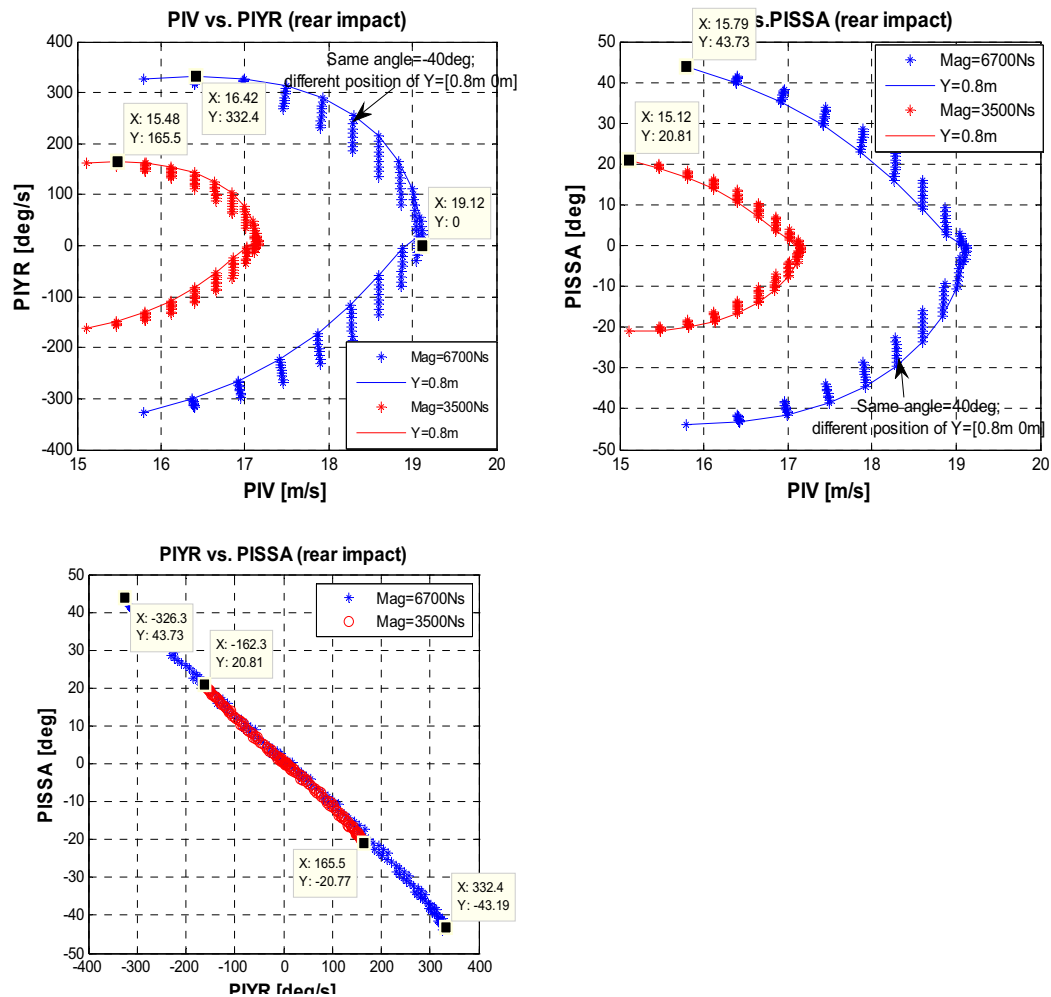


Figure 6.12. Post-impact states of rear-end kick PIT manoeuvre.

The same as rear-end case's figures, side impact plots also cover all possible impact position and angle with weak impulse magnitude (2500 [N]). For side collision, large magnitude impact would threaten the safety of the host vehicle's driver and might result in rollover. Therefore, using side impact it should be done with careful planning, especially for the front side part. Figure 6.13 shows the 'PIYR vs. PISSA' plot of side impact, which covers a wider ratio of PIYR and PISSA than rear-end impact. For smaller PISSA, it is possible to have the same sign PIYR and PISSA through side impact PIT manoeuvre.

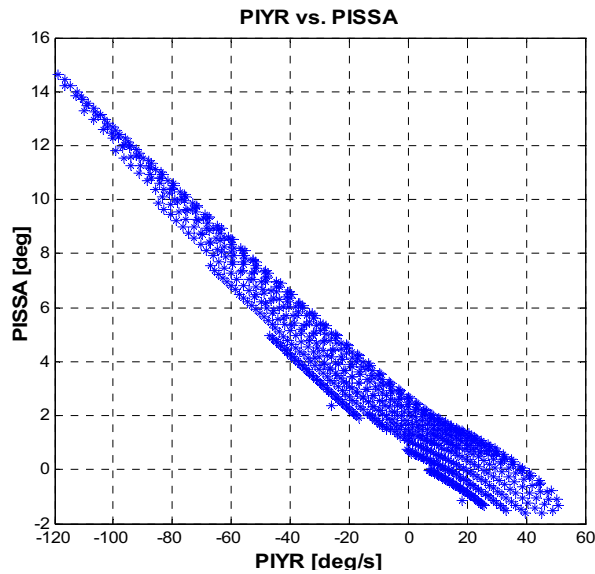


Figure 6.13. *PIYR vs. PISSA of side impact cases.*

6.4.2.3 PIT manoeuvre clouds and capability

By simulating different initial longitude velocity with maximum impulse magnitude, the PIT manoeuvre cloud is plotted as Figure 6.14 shows. From the lower until the higher speeds, 5 [km/h] and 40 [km/h], PISSA increases from 36 [deg] to 67 [deg]. For the most extreme cases, PIYR and PISSA should have opposite sign. It is clear that PIT manoeuvre is limited to a narrow area, despite that it can reach generate yaw rate and slip angle up to 330 [deg/s] and 67 [deg], with alternate signs. Most dots in Figure 6.14 locate at the second and fourth quadrant.

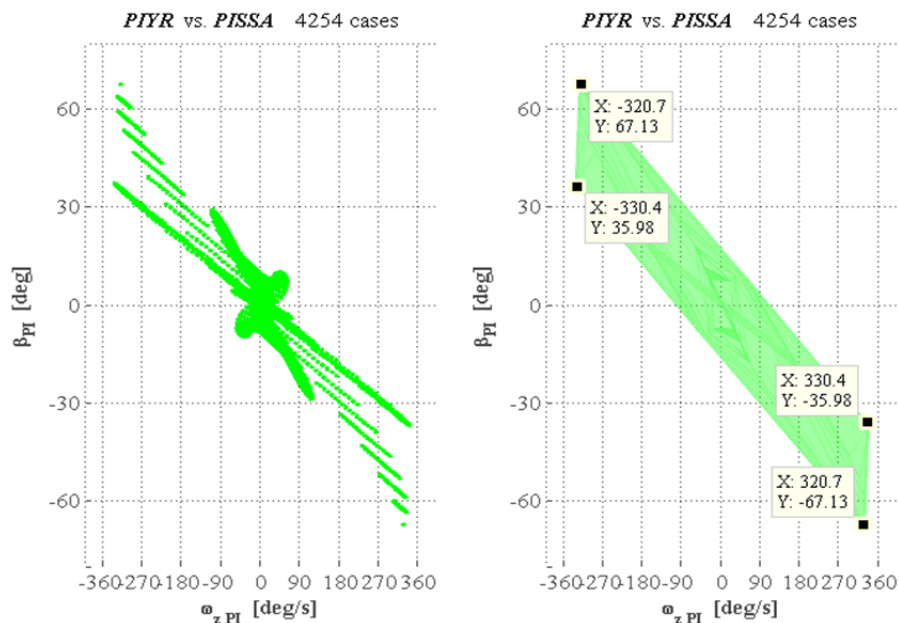


Figure 6.14. *Rig cloud of simulated PIT manoeuvre.*

Rig candidates	Ranked characteristics															
	Driver safety	High reproducibility	Data accuracy	Broad range of impulse positions	Broad range of impulse strength	Gain other tests	Low driver requirements	Broad range of impulse angles	Low damage to equipment	Low construction complexity	Low build-up rig investment	Short rig development time	Fast reload time	Practical movability	Low timing complexity	Low complexity for tesis
PIT manoeuvre	3	3	3	4	3	3	1	3	3	4	4	4	3	3	1	4

Performance 4. Ranked characteristics and performance grade of PIT manoeuvre.

6.5 Built-in actuators

Actuators already installed in production vehicles, Figure 6.15, are used to stabilize them in instable situations, oppositely using the brake system for destabilize the vehicle with the addition of a steer wheel motor that control the front tyres is studied.

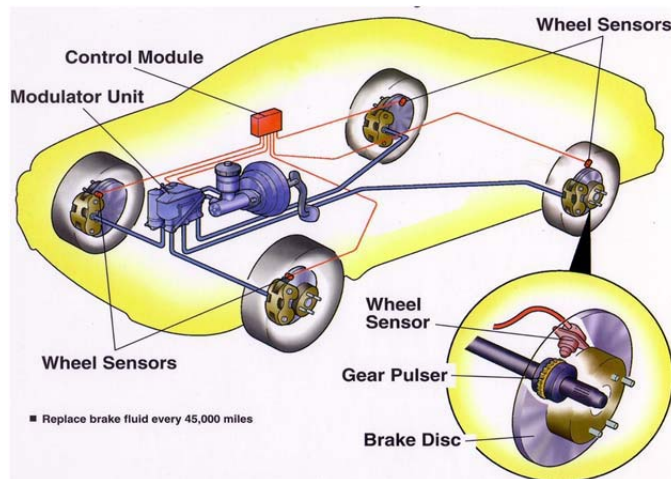


Figure 6.15. Brake system of the Built-in actuators candidate. <Source:(Google) >

Theses built-in actuators mentioned in this section involves steady-state steer and hand brake (brake two tyres in the rear axle). The same as high side slip manoeuvre, commonly known as drifting; it is a cornering technique in which a vehicle is driven beyond its limits of handling at a large side slip angle (Voser C. et al., 2010). The strategy of this sort of steering and braking will be analysed in following. The road condition is assumed to be wet or dry asphalt with road friction coefficient $\mu= 0.5$ or $\mu= 0.9$.

6.5.1 Vehicle dynamic analysis and phase portrait

Use bicycle model to analyse vehicle dynamics, where the front and rear tyres are lumped into a single tyre at each axle and lateral friction represented by $F_{y,r}$ and $F_{y,f}$. After neglected the pitch and roll motion, treated v_x as a time-varying parameter; the lateral and yaw motion could be expressed as equation (6.7) and (6.8).

$$\dot{v}_y = \frac{F_{y,f} \cos \delta + F_{y,r}}{m} - w_z v_x \quad (6.7)$$

$$\dot{w}_z = \frac{a F_{y,f} \cos \delta - b F_{y,r}}{I_{zz}} \quad (6.8)$$

Equation (6.8) indicates that if the rear tyre lateral friction is decreased, yaw rate could increase faster. Thus, hand brake of rear tyre is needed to increase yaw rate. For side slip angle (equation (6.7)), large yaw rate would decrease lateral velocity and thus side slip angle, especially when longitudinal velocity is big. Therefore, the unstable equilibrium of the system defined by above two equations should locate at second or fourth quadrant, where yaw rate and side slip angle have opposite sign. Those unstable regions are the goal for built-in actuator to reach.

Since the longitudinal velocity should be constant during simulation, the thesis adds a simple proportional controller into the system. The feedback signal for controller is longitudinal velocity error $\Delta v_x = v_x - v_x^{ref}$, where the reference longitudinal velocity v_x^{ref} is 8 [m/s]. The output propulsion force is equal to $8000 \cdot \Delta v_x$. The phase portrait is generated by simulating 4-DOF two-track vehicle dynamics model's (shown in section 5.2.1) response at fixed steer angle and fixed longitudinal velocity for a multitude of initial conditions and plotting all of the resulting state trajectories in (β, w_z) plane.

Figure 6.16 shows that there is only one stable equilibrium point, located at (4.7 [deg], 31.54 [deg/s]). Each blue dot represents one initial dynamic state (β_0, w_{z0}) and relevant blue curve is states trajectory as steer angle is 15 [deg] and v_x is 8 [m/s]. All the red circles imply unstable initial states. These points' side slip angle would reduce to less than -90 [deg] for longer simulation time. In this case, it is also impossible for the proportional controller to keep v_x to be 8 [m/s] due to tyre friction limitation.

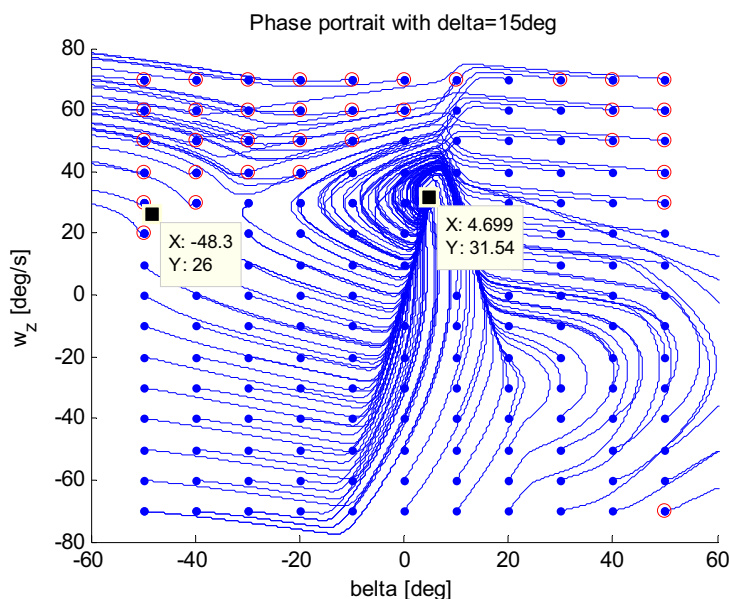


Figure 6.16. Phase portrait of $\delta=15$ [deg] and $v_x=8$ [m/s].

6.5.2 Actuator and friction sensitivity analysis

The strategy for Built-in actuators includes two steps: ramp steer and hand brake. The results of a series of simulations are demonstrated in this section to determine better actuations and its sensitivity for different road conditions ($\mu=0.9$ or 0.5).

6.5.2.1 Steer strategy

This analysis could be separated into three parts: ramp up ratio, ramp down ratio and steer angle magnitude. The tests are did with wet road condition, where $\mu= 0.5$. Initial longitudinal velocity is 12 [m/s], with proportional speed controller to keep it around 8 [m/s].

Figure 6.17 shows the comparison of ramp up steer and step up steer. Comparison figure involve 6 plots: steer and brake actuation, lateral and longitudinal velocity, two post-impact states – side slip angle and yaw rate. Both of these tests are accompanied with hand brake at 0.75 [s]. At 1.5 [s], both tests' steer angle ramp down to -20 [deg] and stop brake. The dynamic states of these two tests are quite similar. Hence, there is no requirement for the ramp up ratio and choose step-up steer for simplification.

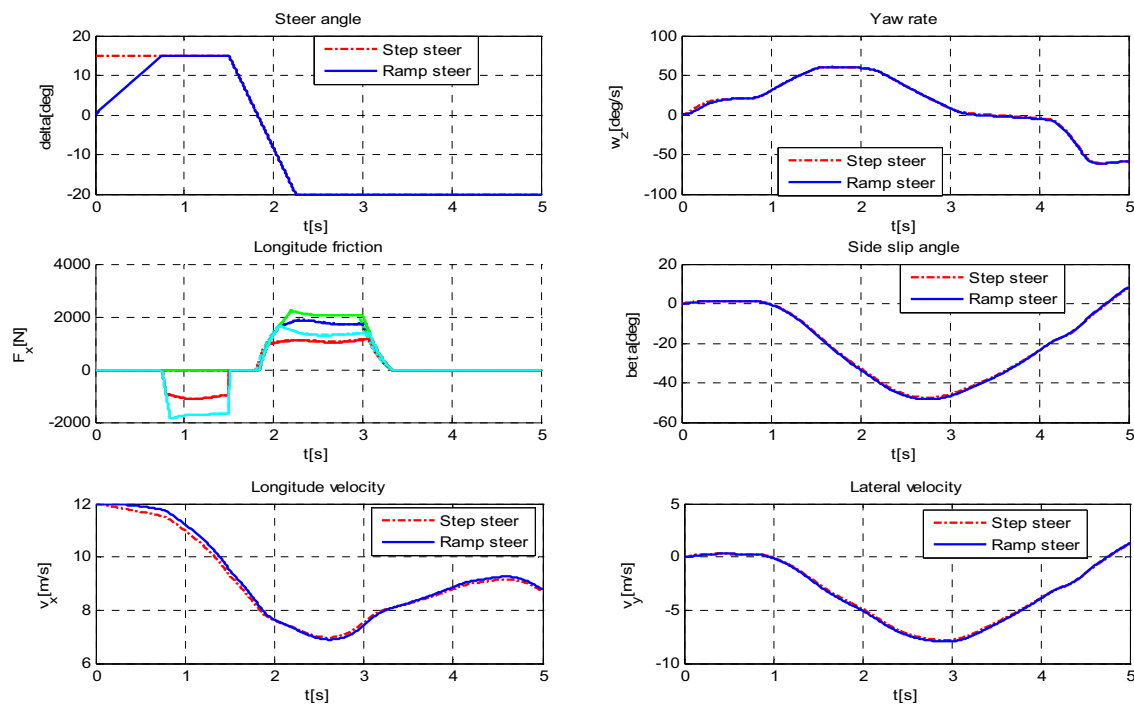


Figure 6.17. Comparison between step-up steer and ramp-up steer.

Four different steer angles are simulated and results are shown in Figure 6.18. As the steer angle increase, the maximum yaw rate and side slip angle would decrease. However, larger steer angle gives quicker increase of yaw rate. Therefore, choose steer angle to be 15 [deg], which have the same maximum yaw rate and side slip angle as 5 [deg] and also destabilize the vehicle fast.

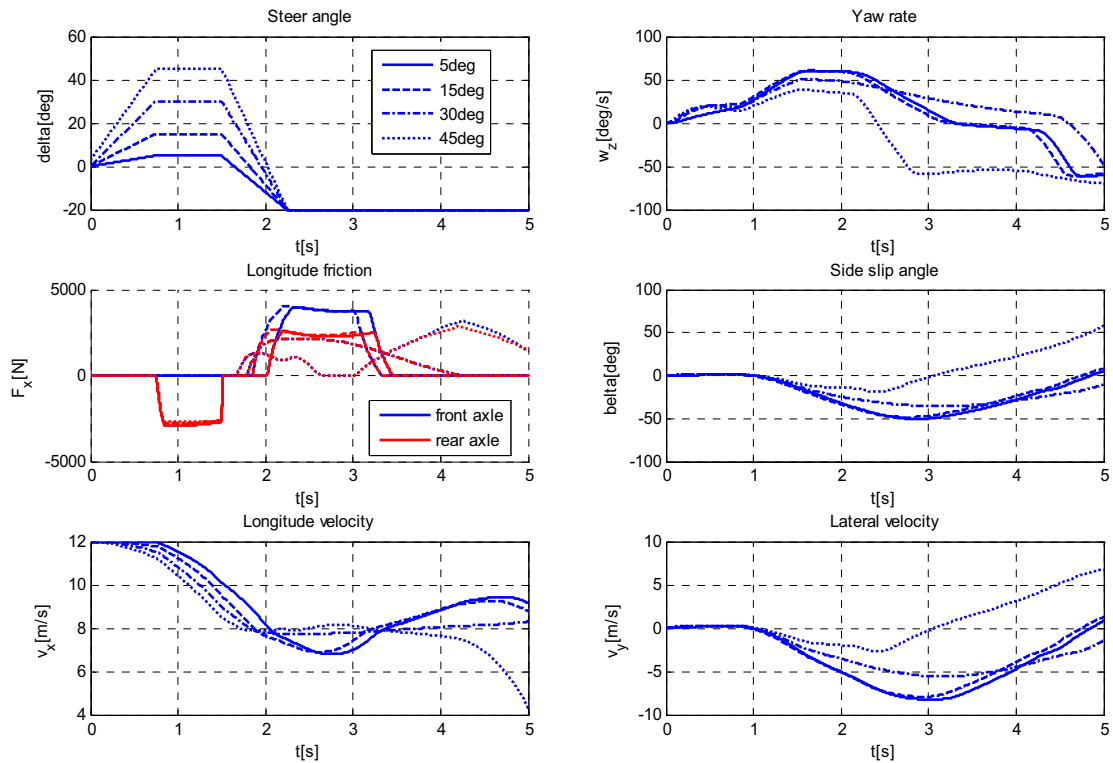


Figure 6.18. Comparison of different steer angle magnitude.

It is easier to image that longer period steer would generate larger yaw rate and side slip angle. Hence, choose to compare the steer strategies that have the same integral but different counter steer methods as shown in Figure 6.19. The ramp down steer strategy would not influence vehicle dynamic states. If the post impact point is defined as the time when steer angle is zero, step down steer strategy is better to get exact post impact states.

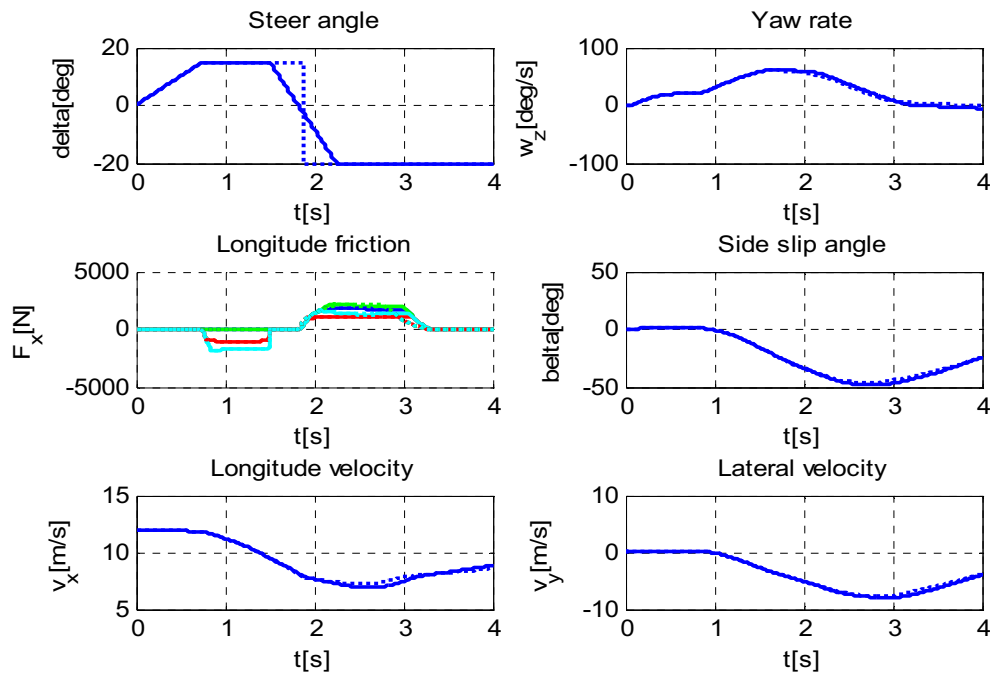


Figure 6.19. Comparison of ramp down steer strategy.

From above analysis, it is clear to see that better steer actuation is: use step-up and step-down strategy with steady-steer angle as 15 [deg]. For larger post-impact states' requirement, prolong the steer and hand brake time is a good solution.

6.5.2.2 Brake strategy

Apart from applying hand brake on both rear tyres, only brake the inner rear tyre is another choice. Thus, the thesis simulate three different cases with the same steer actuation as ramping-up till 15 [deg] at 0.75 [s], last till 1.5 [s] and ramp-down to -20 [deg] at 2.25 [s]. The difference is brake actuation: hand brake during [0.75 1.5] seconds, inner tyre brake during [0.75 1.5] seconds and inner tyre brake during [0.75 1.75] seconds. Comparison result is shown in Figure 6.20.

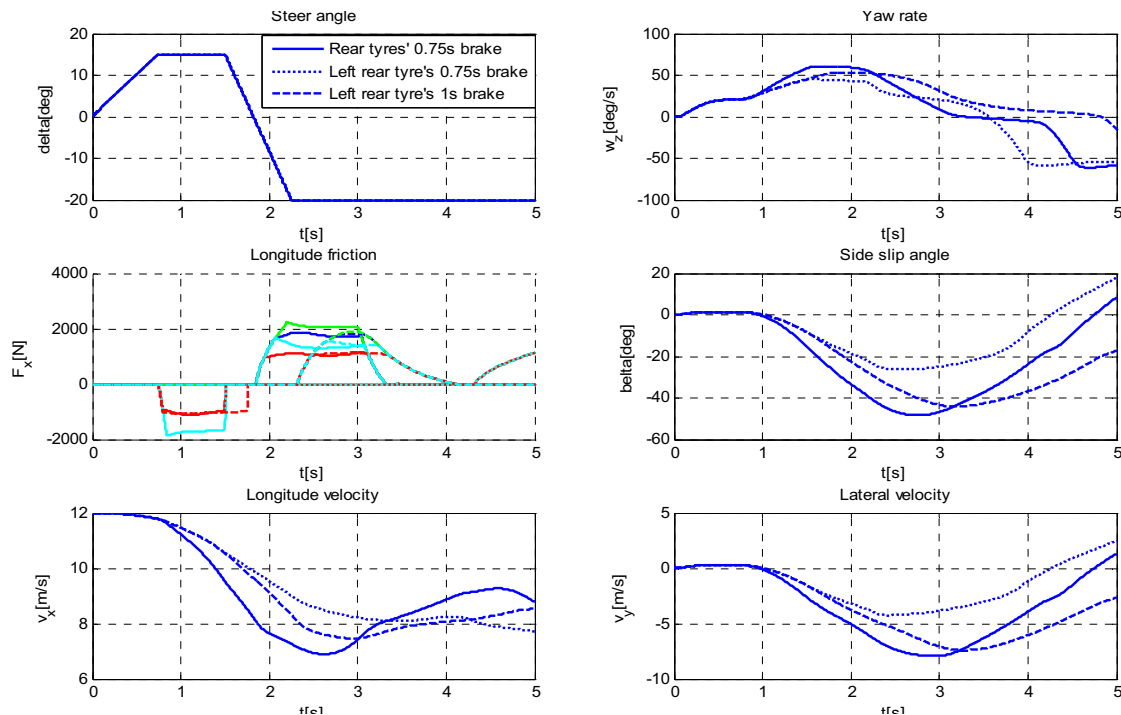


Figure 6.20. Comparison of different brake strategies.

It shows that hand brake is better than only brake inner rear tyre; even after prolonging the braking time of one tyre's case. This is mainly because the outside rear tyre's brake could decrease the arm of force which generate opposite yaw rate. Hence, finally hand brake is chosen to be brake actuation. In addition, as the brake time increases, yaw rate would rise up simultaneously.

6.5.2.3 Sensitivity of road friction coefficient μ

For different accidents, road condition would vary as well. In this case, it is necessary to test the post impact states' sensitivity of different road friction coefficients. Figure 6.21 shows the comparison of $\mu=0.5$ and $\mu=0.9$. Since yaw rate very much relies on the tyre friction, it increases 1.5 times for higher μ case where the tyre forces for yaw destabilization are bigger. In addition, it shows that the difference of side slip angle under these two different road condition is around 6 %.

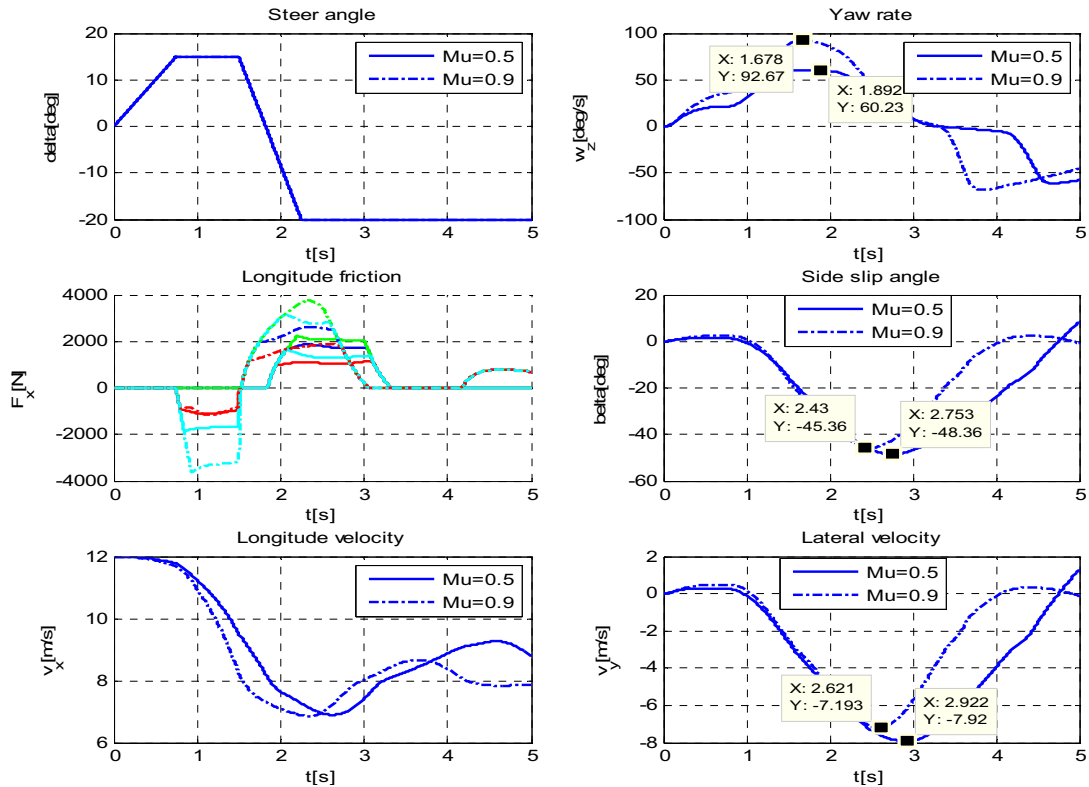


Figure 6.21. Comparison of $\mu=0.5$ or 0.9 with same destabilise strategy.

6.5.3 Actuator strategy analysis

As discussed above, destabilize strategy of built-in actuator is to use step-up and step-down with 15 [deg] steer angle and hand brake after rear tyres are saturated.

For common sense, it is harder to insert a propulsion controller inside the test vehicle. Thus, use higher initial longitude velocity as 20 [m/s] without propulsion controller to test. The three destabilize actuations are shown in Figure 6.22 and the first two actuations state trajectories in phase portrait are shown in Figure 6.23 with red solid curve. The differences of these three actuations are the duration of hand brake and steer. As steer duration larger than 2.25 [s], it is impossible to control the test vehicle, even result in roll-over. Hence, choose 1.75 [s] as the upper bound of steer for later rig capability analysis, which could generate similar yaw rate and side slip angle as longer braking time cases. In Figure 6.22, star represents the time when steer angle back to zero. For detailed description, the two curves in Figure 6.23 represent 15 [deg] steady steer within 1.25 [s]. The hand braking action starts at 0.75 [s] and lasts 0.5 [s] or 1 [s] respectively. The red squares are the dynamic states after the steer angle is back to zero. It is clear to see that all trajectories have entered into the unstable region, which means built-in actuator strategy satisfy our initial goal.

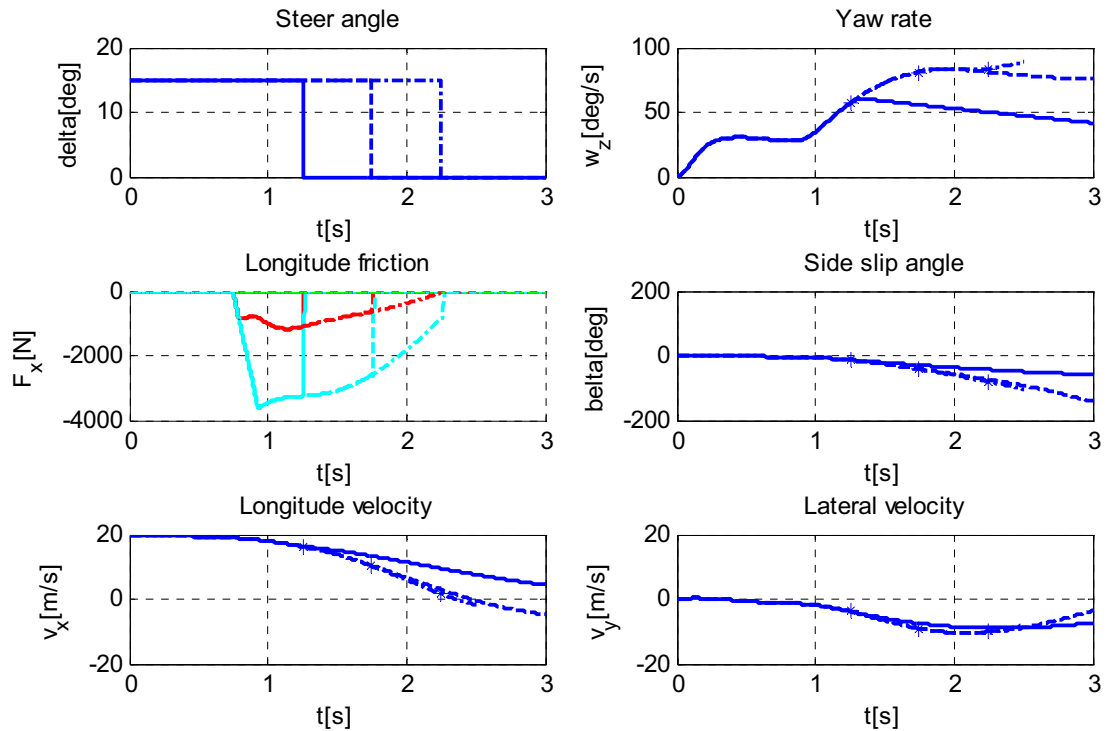


Figure 6.22. Three typical examples with different brake and steer period.

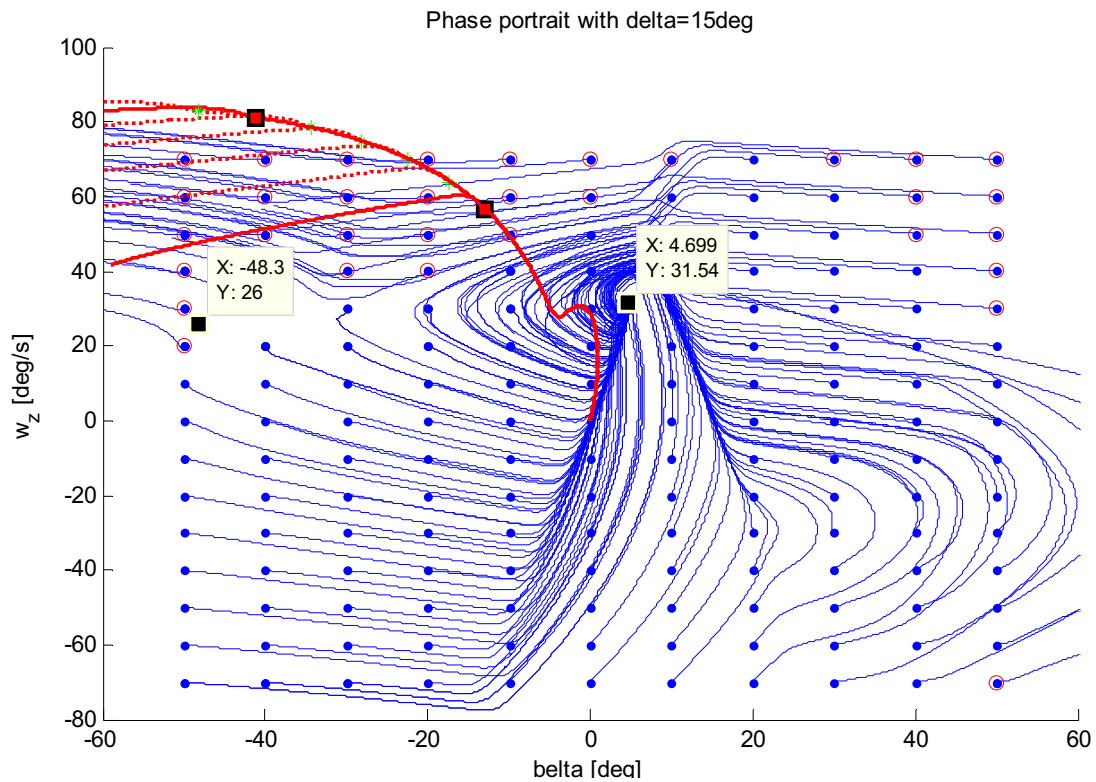


Figure 6.23. State trajectory of typical Built-in actuators strategy.

Except the actuations mentioned above, two sine dwell related destabilize methods are studied as well. First steer manoeuvre is a single cycle input, which is performed at a frequency of 0.7 [Hz], with a 500 [ms] pause between completion of the third quarter

cycle and initiation of the fourth quarter cycle. The second one is increasing amplitude sine dwell, which is also based on one single cycle sinusoidal steering input with pause of 500 [ms] at the beginning of the fourth quarter-cycle of the sinusoid. However, the amplitude of the second half-cycle was 1.3 times greater than the first half cycle for this manoeuvre. Besides, the duration of the second half cycle was 1.3 times that of the first. (Boyd, G.J. et al., 2007)

These two actuation methods result to -2.7 [deg] side slip angle with 23 [deg/s] yaw rate, which are quite weak and impossible to enter into the unstable region shown in Figure 6.16. Consequently, steady-state steer and then hand brake actuation is used to design built-in actuator.

6.5.4 Built-in actuator capability

After choose different initial speed and duration of steer and brake, the post-impact state is plotted in Figure 6.24. It is clear that Built-in actuators can reach large side slip angle; however, it would take relatively longer time and decrease the speed as well. During the increasing period of side slip angle, yaw rate would decrease slowly. The left plot of Figure 6.24 shows that Built-in actuators could only simulate case with opposite sign of side slip angle and yaw rate. The yaw rate generated by built-in actuation should around 100 [deg/s] at most and no boundary for side slip angle.

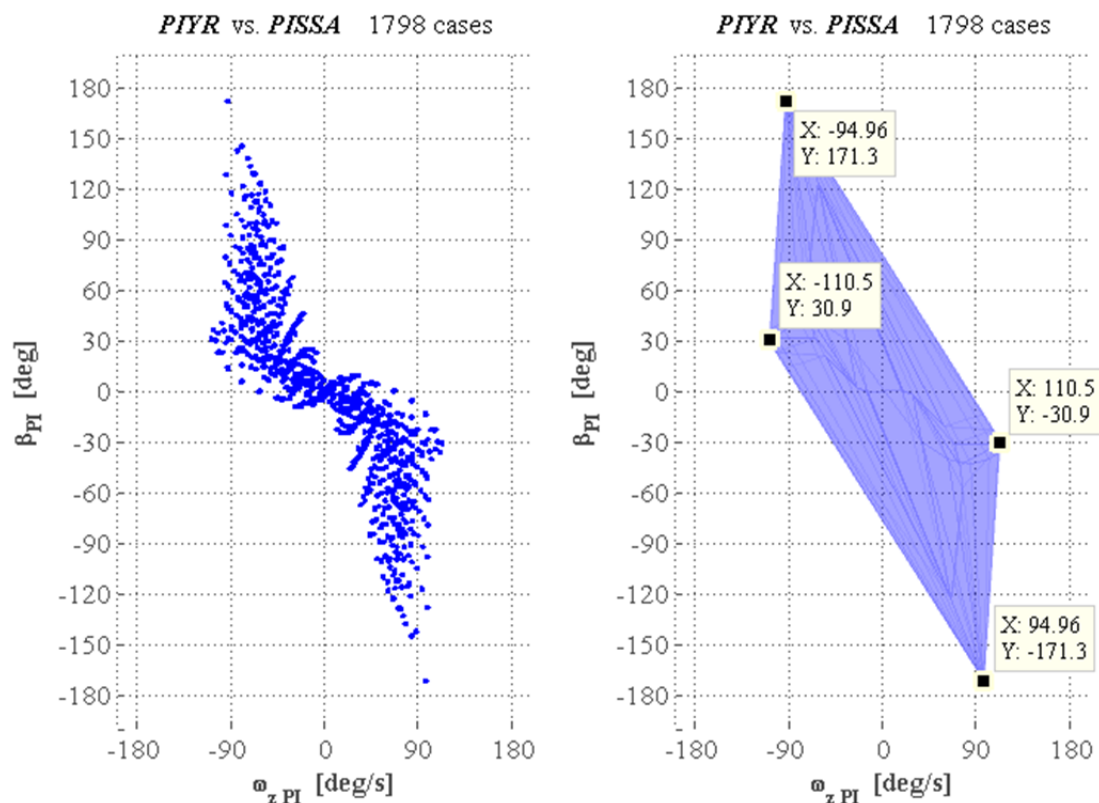


Figure 6.24. Rig cloud of simulated Built-in actuators.

Rig candidates	Ranked characteristics															
	Driver safety	High reproducibility	Data accuracy	Broad range of impulse positions	Broad range of impulse strength	Gain other tests	Low driver requirements	Broad range of impulse angles	Low damage to equipment	Low construction complexity	Low build-up rig investment	Short rig development time	Fast reload time	Practical movability	Low timing complexity	Low complexity for tesis
Built-in actuators	3	4	4	1	3	2	5	3	4	1	4	3	4	5	3	2

Performance 5. Ranked characteristics and performance grade of Built-in actuators.

6.6 Simulator SIM4

Using the Simulator SIM4 at VTI is a very competitive way for research of vehicle and human interaction; but the simulator solution is a very different alternative that should be considered from a special point of view because the operational form and therefore the limitations of it are very different that the other rigs.

Tests that might not be suitable in the real traffic environment, for safety reasons, can repeatedly be simulated in this safe and well equipped installation as meeting traffic, pedestrians, trees and other objects. Virtually the simulator can recreate any traffic situation by combining the visuals, audio and motion through several systems and subsystems. In Figure 6.25 the block “Driver safety system” refer to the protection of the driver and the simulator integrity, meaning that the simulator will not even initiate a risky acceleration that can jeopardize their safety.

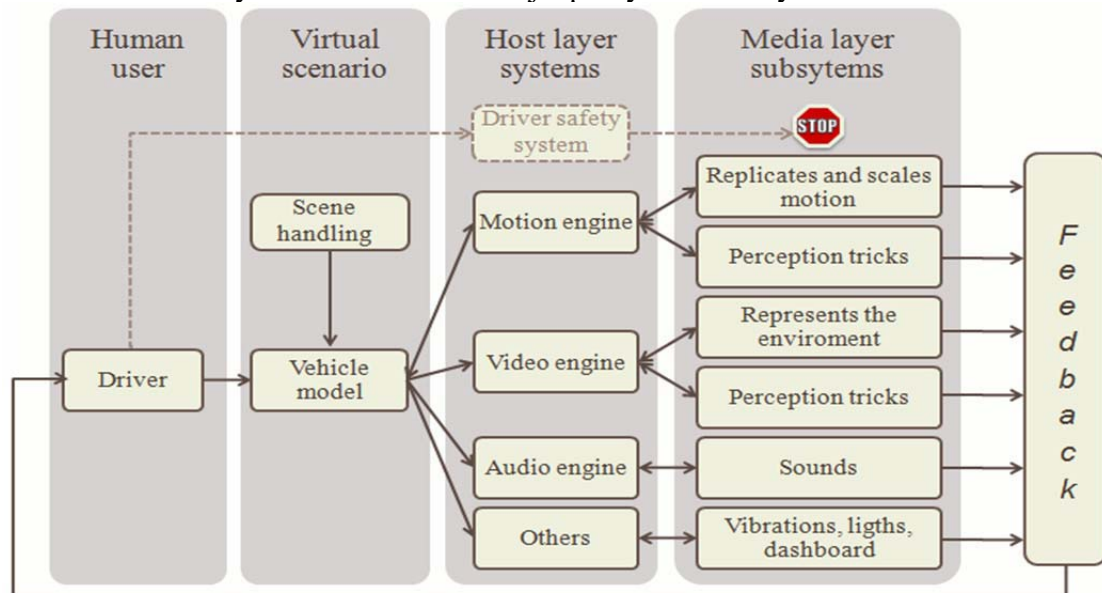


Figure 6.25. Simulator SIM4's basic structure.

The Simulator SIM4 is a hybrid simulator that combines a “cross desk” sliding base and a “hexapod”. The cross desk is a rail system that slides in two orthogonal

directions, and serves as base to the hexapod platform. The hexapod platform sustains the output cabin by six legs that are linear actuators, see Figure 6.26.



Figure 6.26. Simulator SIM4 under construction; sliding base, hexapod and the cabin platform. <Source: (VTI, 2011)>

All the motion variables from the GIDAS cloud can be simulated by the software but replicating the effects of them does have some limitations.

In simulator environment the main goal is not to replicate the intended motion but to make the user believe that he is experiencing this motion. Because the human body mostly feels the lateral acceleration forces on it, the simulator prioritize to recreate them and by tricking the perception in various ways. This perception tricking has become a refined art that extend the acceleration capabilities, for instance masking unreachable accelerations with strong noises or vibrations to distract the driver. Or by anticipating the motion before a curve taking, where the motion engine can prepare the sliding base to a major acceleration by moving it slowly under the detectable threshold gaining rail space. During the verification test the acceleration requested might be unreachable, but without the collision scenario and the input from the tested driver it is not possible to say when the simulator will not be able to continue to feed the driver with acceleration, and even more to be forced to decelerate quickly.

6.6.1 Limitation

The cabin acceleration is useful when the vehicle is generating centripetal acceleration through a curve taking or when accelerating in the conventional way. The former one will be the threshold limit in this comparison, having into account all the time that the comparison is not the same variable than the other alternatives in the sense that this centripetal acceleration limiting yaw rate is not the same as the yaw rate at the vehicle's local coordinates but a effect of the yaw rate at a certain turning speed around a global coordinate.

The yaw rate dependency of turning velocity and the limited acceleration available according to equation (6.9) is valid for planar motion.

$$w_{z,Turn\ Centre} = \frac{a_{n,centripetal}}{v_t} \quad (6.9)$$

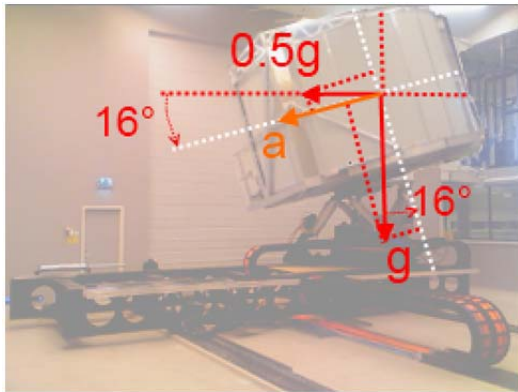


Figure 6.27. Acceleration components, by sliding and tilting, on the driver cabin.
 <Source background: (VTI, 2011)>

The three ways of producing acceleration on the cabins coordinates are:

- Tilting the cabin with the hexapod, trading part of the gravity. This acceleration can last for unlimited amount of time but is just a third part of the gravity, according to the equation (6.10).

$$a_{tilt} = a_{gravity} \cdot \sin(\text{tilt}_{max}) = 9.81 \cdot \sin(16^\circ) = 2.7 \text{ [m/s}^2\text{]} \quad (6.10)$$

- Accelerating the sliding base that supports the cabin at the two directions at the same time according to equation (6.11). This acceleration can last for short period of times and depends much on the drivers input

$$a_{slide} = \sqrt{a_x^2 + b_y^2} = 6.7 \text{ [m/s}^2\text{]} \quad (6.11)$$

- Combining the former ways maximising the acceleration. The tilting acceleration will sacrifice a part of the sliding acceleration but will gain more than it loses. See equation (6.12).

$$a_{tilt \& slide} = a_{tilt} + a_{slide} \cdot \cos(\text{tilt}_{max}) = 9.5 \text{ [m/s}^2\text{]} \quad (6.12)$$

Where do the acceleration threshold reside?

Having prolonged tilt acceleration, or accelerating the sliding base during a short time or a combination of them result in three different thresholds, as seen in Figure 6.28.

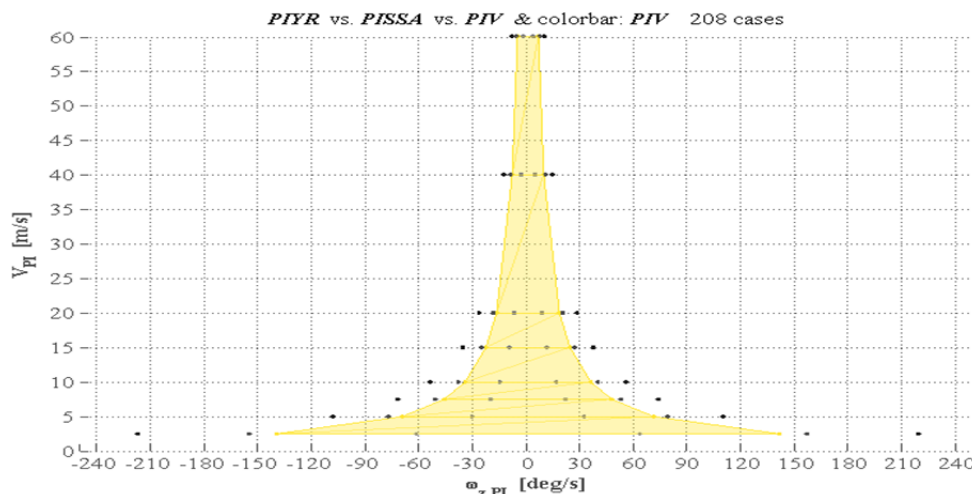


Figure 6.28. Yaw rate threshold according to equation (6.14).

The acceleration threshold used is for simplicity reasons just a mean value between a_{tilt} and $a_{\text{tilt \& slide}}$ according to equation (6.14)

$$a_{\text{tilt}} \leq a_{\text{threshold}} \leq a_{\text{tilt \& slide}} \quad (6.13)$$

$$a_{\text{threshold}} = \frac{a_{\text{tilt}} + a_{\text{tilt \& slide}}}{2} = \frac{2.7 + 9.5}{2} = 6.1 \text{ [m/s}^2\text{]} \quad (6.14)$$

The underestimation is obvious, but rather than an overestimation, for this reason a scaling influence is not employed here. The personnel at VTI said that the acceleration perceived by humans overestimate the acceleration recreated by the simulator. i.e. that the feeling of an acceleration of 1 [m/s] in simulated motion is achieved by sliding the platform just 0.7 [m/s]. This scaling factor is not researched and will not be part of the limitation threshold mapped in Figure 6.29; however this increases by 1.4 the capabilities of the specified accelerations in Table 6.1 & Table 6.2 from a draft data sheet of the projected parameters of the Simulator SIM4.

Table 6.1. Hexapod parameters. <Source: (VTI, 2010)>

	Excursions	Velocity	acceleration
surge	- 408 / +307 mm	+/- 0,80 m/s	+/- 6,5 m/s ²
sway	- 318 / +318 mm	+/- 0,80 m/s	+/- 6,0 m/s ²
heave	- 261 / +240 mm	+/- 0,60 m/s	+/- 6,0 m/s ²
roll	- 16.5 / +16.5 deg	+/- 40 deg/s	+/- 300 deg/s ²
pitch	- 15.5 / +16.0 deg	+/- 40 deg/s	+/- 300 deg/s ²
yaw	- 20.5 / +20.5 deg	+/- 50 deg/s	+/- 350 deg/s ²

Table 6.2. Sliding base parameters. <Source: (VTI, 2010)>

	excursions	velocity	acceleration
Surge (X)	+/- 4000 mm*	2 m/s	+/- 5 m/s ²
Sway (Y)	+/- 2500 mm*	3 m/s	+/- 5 m/s ²

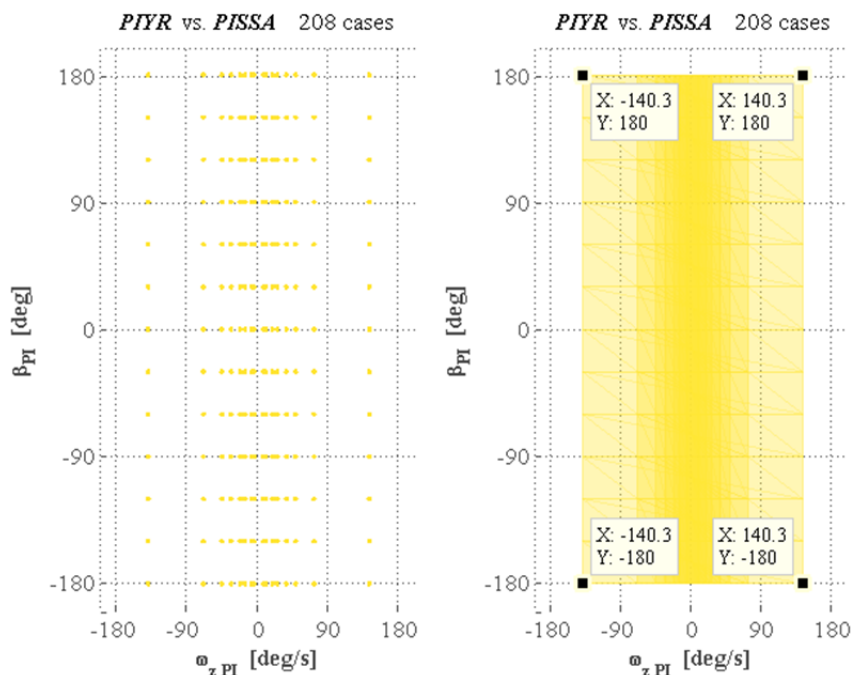


Figure 6.29. . Rig cloud of predicted simulator SIM4.

6.6.2 Advantages

This kind of rigs have been used for decades when training driver and pilots having an environment that brings several advantages as: high safety, reduced time between test sessions, cost effective tests, high repeatability and eliminating external disturbance factors as climate or ground irregularities, possibility to simulate real traffic situations with traffic, pedestrians, meeting traffic, etc. And finally no driver requirement at all, being very advantageous for the psychological approach of common drivers.

6.6.3 Disadvantages

This rig is used as well when testing functions of the vehicle industry and its interactions with the driver. The main drawback is that the states and manoeuvres can not be to extreme or to prolonged, this because of the physical limitation of the rig. Another drawback is that the tests have to be programmed and validated in advance, which could take long time depending on the severity and factors implicated.

Following is not a disadvantage but it is necessary to clarify this: because the budget for buying simulation time is consumed, this budget is not useful for other tests.

For more information about a function evaluation in simulator environment consult the master thesis of (Thor, 2007) made at the operating simulator SIM3 at VTI's head office at Linköping-Sweden.

	Rig candidates						Ranked characteristics									
	Driver safety	High reproducibility	Data accuracy	Broad range of impulse positions	Broad range of impulse strength	Gain other tests	Low driver requirements	Broad range of impulse angles	Low damage to equipment	Low construction complexity	Low build-up rig investment	Short rig development time	Fast reload time	Practical movability	Low timing complexity	Low complexity for tesis
5	Best performance															
4	Very good performance															
3	Good performance															
2	Acceptable performance															
1	Poor performance															
0	No performance															
Simulator SIM4	5	5	5	5	2	0	5	5	5	2	5	3	5	3	3	2

Performance 6. Ranked characteristics and performance grade of Simulator SIM4.

7 Results

In this chapter the results from the different approaches will be summarized and explained from an impartial analysis and first in the chapter Conclusions the results will be handled from a excluding form based on this results, determining the most optimal rig solution.

7.1 Objective evaluation

7.1.1 Rig capabilities on Problem Space

The GIDAS cloud from Problem Space and the clouds from Rig alternatives are combined for to count the enclosed GIDAS cases in each rig volume made by the most external cases in the volume.

Later, comparing the amount of covered GIDAS cases will be the ultimate goal of this thesis, Figure 7.1, having an objective argument in the evaluation. For the 2D projections see Appendix G. Results, cont. Quantifying the capabilities will be done taking into account two aspects, the phase plot area or the plant area that encloses the GIDAS cases in at least one velocity, and the most important, how many GIDAS cases are enclosed inside each Candidate volume.

The vertical variable, PIV, was forced to be plotted within two velocity intervals for practical reasons when selecting and deselecting the cases individually at the counting process.

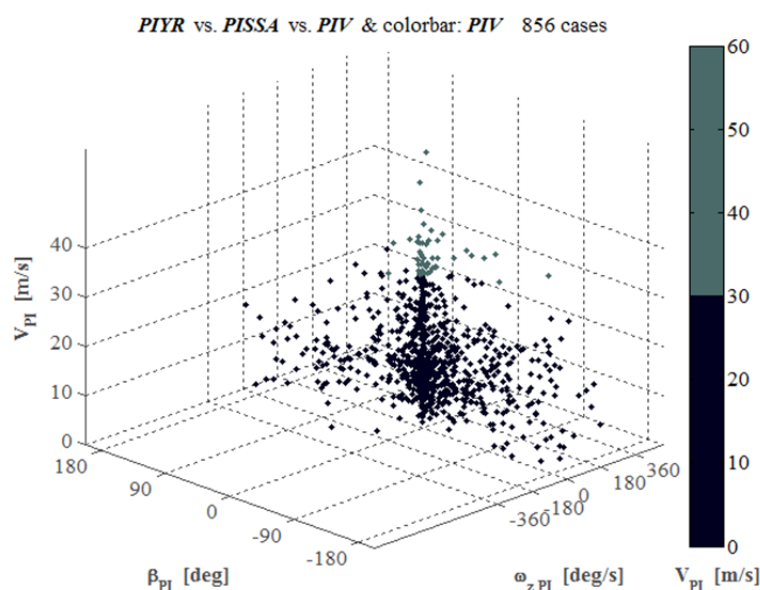


Figure 7.1. GIDAS cloud that attempts to be covered.

Together with each Cloud covering plot there is a Performance radar resulting from of the study in Chapter 6 Rig Candidates uniting the performance grades at each radial characteristic.

7.1.1.1 Kick-plate

The core of GIDAS cloud is as known the most crowded area, diminishing towards the outer ends. Therefore the Kick plate method covers efficiently this trunk in the middle. The narrow extension in yaw rate and slip angle is because of the limited amount of impulse that is possible to reach, and the higher the velocity the more influential it becomes. Despite the reduced space volume Kick plate manage to cover 175 GIDAS cases of 856, making a total coverage of approximately 20 %. The red dots inside the Kick plate volume, in Figure 7.2, indicate cases that are covered by the rig candidate.

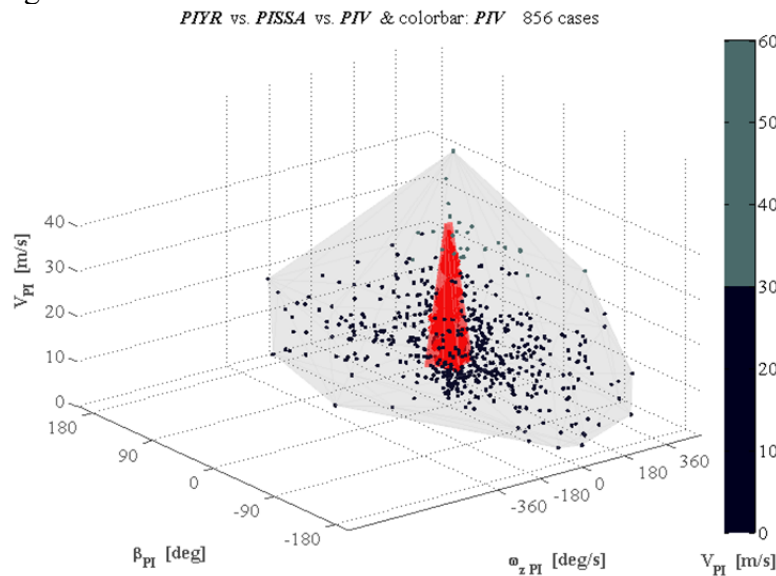


Figure 7.2. Kick plate volume covering GIDAS cloud.

The red line in Figure 7.3 is a graphical representation based on the subjective at Performance 3 vector where it is shown a clear advantage for other tests and otherwise poor performance in the GIDAS coverage area, otherwise a good performance scoring.

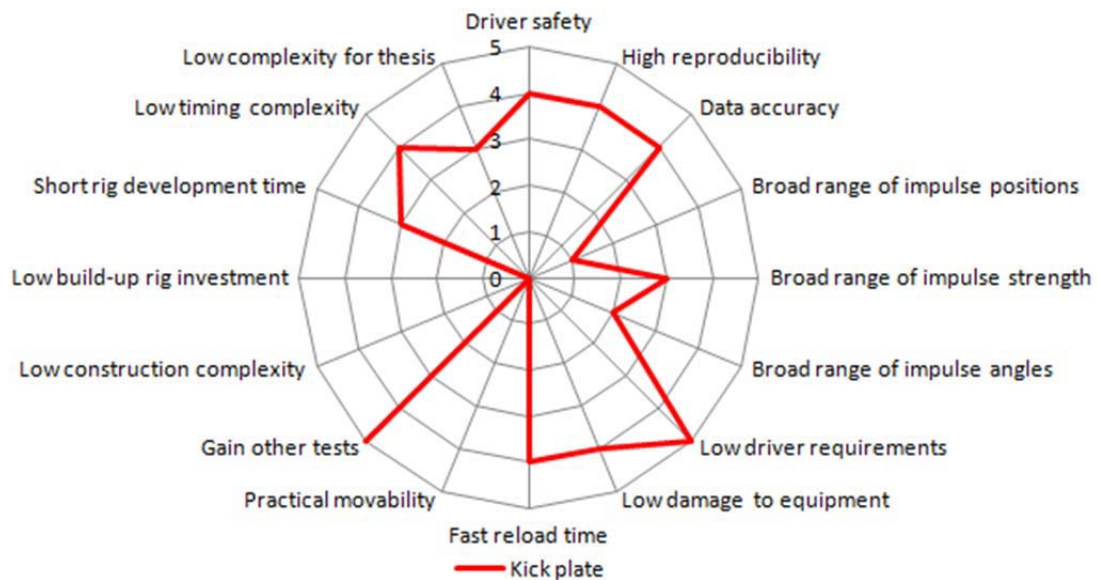


Figure 7.3. Performance radar for Kick plate.

7.1.1.2 PIT-manoeuvre

The PIT manoeuvre cloud covers an oblique wall in the GIDAS cloud, passing through the core. This wall rotates as the velocity rises; i.e. the vehicle adopts higher side slip the higher velocity, with the same collision character. The coverage is very satisfactory being approximately 60 % with 500 GIDAS cases of 856. The green coloured dots in Figure 7.4 are GIDAS cases that have been covered.

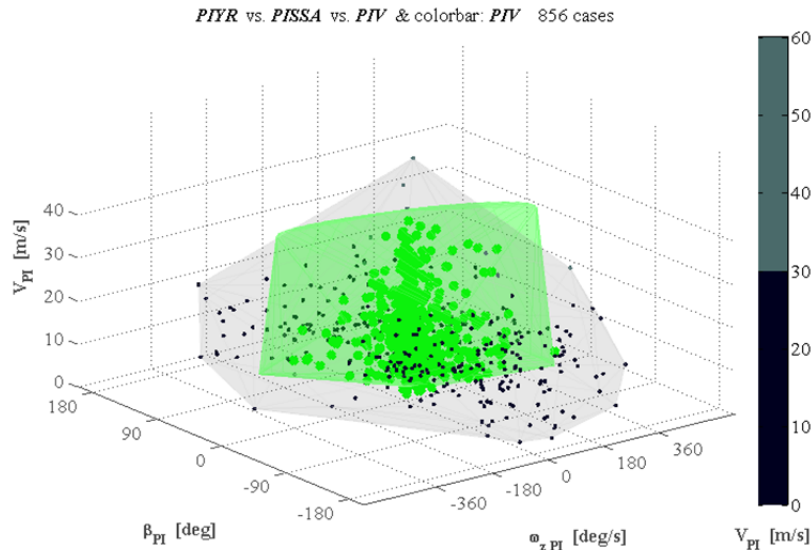


Figure 7.4. PIT manoeuvre volume covering GIDAS cloud.

The green line in Figure 7.5 is a graphical representation based on Performance 4 vector where the advantage are varying across several characteristics and stabilizing in the economical part of the radar. The stable value of four is in the Build-up investment area and three in the cost per test area. The method expects high driver skills or at least a certified test driver with training in the PIT manoeuvre. Most categories are dependent of the timing that is highly done by handcraft.

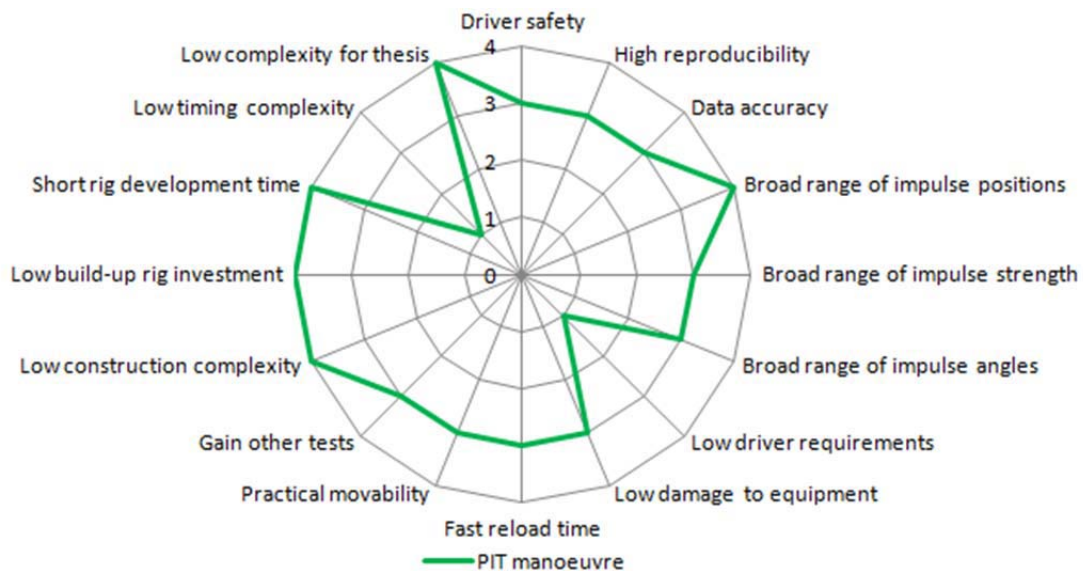


Figure 7.5. Performance radar for PIT manoeuvre.

7.1.1.3 Built-in actuators

The Built-in actuators cloud covers moderately the plant area, yaw rate and side slip, and decreasing very fast truncating at 30 [m/s] or 108 [km/h]. The space volume covers satisfactory 418 GIDAS cases of 856. This is approximately 50 % of the target.

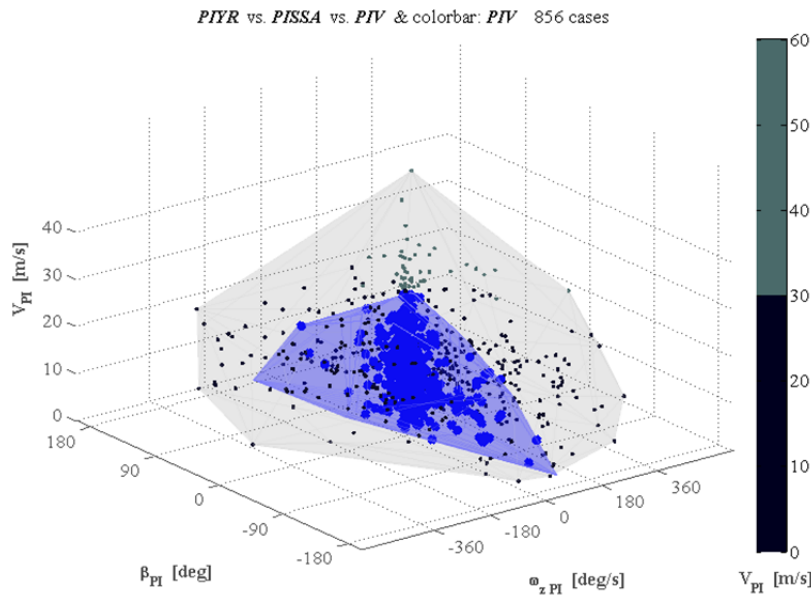


Figure 7.6. Built-in actuators volume covering GIDAS cloud.

For the Built-in actuators, blue line in Figure 7.7, shows the limitation of it in several parts, mainly because is a very complex method that involves automation, however this is beneficial for the high reproducibility, data accuracy and for the cost per test area. The GIDAS coverage is average due to the poor impulse position variation. The lack of robustness results in an average Driver safety.

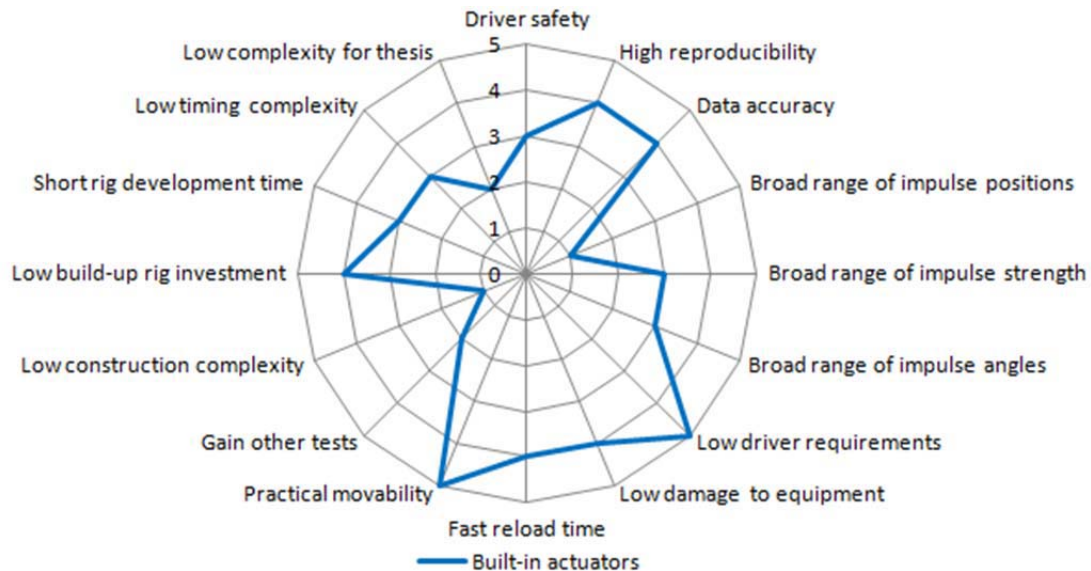


Figure 7.7. Performance radar for Built-in actuators.

7.1.1.4 Simulator SIM4

The simulators capabilities as explained before, distinguish in the operation form significantly, however the limitations of reproducing the states for the driver input, acceleration induced by translational yaw rate, is represented in the spatial volume. Covering approximately 345 GIDAS cases, 40% of 856.

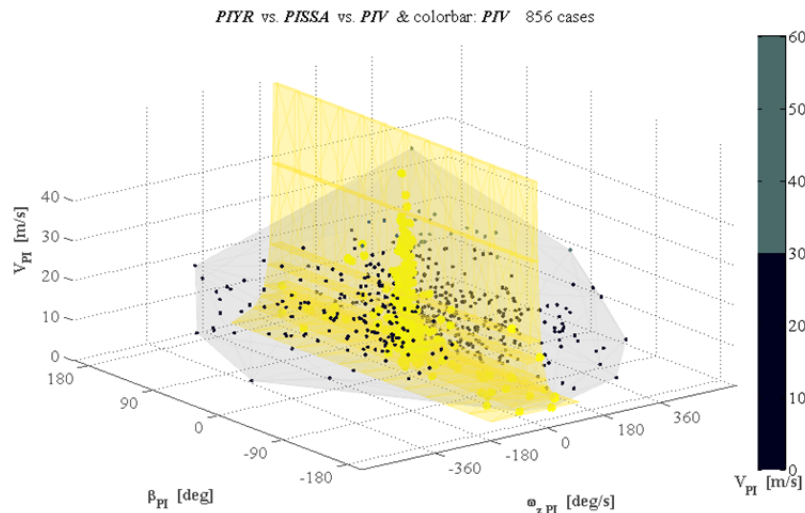


Figure 7.8. Simulator SIM4 volume covering GIDAS cloud.

The Figure 7.9 show the Performance 6 in a yellow line, which perform very good in most of the aspects regarding Testability area and Cost per test area. Some lacks are in the Build-up investment, not the rig that is for rent at an exterior company but the programming of a new utilisation of it, this required for each test to be done, in that sense the budget is already consumed and can not be used to other tests. However the investment is very advantageous in terms of cost per test and especially in the low requirements of drivers, or users that can be in principle anybody.

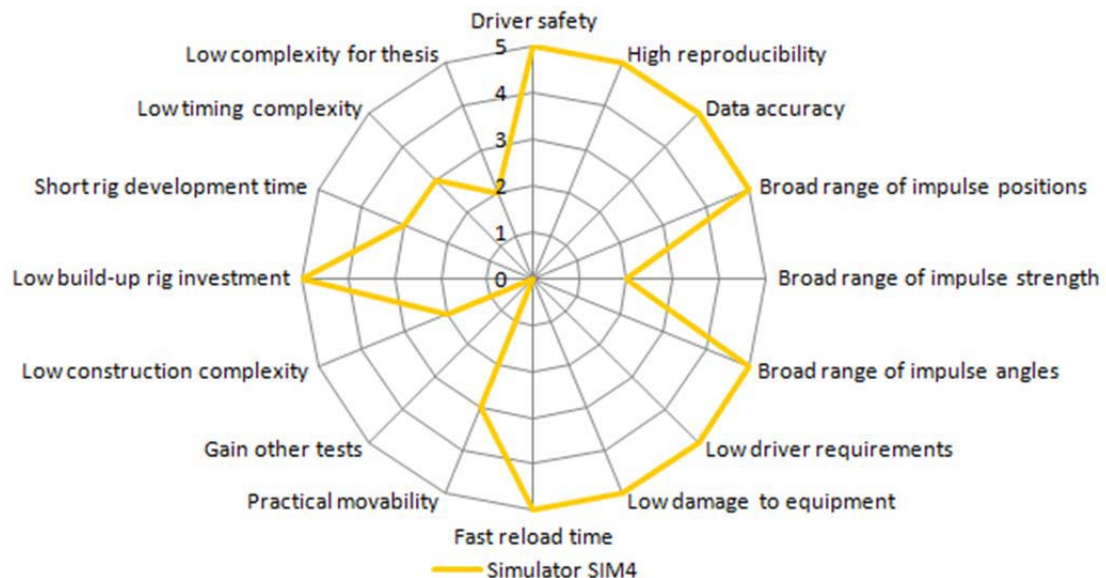


Figure 7.9. Performance radar for Simulator SIM4.

7.1.1.5 Comparison

Comparing the candidates rig clouds and volumes to each other brings more understanding of the different shapes and characteristics from each candidate. In Figure 7.10 the candidate simulation is represented with colour dots that are counted and specified at the bottom figure legend.

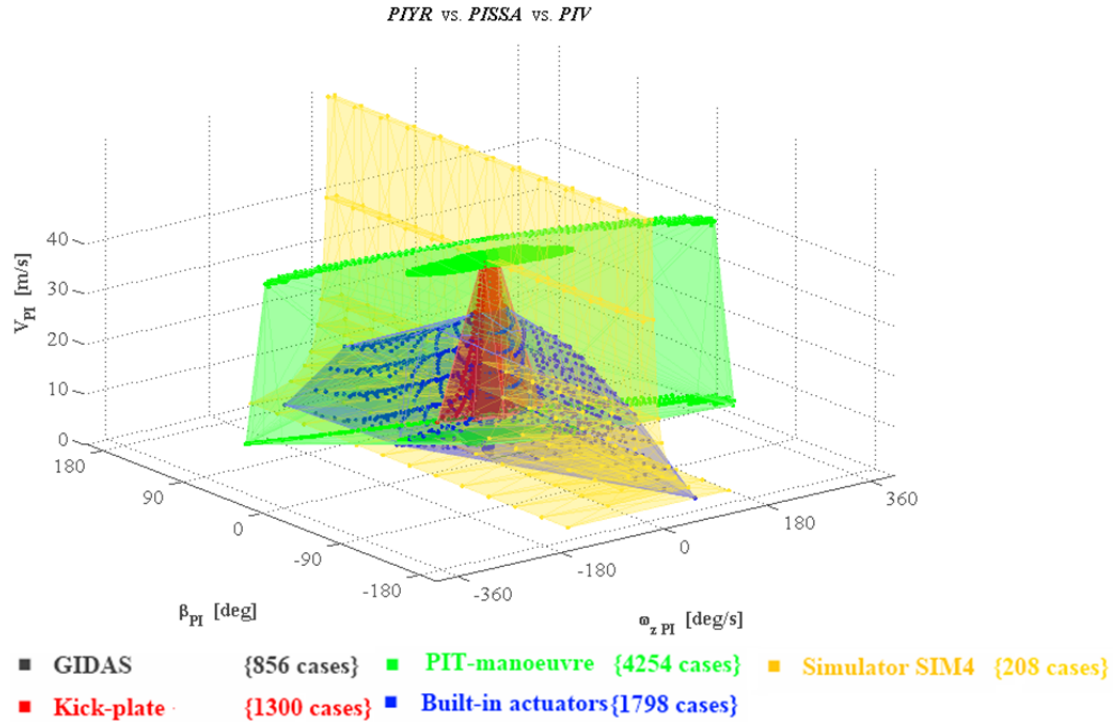


Figure 7.10. Simulation of rig candidates in the Post-Impact problem space.

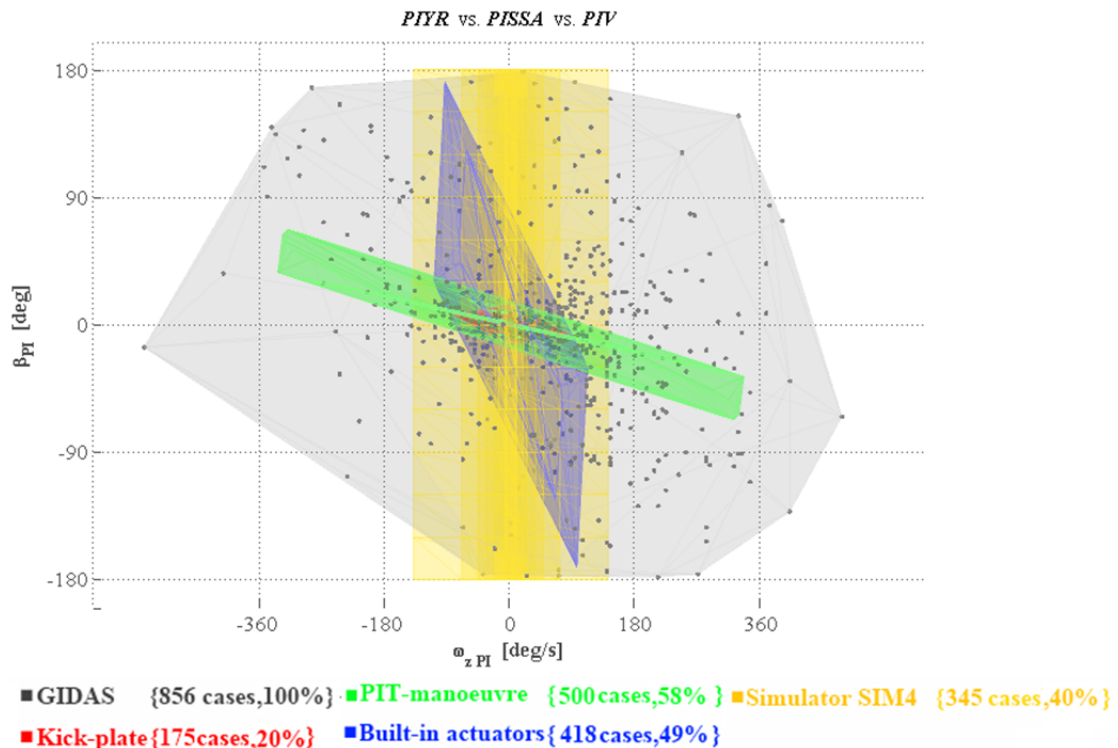


Figure 7.11. Rig candidates covering the GIDAS cloud, XY view.

From the top view (XY-view) the performance capabilities of the candidates can be seen as colour clouds that extends in several directions, each point on the clouds represent a Post-Impact state in PIYR and PISSA. The candidate clouds enclose the plant area of cases that have been covered within at least one velocity. Special shapes characterize each candidate, most notorious is the shape of the PIT manoeuvre that extends in a oblique bar across the second and fourth quadrant in Figure 7.11.

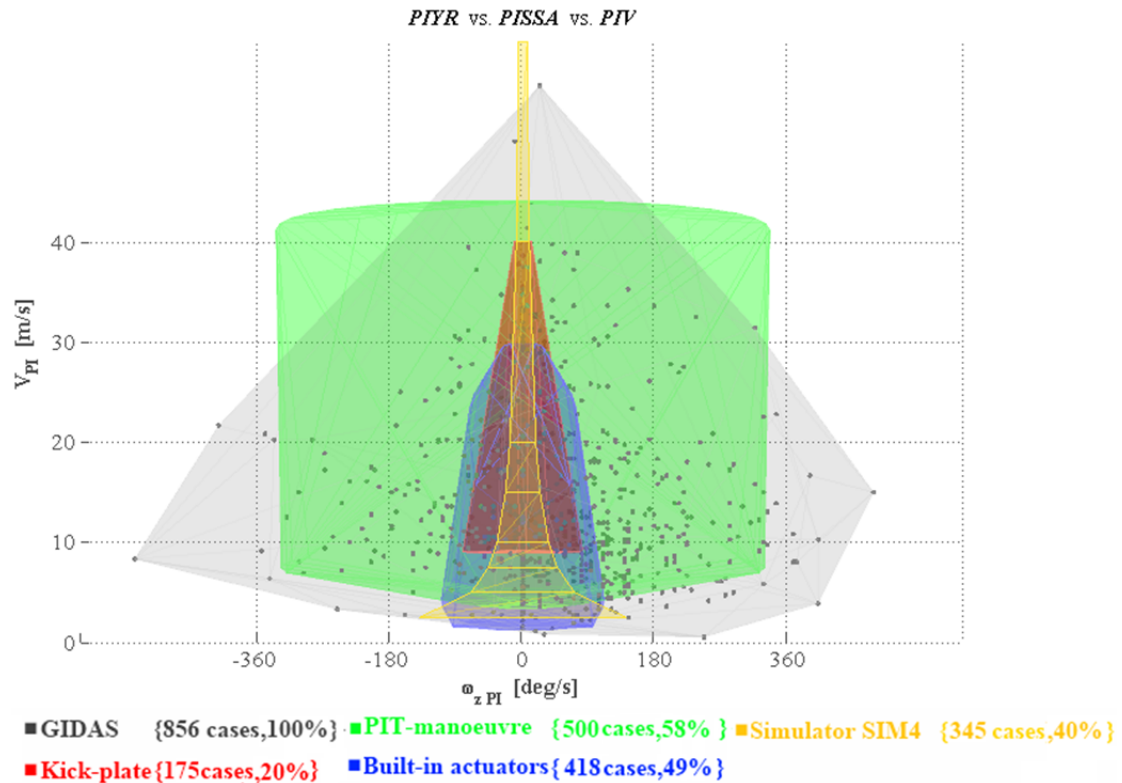


Figure 7.12. Rig candidates covering the GIDAS cloud, XZ view.

In Figure 7.12 it is evident that the capabilities differ a lot and have special shapes that are proper to the rig. In the same form these points have been covered in at least one side slip angle. The Kick plate, Built-in actuators and Simulator SIM4 shows a dependency of the velocity to cover the yaw rate problem space.

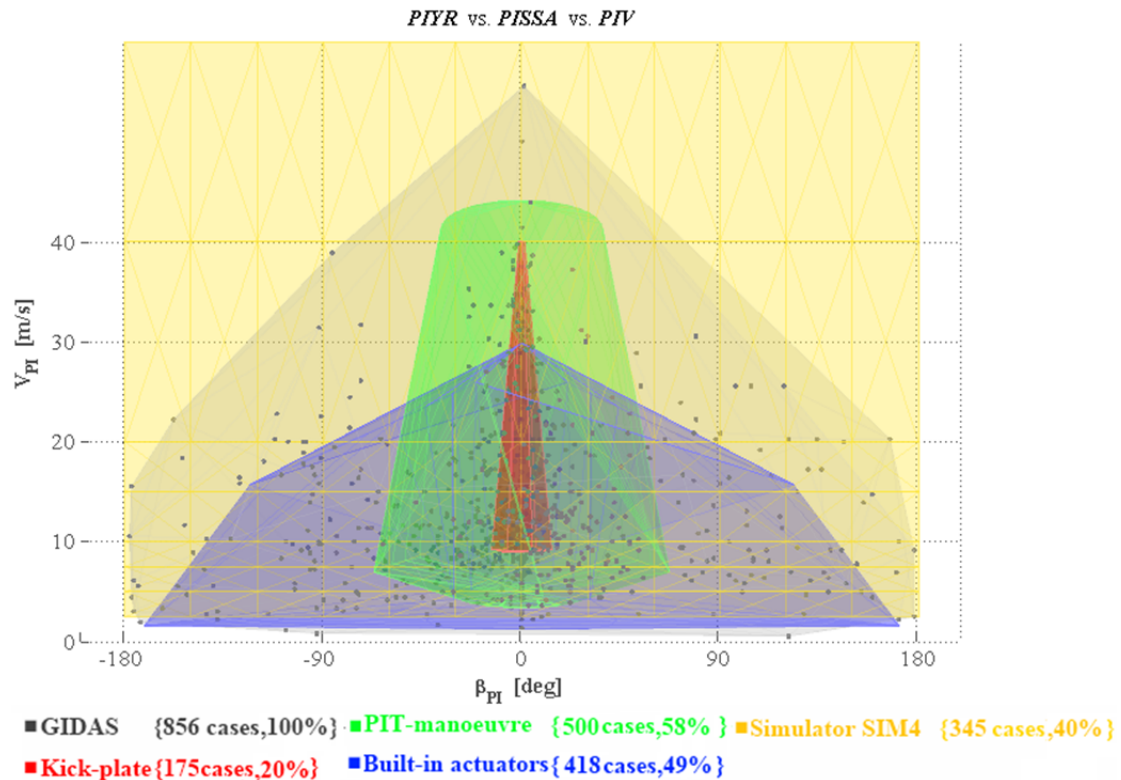


Figure 7.13. Post Rig candidates covering the GIDAS cloud, XY view.

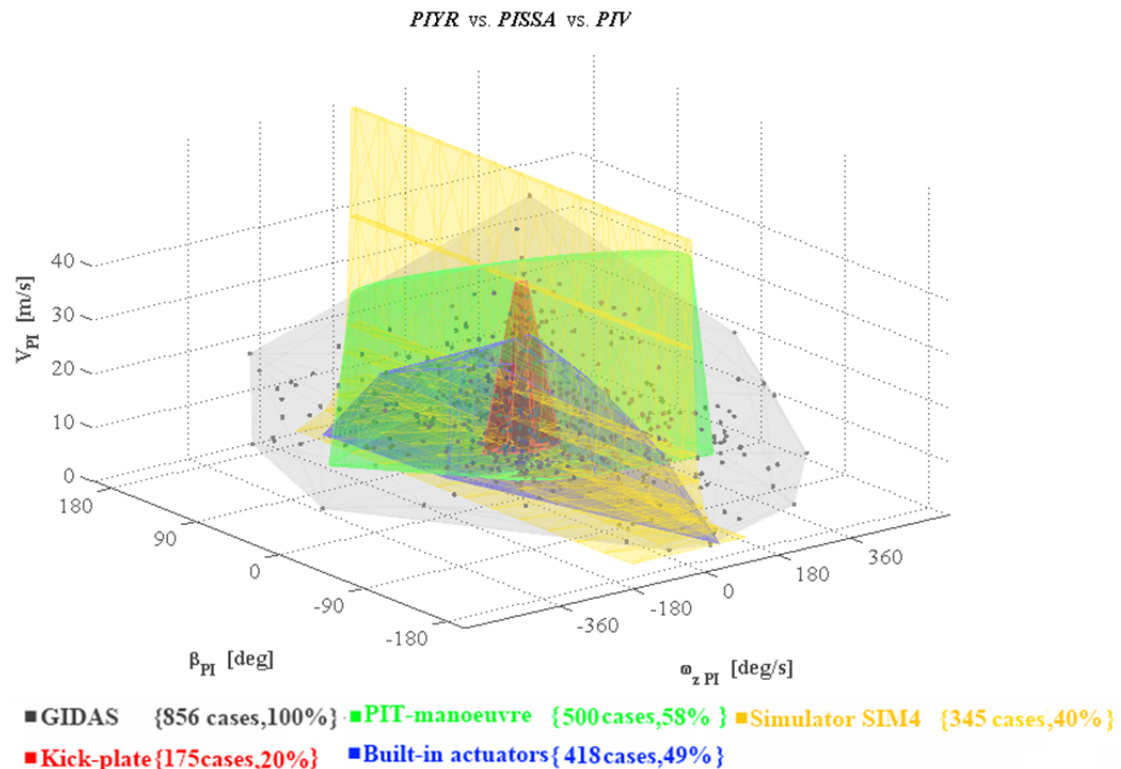


Figure 7.14. Rig candidates covering the GIDAS cloud, 3D view.

The 3D view is useful when analysing the cases, rotating and zooming into the areas of interests. Nevertheless interesting to appreciate the volume shapes from all three coordinates even at from a static plot, see Figure 7.13 and Figure 7.14.

In Table 7.1 the results from the GIDAS coverage analysis shows the Phase plot coverage in at least one velocity and the number of cases enclosed by the rig volume. Note how the PIT manoeuvre encloses almost the 60 % of the GIDAS cloud with just an 8.3 % of the XY planar area, being the most promising alternative from this point of view. Followed closely by the Built-in actuators with almost 50 % and by the Simulator SIM4 with 40 %. The Kick plate has a poor coverage in both Phase plot area and GIDAS cloud coverage.

Table 7.1. Result of plant area covering and GIDAS cloud covering.

Data sample	Phase plot area [deg ² /s]	%	cases	%
GIDAS	255799	100 %	856	100 %
Kick-plate	2168	0.8%	175	20 %
PIT-manoevre	21210	8.3%	500	58 %
Built-in actuators	32091	12.5%	418	49 %
Simulator SIM4	100800	39.4%	345	40 %

7.1.2 Ten representative cases

To describe how rigs would be used to simulate real accidents, ten typical cases were chosen as examples to analyse. With PIV within 21 [km/h] to 92 [km/h] these ten cases almost cover all the light collisions, such as PIYR lower than 200 [deg/s] and also one pure side slip case. Figure 7.15 shows their distribution in GIDAS database, where red star is the real case and blue one is mirrored.

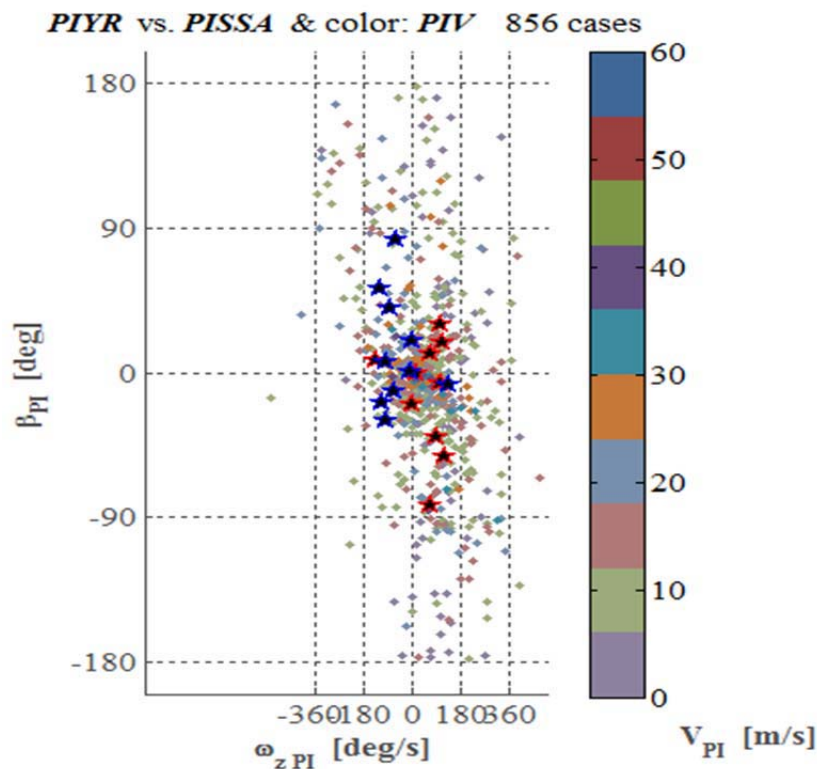


Figure 7.15. Ten cases' distribution in GIDAS database.

If PISSA is classified into four parts: <-20 [deg], $[-20\ 0]$ degrees, $[0\ 20]$ degrees and >20 [deg]; PIYR is sorted into two parts: $[0\ 80]$ degrees and >80 [deg] (mirror if needed), there are eight groups are obtained. Besides, after added one group with pure side slip angle (PISSA = 0 [deg]), nine groups are generated to describe the post impact states' distribution. The same as Figure 7.15, if PIV is not considered in the percentage distribution, 636 cases (74.3 % of 856) are covered by these representatives. The non-involved accident cases are: 73 zero accident cases (located at the origin point in Figure 7.15), 96 large yaw rate accident cases (over $|200|$ [deg/s]) and 51 small positive yaw rate with large positive side slip angle accident cases, which could only be simulated by PIT manoeuvre but under the risk of driver safety. The detailed representative Cases and their group distribution are shown in Table 7.2.

Compared to Chromosome groups (Yang, 2009), there are eight groups that are not included because:

- One is pure side slip, the same as representative Case 3.
- Four Chromosome groups have too large yaw rate (over 200 [deg/s]).
- Chromosome Group 6 lacks information about side slip angle and is ignored as well.
- Two other Chromosome groups belong to the same representative group as other Chromosome groups (No.7 and No.10), which should have the same simulation rig strategy.

Consequently, except large PIYR cases, all chromosome cases' groups are covered by these ten representatives.

Table 7.2 Representative cases.

Case No.	Key Characteristics					
	PIV [km/h]	PISSA [deg]	PIYR [deg/s]	Imp. Area	Road Type	Road Layout
1	61-120	≤ -20	0-80	Front	motorway	Continuous
2	61-120	-20-0	0-80	Rear	Any	Any
3	21-60	Any	0	Side	Any	Any
4	21-60	0-20	0-80	Side	Urban road	Intersection
5	21-60	≤ -20	≥ 80	Side	Country road	Continuous
6	21-60	≤ -20	≥ 80	Front	Urban road	Intersection
7	21-60	-20-0	≥ 80	Side	Country road	Continuous
8	61-120	-20-0	≥ 80	Rear	Any	Any
9	21-60	0-20	≥ 80	Side	Country road	Intersection
10	21-60	≥ 20	≥ 80	Side	Country road	Intersection

7.1.2.1 Description and rig simulation

There are three cases demonstrated here, which could be simulated by actuator, kick plate and PIT manoeuvre separately. The other seven cases are shown in Appendix A. Since kick plate is a quite weak rig alternative, actuator could also simulate the accident that kick plate does. For PIT manoeuvre, it is only implemented when none of the other two are available, because of its inaccurate and dangerous properties.

7.1.2.1.1 Built-in actuator implemented Case 1

(Chromosome Group No. 8)

Description:

Table 7.3. GIDAS given post-impact states of Case 1.

PIV [km/h] or [m/s]	PISSA [deg]	PIYR [deg/s]
92 or 25.56	-83	63

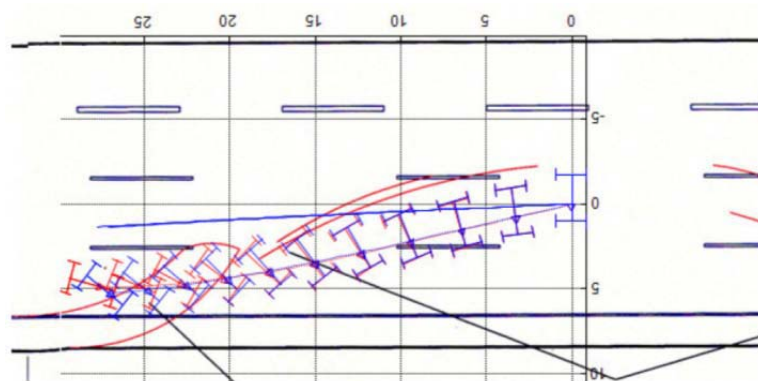


Figure 7.16. Trajectory after first collision of Case 1. <Source: (Yang, 2009)>

The accident happened at the motor way with continuous road, and finally results in rollover with three collisions in total. The initial velocity is 120 [km/h] and side slip angle before collision is -90 [deg]. First crash happened at the front, with 174 [deg] impulse angle and 6452 [Ns] magnitude. Therefore, the host car has positive yaw rate and huge negative side slip angle, which generate the second collision on the curb fender. The trajectory is shown in Figure 7.16.

Rig simulation:

- Kick plate:

PISSA = -83 [deg] is far away from the capability of kick plate. Kick plate could not be used in this case.

- Built-in actuators:

The steer strategy and results are shown in Figure 7.17. The steady steer angle is 15 [deg], with step-up and lasts 1 [s]. Hand brake starts at 0.2 [s] when both rear tyres are almost saturated. Yaw rate decrease slowly after stopping hand brake and side slip angle keep decrease. At 1.78 [s] the post impact states are shown in Table 7.4. The largest difference between rig and GIDAS result is yaw rate, which is 8.9 %.

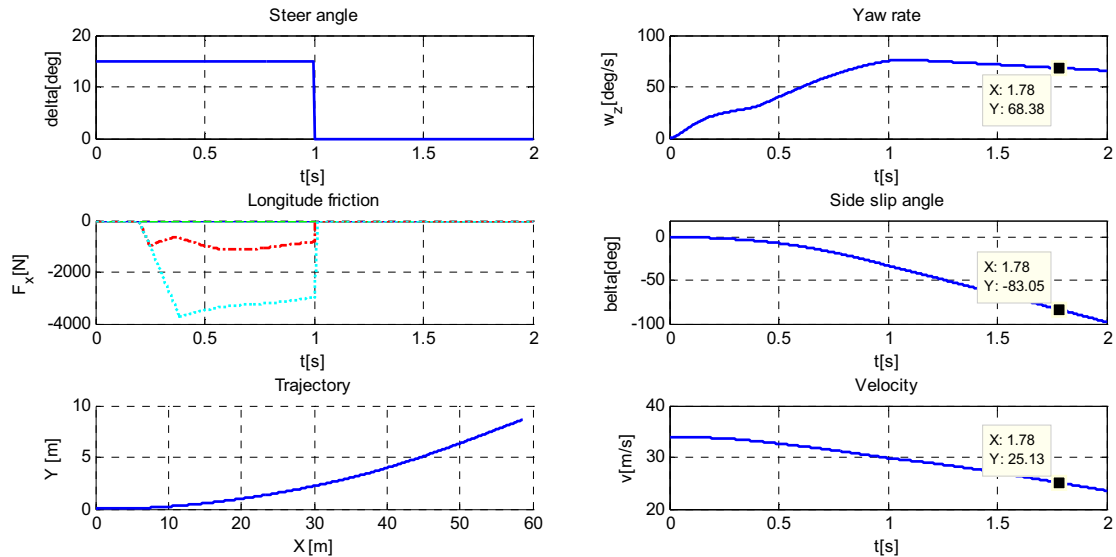


Figure 7.17. A Built-in actuators strategy of Case 1.

Table 7.4. Post impact states comparison of Case 1.

	PIV [km/h] or [m/s]	PISSA [deg]	PIYR [deg/s]
GIDAS	92 or 25.56	-83	63
Built-in actuators	90.5 or 25.13	-83	68.4

– PIT manoeuvre:

The absolute ratio between yaw rate and side slip angle of PIT manoeuvre are always within [4 10], which is not possible to simulate this case. The huge side slip angle of this case is resulted by the initial side slip angle before collision, but not the collision itself. Even if choosing PIT manoeuvre, large impulse magnitude would be needed to generate this large PISSA which is not safe enough. Consequently, PIT manoeuvre is not implemented here.

7.1.2.1.2 Kick plate implemented Case 2

(Chromosome Group No.11)

Description:

The accident happened at the entry of motor way with continuous road. Four collided vehicles were involved in this accident process. For first collision, it is located at the left rear end with perpendicular impulse and 1750 [Ns] magnitude, and generate positive yaw rate with quite small side slip angle. The second collision is happened at the curb fender. Figure 7.18 shows the real collision trajectory through red line and post-impact states after first collision is exhibited in Table 7.5.

Table 7.5. GIDAS given post-impact states of Case 2.

PIV [km/h] or [m/s]	PISSA [deg]	PIYR [deg/s]
79 or 21.94	-1	11

Contents in this appendix are only found in the confidential variant of the report.

Figure 7.18. Trajectory after first collision of Case 2.

Rig simulation:

– Kick plate:

We know as PIV increases, the capability of kick plate would decrease a lot. However, this case has really small side slip angle and yaw rate, which are possible to use kick plate to reach even at large PIV. There are 5 optional kick methods in kick plate, in which 3 of them could be used to simulate this case: rear tyre kick with short depth plate, rear tyre kick with long depth plate and two short plates' kick method. Since the short depth plate strategy could be repeated by the other two strategies, only simulate one short depth strategy instead all of the three methods.

– *Rear kick with short depth plate:*

No matter if the plate is long depth or short depth, the kick starts when the distance between rear axle and end edge of sliding plate is 1.62 [m]; assuming that the plate acceleration is larger than 1g at the beginning or say the plate acceleration would not influence kick result dramatically. Otherwise, longer distance is needed and also possible. The direction of plate movement is from left to right, which generate negative lateral friction. The kick time is 75 [ms] and following table shows the PI states at 0.9 [s]. The largest difference of post impact states between GIDAS and kick plate is around 4 %. Other post-impact states' comparisons are shown in Table 7.6.

Table 7.6. Post impact states comparison of Kick plate with Case 2.

	PIV [km/h] or [m/s]	PISSA [deg]	PIYR [deg/s]
GIDAS	79 or 21.94	-1	11
Rear tyre kick	79.2 or 22	-1	10.6

– Built-in actuators:

Since PIYR and PISSA are relevantly too small, counter steer destabilize method is used for actuator. At first, 15 [deg] steady steer generates large yaw rate and decreases lateral velocity to generate negative side slip angle at the same time. Then counter steer to decrease yaw rate until 11 [deg/s] and side slip angle is -1 [deg]. The total destabilization time is 0.25 [s] with only 90 [ms] hand brake with 15 [deg] step steer,

which are shown in Figure 7.19. The comparison results are shown in Table 7.7, which has 5% difference at most.

Table 7.7. Post impact states comparison of Actuator with Case 2.

	PIV [km/h] or [m/s]	PISSA [deg]	PIYR [deg/s]
GIDAS	79 or 21.94	-1	11
Built-in actuators	77.62 or 21.56	-0.98	10.82

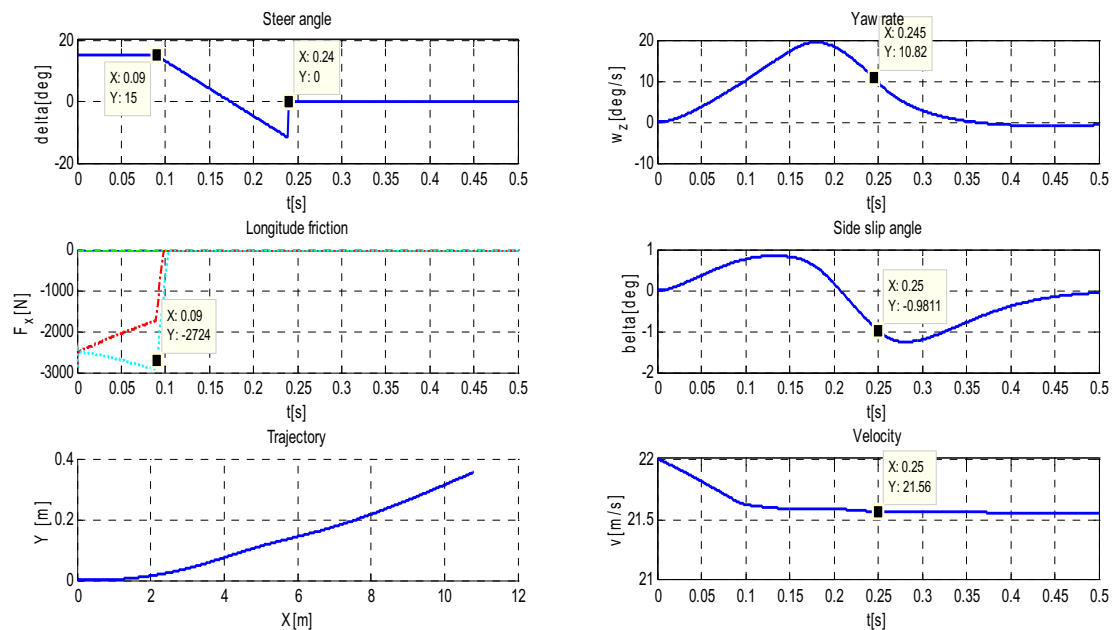


Figure 7.19. A Built-in actuators strategy of Case 2.

- PIT manoeuvre:

For smaller post impact state cases, PIT manoeuvre is more inaccurate compare to other rig alternatives. This is because real collision is hard to control for impact position, angle and so on. Besides, the restitution and friction coefficient on collision point are experimental data, which has error included. In this case, PIT manoeuvre would not be tested.

7.1.2.1.3 PIT manoeuvre implemented Case 7

(Chromosome Group No.10)

Description:

This accident happened at an intersection of country road. The first kick is located at the left rear end, with impulse angle is -16 [deg] and magnitude is 5288 [Ns]. The generated large negative PIYR render the host vehicle run to the pole and secondly crashed on the left rear side and stopped. The first rear end kick generates negative yaw rate and small positive side slip angle, which are shown in Table 7.8. The initial velocity is 29 [km/h] and without side slip before collision. The real collision trajectory is shown in Figure 7.20 with red.

Table 7.8. GIDAS given post-impact states of Case 7.

PIV [km/h] or [m/s]	PISSA [deg]	PIYR [deg/s]
44 or 12.2	8	-138

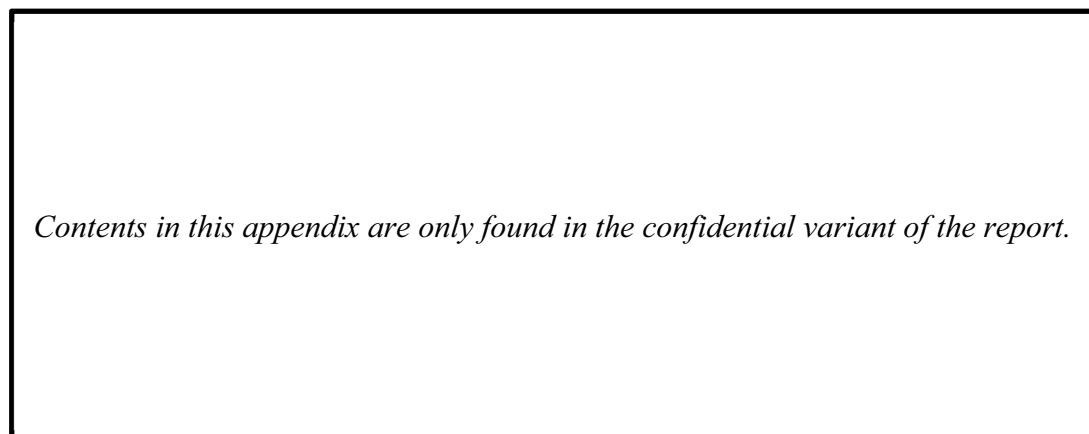


Figure 7.20. Trajectory after first collision of Case 7.

Rig simulation:

- Kick plate:

PIYR is over the capability of kick plate, so that kick plate is not a candidate rig in this case.

- Built-in actuators:

With the actuator is easier to reach cases that have opposite PISSA and PIYR signs. This is mainly because large yaw rate is good to increase the opposite side slip angle. However, Built-in actuators is not capable to reach huge yaw rate, or even it could reach -138 [deg/s], the side slip angle would also quite big at the same time. Besides, this kind of light rear end kick is quite suitable to use PIT manoeuvre, and actuator is not been considered here.

- PIT manoeuvre:

During the collision, impulse is the main domination of post impact states compared to tyre friction. Therefore, assuming this is the only point of contact of the vehicle with an impulse angle equal to -16 [deg]; the PISSA should be negative, which disregards the given states. This is because GIDAS may not consider friction on the collision surface.

Compared to PIYR, PISSA is quite small, which implies that impulse is almost perpendicular to the collision surface. The collision surface friction on host vehicle should be positive, which would generate negative PIYR and positive PISSA. Therefore, both impulse angle and magnitude increase. To fulfil the safety requirement the impulse angle is 12 [deg] and the impulse magnitude is 6500 [Ns], the detailed post impact states shown in Table 7.9. The maximum difference is PISSA, with 60% error.

Table 7.9. Post impact states comparison of tuned impulse and GIDAS.

	PIV [km/h] or [m/s]	PISSA [deg]	PIYR [deg/s]
GIDAS	44 or 12.2	8	-138
Tuned GIDAS	43 or 11.9	13	-112

Assuming the μ on the collision surface is 0.5, the collision angle would be 16 [deg], the same as GIDAS given impulse angle. Then CoR is set to be 0.8, where less energy losses are consumed with proper vehicle protection. The detailed PIT manoeuvre strategy and post impact states comparison, trajectory is shown in Table 7.10, Table 7.11 and Figure 7.21 respectively. The maximum difference between PIT manoeuvre and GIDAS is 37 %, which is better than the tuned data by increasing the impulse magnitude with 3.5 %.

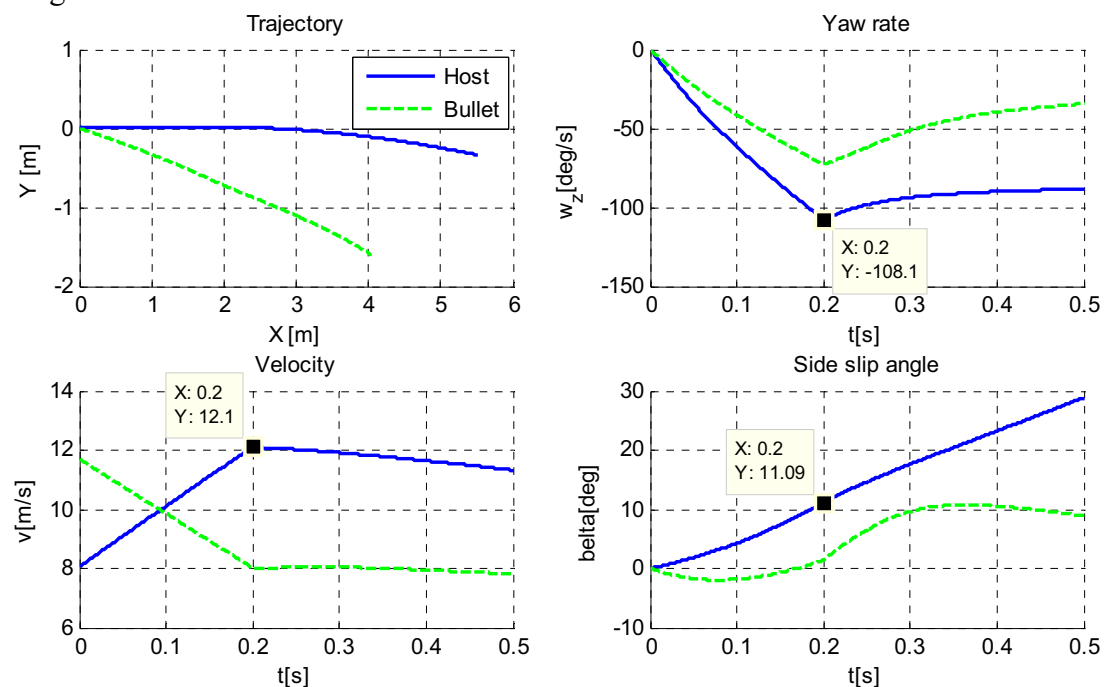


Figure 7.21. Host and bullet vehicle dynamic states during and after collision.

Table 7.10. A PIT manoeuvre strategy of Case 7.

	Impulse position		V0 [km/h] or [m/s]	Collision angle [deg]	Imp. angle [deg]	Imp. magnitude [Ns]
	X [mm]	Y [mm]				
GIDAS	4100	-700	29 or 8.1	—	-16	5288
New host	4100	-700	29 or 8.1	-16	10	6720
New Bullet	140	400	29 or 8.1	16	-154	6720

Table 7.11. Post impact states comparison of PIT manoeuvre with Case 7.

	PIV [km/h] or [m/s]	PISSA [deg]	PIYR [deg/s]
GIDAS	44 or 12.2	8	-138
PIT manoeuvre	43.5 or 12.1	11	-108

7.1.2.2 Summary

Kick plate can only simulate weak accident cases. Since rear kick is much easier to destabilize the car, larger range of crash case with different sign yaw rate and side slip angle could be simulated by kick plate (representative case 2). For same sign yaw rate and side slip angle, the limitations for them are 37 [deg/s] and 5 [deg] respectively.

The Built-in actuator can simulate almost all weak accident cases with PIYR and PISSA have different sign (top 3 representative cases in Table 7.2). For severe collision, larger side slip angle is easier to be simulated (representative case 5 and 6 in Table 7.2). There are two kinds of accident case that actuator is hard to reach: PIYR and PISSA have same sign (representative case 4, 9 and 10 in Table 7.2) or different sign but the absolute ratio of PIYR and PISSA is too large (representative case 7 and 8 in Table 7.2). The main reason for these is that the Built-in actuator takes longer time to destabilize the host vehicle compare to other rig alternatives, which determines that yaw rate would contribute great on the side slip angle. Side slip angle is inversely proportional to the yaw rate.

PIT manoeuvre is more flexible but inaccurate compared to other rigs. In this case, the suggestion is to only use PIT manoeuvre when other two rigs could not reach the PI states, like severe crash case with same sign side slip angle and yaw rate (representative case 4 in Table 7.2), different sign but large absolute ratio between yaw rate and side slip angle (representative case 7 and 8 in Table 7.2). However, if the crash is so severe that it needs large impulse magnitude, PIT manoeuvre could not help to simulate it (representative case 9 and 10 in Table 7.2).

When choosing these 10 representative cases as a base, Kick plate can cover 10 %, Built-in actuator covers 50 % and PIT manoeuvre would be used for 30 % cases but its capability could cover around 50 % within safety limit.

Since Simulator SIM4 cannot replicate the dynamic motion, its coverage is counted through the clouds shown capability, where only 20 % cases could be reproduced. The coverage comparison of rig alternatives between ten case and GIDAS database is shown in Table 7.12. The hardest case is severe collision with PIYR and PISSA having same sign. Beyond that case, almost all other weak situations could be tested by these three rig alternatives, which cover almost 63 % GIDAS database accidents.

It shows that the rank of rig alternatives would not change, but the coverage is a slightly different, especially for Simulator SIM4 and Kick plate. This is because these ten cases are severe collisions, where PIYR always is larger than 65 [deg/s]. Hence, it is hard for Simulator SIM4 and Kick plate to reach such large PIYR. The hardest case is severe collision with PIYR and PISSA having same sign. Beyond that case, almost all other weak situations could be tested by these three rig alternatives, which cover almost 63 % GIDAS database accidents.

Table 7.12. Ten cases coverage of rig alternatives.

Data sample	cases	%
GIDAS representative cases	10	100 %
Kick-plate	1	10 %
PIT-manoevre	5	50 %
Built-in actuators	5	50 %
Simulator SIM4	2	20 %

7.2 Subjective evaluation

7.2.1 Ranked characteristics

The interview resulted in the following rating of characteristics, Table 7.13, and the following thoughts were synthesized from the conversation with the personnel.

Table 7.13. Ranking of characteristic importance.

Rank	Ranked characteristics	a	b	c	d	e	f	g	h	i	j	Avg
1	Driver safety	10	10	10	10	10	10				9	9.9
2	High reproducibility	8	9	8	10	9	8	5	10	7	8	8.2
3	Data accuracy	10	9.5	8	7	4	4	5	10	7	8	7.3
4	Broad range of imp. positions	7	8	4	5	5	7	7	6	10	8	6.7
5	Broad range of imp. strength	8	8	5	5	5	5	7	6	9	8	6.6
6	Gain other tests	5	6	4	7	4		9	6		8	6.1
7	Low driver requirements	3	6	8	7	3	7	5		7	8	6.0
8	Broad range of impulse angles	6	6	6	5	5	4	7	6	10	3	5.8
9	Low damage to equipment	3	4	6	10	8	7	9	2	5	4	5.8
10	Low construction complexity	3	5	6	5	2						4.2
11	Low build-up rig investment	5	3	6	7	1		5	0	5	4	4.0
12	Short rig development time	4	4	6	5	1						4.0
13	Fast reload time	3	3	3	2	5	7	5		3	3	3.8
14	Practical movability	6	2	4	1	1	3	5		3	9	3.8
15	Low timing complexity	3	4	2	5	3						3.4
16	Low complexity for thesis	3	5	6	0	3						3.4

The most important characteristic is as denoted already in the introduction chapter, the driver safety. Successively the average points decreases from 9.9 until the lowest 3.4. These numbers reflects the importance of the evaluation criteria. This will be useful when analysing the grades of each solution in these criteria.

7.2.2 Performance Matrix

In this section the results from performance of rig alternatives, simulation and literature study will be used to select the most fitted solution according to the individual performance grades in each criteria and the importance score of each criteria. The grades are subjective judgements based on the present knowledge of the rig solutions.

The performance matrix shows in warm colours the performance of each candidate trough increasing the "redness" colours in Performance 7 to represents the better performance at every characteristic. The control item, i.e. The ideally perfect rig have a qualification of the maximum five in all of the characteristics, showed in the deep orange row above the performance matrix.

Rig candidates		Ranked characteristics																	
		Driver safety	High reproducibility	Data accuracy	Broad range of impulse positions	Broad range of impulse strength	Gain other tests	Low driver requirements	Broad range of impulse angles	Low damage to equipment	Low construction complexity	Low build-up rig investment	Short rig development time	Fast reload time	Practical movability	Low timing complexity	Low complexity for thesis		
5	Best performance																	≥ 70	
4	Very good performance																	≥ 60	
3	Good performance																	≥ 50	
2	Acceptable performance																	< 50	
1	Poor performance																		
0	No performance																		
Importance of qualification -->		9.9	8.2	7.3	6.7	6.6	6.1	6.0	5.8	5.8	4.2	4.0	4.0	3.8	3.8	3.4	3.4		
Perfect Rig (Control item) -->		5	5	5	5	5	5	5	5	5	5	5	5	5	5	5	5	444	100 %
Skidcar system		5	0	0	1	0	3	0	1	5	5	5	5	5	5	0	5	225	51 %
Water cannon		3	4	4	1	0	2	3	1	4	3	4	4	3	4	5	4	259	58 %
Kick plate		4	4	4	1	3	5	5	2	4	0	0	3	4	0	4	3	274	62 %
PIT manoeuvre		3	3	3	4	3	3	1	3	3	4	4	4	3	3	1	4	270	61 %
Built-in actuators		3	4	4	1	3	2	5	3	4	1	4	3	4	5	3	2	284	64 %
Simulator SIM4		5	5	5	5	2	0	5	5	5	2	5	3	5	3	3	2	349	78 %

Performance 7. Ranked characteristics and Performance matrix.

The colour code helps in visualizing the "good spots" and helps to understand the candidates as group revealing common faults and common strengths.

The tree highest percentages will be the most interesting solutions for a further development, marked with bold text, the colour circle at its left indicates the interval the percentage corresponds to in the right end of the matrix.

Further, as the thesis advanced and the most outstanding candidates were graded again with the same principle and using the average of the characteristic groups. The numbers in the Characteristics column in Table 7.14 corresponds to the first rank of characteristics averaged from table Table 7.13.

Table 7.14. Main characteristic groups of average importance points

Rank	Ranked final characteristics	Characteristics	Avg.
1	Test ability	[2,3]	7.7
2	GIDAS coverage	[4,5,8]	6.4
3	Cost per test	[7,9,13,14]	4.8
4	Build-up investment	[6,10,11,12,15]	4.3

The result ratifies that the performance of Simulator SIM4 is very advantageous for the desired tests; the second most advantageous candidate is again the Built-in actuators achieving a stable score through the Performance 8. The third place is the PIT manoeuvre that follows very closely to the Built-in actuators. The same information is shown in the performance radar in Figure 7.22.

Final rig candidates	Final characteristics				
	Test ability	GIDAS coverage	Cost per test	Build-up investment	
	7.7	6.4	4.8	4.3	
	5	5	5	5	116 ● 100 %
Kick plate	3	1	4	1	53 ● 46 %
PIT manoeuvre	2	5	3	3	75 ● 64 %
Built-in actuators	3	4	4	3	81 ● 70 %
Simulator SIM4	5	3	5	4	99 ● 85 %

Performance 8. Rig performance in each Characteristic group.

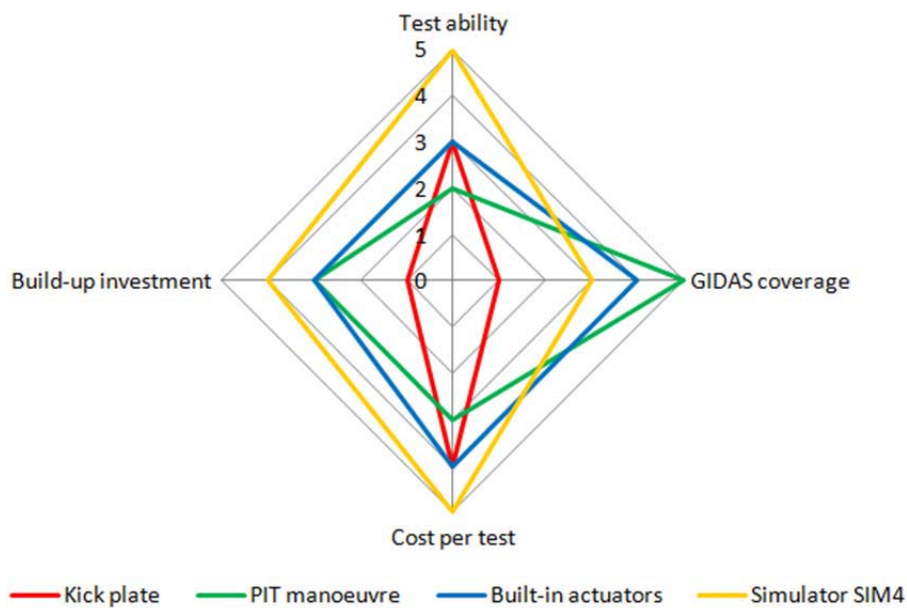


Figure 7.22. Performance radar for the final candidates in characteristic groups

Another clear way to see the rig grades is in radar with the characteristics axis ordered in the importance order, clockwise starting from the top. In Figure 7.23. It is evident that the performance in the most valuable area is dominated by the Simulator SIM4, followed by PIT manoeuvre which ratifies the numerical evaluation made.

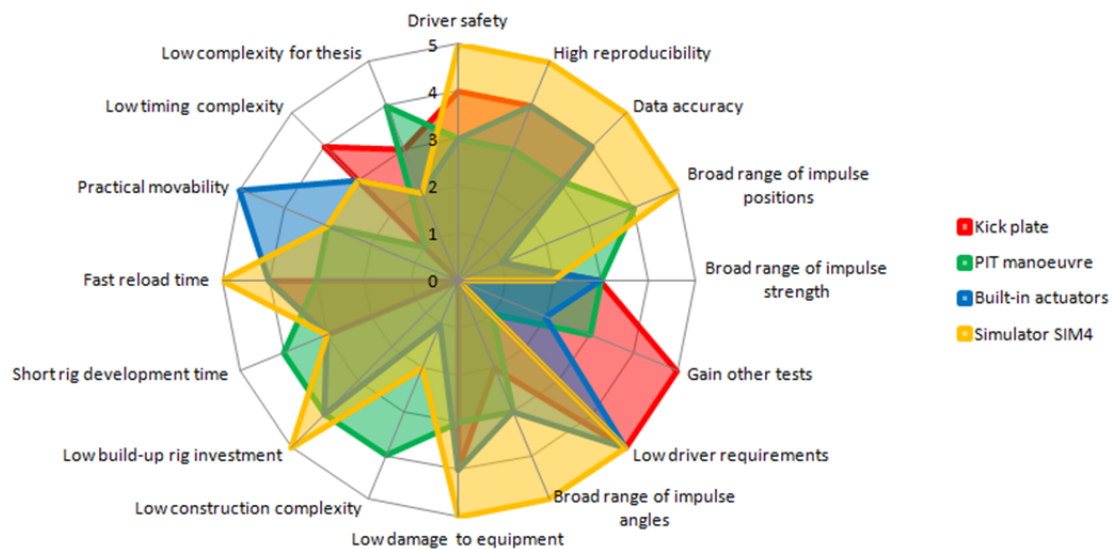


Figure 7.23. Rig candidates in the ranked radar, clockwise increasing from top.

7.2.3 Brief feedback from interview

7.2.3.1 Why is the Post Impact rig important for Volvo PV?

"The rig is important for the safety leadership and for the company's vision 2020, with new test methods there is possible to approach more accidents. Improving stability control functions gains the corporation goals and internally Development and Verification departments benefits having more tools to support the measurements. The Post-Impact functions as PIB & PISC are important to Volvo and need to be verified."

7.2.3.2 Which other test do you think it could be useful for?

"The vehicle instability and driver safety is a wide research area where several test could be performed, just some examples are: as seats side support and seat belts tensioning in crash related tasks, air bag deployment in MEA, etc. The most of the crash tests do not have the human response due to obvious reasons; however a rig that can grasp that critical factor in a safe method would be desirable. Sensors and other hardware can be tested on production cars."

7.2.3.3 Free thoughts and feedback

Reaching the Post-Impact states is the most important regarding the data accuracy, and the drivers' feedback from the added benefit is critical, therefore the radio controlled option is not suitable for this purpose. Aspects as the drivers panic level is very important in reaction time and can hardly be simulated without the drivers' awareness in a practical frame. For this reason the Simulator is very advantageous due to the guaranteed safety all the time, light crash scenarios have been simulated with the surprise factor. Drivers can withstand up to $2-3 \cdot g$ [m/s^2] in a test, higher than that it becomes dangerous.

The function of the rig is mostly meant to replicate the destabilized motion states, for which the safety of the driver and the test environment should be ranked far way higher than the other criteria. Test methods as the water canon can imply high risks with unwanted deployment. The Kick plate concept is good provided good capabilities. Regarding the impact locations the efforts should be concentrated at the rear and from the sides, the essential here are the impulse angle and the impulse position, maybe the impulse magnitude as well. Enhanced cars can supply protection to driver and equipment.

The movability is good for creating different ground friction without the need to build up artificial pavements. This capability reduces the dependence on climate factors and cost less in that way. However the price is almost not influential if the equipment fulfils the result requirements.

7.2.3.4 Discussion about completeness of criteria

The difficulty to retain a surprise effect in some methods diminish their usefulness to study the psychological and emotional behaviour by the drivers, for instance: letting the test drivers ignore the strong instability ahead will hardly be permissible to working laws, this criteria is not graded and studied because there is no study in this legal matter. The simulator solution has advantages for this study, where the safe and controlled motions are monitored all the time, letting the surprise factor being feasible.

8 Conclusions

The research in the present work is pioneer in many aspects; GIDAS problem space knowledge, application of a combined collision method in real accident cases, and the result oriented evaluation of verification method for driver interaction during PI control.

- GIDAS problem space; because the enormous amount of information in the database just the critical, Post-impact yaw rate and side slip angle, variables were analysed. The phase plot shows a clear accumulation along the zero yaw rate and slip angle, probably due to pitch rate and low induced rotational impulse. The variable intervals to focus the efforts are:
 - PIV, from 20 [km/h] up to 60 [km/h]
 - PIYR, from -90 [deg/s] up to 90 [deg/s]
 - PISSA, from -30 [deg] up to 30 [deg]
- GIDAS coverage or objective criteria; rig candidate that have the best performance according to the results in Table 7.1, the PIT manoeuvre profiles as the foremost candidate to cover the GIDAS cloud, 60 % of the GIDAS cloud coverage. The Phase plot area is not as important as the GIDAS cases coverage but gives a measure of the rig capabilities over the two most important variables of the thesis. In this study the rig that covers most PIYR/PISSA area is the Simulator SIM4 with almost 40 % followed by the Built-in actuators.
- Practical aspects (subjective); regarding performance over several criteria the Simulator SIM4 has a clear advantage over all candidates due to the test friendly environment and low cost per test scores, as the grades in Performance 7 & Performance 8 shows. The second and the third candidates (Built-in actuators and PIT manoeuvre) are very close to each other, being switched with slight grade changes on the rig performance grades. These grades are very susceptible to change with improvements, which of course have a resource cost, but this criteria showed to be dispensable or less important.
- The collision model, which is a combination of a matrix method based on momentum-conservation and vehicle dynamics, implemented in Matlab/Simulink model could be used to estimate the post-impact states from requested pre-impact states in an acceptable accuracy.
- Three verified GIDAS representative cases are analysed in detail and demonstrate the method of proposed collision model. With well-matched reconstruction result, these examples kind of validate both collision model and Simulink model for further rig analysis.
- Three feasible rigs: Kick plate, PIT manoeuvre and Built-in actuators are studied in detail using the collision model.

- Ten cases are used to identify the rig capabilities. These ten cases are particularly analysed using the database documents and reconstructed through three feasible rigs, where eight of the ten cases are reconstructable.

9 Future work

The future work that can be useful for the PIC project, and for the series of thesis work within the cooperation Volvo Cars Company and Chalmers Technical University, are presented in both short term and long term.

Short term (<6 months):

- Some rig alternatives have appeared during the thesis but have not been developed further for time reasons, these candidates and the combinations of them can be analysed with the same software and implement in the evaluation; candidates that have not been analysed are:
 - Kick bar that consists of a retractile arm that pushes the vehicle body as it passes through. A protective plate mounted at the host car will prevent further damage to the host car, in the same form as the PIT manoeuvre cars have enhanced protection. Possible some soft material with known coefficients will be the contact output.

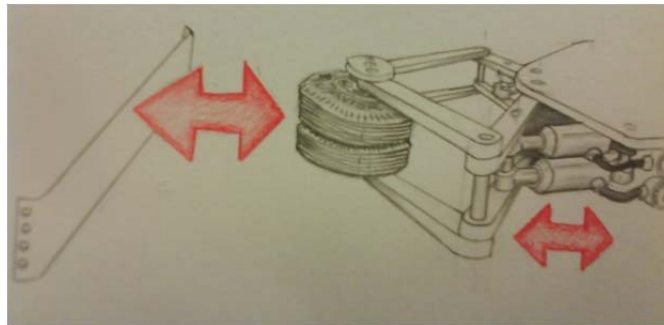


Figure 9.1 Kick bar sketch showing an example of the principle.

- A combination of the PIT manoeuvre and a Kick bar will take care of some deficient of both alternatives, but raising the complexity, cost, and development time, and might decrease the movability or other aspects, however this combination is worth to study further.
 - Another suggestion that appeared during the thesis was a Fifth wheel car that deploys a fifth tyre to the ground when desiring a sudden destabilisation force. The tyre could probably be oriented in an oblique direction from the longitudinal axis and positioned under the trunk of the car. Advantages and disadvantages are balanced by the efficiency in the GIDAS coverage and the influence in the natural inertia parameters of the test vehicle.
- Develop the simulation model with more degrees of freedom, especially with pitch dynamics and simulating the behaviour of tyre lifting from the ground without/before rollover.
 - Develop the automatic script for post processing of the simulation output, enhancing the analysis time. i.e a program that plots requested variable combinations trying to require less time and energy to interpret the information of the researcher. For instance SIL/HIL tests will benefit of that visualization tool.

- Make a more deep study of the influences of the delimitation assumption with an improved model. Some influences have been studied but there are more influences that should be carried out provided time.
- Ask for newest GIDAS or other database with complete data sets for vehicle dynamics, despite of if there are just a few cases but with recorded accident data. Or request logged data from the existent crash test at the correspondent Volvo department.

Long term (>6 months):

- Implement the Simulator SIM4 method by a team with deep programming skills requirements in both high application and hardware near programming. Some experience with simulators will be desired as well as knowledge of Vehicle dynamics and HIL-testing. A similar study to the one in (Thor, 2007) but with the Simulator SIM4 might be interesting.
- Implementation of the Built-in actuators because it has a good performance in the subjective grades for testing PIC function. This method can be completed with a helmet mounted display similar to the ones the airplane fighters use. By this way, making it possible to project traffic situations that improve the psychological capabilities for the human study.

10 References

- Anderson, A. (2009). *Implementation, validation and evaluation of an ESC system during a side impact using an advanced driving simulator*. Department of Electrical Engineering, Tekniska Högskolan i Linköping, LITH-ISY-EX--09/4234--SE, Linköping, Sweden.
- Antonietti, V. (1998). *Estimating the coefficient of restitution of vehicle-to-vehicle bumper impacts*. Society of Automotive Engineers, SAE Tech. paper 980552.
- Beltran J. & Song Y. (n.d.). *Share disc for this thesis*. Retrieved from VCC: Z:\PostImpactControl-vcc34520\PostImpactStabilityControl\MScThesisDescription_PIC_DrvrInteract_Verif
- Boström, O. et al. (1996). *A new neck injury criterion candidate-based on injury findings in the cervical ganglia after experimental neck extension trauma*. Proceedings of the IRCOBI Conference on Biomechanics of Impacts, Dublin, Ireland, pp 123-126.
- Boyd, G.J. et al. (2007). *Light vehicle ESC performance test development, NHTSA*. Paper No. 07-0456.
- Brach, R. (2003). *Modelling of low-speed, front-to-rear vehicle impacts*. Society of Automotive Engineers, SAE Tech. paper 2003-01-0491.
- Cannon, J. (2001). *Dependence of a coefficient of restitution of geometry for high speed vehicle collisions*. Society of Automotive Engineers, SAE Tech. paper 2001-01-0892.
- Cartype.com. (2011). *CARTYPE.COM*. Retrieved April 1, 2011, from http://www.cartype.com/pages/4693/volvo_s60_sedan__2011
- Cliff, W., & Montgomery, D. (1996). *Validation of PC-Crash a momentum based accident reconstruction program*. Society of Automotive Engineers, Paper number 96-0885.
- Coelingh, E. (2005). *Active Safety and Complete Vehicle Control*. Proceedings, 1st AUTOCOM Workshop on Preventive and Active Safety Systems for Road Vehicles, Istanbul, Turkey.
- Eichberger, A. et al. (1998). *Evaluation of the applicability of the neck injury criterion (NIC) in rear end impacts on the basis of human subject tests*. Proceedings of the IRCOBI Conference on Biomechanics of Impacts, Gothenburg, Sweden, pp. 321-333.
- EuroNCAP. (2011, 3 31). *European New Car Assessment Programme homepage*. Retrieved March 31, 2011, from www.euroncap.com
- GIDAS. (n.d.). *RECO_US, Codebookexport*. Retrieved from Z:\PostImpactControl-vcc34520\PostImpactStabilityControl\MScThesis_PostImpactStabilityControl_Yang\MSc.thesis_PISC\DAQ\SAFER\REKO_US.doc
- Gillespie T.D. . *Fundamentals of Vehicle Dynamics*. Society of Automotive Engineering.
- GmbH, H.-B. (2010). *Datasheet Kick plate*. HMP-Bau GmbH.
- Google. (n.d.). *Google Image Search*. Retrieved April 1, 2011, from [Google.com: www.google.com/imghp?hl=en&tab=wi](http://www.google.com/imghp?hl=en&tab=wi)
- ITE. (2010). *Intersection Design Guidelines*. Retrieved April 1, 2011, from Institute of Transportation Engineers homepage: <http://www.ite.org/css/online/DWUT10.html>
- Jalopnik.com*. (2009). Retrieved April 31, 2011, from Forum: www.jalopnik.com/#/15250843/ford-engineers-strap-giant-water-cannon-to-volvo;www.jalopnik.com/5251098/riding-the-volvo-water-cannon;www.youtube.com/watch?v=40o6jgzZij0
- Langwieder, K. et al. (1999). *RESICO-Retrospective Safety Analysis of Car Collisions Resulting in Serious Injuries*. GDV 9810, Munich, Germany.
- Monson, K. G. (1999). *Determination and mechanisms of motor vehicle structural restitution from crash test data*. Society of Automotive Engineers, SAE Tech. paper 1999-01-0097.
- NHTSA. (2004). *National Highway Traffic Safety Administration homepage*. Retrieved March 31, 2011, from www-nrd.nhtsa.dot.gov/Pubs/TSF2004.pdf

- Pacejka, H. (2006). *Tyre and Vehicle Dynamics (2nd Ed)*. Society of Automotive Engineers, Inc., SAE ISBN 0 7680 1702 5, Warrendale, PA. USA.
- Petersson, E., & Tidholm, D. (2007). *Vehicle Stability Control for Side Collision by Brake and Steering Wheel Torque Superposition*. Department of Signals and Systems, Chalmers University of Technology, MSc. Thesis EX031/2007, Gothenburg, Sweden.
- Pinellas County, S. O. (2007). *Pursuit operation of sheriff's office vehicles*. General Order 15-2. Florida, USA.
- pistonheads.com*. (2010). Retrieved March 31, 2011, from Forum: www.pistonheads.com/gassing/topic.asp?t=836562
- rockingham.co.uk*. (2011). Retrieved April 1, 2011, from Rockingham Motor Speedway homepage: www.rockingham.co.uk/oem/wetgrip.asp
- Segel, L. (1956). *Theoretical prediction and experimental substantiation of the response of the automobile of steering control*. Proceedings of Institute of Mechanical Engineers, pp. 310-330.
- Skidcar.com*. (2011). Retrieved April 1, 2011, from Skidcar System homepage: www.skidcar.com
- Thor, M. (2007). *The Efficiency of Electronic Stability Control after Light Collisions*. Department of Applied Mechanics, Chalmers University of Technology, MSc. Thesis 2007:02, ISSN 1652-8557, Gothenburg, Sweden.
- Trafikverket. (2010). *Variation of crash severity and injury risk depending on collision with different vehicle types and objects*. Retrieved April 1, 2011, from Swedish Transport Administration homepage: http://www.trafikverket.se/PageFiles/3535/variation_of_crash_severity_and_injury_risk_dependig_on_collisions_with_different_vehicle_types_and_objects.pdf
- uptodatedesign.com*. (2008). *UPTODATEDESIGN.COM*. Retrieved 12 2010, from <http://www.uptodatedesign.com/2008/12/2009-volvo-s60-concept-as-best-car-design/2009-volvo-s60-concept-3/>
- Volvo Cars Corporation. (2009). *Corporate Report 2009/10*. Retrieved March 31, 2011, from Volvo Cars Corporation homepage: http://www.volvocars.com/intl/top/about/corporate/volvo-sustainability/reports/Documents/Volvo_PV_Foretagsrapport_09_10_ENG.pdf;www.volvocars.com/se/all-cars/volvo-s60/Pages/default.aspx
- Voser C. et al. (2010). *Analysis and control of high sideslip manoeuvre, Vehicle system Dynamics, Vol. 48*. Page 317 – 336.
- VTI. (2011). Retrieved April 1, 2011, from Swedish National Road and Transport Research Institute homepage: www.vti.se/templates/Page___11861.aspx
- VTI. (2010). *Sim4 – Technical description (Draft)*. Swedish National Road and Transport Research Institute.
- Yang, D. (2009). *Method for Benefit Prediction of Passenger Car Post Impact Stability Control*. Department of Applied Mechanics, Chalmers University of Technology, Master's Thesis 2009:06, ISSN 1652-8557, Gothenburg, Sweden.
- Zhou, J. et al. (2008). *Collision model for vehicle motion prediction after light impacts. Vehicle System Dynamics, 46:1,3-15*. Department of Mechanical Engineering, University of Michigan, USA ISSN 0042-3114 print/ISSN 1744-5159 online, Ann Arbor, MI, USA.

Appendix A. Notations

The entire notation is for the host vehicle if nothing else is clarified.

Roman upper case letters

BX	:	Vehicle body length
BY	:	Vehicle body width
D_s	:	Total suspension roll damping
F_i	:	Force at the CoG along the index coordinates
I_i	:	rotational inertia around the index coordinates
I_{ang}	:	Angle of impact precedence, GIDAS coordinates.
I_{mag}	:	Impulse magnitude of impact
K_s	:	Total suspension roll stiffness
L	:	Vehicle wheelbase length
M_i	:	Torque at the CoG around the index coordinates
SLf	:	Suspended (mass) length to the front axle
V_i	:	Vehicle velocity at the CoG along the index coordinates

Roman lower case letters

l_{tw}	:	Track width length
l_i	:	Distance from CoG to index axle, vehicle body length
m	:	Total vehicle mass
p	:	Impulse
t	:	Time
w_i	:	Yaw rate around index axis
$xPos$:	X position of impact, GIDAS-coord
$yPos$:	Y position of impact, GIDAS-coord

Greek uppercase letters

Δ	:	Difference
Γ	:	Deformation angle of host vehicle

Greek lowercase letters

β_i	:	Side slip angle at index position or time point
ε	:	Yaw deviation angle
λ	:	Vehicle mass distribution coefficient
μ	:	Friction coefficient

Index

l	:	Host vehicle
2	:	Bullet vehicle
c	:	Collision
f	:	Front axle
r	:	Rear axle
s	:	Suspended mass
PI	:	Post-Impact
x	:	Along/around x axis
y	:	Along/around y axis
z	:	Along/around z axis

Abbreviations & acronyms

CoG	:	Centre of gravity
CoR	:	Coefficient of restitution
DOF	:	Degree of freedom
PI	:	Post-Impact
PISSA	:	Post-Impact side slip angle
PIV	:	Post-Impact velocity
PIYR	:	Post-Impact yaw rate

Coordinate systems

The both coordinate systems that have been used are:

- The vehicle ISO-car coordinates, (ISO 31/1000/80000):

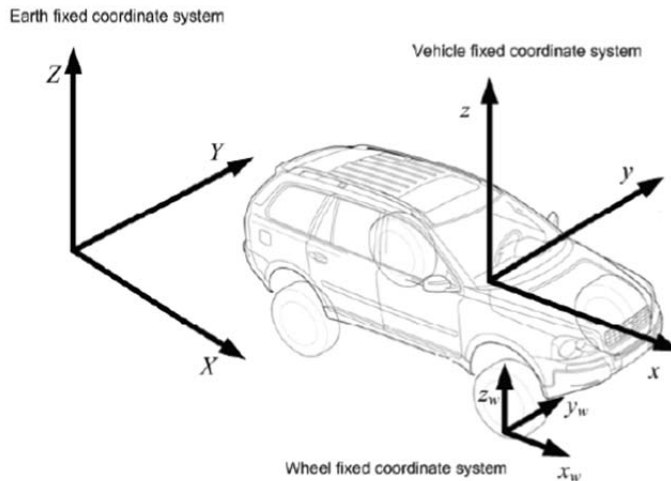


Figure A. 1. The different coordinate subsystems ISO-car coordinates. <Source: (Thor, 2007)>

The ISO-coordinate system is described in several subsystems that are interrelated by Euler's Angles transformation matrixes (Gillespie T.D.). Note the direction at which the positive axes are pointing at. In especially the x- and y-axis of the car body.

– GIDAS car coordinates

This coordinate system have slightly differences in relation with the ISO system, most the direction in which the axes positive direction points at, and turns around.

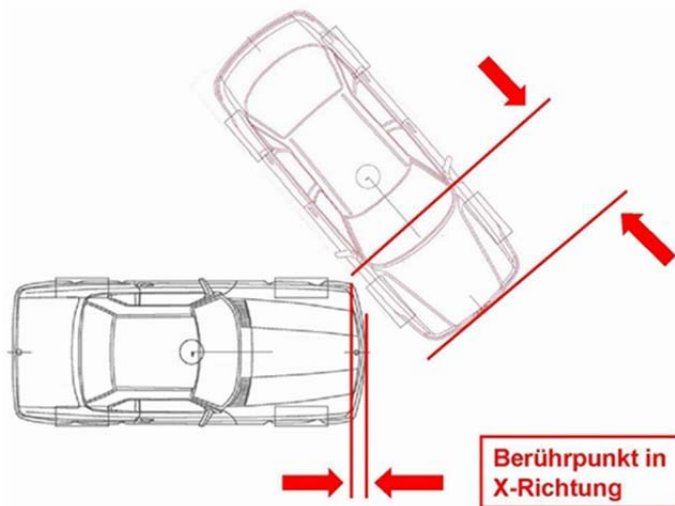


Figure A. 2. x-coordinate in GIDAS coordinate system. <Source: (GIDAS)>

The x-coordinate begins at the very front of the vehicle, prolonged until the vehicles end, in the S60 Volvo approx. 4.6 meters. I.e. There entire car are in the positive x-axis in the GIDAS-car coordinate system.

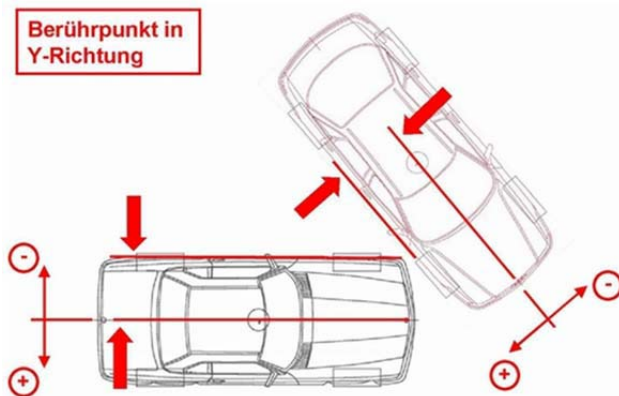


Figure A. 3.y-coordinate in GIDAS coordinate system. <Source: (GIDAS)>

The y-coordinate zero position is located at the middle section of the car in transversal meaning, and congregates at the zero-position of x-coordinate at the front of the car. Therefore the origo of this system is located at the middle of the front of the vehicle. The positive y-axis points at the left of the car, in opposite to the ISO coordinates.

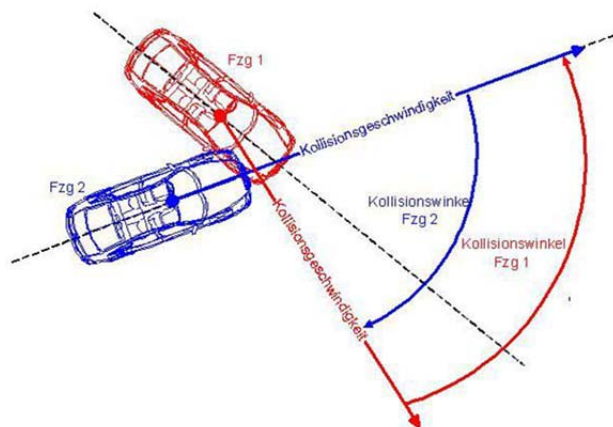


Figure A. 4.Impulse angle in GIDAS coordinate system. <Source: (GIDAS)>

The precedence of the impulse is described by an angle that swaps the space from the positive x-axis to the negative x-axis. I.e. The angles lay in between -180 and 180 degrees, making the zero degree an impact from the behind and an angle of 180 or -180 an impact from the front. For more information about the units, the transformations made consult (GIDAS).

Vehicle parameters

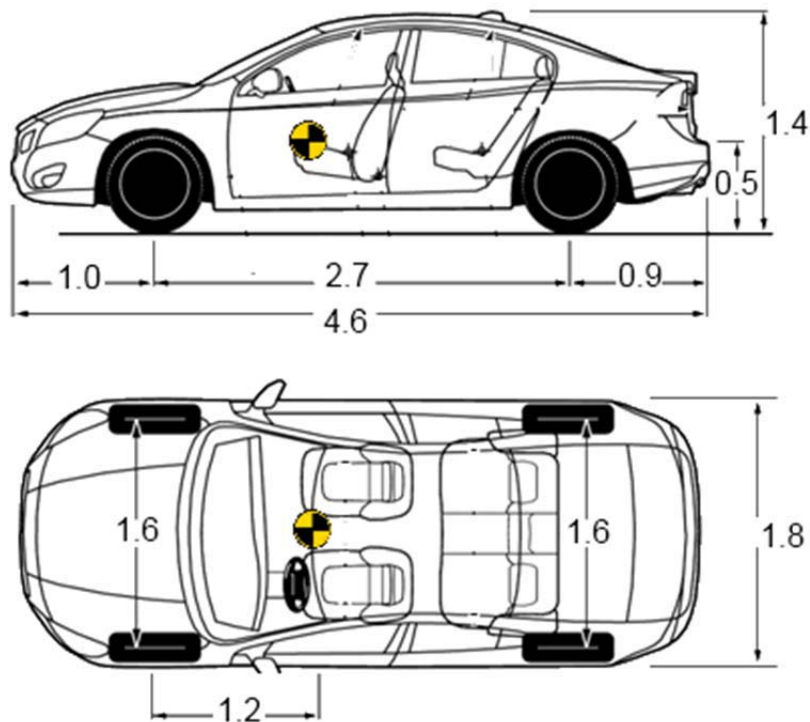


Figure A. 5. Vehicle dimensions VOLVO S60. <Source background: (Cartype.com, 2011)>

The car used to simulate the most of the studies in the thesis is the Volvo S60 with the following parameters:

$$m = 1625 \text{ [kg]}$$

$$I_{zz} = 3260 \text{ [kgm}^2\text{]}$$

$$I_{xx} = 3000 \text{ [kgm}^2\text{]}$$

$$L = 2.715 \text{ [m]}$$

$$\lambda = 0.45$$

$$l_{tw} = 1.56 \text{ [m]}$$

$$SLf = 1.0 \text{ [m]}$$

$$BX = 4.6 \text{ [m]}$$

$$BY = 1.8 \text{ [m]}$$

Collision analysis variables

V_{1x} : post-impact longitudinal velocity of host vehicle in its local coordinate.

V_{1y} : post-impact lateral velocity of host vehicle in its local coordinate.

Ω_{1z} : post-impact yaw rate of host vehicle in its local coordinate.

Ω_{1x} : post-impact roll rate of host vehicle in its local coordinate.

V_{2x} : post-impact longitudinal velocity of bullet vehicle in its local coordinate.
 V_{2y} : post-impact lateral velocity of bullet vehicle in its local coordinate.
 Ω_{2z} : post-impact yaw rate of bullet vehicle in its local coordinate.
 Ω_{2x} : post-impact roll rate of bullet vehicle in its local coordinate.
 v_{1x} : pre-impact longitudinal velocity of host vehicle in its local coordinate.
 v_{1y} : pre-impact lateral velocity of host vehicle in its local coordinate.
 w_{1z} : pre-impact yaw rate of host vehicle in its local coordinate.
 w_{1x} : pre-impact roll rate of host vehicle in its local coordinate.
 v_{2x} : pre-impact longitudinal velocity of bullet vehicle in its local coordinate.
 v_{2y} : pre-impact lateral velocity of bullet vehicle in its local coordinate.
 w_{2z} : pre-impact yaw rate of bullet vehicle in its local coordinate.
 w_{2x} : pre-impact roll rate of bullet vehicle in its local coordinate.
 P_{1x} : x-component of collision-induced impulse acting on the host vehicle in its local coordinate.
 P_{1y} : y-component of collision-induced impulse acting on the host vehicle in its local coordinate.
 P_{2x} : x-component of collision-induced impulse acting on the bullet vehicle in its local coordinate.
 P_{2y} : y-component of collision-induced impulse acting on the bullet vehicle in its local coordinate.
 (x_A, y_A, z_A) : host vehicle collision position in x-, y-, and z-axis.
 $(x_{A'}, y_{A'}, z_{A'})$: bullet vehicle collision position in x-, y-, and z-axis.
 θ : collision angle.
 θ_1 : The angle between the x-axle of earth fixed coordinate and host vehicle local coordinate.
 θ_2 : The angle between the x-axle of earth fixed coordinate and bullet vehicle local coordinate.
 (ξ_1, d_1) : host vehicle collision position in planar spherical coordinate.
 (ξ_2, d_2) : bullet vehicle collision position in planar spherical coordinate.
 F_{yf} : front tyre lateral friction.
 F_{yr} : rear tyre lateral friction.

Appendix B. Assumptions influence

The Base line consists of simulations with the bicycle model with magic formula tyre model, no longitudinal friction on tyres, $\mu=0.6$ for lateral friction on tyres and car fixed impulse angle, as the Water cannon.

Impulse shape influence

With the Bicycle model, magic formula tyre model and no longitudinal friction on tyres, $\mu=0.6$.

- Sinus shape: Sinus shaped impulse, double amplitude to compensate for the flanks of the smooth shape, red colour, used in (Anderson, 2009).
- Curve shape: A curved shape from the recommendation of impulse shape in (Anderson, 2009)
- Square shape, Baseline: The square shaped impulse, blue colour used in (Thor, 2007) & (Yang, 2009).

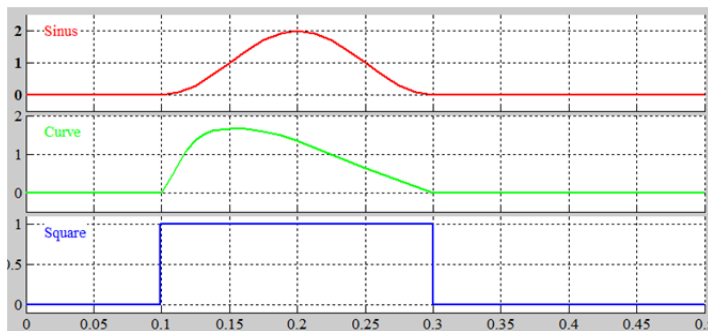


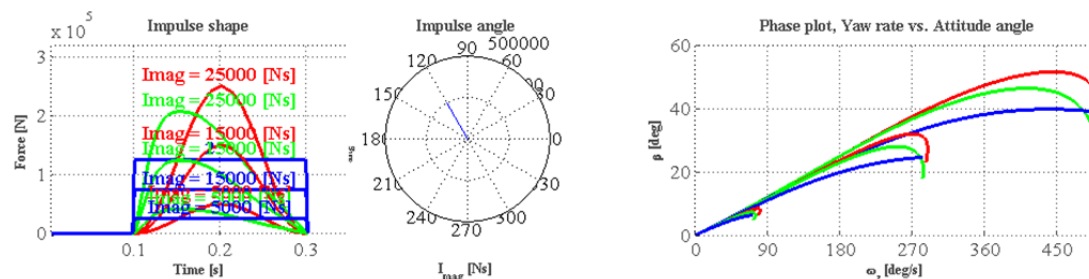
Figure A. 6. Three impulse shapes.

```

%% Time space config %%%%%%%%%%%%%%%%%%%%%%%%%%%%%%%%%%%%%%%%%%%%%%%%%%%%%%%%%%%%%%%%%%%%%%%%%
ctime = 0.2;      % Collision duration time[s]
stime = 0.002;   % Sampling time [s]
etime = 0.1+0.2; % Simulation end time [s]

##### Pre-Prblem space #####
Fmag = (5:10:25)'*1000/ctime; % (kNs)*1000/s
Fang = (120)'*pi/180; % (deg)*pi/180 [rad]
FxPos = (1.8)'; % (m) [m]
FyPos = (-0.7)'; % (m) [m]
vx_init = (40)'/3.6; % (kph)/C [m/s]
    
```

Figure A. 7. Impulse parameters, $I_{mag} = 5000, 15000, 25000$ [Ns].



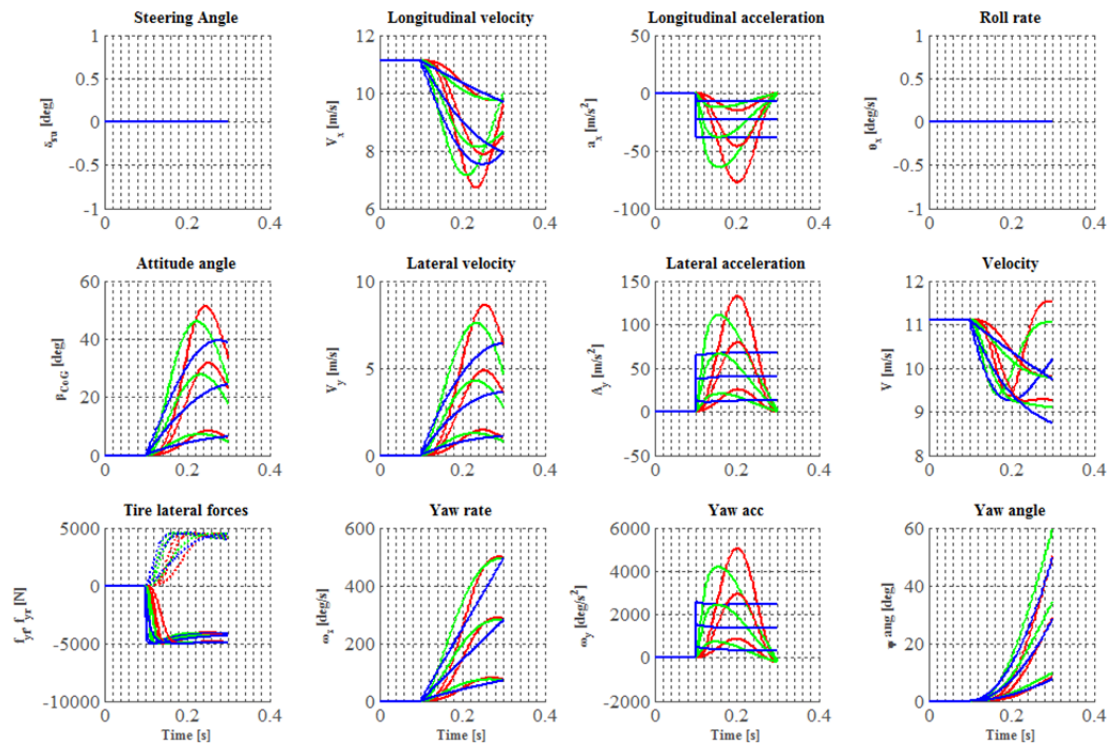


Figure B. 1. Impulse shape influence on the PI states.

Increasing the impulse from 5000 [Ns], considered as light impact, up to 25000 [Ns] or the three times the average of the impulse magnitude from GIDAS shows that somewhere near 15000 [Ns] the idealization of a square shape and the sinus shape do not follows the curved shape in all the PI states, differing by:

- PISSA -20 % between Curve shape to Baseline in 15000 [Ns] and -38 % in 25000 [Ns] impulse.
- PIYR 0 % in for all shapes over all impulse strengths.
- PIV 5 % between Sinus shape to Baseline in 15000 [Ns] and 15 % in 25000 [Ns] impulse.

The differences of the different states at the light impulse of 5000 [Ns] can barely sees, however the yaw rate and side slip differs slightly across the collision time section and reunites at the PI time point. PIYR do not differ at all in the PI time point, if the impulse amount is the same for all shapes and strengths. The blue baseline has a step in the acceleration subfigures, that step is just about to reunite to the other lines as quick as it raised in the next simulation step.

Tyre model influence

Magic formula tyre model: A quasi empirical model (Pacejka, 2006), in blue.

Linear tyre model: Constant lateral force stiffness and a saturation point, in red.

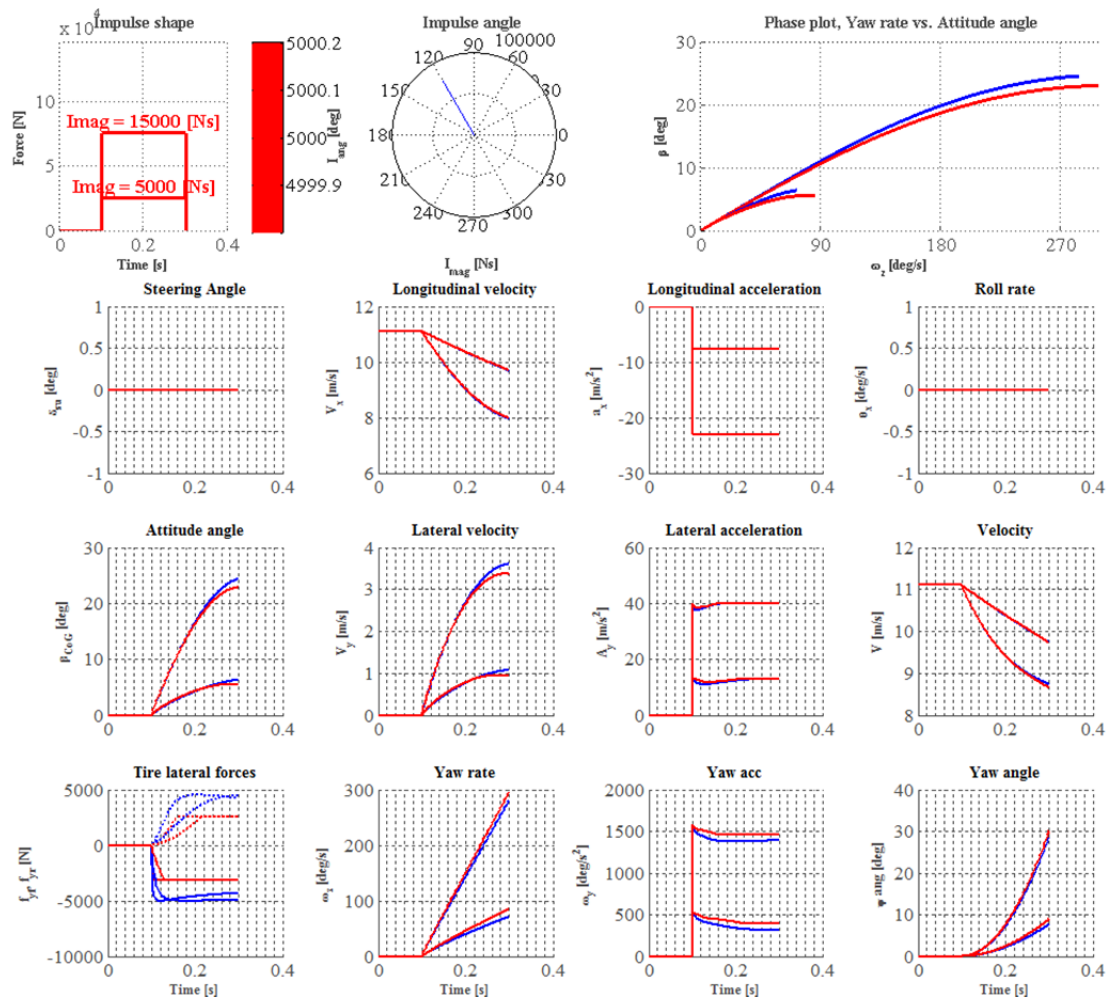


Figure B. 2. Tyre model influence on the PI states

The percent deviations from Baseline diminish the higher impulse magnitude. PIYR suffers more deviation than PISSA, PIV and other less significant variables remains almost the same. The tyre forces show that the different models have a different saturation point but very similar slope at the unsaturated part. The dotted lines correspond to the rear axle. The less resistance to turn in the case of the linear tyre model make it achieve higher yaw acceleration than the baseline. The saturation point of the linear model is reached at μ times the normal load at the tyre. What is to consider is that the bicycle model do not have any weight nor load transfer which have influences in the tyre capabilities. The height of the impact and its relation to the CoG has significant possibility to transfer load, until the tyre saturates, in some accident cases. This question of the tyre model influencing until a critical threshold is not possible to answer at a general form without better vehicle model than the bicycle model.

Appendix C. Filters

From the initial GIDAS database there are 14638 passenger car collisions, Figure C. 1, from there are filters applied in order to focus on the cases that are relevant to the PIC functions. In the work (Yang, 2009) the author filters out 944 PISC relevant cases which represents approximately the 7 % of the initial 14638 cases in the record.

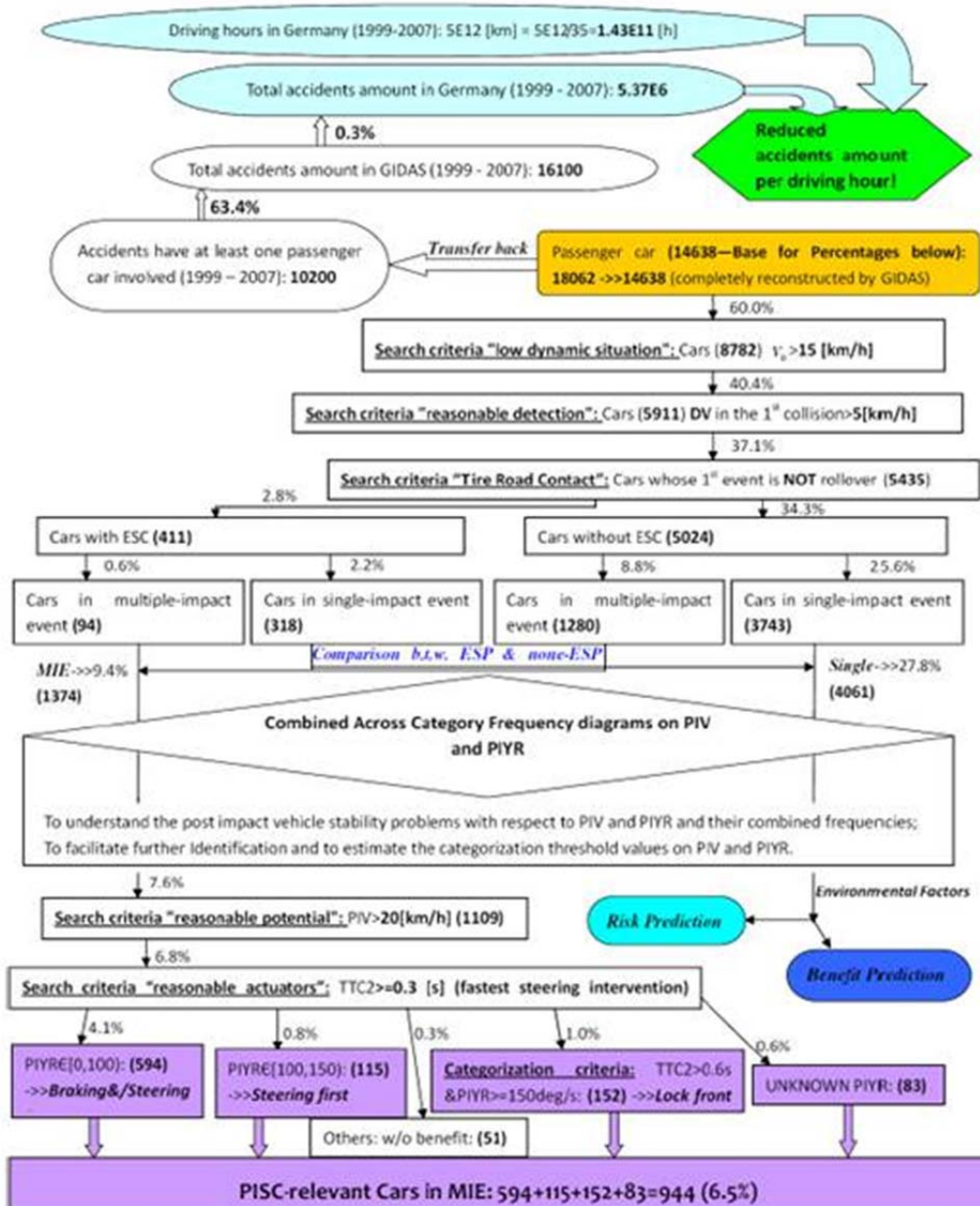


Figure C. 1. Filtering chart for PISC relevant cases. <Source: (Yang, 2009)>

Further releasing the filters:

- Search criteria "low dynamic situation": Cars (8782) $V_0 > 15$ [km/h],
- Search criteria "reasonable detection": Cars (5911) DV in the 1st collision > 5 [km/h], and
- Search criteria "reasonable potential": Cars (1109) $PIV > 20$ [km/h]

will made accessible 119 cases having a PIC-relevant 1063 cases GIDAS database, as seen in Figure C. 2.

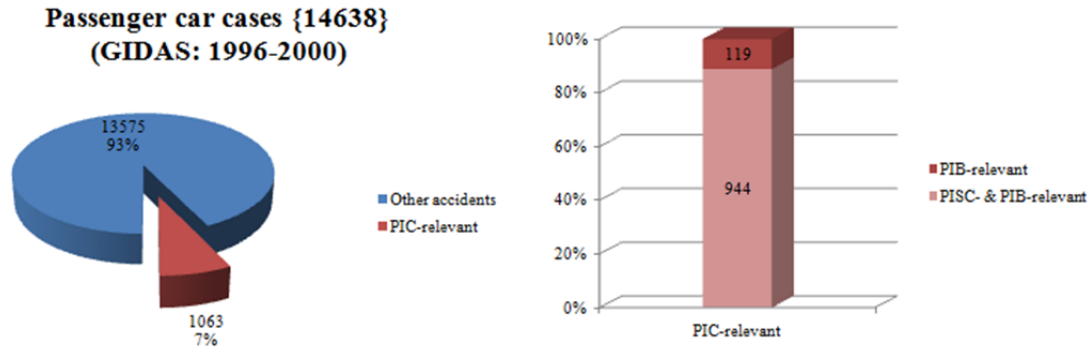


Figure C. 2. Share of multi event accidents from accident databases.

These 1063 PIC relevant cases have valuable information for the study but have unknowns and irrational data mixed in the useful data, therefore sorting out these and mapping where the gaps of them will appear facilitates the correct interpretation. The distribution of the cases that are eliminated fortunately appears to be distributed evenly across the vehicle, shown in Figure C. 3. The criteria of the filtering from GIDAS database to PIC-relevant will be found in the thesis work (Yang, 2009). From the initial 14638 cases of passenger car accidents are 1063 PIC-relevant cases separated for further handling. The refining process of the cases for the pre impact problem space and the post impact problem space is specified in Figure, following three Filtering steps:

- Step 1. Take care of all unknown data in pre impact problem space
- Step 2. Take care of the irrational data of the pre impact problem space
- Step 3. Takes care of the unknowns data in post impact problem space

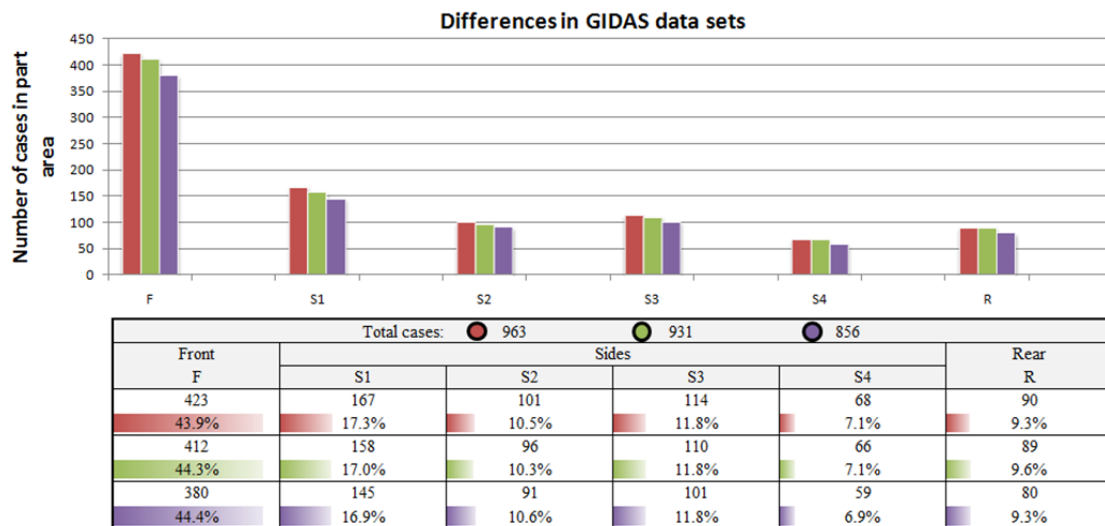


Figure C. 3. Differences in data sets showing an even distribution of the reduced data.

Table C. 1. Filter and refining process in three steps.

Cases after filter	Filter	Gain/Drop	Total G/D (%)
STEP 1.			
1063	PIC-relevant cases		
995	Crash weight \sim 1,135,9999,14009,blanks	-68	
1025	Crash weight II = empty weight + 150 [kg]	30	
1018	$\Delta V \sim$ 9999 [m/s]	-7	
1011	Parts \sim 5,6	-7	
1006	$lang \sim$ 999,9999 [deg]	-5	
971	$lx \leq$ 460 [cm]	-35	
964	$ ly \leq$ 90 [cm]	-7	
963	Vehicle width < 2100 [mm]	-1	
963	if($lang == 360, lang=0$)	0	-100
			-100 (-9.5%)
STEP 2.			
961	Front $90 < lang < 180$; Front $-90 > lang > -180$	-2	
956	Front $lx < 200$	-5	
949	Rigth $0 < lang < 180$	-7	
949	Rigth $ly > 0$	0	
948	Rigth if($PIYR == 1438$)	-1	
943	Left $0 > lang > -180$	-5	
943	Left if($lang == 180, lang = -180$)	0	
937	Left $ly < 0$	-6	
937	Back $-90 < lang < 90$	0	
936	Back $lx > 200$	-1	-27
931	$lmag < 30$ kNs	-5	-5
			-132 (-12.4%)
STEP 3. (Obs! Individually)			
856	if($PIV == 9999, PISSA == 9999$)	75	-207 (-19.5%)
860	if($PIV == 9999, PIYR == 9999$)	71	-203 (-19.1%)
856	if($PISSA == 9999, PIYR == 9999$)	75	-207 (-19.5%)

The enormous amount of data in this database is not all necessary for the thesis, which is the reason of cropping the useful data in a more accessible datasheet (Sorted_1063) improving the filtering capabilities that are in apparent conflict in the original Excel Sheet (Crude).

Appendix D. Problem Space, cont.

Figures that continue from the Chapter Problem Space

Pre-Impact Problem Space

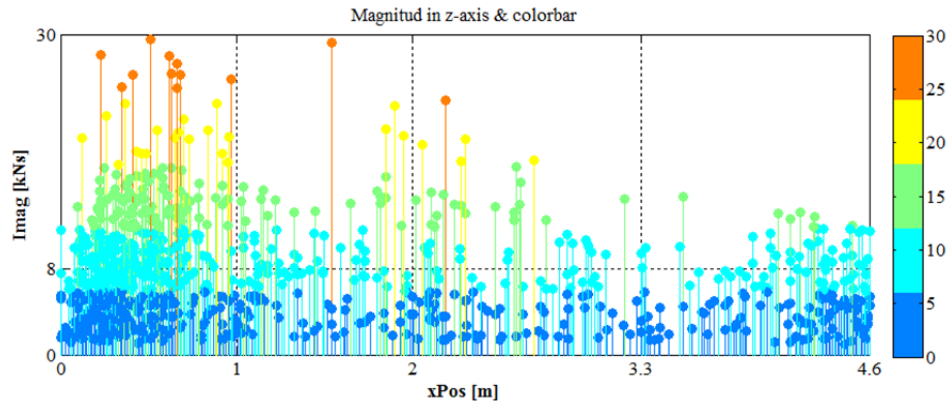


Figure D. 1. Pre-Impact problem space, Impulse physical and magnitude distribution, side view.

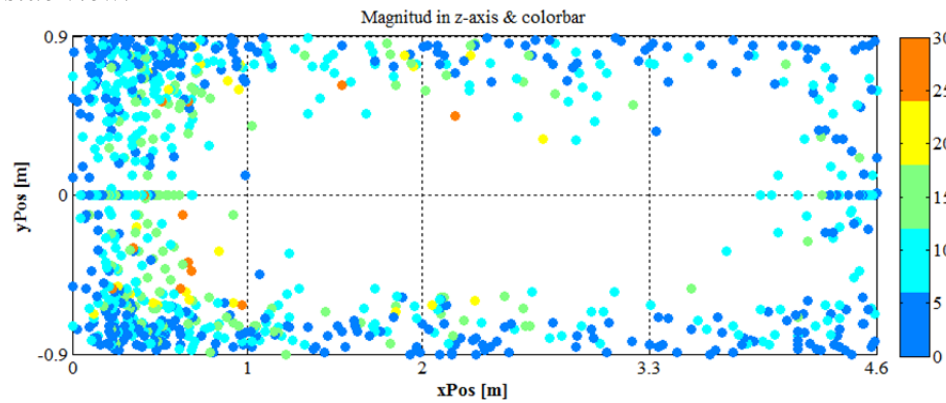


Figure D. 2. Pre-Impact problem space, Impulse physical and magnitude distribution, top view.

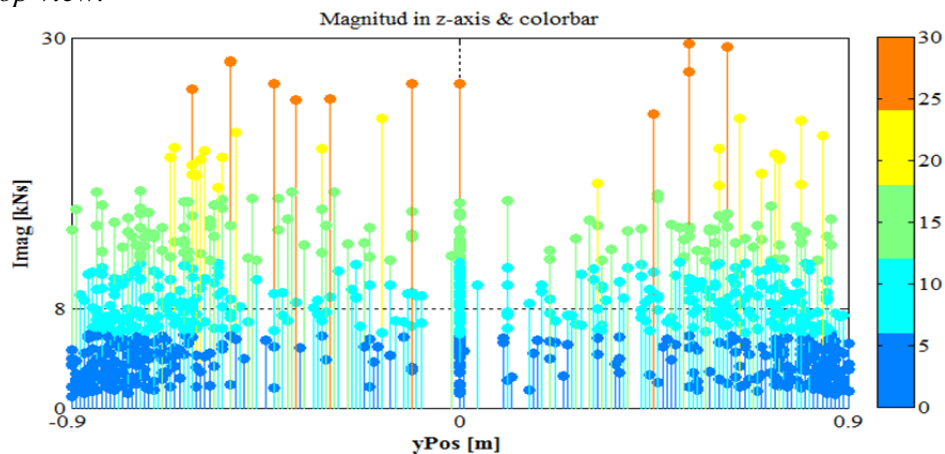


Figure D. 3. Pre-Impact problem space, Impulse physical and magnitude distribution, front view.

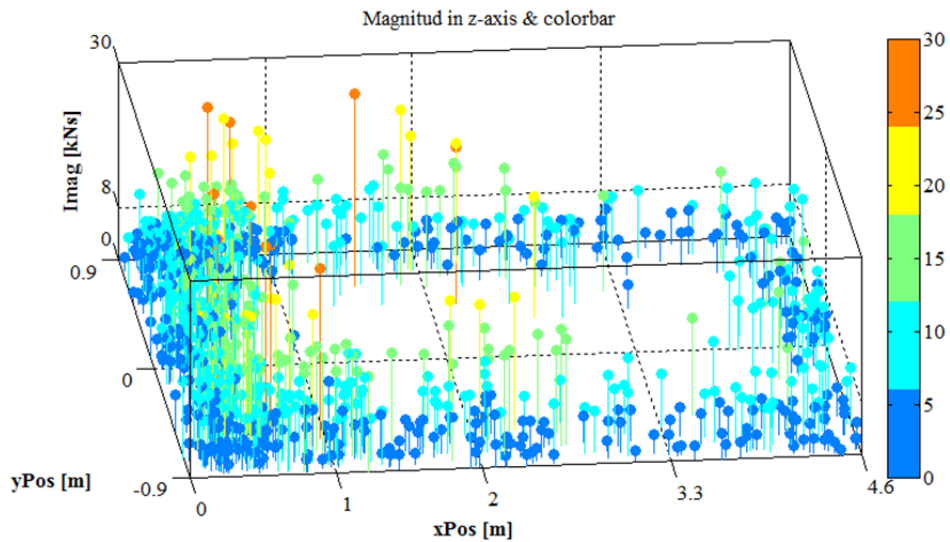


Figure D. 4. Pre-Impact problem space, Impulse physical and magnitude distribution, 3D view.

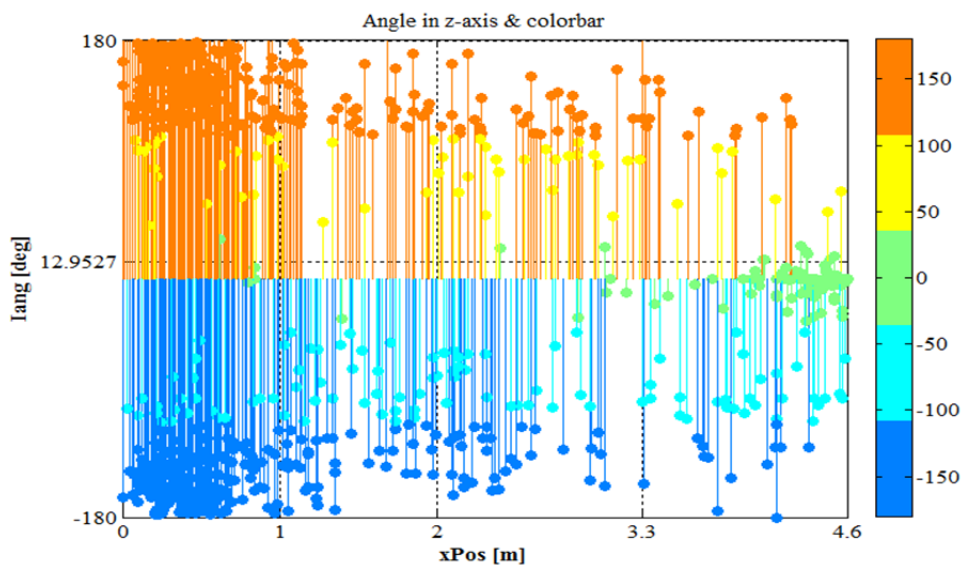


Figure D. 5. Pre-Impact problem space, Impulse physical and angle distribution, side view.

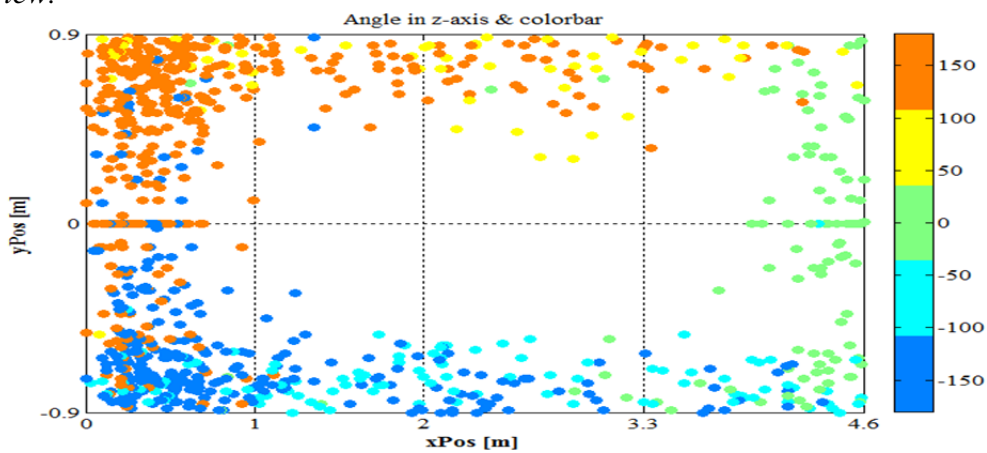


Figure D. 6. Pre-Impact problem space, Impulse physical and angle distribution, top view.

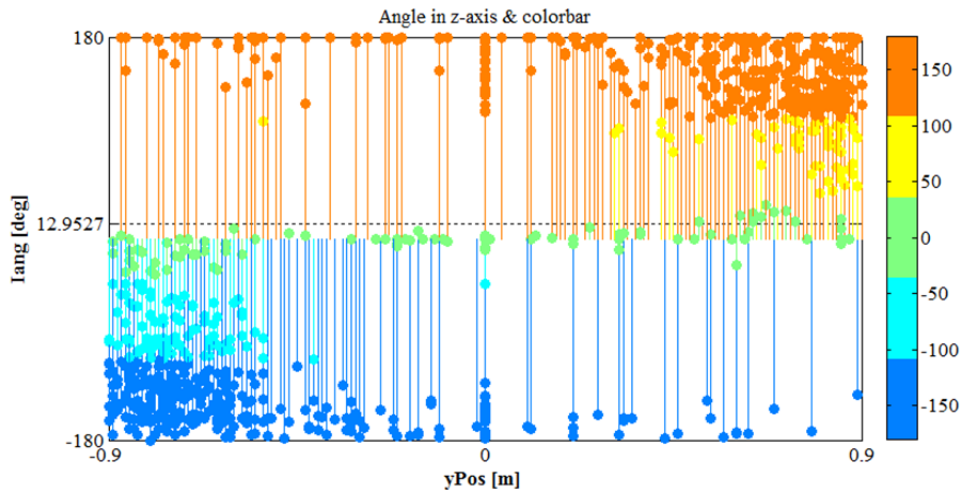


Figure D. 7. Pre-Impact problem space, Impulse physical and angle distribution, front view.

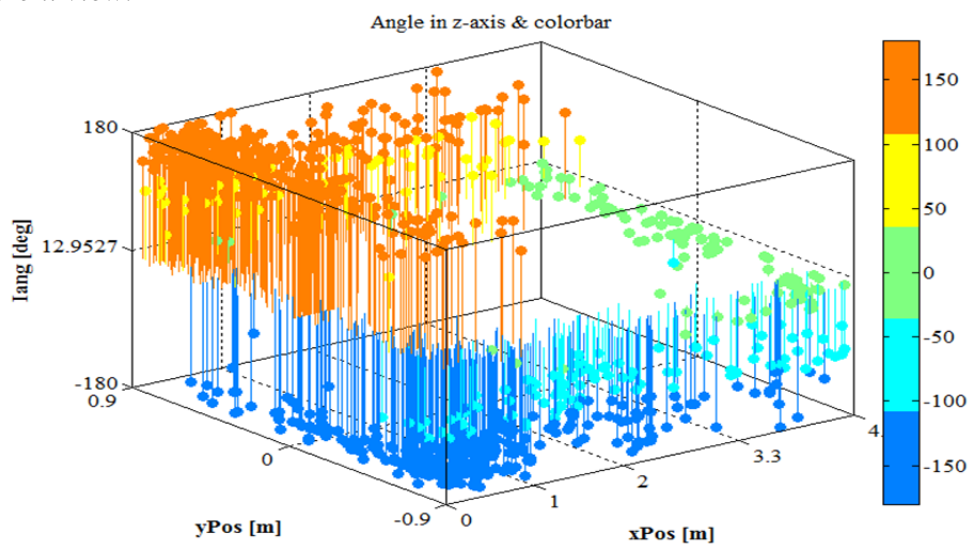


Figure D. 8. Pre-Impact problem space, Impulse physical and angle distribution, 3D view.

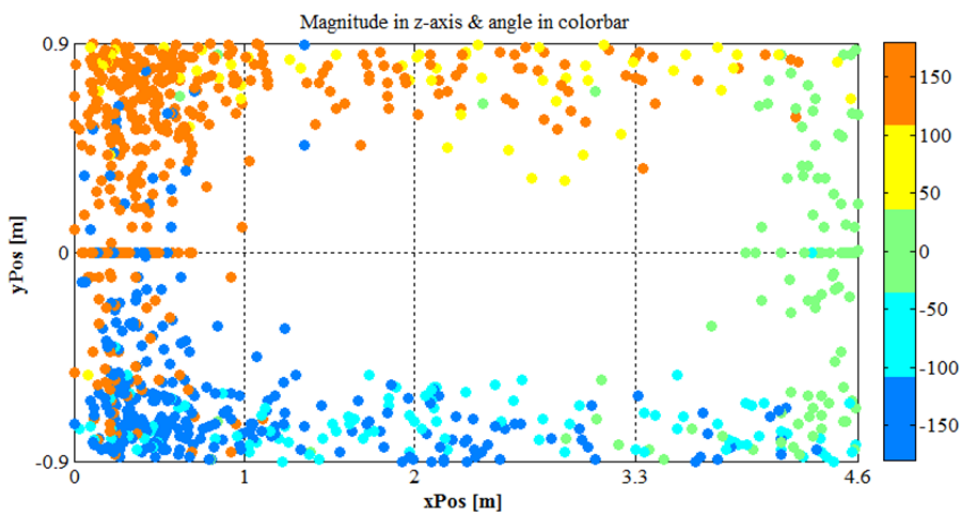


Figure D. 9. Pre-Impact problem space, Impulse physical, magnitude and angle distribution, top view.

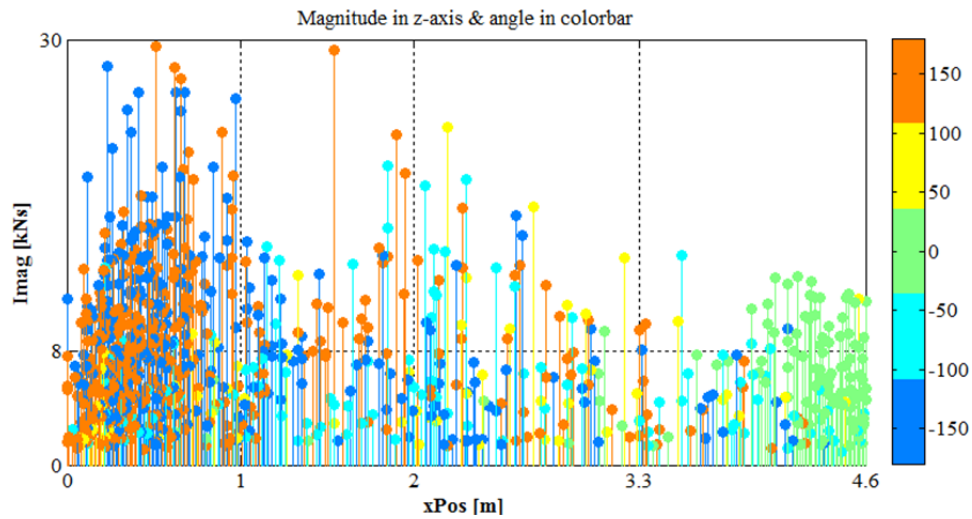


Figure D. 10. Pre-Impact problem space, Impulse physical, magnitude and angle distribution, side view.

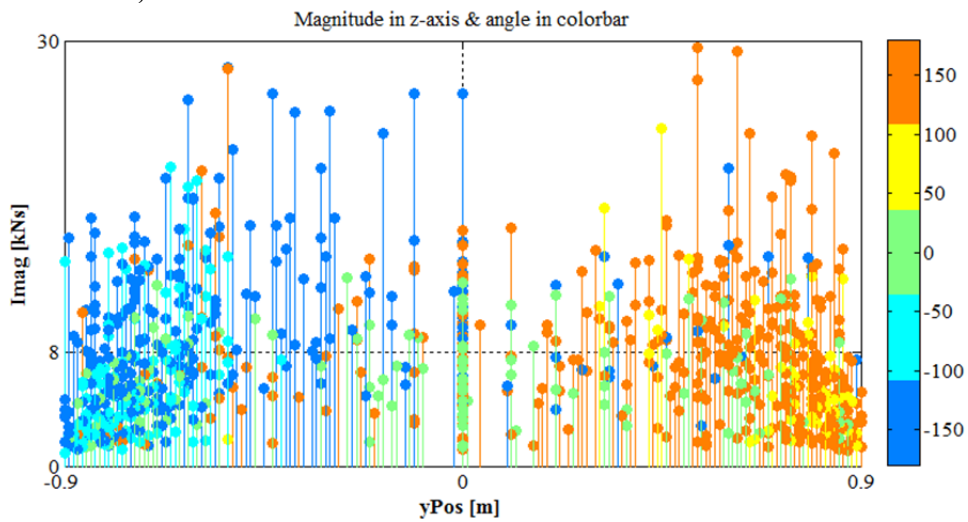


Figure D. 11. Pre-Impact problem space, Impulse physical, magnitude and angle distribution, front view.

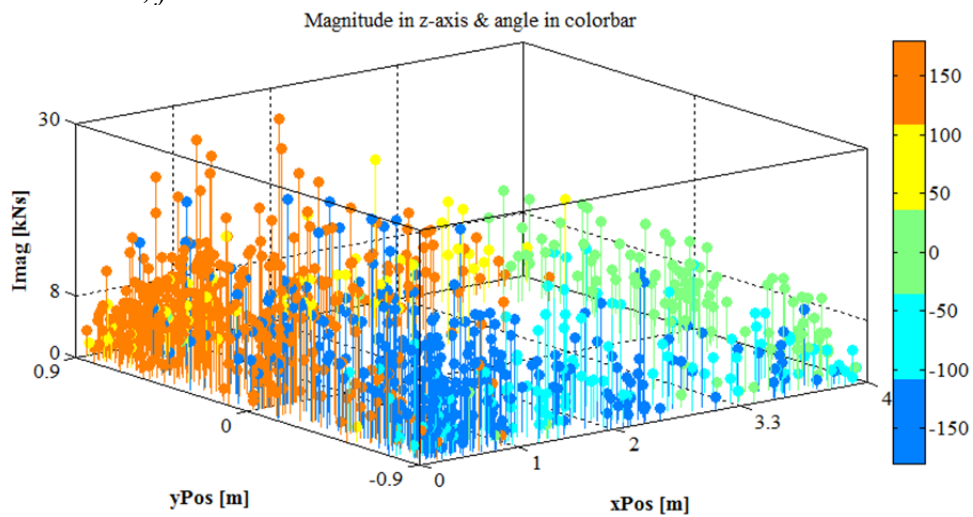


Figure D. 12. Pre-Impact problem space, Impulse physical, magnitude and angle distribution, 3D view.

Post-Impact Problem Space

The mirrored data is available in the Excel/Matlab codes at (Beltran J. & Song Y.).

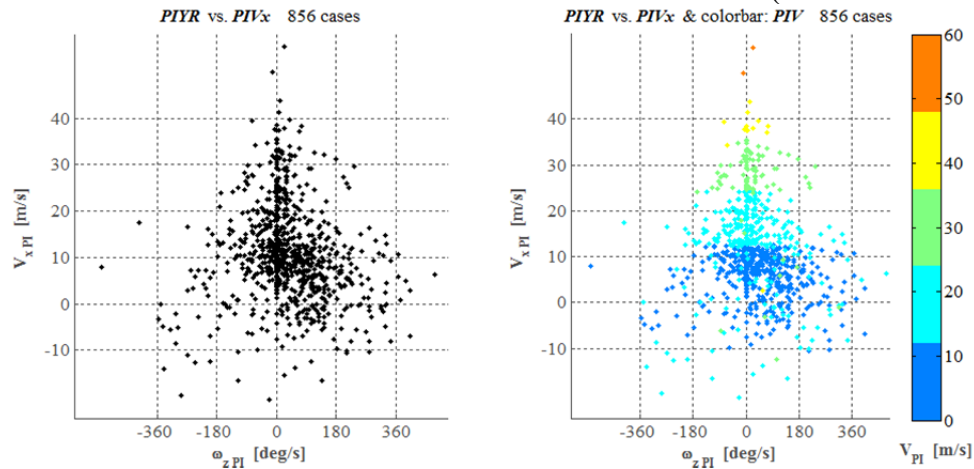


Figure D. 13. Post-Impact problem space, PIYR and PIVx.

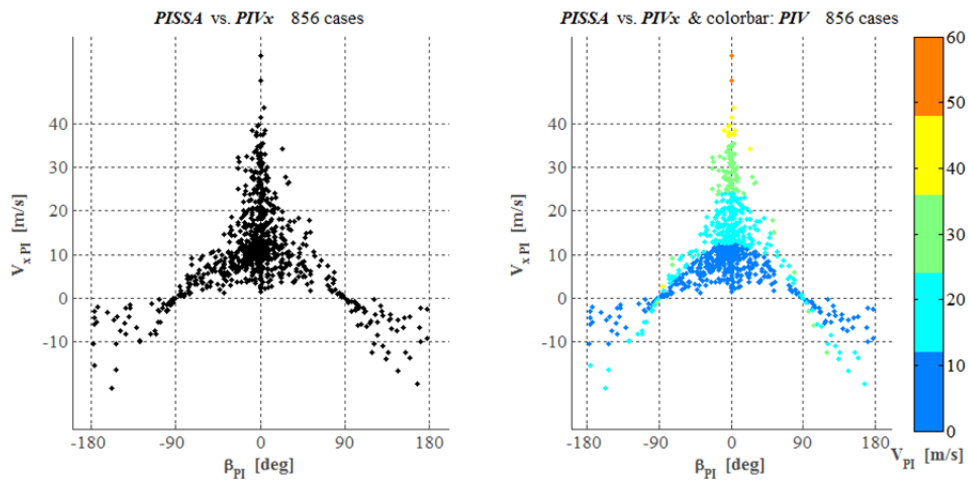


Figure D. 14. Post-Impact problem space, PISSA and PIVx.

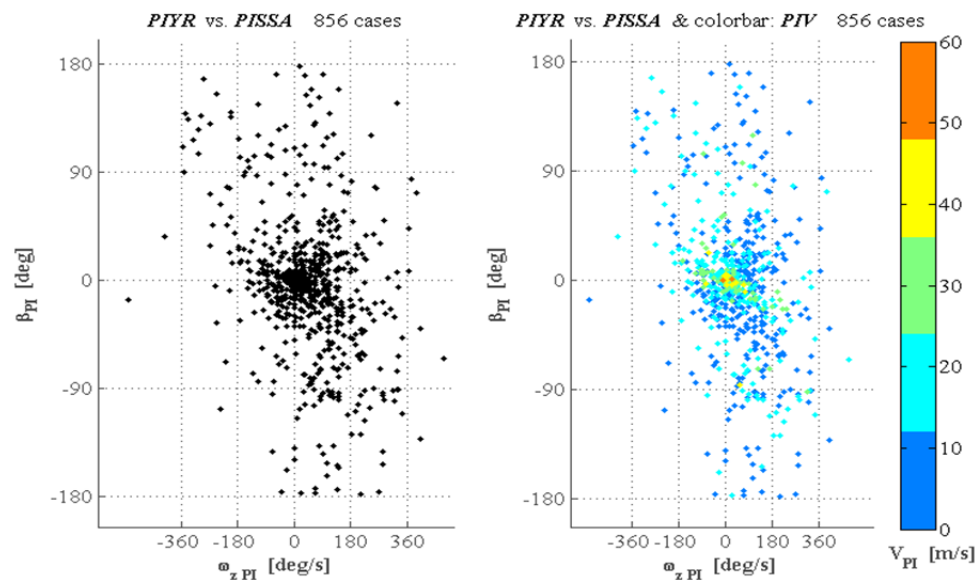


Figure D. 15. Post-Impact problem space, PIYR and PISSA.

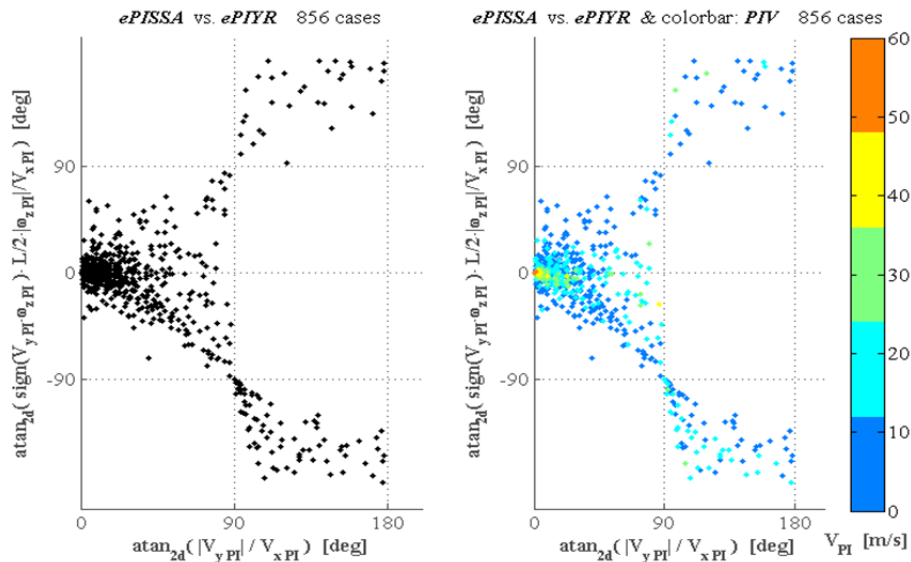


Figure D. 16. Post-Impact problem space, *ePISSA* and *ePIYR*.

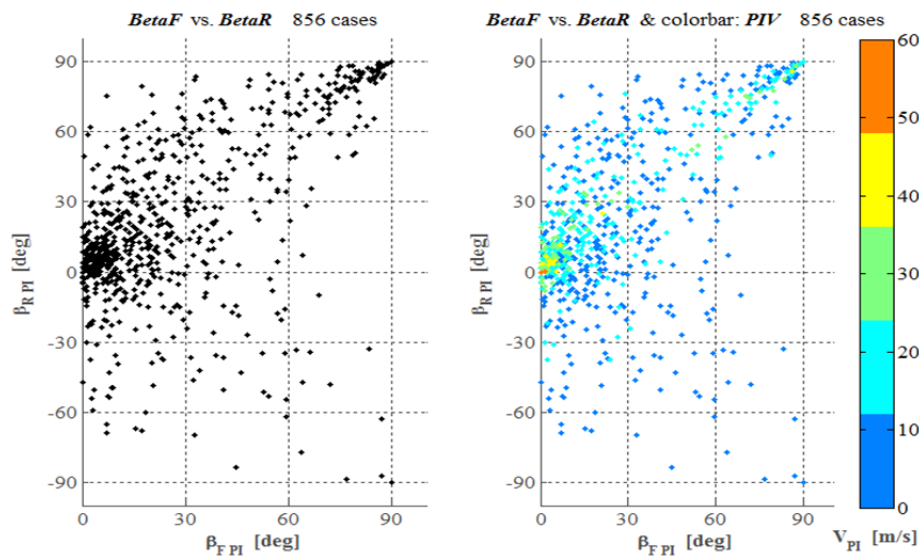


Figure D. 17. Post-Impact problem space, *BetaF* and *BetaR*.

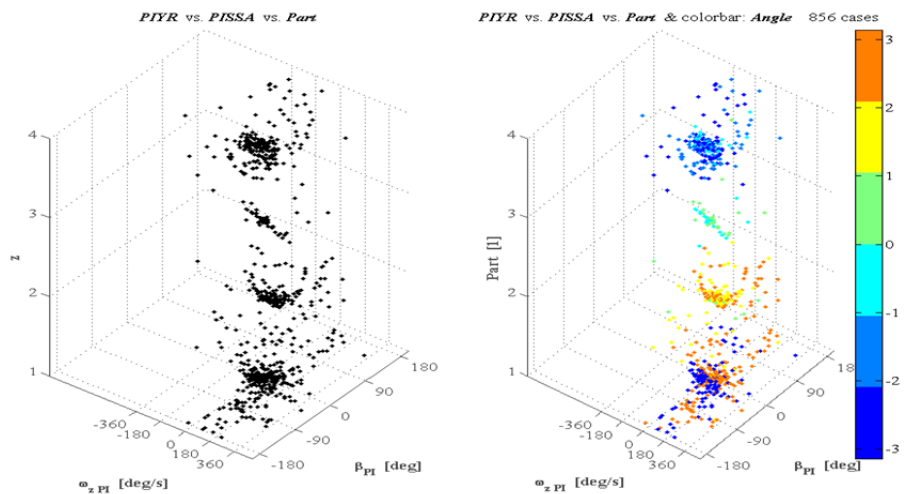


Figure D. 18. Example of the different variable combinations and points of view.

Appendix E. Interview questioner

Contents in this appendix are only found in the confidential variant of the report.

Appendix F. Collision Model

Collision Model Specific Term in Matrix

$$A_{11} = \begin{pmatrix} m_1 & 0 & -m_1 \frac{\Delta t}{2} V_{1y} & 0 \\ 0 & m_1 + \frac{\Delta t}{2} \cdot \frac{C_{f1} + C_{r1}}{V_{1x}} & m_1 \frac{\Delta t}{2} V_{1x} + \frac{\Delta t}{2} \frac{a_1 C_{f1} - b_1 C_{r1}}{V_{1x}} & -m_{R1} h_1 \\ 0 & \frac{\Delta t}{2} \cdot \frac{-a_1 C_{f1} + b_1 C_{r1}}{V_{1x}} & -I_{zz1} - \frac{\Delta t}{2} \frac{a_1^2 C_{f1} + b_1^2 C_{r1}}{V_{1x}} & -I_{xz1} \\ 0 & -m_{R1} h_1 & I_{xz1} - m_{R1} h_1 \frac{\Delta t}{2} V_{1x} & I_{xxs1} + \frac{\Delta t}{2} D_{s1} \end{pmatrix}$$

$$A_{13} = \begin{pmatrix} -1 & 0 & 0 & 0 \\ 0 & -1 & 0 & 0 \\ -y_A & x_A & 0 & 0 \\ 0 & -(z_A - h_1) & 0 & 0 \end{pmatrix}$$

$$A_{22} = \begin{pmatrix} m_2 & 0 & -m_2 \frac{\Delta t}{2} V_{2y'} & 0 \\ 0 & m_2 + \frac{\Delta t}{2} \cdot \frac{C_{f2} + C_{r2}}{V_{2x'}} & m_2 \frac{\Delta t}{2} V_{2x'} + \frac{\Delta t}{2} \frac{a_2 C_{f2} - b_2 C_{r2}}{V_{2x'}} & -m_{R2} h_2 \\ 0 & \frac{\Delta t}{2} \cdot \frac{-a_2 C_{f2} + b_2 C_{r2}}{V_{2x'}} & -I_{zz2} - \frac{\Delta t}{2} \frac{a_2^2 C_{f2} + b_2^2 C_{r2}}{V_{2x'}} & -I_{xz2} \\ 0 & -m_{R2} h_2 & I_{xz2} - m_{R2} h_2 \frac{\Delta t}{2} V_{2x'} & I_{xxs2} + \frac{\Delta t}{2} D_{s2} \end{pmatrix}$$

$$A_{23} = \begin{pmatrix} 0 & 0 & -1 & 0 \\ 0 & 0 & 0 & -1 \\ 0 & 0 & -y_{A'} & x_{A'} \\ 0 & 0 & 0 & -(z_{A'} - h_2) \end{pmatrix}$$

$$A_{31} = \begin{pmatrix} 0 & 0 & 0 & 0 \\ 0 & 0 & 0 & 0 \\ 0 & 0 & 0 & 0 \\ \cos\Gamma & \sin\Gamma & d_c \cos\Gamma - d_a \sin\Gamma & 0 \end{pmatrix}$$

$$A_{32} = \begin{pmatrix} 0 & 0 & 0 & 0 \\ 0 & 0 & 0 & 0 \\ 0 & 0 & 0 & 0 \\ -\sin\theta_2 \sin\Gamma - \cos\theta_2 \cos\Gamma & \sin\theta_2 \cos\Gamma - \cos\theta_2 \sin\Gamma & d_a \cos\Gamma - d_b \sin\Gamma & 0 \end{pmatrix}$$

$$A_{33} = \begin{pmatrix} 1 & 0 & \cos\theta_2 & -\sin\theta_2 \\ 0 & 1 & \sin\theta_2 & \cos\theta_2 \\ \mu \cos\Gamma + \sin\Gamma & \mu \sin\Gamma - \cos\Gamma & 0 & 0 \\ 0 & 0 & 0 & 0 \end{pmatrix}$$

$$B_{12} = -e[(-v_{2x'} \sin\theta_2) \cdot \sin\Gamma + (v_{1x} - v_{2x'} \cos\theta_2) \cdot \cos\Gamma]$$

$$B = (m_1 v_{1x} \quad 0 \quad 0 \quad m_2 v_{2x'} \quad 0 \quad 0 \quad 0 \quad 0 \quad 0 \quad 0 \quad B_{12})'$$

Appendix G. Results, cont.

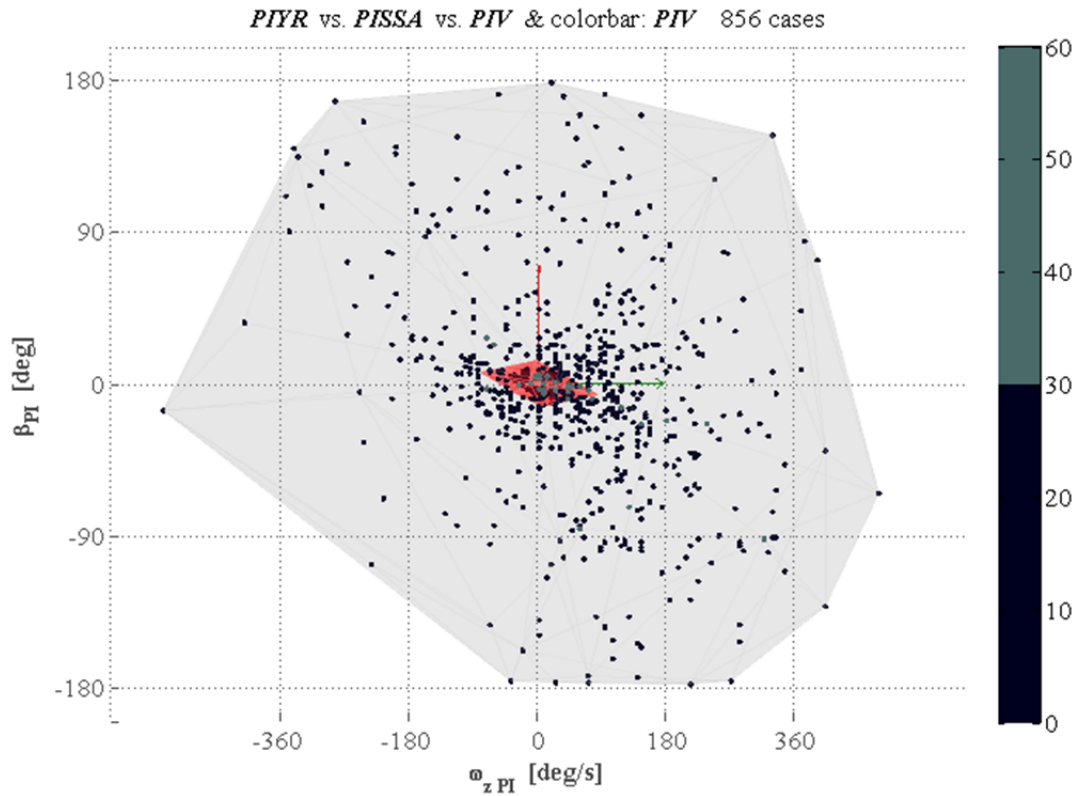


Figure G. 1. Kick plate volume covering GIDAS cloud, XY view.

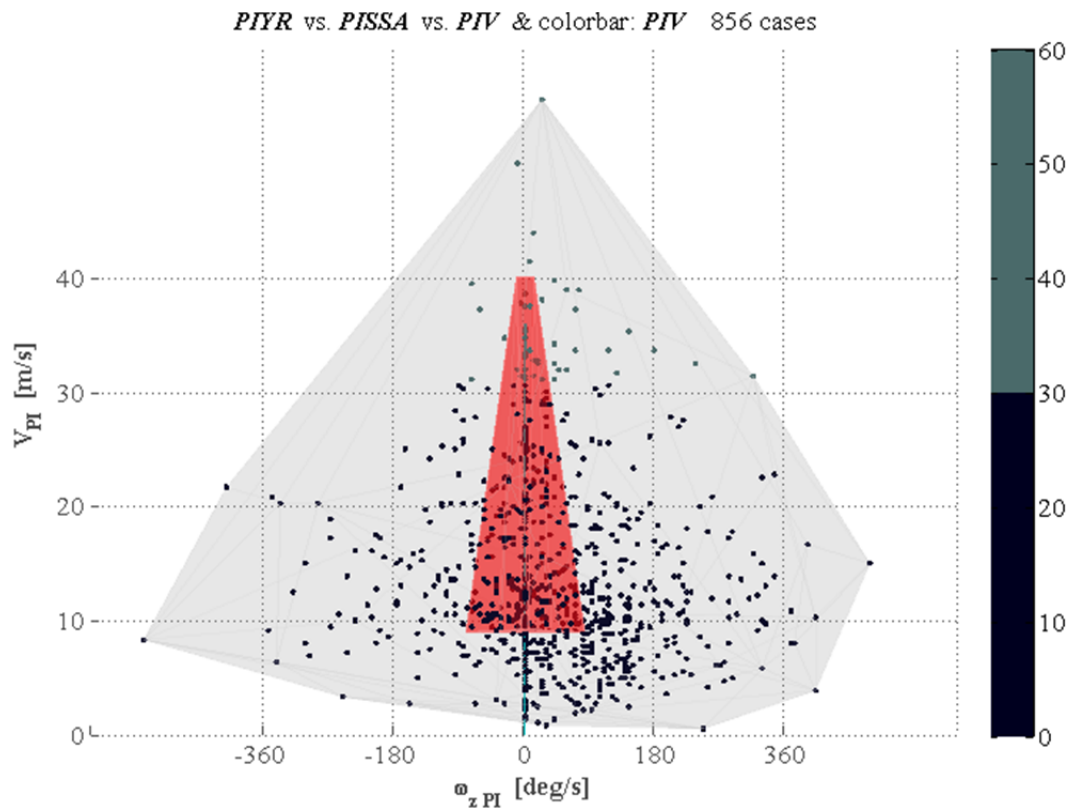


Figure G. 2. Kick plate volume covering GIDAS cloud, XZ view.

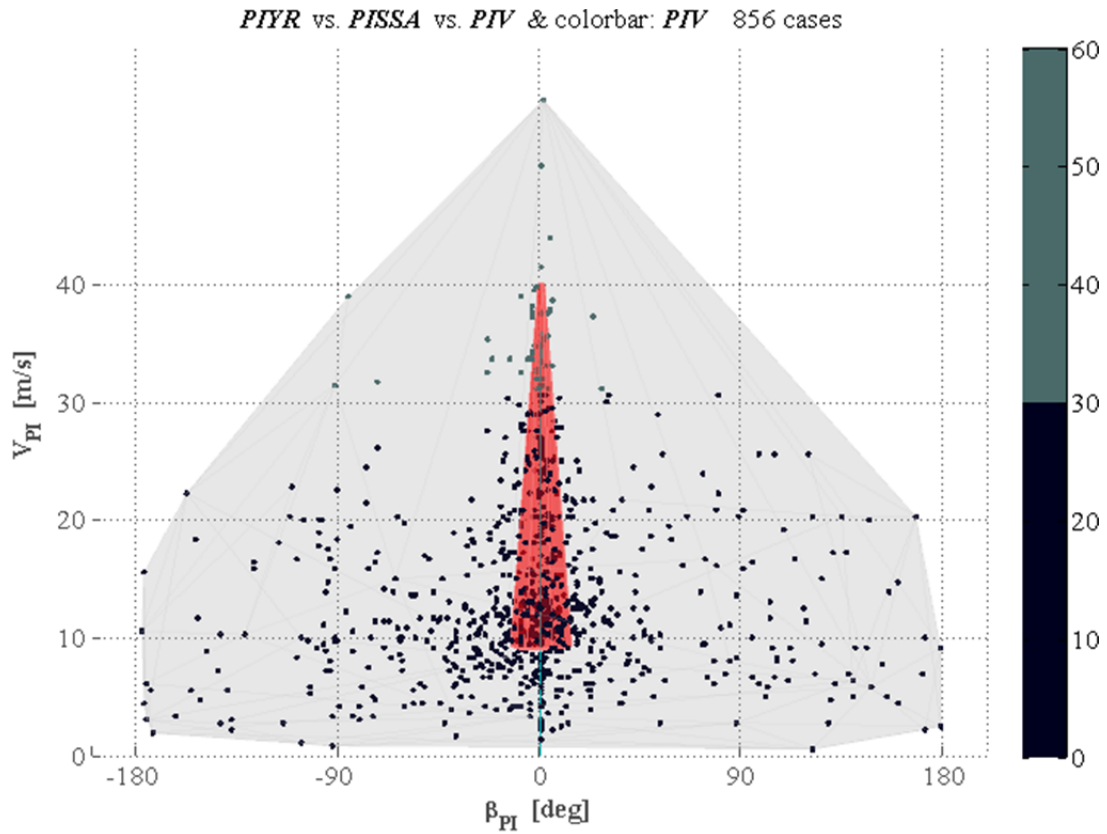


Figure G. 3. Kick plate volume covering GIDAS cloud, YZ view.

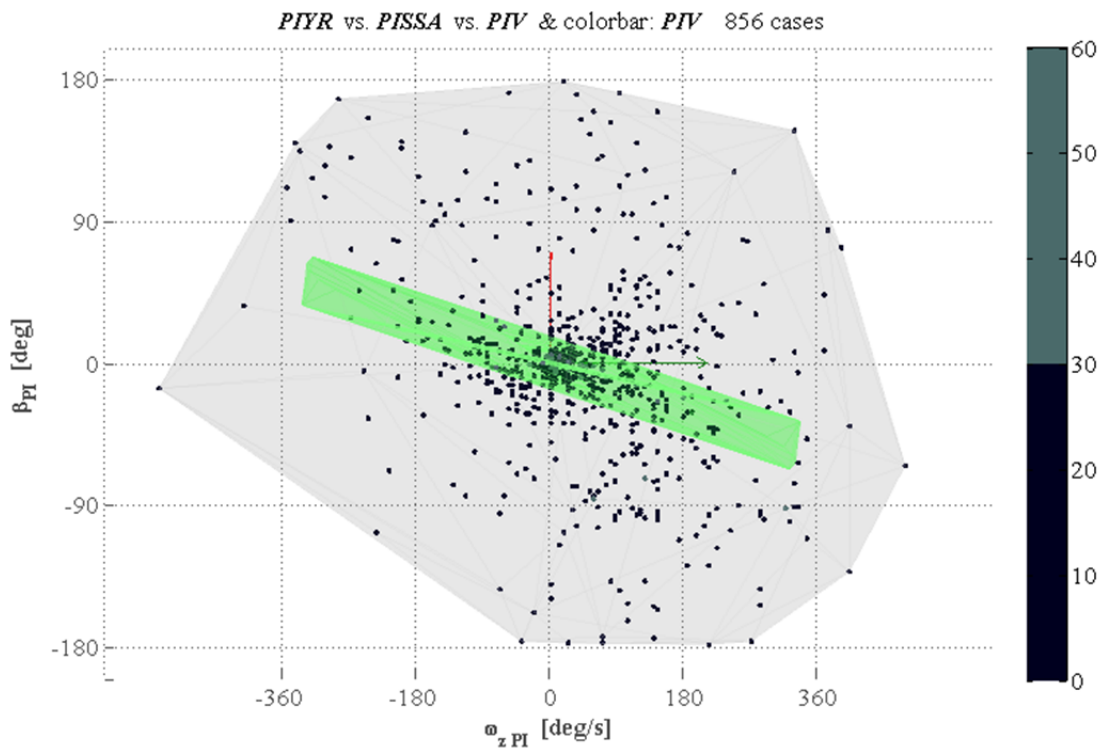


Figure G. 4. PIT manoeuvre volume covering GIDAS cloud, XY view.

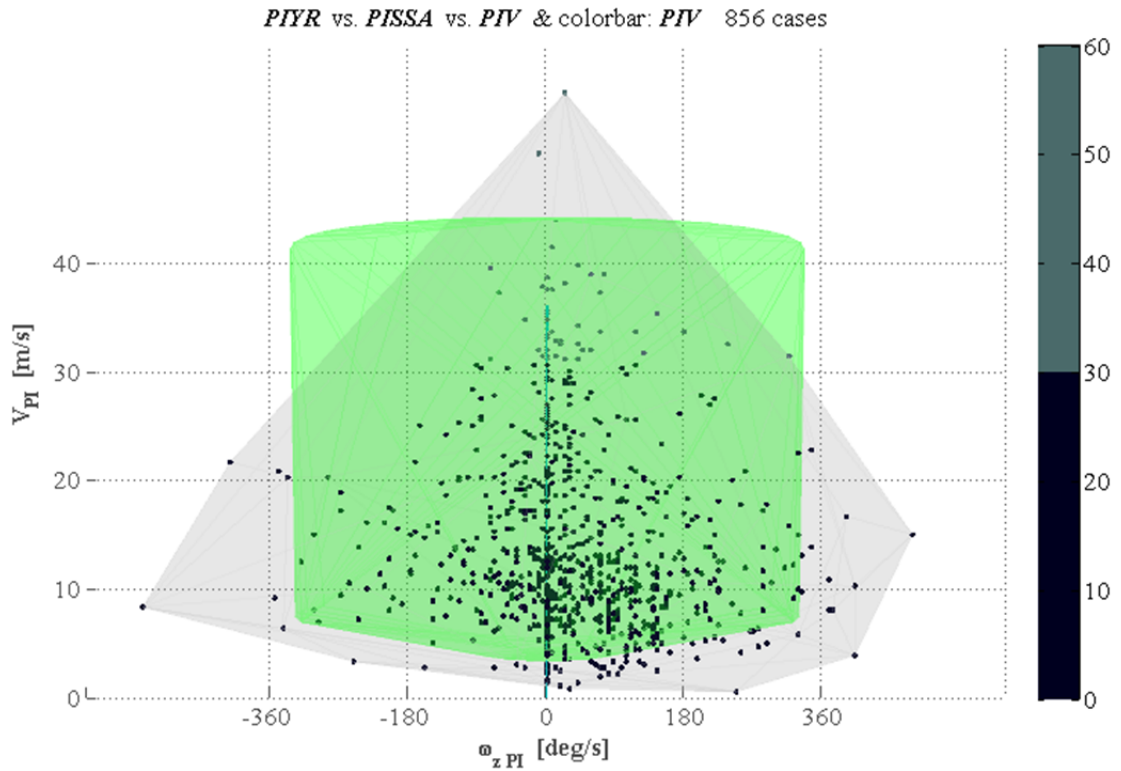


Figure G. 5. PIT manoeuvre volume covering GIDAS cloud, XZ view.

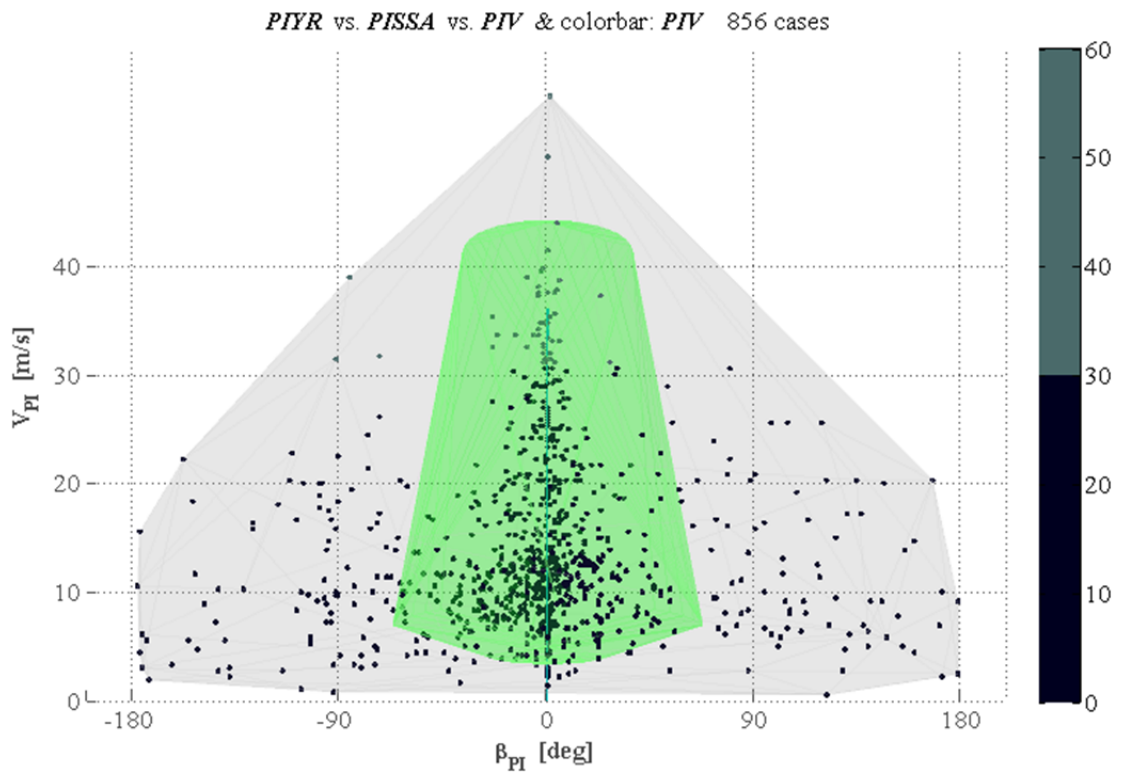


Figure G. 6. PIT manoeuvre volume covering GIDAS cloud, YZ view.

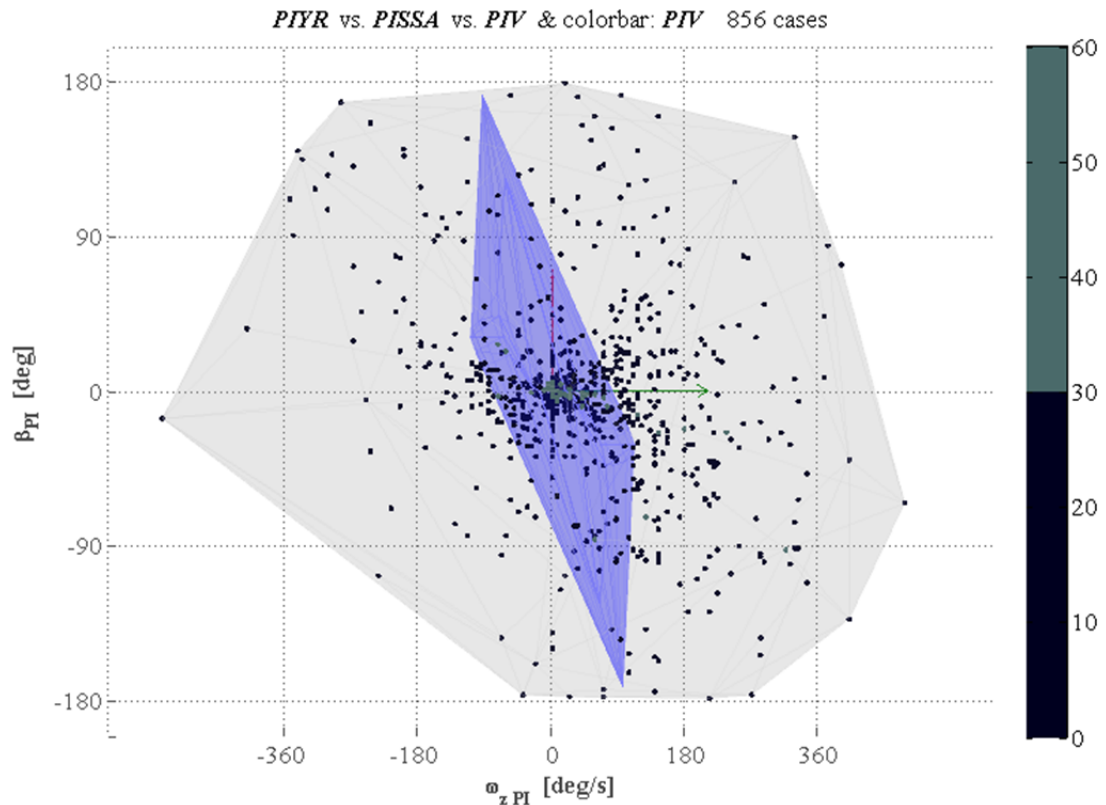


Figure G. 7. Built-in actuators volume covering GIDAS cloud, XY view.

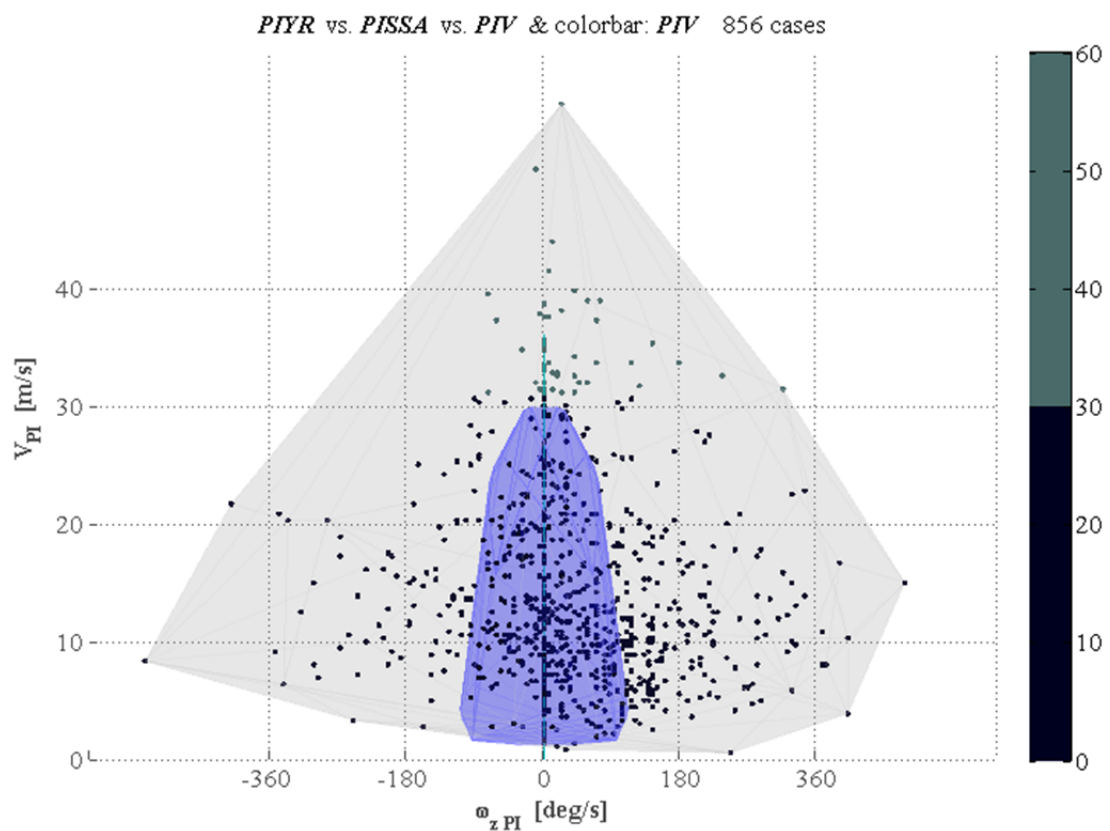


Figure G. 8. Built-in actuators volume covering GIDAS cloud, XZ view.

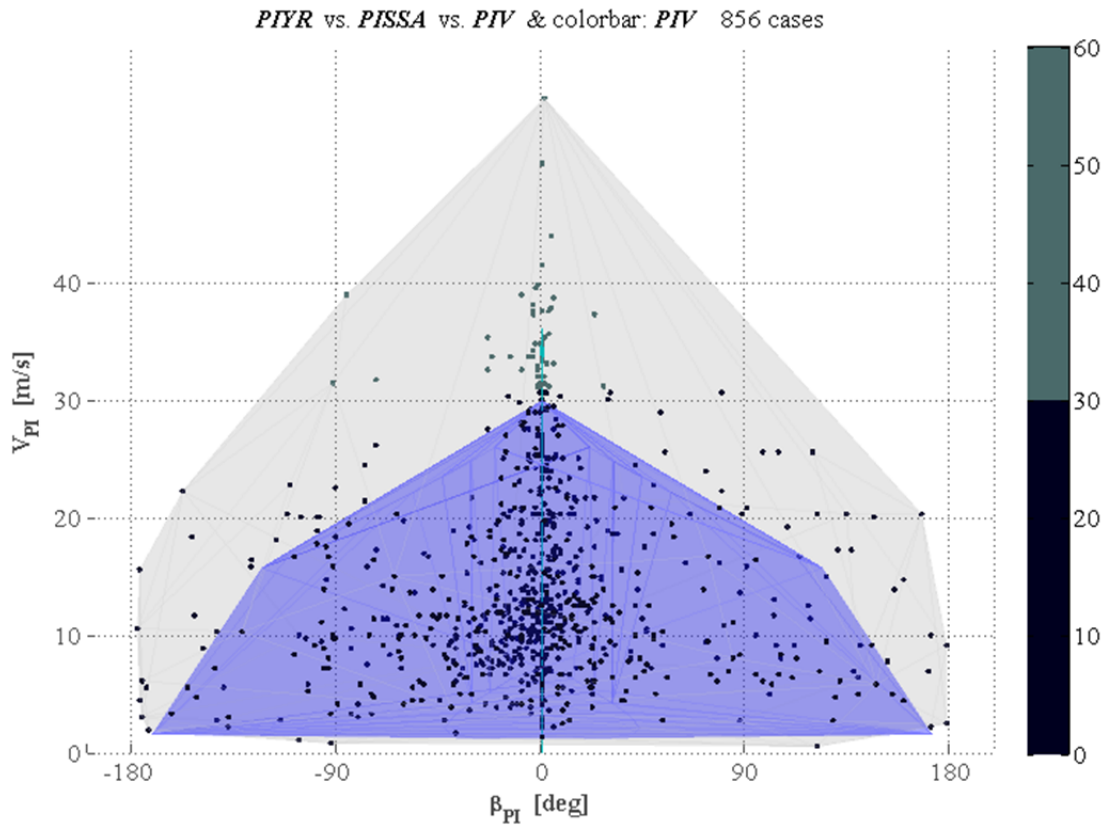


Figure G. 9. Built-in actuators volume covering GIDAS cloud, YZ view.

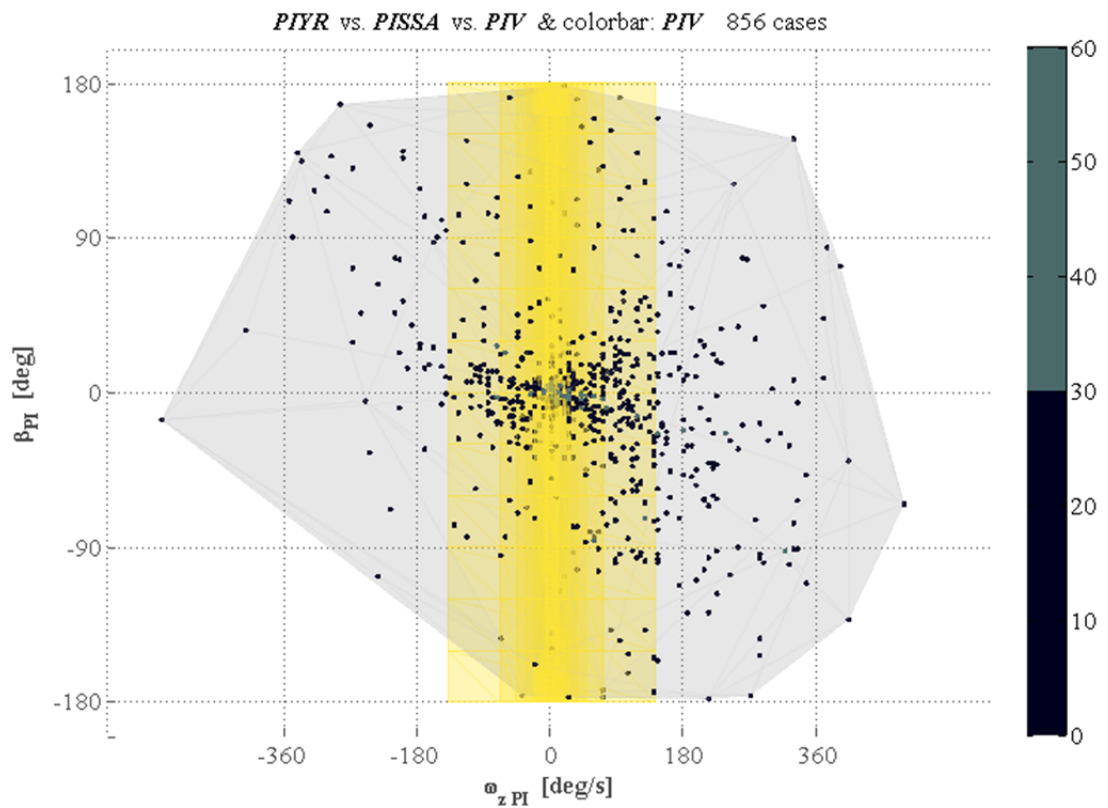


Figure G. 10. Simulator SIM4 volume covering GIDAS cloud, XY view.

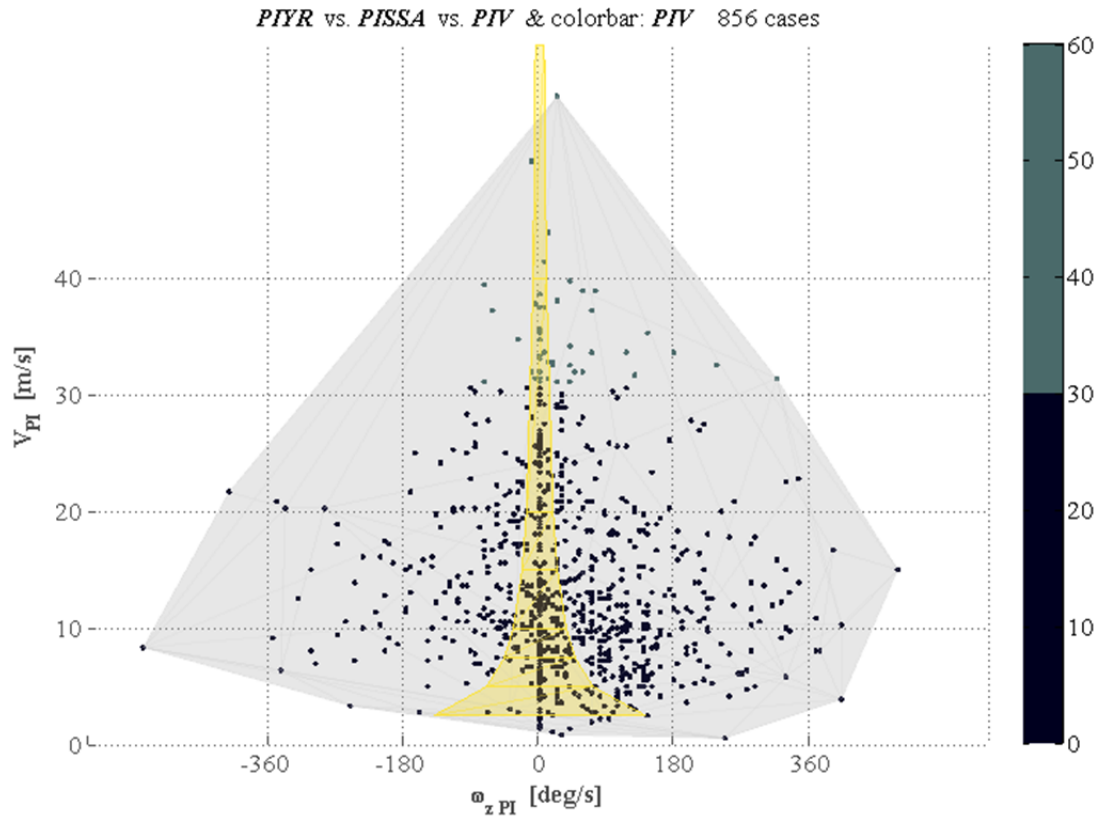


Figure G. 11. Simulator SIM4 volume covering GIDAS cloud, XZ view.

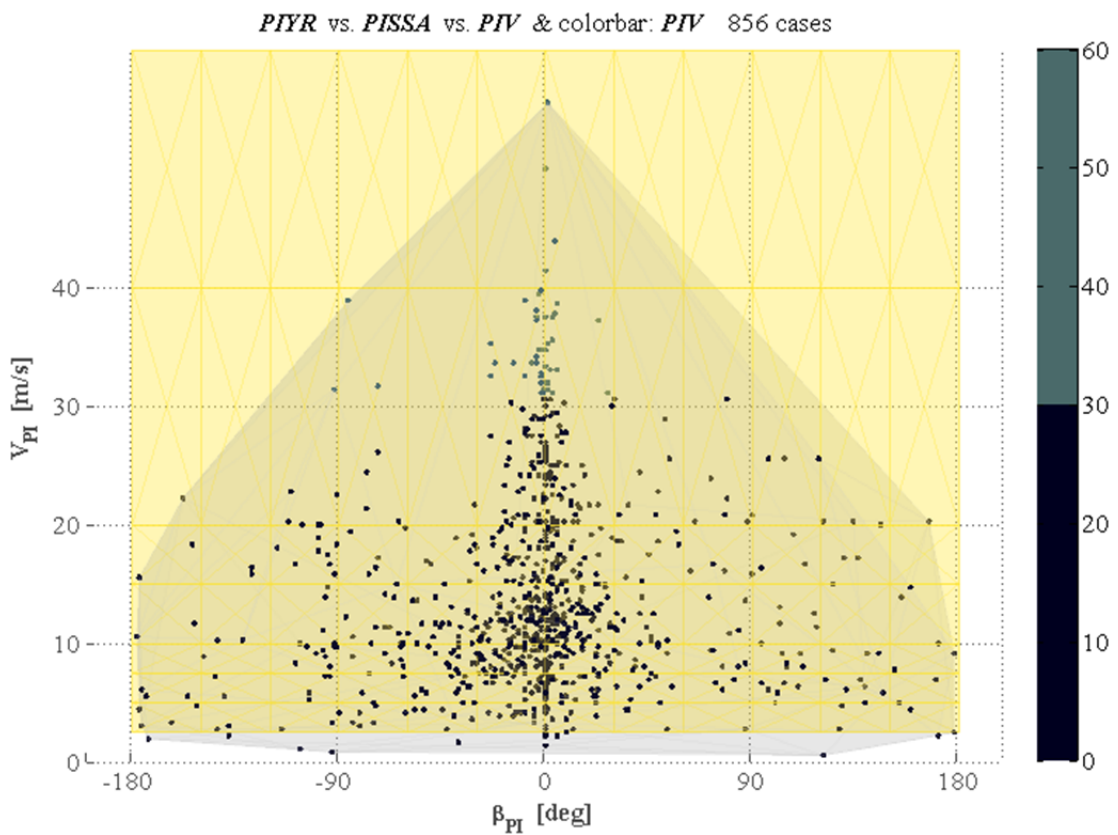


Figure G. 12. Simulator SIM4 volume covering GIDAS cloud, YZ view.

Appendix H. Other 6 GIDAS verification cases

Contents in this appendix are only found in the confidential variant of the report.

Appendix I: Other 7 reproduced cases

Contents in this appendix are only found in the confidential variant of the report.